STATE OF THE ART OF CONDUCTOR GALLOPING

A complementary document to "Transmission line reference book –Wind-induced conductor motion Chapter 4: Conductor galloping," Based on EPRI Research project 792

Task Force B2.11.06

Members:

Lilien, Jean-Louis - Belgium (Convenor)
Van Dyke, Pierre - Canada (Secretary)
Asselin, Jean-Marie - Canada
Farzaneh, Masoud - Canada
Halsan, Kjell - Norway
Havard, Dave - Canada
Hearnshaw, Dave - England
Laneville, André - Canada
Mito, Masataka - Japan
Rawlins, Charles B. - USA
St-Louis, Michel - Canada
Sunkle, Dave - USA
Vinogradov, Alexandre - Russia

International expert who contributed:
Yamaguchi, Hiroki - Japan

The authors of this brochure have asked detailed comments to:
Tunstall, M.J. (former chairman of B2.11.06) - UK
Ervik, M. - Norway
Obrö, H. - Denmark
Okumura, T. - Japan
Shkaptsov, V. - Russia

FOREWORD TO THE GALLOPING BROCHURE

Of all the wind induced motions of Overhead Transmission Line conductors or other suspended cables, galloping is the most noticeable and spectacular and the resulting damage can be equally dramatic and very costly, with broken conductors and fittings, damaged tower components and even whole towers collapsing! The consequential economic and social costs of power loss to whole areas can also be very considerable.

Galloping is an oscillation of single or bundled conductors due to wind action on an ice or wet snow accretion on the conductors, although there are recorded instances of non-ice galloping arising from the conductor profile presented to the wind. Conductor motions are characterised by amplitudes that may approach or exceed the conductor sag (possibly >10m) and depending on the amplitudes and number of loops, frequencies up to 3 Hz.

Galloping of conductors received particular emphasis by incorporation of a CORECH work group within Task Force 6 (Galloping) of CIGRE SCB2 WG11. The focus was on field observations of galloping, effectiveness of control devices, documentation of damage, refinement of clearances required for design to avoid flashovers and instrumentation to record galloping. Emphasis was also placed on research on aerodynamics, on shapes of accretions of ice or wet snow and on the development of theories describing galloping behaviour. A galloping reporting format for the field was published in 1995 and a 'State of the Art' report reviewing galloping control methods was published in 2000.

This brochure is both up to date and comprehensive in its treatment of this important topic and will be valuable both to researchers, who are seeking to better understand the fundamental causes of galloping and Transmission Line engineers, who are faced with the practical consequences of galloping on their lines and need to find remedies. It will also compliment the revised EPRI 'Orange Book'.

In conclusion, I would like to recognise the hard work of the Task Force volunteers who have carried this work through to completion and thank them on behalf of CIGRE and the wider industry.

David Hearnshaw C Eng

Convenor, SCB2 WG11

09 December 2005

CIGRE ad hoc SC

CONTENT

1. Executive summary

Galloping is a low frequency, high amplitude wind induced vibration of both single and bundle conductors, with a single or a few loops of standing waves per span. Frequencies can range from 0.1 to 1 Hz and amplitudes from ± 0.1 to ± 1 times the sag of the *span*. In the case of distribution lines, amplitudes of up to 4 times the *sag* can occur. Galloping is generally caused by a moderately strong, steady crosswind acting upon an asymmetrically iced conductor surface. Galloping is usually observed with limited amounts of ice but there have been some examples of non-ice galloping. The large amplitudes are generally but not always, in a vertical plane whilst frequencies are dependant on the type of line construction and the oscillation mode excited. Winds approximately normal to the line with a speed above a few m/s are usually required and it cannot be assumed that there is necessarily an upper wind speed limit.

Galloping has a major impact on the design of overhead lines, for both clearances and tower loadings, as large load variations may occur between phases and even between each side of a given tower, causing horizontal and vertical bending as well as torsional loads on towers and crossarms. Due to the large amplitudes, breaking bending loads may be reached at conductor attachment points and tower bolt failures have been observed. Wear also results at some locations (e.g. - yoke plates and insulator pins), which may only become evident with severe consequences much later, possibly during other seasons.

Torsional motion of the earthwire or phase conductors (single or bundle) may occur with very significant amplitudes. In the case of bundles, collapse may occur causing problems at suspension arrangements.

Types of Motion

Galloping takes the basic form of standing waves and traveling waves, or a combination of the two. The standing waves may occur with one or up to as many as ten loops in a span. Small numbers of loops predominate.

Observed peak-to-peak amplitudes of galloping are often as great as the sag in the span and are sometimes greater, especially in short spans. Amplitudes approaching the sag in magnitude have been observed with as many as three loops in the span but beyond that number, the amplitudes become smaller.

The predominant conductor motions in galloping are vertical but there is often a horizontal component of motion transverse to the line. The vertical and horizontal motions are often out of phase, so that a point on the conductor near the mid-loop traces an elliptical orbit.

When galloping occurs with one loop in the span, there may be significant longitudinal movement of the conductor (in the direction of the line). Peak-to-peak swings of the order of ½ meter have been observed. These motions are most noticeable in longer spans.

Twisting motion of single conductors during galloping is difficult to discern from the ground, but it has been detected and measured by the attachment of suitable targets to the span. Peak-to-peak rotations greater than 100° have been observed and the torsional movement during the galloping limit cycle (the elliptical orbit) has the same frequency as the vertical motion, although it is generally out of phase with it.

Damage and Other Consequences

Galloping has caused various kinds of structural damage in overhead lines. Some types of damage result directly from the large forces that galloping waves or loops apply to supports. For example, crossarms have failed on both wooden and metal structures. Conductor ties on pin-type insulators have been broken and support hardware has failed. In other cases, cotter pins have been damaged and insulator strings have consequently uncoupled.

Dynamic shock loading occurs when a steep-fronted galloping wave is reflected at a tower. Repeated reflections can cause vibration damper weights to ‘droop’ and in extreme cases, damper messenger cables to break, dropping the damper weights.

Dynamic loads have also caused loosening of crossarm and bracing bolts in tower structures and loosening of wood poles in the ground. Jumpers at deadend towers have been thrown up onto crossarms.

When galloping amplitudes are great enough to permit flashover between phases or from phase to ground, arcing damage to conductor surfaces results. The damage has been significant enough in some cases to cause broken strands in conductors and to result in complete failure of earthwires or even phase conductors.

Forced outages caused by galloping result in loss of revenue and sometimes in other costs associated with re-establishing service. These consequences are generally considered to be more severe than direct damage to lines.

Amplitudes

For single conductors, the curve defining the maximum amplitude over conductor diameter, is given by:

$$\frac{A_{pk-pk}}{\phi} = 80 \ln \frac{8f}{50\phi} \tag{1.1}$$

where A the peak-to-peak amplitude (m), ϕ the (sub)conductor diameter (m) and f the sag of the unloaded span (m) at 0ºC.

For bundle conductors, limited to observations of galloping with wind speed up to 10 m/s:

$$\frac{A_{pk-pk}}{\phi} = 170 \ln \frac{8f}{500\phi} \tag{1.2}$$

Design load

- Anchoring level: tension load extremes during galloping can range from 0 to 2.2 times the static value (with ice but no wind). Nevertheless, ice loads during the most severe galloping are generally very limited so that, in absence of particular data, static value to consider can be evaluated at 0°C without ice load.
- Suspension level: vertical load extremes during galloping can range from 0 to 2 times the static value

Protection Methods

There are three main classes of countermeasure employed against galloping:

1. Removal of ice or preventing its formation on conductors.

2. Interfering with the galloping mechanisms to prevent galloping from building up or from attaining high amplitudes.

3. Making lines tolerant of galloping through ruggedness in design, provision of increased phase clearances or controlling the mode of galloping with interphase ties.

An overview of existing techniques is given as follows:

Table: Overview of existing countermeasure against galloping

NO	DEVICE NAME	APPL'N	WEATHER CONDITION		LINE CONSTRUCTION			COMMENTS
			Glaze	Wet snow	Dist'n	Single trans'n	Bundle	
1	Rigid Interphase Spacer	Widely used	Yes	Yes	Yes	Yes	Yes	Prevents flashovers, reduced galloping motions
2	Flexible InterphaseSpacer	Widely used	Yes	Yes	Yes	Yes	Yes	Prevents flashovers, reduced galloping motions
3	Air Flow Spoiler	Widely used	Yes		Yes	Yes	Yes	Covers 25% of span Limited by voltage. Extensive field evaluation
4	Eccentric Weights & Rotating Clamp Spacers	Used in Japan	No	Yes	No	Yes	Yes	Three per single span. One per spacer per subconductor
5	AR Twister	Used in USA	Yes		Yes	Yes	Yes	Two per span
6	AR Windamper	Used in USA	Yes		Yes	Yes	Yes	Two per span
7	Aerodynamic Galloping Controller (AGC)				Yes	Yes		Number based on analysis
8	Torsional Control Device (TCD)	Used in Japan		Yes	No		Yes	Two per span
9	Galloping Control Device (GCD)	Used in Japan		Yes	No		Yes	Two per span
10	Detuning Pendulum	Widely used	Yes		Yes	Yes	Yes	3 or 4 per span. Uses armor rods if tension is high. Most extensive field evaluations
11	Torsional Damper and Detuner (TDD)	Experim ental	Yes	Yes	No	No	Yes	2 or 3 per span

2. Introduction

Galloping of iced conductors has been a design and operating problem for electric utilities since the early 1900s. Over the years, it has been the subject of numerous investigations and research programs, resulting in better understanding of galloping mechanisms and in the development of devices and procedures to combat its effects. However, the EPRI Reference Book, "Wind-Induced Conductor Motions," [EPRI, 1979] remarked in 1979,

"Progress, both in analytical attack on the problem and in development of countermeasures, has been slow. Forty-five years after publication of Den Hartog's analysis, important questions remain as to which variables and mechanisms are significant, and validation of theories of galloping is still not satisfactory. No practical protection method has been developed that is recognized as fully reliable."

The EPRI book's chapter dedicated to galloping gave an extensive summary of the state-of-the-art at that time [Rawlins, 1979].

There has been continued research effort since publication of the book, with resulting significant advances in the technology. The purpose of the present report is to describe these advances, to put them in context for designers and operators of overhead lines, and to point the direction for future research on the subject. It should be noted that, at the time of writing, work was in progress at EPRI to produce a second, revised edition of the book. The new edition may be expected to incorporate material on many of the advances discussed below, especially if they can be put to immediate practical use. However, this brochure, with its emphasis on technical depth, should continue to serve as a prime knowledge base for future development and progress in understanding and control of galloping.

Advances during the period 1979 to 2006 fall in several categories. Of particular importance is the development of several countermeasures that appear to be reliable enough to find common usage on operating lines. These include the conductor construction known as "T2" in which two conventional conductors are twisted together; airflow "spoilers" which impart a figure-8 outline to the conductor span over part of its length; offset masses; and detuning pendulums. Other devices, showing promise in development programs, include torsional dampers for use on bundled conductors. Although they are not a recent development, interphase spacers have found increasing use and acceptance in recent decades.

Advances have also occurred in guides for the design of electrical clearances to accommodate galloping motions without flashovers. Several independent analyses of a large data bank of galloping observations have yielded improved guides to maximum expected amplitudes; and a systematic study of films of galloping events has provided better definition of the shapes of galloping orbits.

Although the accumulation of field observations has markedly slowed since 1980, methods of obtaining data from the field have improved. First, CIGRE WG11 has issued a document standardizing the acquisition and reporting of such observations. Second, and more significant, there has been a proliferation of instrumented test lines and test sites where much more comprehensive information on natural galloping is acquired. This information is of critical importance in developing and validating analytical models of galloping mechanisms.

The analytical area is another category that has shown advances since 1979. The advances have been spurred by access to more powerful computer analysis software. Actual overhead lines are much more complex than was visualized by the theoretical models in use at that earlier time. This is particularly true for bundled conductors, but is also the case in multi-span line sections even for single conductors. The advanced software has allowed investigation of the impact of these complexities, for example through computer simulations and through eigenanalysis.

There has been increasing success in simulating in the computer actually observed galloping behavior in field test spans and, even more so, the measured behavior in dynamic wind tunnel tests.

A fully satisfactory analytical attack depends upon reliable data on the aerodynamic characteristics of the ice shapes that actually occur on overhead lines and cause galloping. Galloping technology remains deficient in this area. Although a few samples of such ice shapes have been obtained and evaluated in wind tunnel tests, there is as yet no case where such a shape, with its aerodynamic characteristics, can be associated with an actual galloping event. There are several cases where the association between such characteristics and actual galloping has been established for artificial shapes, but the relationship between these shapes and actual icing deposits is not completely clear because of differences in surface texture and the degree of uniformity along the conductor. A 1988 paper remarked [Rawlins and Pohlman, 1988]:

"… Galloping technology seems to divide naturally into a mainly meteorological segment which is inherently random, and a basically deterministic segment that is driven by … the first segment. The pivot between the two segments is … (aerodynamic) information on ice shapes. The deterministic segment cannot be exploited without a fund of data at this pivot."

It should be added that the deterministic segment cannot even be *validated* without data at this pivot.

In the following chapters, the members of the Task Force on Galloping describe advances in the various areas of galloping technology mentioned above, as well as others, in order to bring into focus the present state-of-the-art.

The target groups for this brochure can be defined as follows:

Researchers, to state the general agreement of the art among the different researchers in the field and to form a better base for cooperation with the other target groups mentioned below.

Overhead line engineers, to understand the background existing behind IEC methods from one side, to think about system design taking into consideration galloping loads and clearances at early stage and not simply to verify structure against galloping problems, to give them trends to decrease galloping loads and clearances for uprating, refurbishment as well as designing new lines.

Technical group like equipment suppliers, to help them providing new design of line components as well as retrofit methods.

IEC and other organisations submitting recommendations and standards, like CENELEC and IEEE, the CIGRE brochure being eventually technical base for the methods to be suggested in overhead line design against galloping.

This brochure is accompanied by a CDrom showing the best videos taken during either actual galloping on lines or galloping obtained with artificial ice shape. Some wind tunnel galloping is also shown.

3. Cost of galloping

Galloping is not just a spectacular and annoying phenomenon: in some cases it may have very costly consequences. The costs associated with galloping events can be due to damaged components requiring inspection and repair or to the consequences of repeated power interruptions. Costs may range from very low to extremely high, depending on the circumstances of each case.

There are also costs related to the prevention of galloping. Increased conductor clearances and the use of anti-galloping devices generate direct costs whilst investments in studies, research and development also have to be considered. This chapter will show that galloping can have a serious cost impact and what aspects should be considered.

3.1 Costs Related to Galloping Events

3.1.1 Damage Repair

Galloping does not necessarily damage transmission lines components and most of the time it does not. When it occurs however, damage may range from minor, such as conductor strand burn (which is quite common), to extreme, such as line collapse as the result of conductor breakage or dynamic overload. The repair costs will vary greatly depending on the extent of the damage. Repair of broken conductor strands may cost a few thousands dollars for easy access lines. For lines in remote area or those that are not easily accessible, such as river crossings, special techniques may have to be used such as helicopter work. Costs may then increase significantly. Although rare, line collapses due to galloping have occurred. As an example, galloping has been observed to have triggered a cascade failure of a section of a HV line during the 1998 ice storm that affected the north east of North America. Another case was reported in 1997 when two 120 kV towers collapsed due to a conductor breakage under galloping conditions. Costs range from less than 100 k$ for the two towers to millions of $ for the EHV line cascade in 1998. Experience from Russia shows that tower collapse can cost 50 k$ per tower for 110-220 kV lines, whilst repairing one suspension insulator string can cost 2-4 k$.

3.1.2 Inspection

A galloping event causing the repeated trip-out of lines may require an emergency inspection to identify the cause and apply remedial measures. This has to be done in bad weather at unpredictable moments. Otherwise, depending on the utility's practices, an inspection of the lines that galloped may have to be performed to detect any damage. This may be done either by a ground crew or by helicopter. The costs may not appear significant if this work is considered as part of the normal tasks of the maintenance crews. However, as the work is often unplanned, it may introduce additional costs.

3.1.3 Loss of revenue

Most of the time, line trip-out due to galloping will be of short duration with negligible effect on the utility's revenues. In some cases, repeated flashovers will cause the automatic protection systems to open the circuit until the cause of the fault is identified and repaired. A real loss of revenues will result if there is no alternate route to reach the customer and the cost of galloping may then be significant. As an example, in a recent galloping event a loss of 200 MW for 2 hours was reported. Depending on energy costs, this represents a significant amount of revenue.

3.1.4 System reliability and quality of service

There is no doubt that many utilities are increasingly concerned about the impact of galloping on system reliability and the quality of service but establishing the cost of galloping with regards to those factors is problematic. There may be no direct costs, as customers will seldom get compensation for a short duration power failure. However, transmission system owners may sustain significant costs if the system operator has to call up more expensive generation to maintain system security. Indirect costs may certainly be important; for example, it may be necessary to have a backup line for important industrial customers, such as aluminium smelters. There may also be a risk of losing hi-tech customers who are very sensitive to power quality.

3.1.5 Social impacts of outages due to galloping

3.1.5.1 Impact on utility image

All unscheduled interruptions in supply to customers result in adverse publicity. The extent of the adverse publicity will be influenced by a number of factors: for example, the number of customers affected, the duration of the failure and the time of the year when the failure occurs. If the outages are frequent and last for long periods during the winter season, the utility can expect adverse publicity from the national media. This may adversely influence public confidence in the company and also the share values for public limited companies. However, there can be a positive side to failures in that increased public awareness of the importance and vulnerability of transmission systems can be used to help justify investments in maintenance or in the application of countermeasures.

3.1.5.2 Impact on hospitals

Outages caused by galloping are normally short, but even short outages can be critical in hospitals. Most countries require that hospitals have back-up power supplies in case of power outages, so the impact on hospitals should be limited. If the back-up power supply fails, it is more likely that public criticism will be directed at the hospitals rather than at the utility involved.

3.1.5.3 Impact on production industry

Some types of industry are very sensitive to both power outages and power quality. Heavy industries, like aluminium smelters, may have huge start up costs if a long outage causes the cessation of production. Other industries, like paper mills, require good power quality to avoid interruptions in production. In some countries, the utilities have to pay compensation to industrial costumers for the power that has not been supplied. The compensation rate will depend on the type of industry. Examples from Norway for other types of failures show that a short outage lasting for few minutes can cost more than 100,000 US$ and an outage to an aluminium smelter could cost the power utility about 150,000 US$ per hour. In this case, compensation costs could easily be much larger than the costs of repairing damage to towers and line components if the outage were to last for several hours.

If production industries have too many interruptions in their power supplies, they will evaluate alternative on-site power sources such as gas turbines to avoid power outages. This will result in loss of income for the power utility.

3.1.5.4 Impact on population confidence and safety

Outages will always have a negative impact on confidence in the utility, especially among the affected customers. Normally the customers will not know or care about the reason behind the failures that occur and they are unlikely to have any knowledge of the phenomenon of conductor galloping. People living in the vicinity of galloping lines may observe the phenomena and be concerned about damage to property or person due to broken conductors or falling towers. This may, in turn, result in questions being raised about the professional competence of the utility.

When a line gallops severely and for a significant period of time, the failure of a component is always a possibility. In this case, measures may have to be taken to keep people away from the galloping line. Such a situation happened when a 4-conductor bundle line passing over a highway was experiencing galloping and the traffic had to be stopped for a few hours. In another case, during the 1998 ice storm in Canada, access to the Montreal city area was closed because a twin bundle line was galloping.

3.2 Costs Related to Prevention of Galloping

3.2.1 Design criteria

It has been the practice in many utilities to increase conductor clearances in order to minimise the risks of flashovers between conductors. Different approaches have been used, generally based on the theoretical shape and size of the galloping conductors' trajectory. Although more realistic clearance requirements have been made possible by field observations, this approach is costly because it is usually applied to complete sections of lines, assuming that galloping can happen anywhere. The actual cost of this approach can only be established for each specific case. In fact, conductor

clearances are also dictated by other considerations, such as live-line maintenance, so that the potential impact of galloping may be reduced. Nevertheless, any additional clearance due to galloping means higher towers and higher mechanical loads, leading to heavier and costlier towers and foundations.

3.2.2 Anti-galloping devices

Anti-galloping devices can be retrofitted on existing lines that experience galloping. This situation is the most common and the easiest to manage because the field experience exists to justify the decision. These devices can also be used on new lines as part of a design approach to prevent galloping. In these cases, the galloping experience of other lines in the same area can be taken into account. However, in cases where there is no other line in the area and the concern about galloping is based on an evaluation of the terrain conditions and climatic data, then the decision is difficult. A cost comparison between increasing the clearances and using anti-galloping devices must be made.

In addition to the cost of purchasing and installing the devices, the maintenance costs have to be considered because each piece of equipment installed on conductors may be a source of problems in the future. For example, the device itself may become defective or create damage to the conductor due to the effect of aeolian vibration. Experience has shown that inappropriate devices may cause more damage than the benefits they provide. A serious situation was experienced in 1993 when multiple conductor breakages occurred at the attachment points of anti-galloping devices on a 120 kV line. This was due to aeolian vibration entrapment between the devices. Thousands of people were left without an electrical supply for nearly two weeks during the cold season. Conductors had to be replaced on many km of lines. Data on the actual cost of this event are not available, but it was certainly in the order of millions of dollars.

3.2.3 Research and Studies

Because galloping exists and has created concerns among utilities for nearly 75 years, considerable expenditure has been made on field observations, studies and the research and development of countermeasures. The efforts dedicated to this phenomenon have varied widely with time but even today, hundreds of thousands dollars, if not million, are invested every year to better understand the galloping phenomenon and develop efficient means for the protection of transmission lines against it.

4. The appearance and the occurrence of galloping

4.1 Types of motion

In gross terms, galloping is a vertical oscillation of the conductor span in one- or a few loops. However, it usually incorporates other, less visible, twisting, lateral and longitudinal motions.

The most common design of overhead transmission lines consists of many spans of similar length supported on steel lattice towers with suspension insulators. Galloping of these lines is usually in one or two loops with generally similar amplitudes in each span. Aside from the clearly visible vertical motions, there are usually noticeable longitudinal motions of the suspension insulator strings. The upward half of the cycle of motion is larger than the downward motion due to longitudinal insulator swing, and the conductor can move above the horizontal. The galloping motions can be large enough to cause flashovers between adjacent phases, especially when the phases are above each other. Occasionally, the vertical motion may result from a combination of modes, including one-, two-, three-, and four-loop motions. The single loop mode can occur even on relatively long spans.

The swinging of the suspension points longitudinally to the line, referred to above, are caused by the variations in tension that can accompany galloping, and they act to couple the galloping motions in adjacent spans. The spans are then not autonomous. Instead, the section as a whole has normal modes, each of which involves participation of every span in the section. There is generally a multitude of such modes, each at a different frequency, and each displaying a different combination of relative amplitudes in the various spans.

When the spans are on quasi fixed supports, such as in many lower voltage distribution lines, the motions are commonly in the two-loop mode but with very high amplitudes (several times the sag has been observed), in such severe cases tension changes, despite the two loops mode, can be quite high. The amplitudes are again similar to each other in the different spans, due to feed-through at the supports, which can occur because this class of line is frequently supported on wood poles with crossarms, which allow some longitudinal support point movement. In addition to causing flashovers between phases, galloping can damage this type of structure due to twisting of the wood crossarms and poles accompanying synchronous motions of the phases.

The conductor may twist during galloping. This is seldom visible for single conductors, but is readily apparent in bundled conductors through rocking motion of the spacers. The twist is synchronized with the vertical motion. The vertical motion of galloping may be accompanied by horizontal motion, but this is usually, and perhaps generally, less than one third of the vertical component.

Short line sections between dead-ends are the most common design of overhead lines. Figure 4.1 illustrates the four lowest-frequency modes for such a line section having four suspension spans of 160, 180, 190 and 195 m between dead-ends. Calculations, using a linear analysis of the motions, show that for the modes at 0.386 and 0.403 Hz, there is only small variation in tension during galloping. This is because, when one span is at its upward extreme of motion, there is another span at the downward extreme. The variations in arc length of the two spans compensate each other by means of swinging of the suspension support between them.

In the mode at 0.516 Hz in Figure 4.1, all spans move in phase so there is less ability for arc length compensation between spans to occur. As a result, this mode displays significant tension variations during galloping, rather like the pseudo-fundamental in a dead ended span, which we discuss below.

The least common design of overhead transmission line span is that with tension towers at both ends. When the galloping takes place in such a span and if the towers are stiff enough (this may not be the case for wood poles), the motions are independent of what is taking place in adjacent spans. The galloping may display modes with 1, 2, 3, etc, loops. The modes with even numbers of loops conform in frequency and mode shape to simple taut-string theory. The odd-numbered modes, however, have higher frequencies than predicted by string theory, and their mode shapes take the form of sine waves with an offset. They are called pseudo-modes because of these differences.

These odd modes, especially the pseudo-fundamental, are marked by significant variations in conductor tension even for small galloping amplitudes. These variations occur because the galloping loops are superimposed upon the curvature of the sagged conductor. This results in a difference in the arc length of the conductor between its upper and lower extremes of motion, as illustrated in the top panel of Figure 4.2. Since the supports of a dead ended span are nominally rigid, this variation in arc length must be accommodated through conductor strain, with resulting variations in tension. These tension variations lead to an offset of the sine wave synchronous with its deflection, resulting in loop shapes such as in the second

panel of Figure 4.2. The lowest odd mode, the pseudo-fundamental, may have enough offset that it appears to have three-loops, as in the third panel. Dead-end spans experience the highest forces applied to the structures during galloping.

There are certain modes that, even in suspension spans, are autonomous to the span. These are the modes that have even numbers of loops in the span. These modes cause only slight variations in conductor tension, and thus produce little motion at suspension supports. Thus, there is no significant coupling to adjacent spans.

Spans are often observed to gallop in a combination of two or more of the modes that are available to them. For example, a suspension span may move simultaneously in a mode of the section and in its own autonomous 2-loop mode. This type of behaviour is discussed in more detail in section 4.2.1 Galloping observations by measurement and data analysis.

The vertical component of galloping, and the longitudinal motions at suspension supports, are important relative to the infringement of electrical clearances, both in spans and at supports. They are also closely associated with the conductor tension variations, which can be large, and the dynamic forces transmitted to insulators and supporting structures.

The above discussion neglects the torsional component of galloping motion, as well as motions lateral to the span. Both of these also have normal modes by span and by line section. Those components can have important effects in relation to aerodynamic mechanisms that cause galloping, and they are discussed in the next part of this chapter.

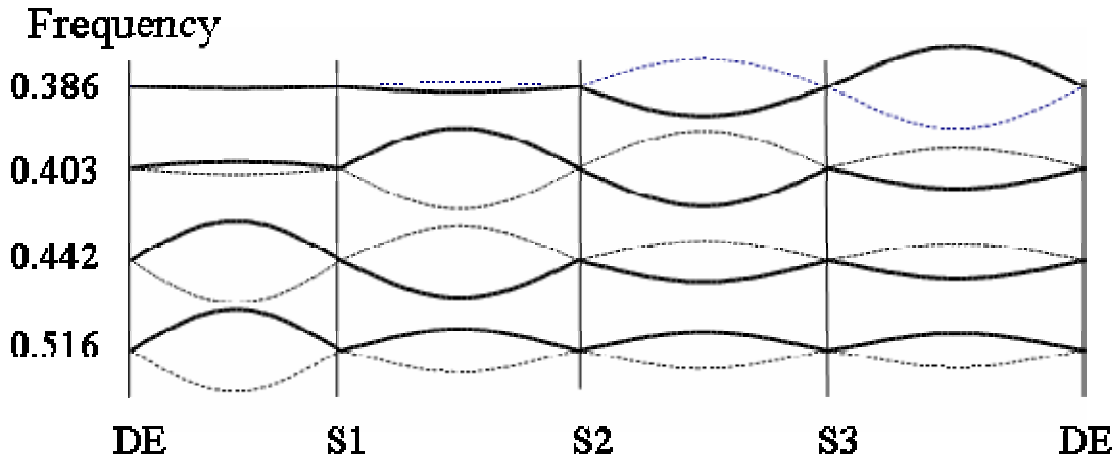

Figure 4.1: Typical one-loop mode shapes (4 span sections). The three first ones are “up-and-down” modes (some spans are moving up when others are moving down with a global compensation effect). The fourth one is the “up-up” mode when all spans are synchronously going up or down. This last is related to large tension variation and its shape is an offset sinusoid.

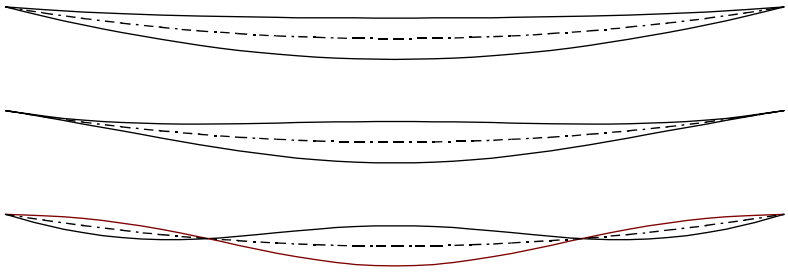

Figure 4.2: Possible forms of the pseudo-fundamental mode

4.2 Causes of galloping

Galloping is a large amplitude (several metres), low frequency (fraction of Hz), wind-induced oscillation. In the vast majority of cases, an ice accretion is present on the conductor: this has the effect of modifying the conductor's cross-sectional shape such that it becomes aerodynamically and/or aeroelastically unstable [Blevins, 1990; Den Hartog, 1932; Edwards and Madeyski, 1956; Koutselos and Tunstall, 1988; Lilien and Ponthot, 1988; Lilien and Dubois, 1988; Nakamura, 1980; Nigol and Buchan, 1981; Rawlins and Pohlman, 1988; Richardson et al., 1963; Tunstall and Koutselos, 1988].

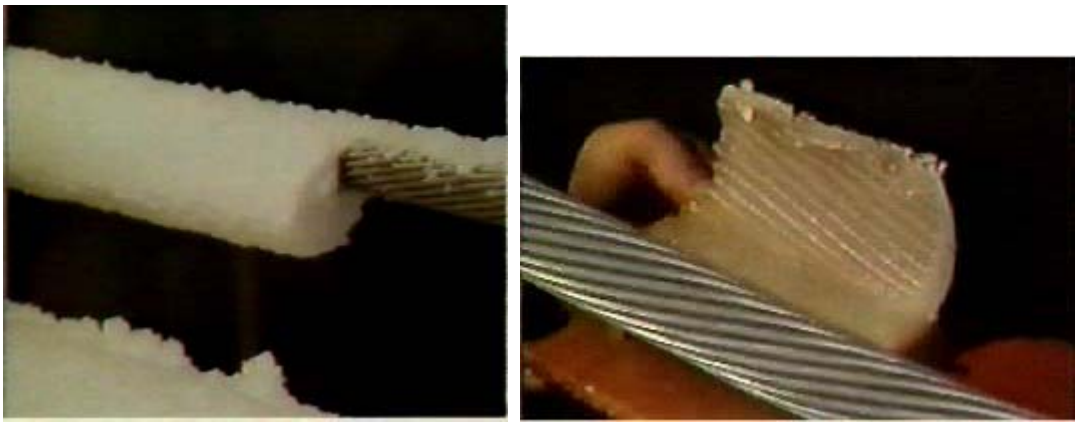

Figure 4.3: Typical ice shapes as observed on power lines, at instant close to galloping events

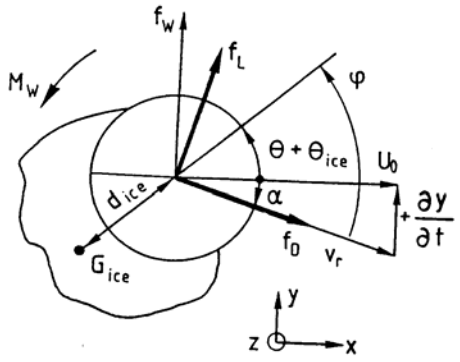

Figure 4.4: Aerodynamic forces acting on an iced conductor. U_0 is the horizontal wind velocity. Vr is the relative wind velocity taking into account conductor vertical velocity. Drag force (f_D) , lift force (f_L) and pitching moment (M_W) can thus be obtained on such asymmetric shape. Compared to v_r direction, the position of ice (its centre of gravity) is defined by φ, the angle of attack. This one is influenced by conductor rotation (torsion) and conductor vertical velocity. f_D , f_L and M_W depends on the angle of attack as detailed on equation (4.1) and shown on Figure 4.5 for a particular ice shape.

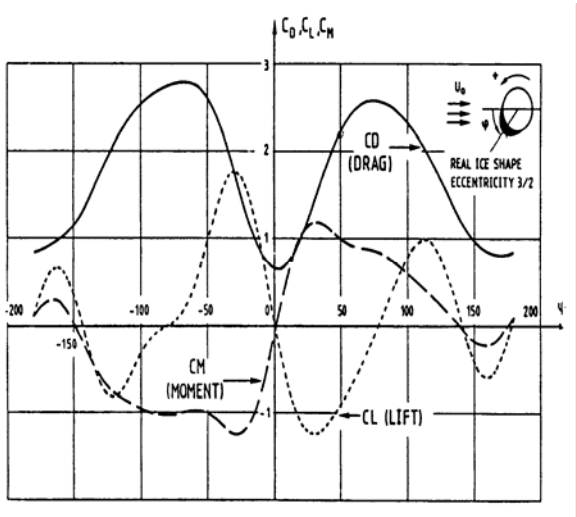

Figure 4.5: Typical aerodynamic lift, drag and moment versus angle of attack. Ice thickness 24 mm over a subconductor diameter of 32.4 mm. These coefficients are wind velocity independent in the range of galloping. (0º angle of attack when ice is facing the wind).

LIFT positive upwards; Pitching moment and angle of attack positive anti-clockwise. Zero angle when ice is facing the wind and in horizontal position. Major similarities exist between different ice thicknesses and in general for any typical shapes, but this is no more valid for very thin ice thickness. Other curves are also shown in Figures 6.27 to 6.30 in section 6.

Ice eccentricity (ε) is defined as: ε =ice thickness / (d/2) where d is the conductor diameter.

Equations (4.1) are the definition of aerodynamic drag (f_D) and lift forces (f_L) (N/m) as well as pitching moment (M_W) (N.m/m) per unit length. ρ_{air} is the air density (about 1.2 kg/m^3), v_r is the relative wind velocity (m/s) and d the conductor diameter (m) (without ice). φ is the angle of attack (abscissa of Figure 4.5).

$$\left.\begin{array}{lll} f_D = k_D v_r^2 C_D(\varphi) & f_L = k_D v_r^2 C_L(\varphi) & M_w = k_M v_r^2 C_M(\varphi) \\ k_D = \frac{1}{2}\rho_{air} d & k_M = \frac{1}{2}\rho_{air} d^2 & \end{array}\right\} \qquad (4.1)$$

As will be seen later, when the aerodynamic coefficients are such that the conductor is unstable, it may extract energy from the wind as it starts to move, allowing the amplitude of the motion to grow. The final amplitude is, of course, limited by the balance between the energy extracted and the energy dissipated during a cycle of motion.

Thus, galloping is NOT a forced oscillation, it is a self-excited phenomenon. It may (and does) occur during both 'steady' and turbulent winds. The forced response of an overhead line to the turbulence of the natural wind (buffeting), which is not galloping, also occurs in the low frequency modes of conductor spans and the identification of buffeting as compared to galloping is dealt with in Section 5.3.1. The effects of turbulence on galloping itself is discussed in Section 5.1.4.

An aerodynamic instability can arise when the aerodynamic lift and drag acting on the iced conductor, as functions of angle of attack of the wind, provide a negative aerodynamic damping. This negative aerodynamic damping generally increases in magnitude as the wind velocity increases so that, at some critical velocity, the sum of the aerodynamic damping and mechanical damping in the conductor system becomes zero. Unstable motion can then develop, usually in the vertical direction [Den Hartog, 1932].

An aeroelastic instability is much more complex and will always involve more than one type of conductor motion (degree of freedom) - typically vertical and torsional motion - whereas an aerodynamic instability may involve only one. The aeroelastic instability is only possible because of a strong interaction between the aerodynamic properties of an iced conductor, as functions of angle of attack, and the structural properties of the iced conductor system. Bundled conductor systems are particularly susceptible to aeroelastic instability because their natural frequencies in vertical, horizontal and torsional motion tend to be very close together. This is true for any number of loops and there is no easy design means available for separating them. A change in effective angle of attack of the iced conductor - induced, for example, by vertical motion - leads to changes in all three aerodynamic forces (see Figure 4.4). Because of the close proximity of the natural frequencies in a bundle, the vertical motion is then readily coupled to horizontal and torsional motion. Of these, vertical-torsional coupling is usually the most significant and can lead to some spectacular galloping of conductor bundles.

The gravitational moment provided by the eccentricity of the ice and the aerodynamic moment characteristic of an iced conductor can have a strong effect on the conductor's torsional stiffness - and, hence, torsional frequency. This can lead to a convergence of the vertical and torsional frequencies, even for single conductors where these frequencies are otherwise well separated. An aeroelastic instability may then ensue.

Galloping is NOT a forced oscillation, it is a self-excited phenomenon. It may (and do) occur, but not only, during constant wind.

The links between galloping and the two other main types of overhead line vibration - namely, aeolian vibration caused by vortex shedding and wake-induced oscillation in bundles - are very tenuous. All of these phenomena have their own physics and their own range of frequencies, galloping being associated with the lowest frequency range (typically, 0.1 to 1 Hz). Because the corresponding motion velocity of galloping is relatively low, the conversion of wind energy to conductor kinetic energy leads to the possibility of very high amplitudes. Amplitudes in excess of the conductor sag and, indeed, of 15 m peak-to-peak have been recorded.

Identification of buffeting Vs galloping has already been discussed in section 3.1.2 and the effect of wind turbulence on galloping will be discussed in section 3.1.2.

Finally, it should be noted that most theoretical studies of galloping employ wind tunnel data that have been measured for winds perpendicular to the conductor axis. The complexity of fluid flow is such that these data may not be reliably used for studies involving non-perpendicular (yawed) winds by resolving the data into components perpendicular and longitudinal to the conductor. This subject will be covered with more details in section 4.3.2.3.

4.3 Ice Forms

Galloping requires moderate to strong wind at an angle greater than about 45° to the line, a deposit of ice or rime upon the conductor lending it suitable aerodynamic characteristics, and positioning of that ice deposit (angle of attack) such as to favor aerodynamic instability. The ice, wet snow or rime deposit has to have strong adhesion to the conductor.

A classification of icing forms has been proposed in Technical Brochure No. 179, by a CIGRE working group. (CIGRE TB179, 2000). They divided icing into six different types.

Precipitation icing:

(1) Glaze, density 0.7 to 0.9, also called "blue ice", is due to freezing rain, pure solid ice, and has very strong adhesion, sometimes forms icicles, and occurs in a temperature inversion situation. Accretion temperature conditions -1°C to -5°C.

(2) Wet snow, density 0.1 to 0.85, forms various shapes dependent on wind velocity and torsional stiffness of the conductor. Depending on temperature, wet snow may easily slip off or if there is a temperature drop after accretion, it may have very strong adhesion. Accretion temperature conditions +0.5°C to +2°C.

(3) Dry snow, density 0.05 to 0.1, is a very light pack of regular snow, which is easily removed by shaking the conductor.

In-cloud icing:

(1) Glaze due to super cooled cloud/fog droplets (similar to precipitation icing).

(2) Hard rime, density 0.3 to 0.7, has a homogenous structure and forms a pennant shape against the wind on stiff objects but forms as a more or less cylindrical coating on conductors with strong adhesion.

(3) Soft rime, density 0.15 to 0.3, has a granular "cauliflower-like" structure, creating a pennant shape on any profile, with very light adhesion.

Hard rime and glaze deposits are tenacious enough, and have sufficient strength and elasticity, that galloping motions do not dislodge them.

Wind-driven wet snow may pack onto the windward sides of conductors, forming a hard, tenacious deposit with a fairly sharp leading edge. The resulting ice shape may permit galloping.

4.4 Factors influencing galloping

Without further discussion, we summarise these factors as following:

- ice accretion type and shape (eccentricity, weight, aerodynamic properties)
- wind velocity (with limited effects of turbulence and orientation as detailed)
- conductor self-damping (vertical, torsion) in the low frequency range (including span end-effects)
- span lengths (including all spans of a section) and section length
- longitudinal stiffness at attachment point on tension tower
- yoke plate assembly (tension and suspension tower) (torsional stiffness effect)
- number of subconductors and their arrangement
- subconductor spacing
- sagging conditions (effect on vertical frequencies)
- spacers (kind of spacer, location, eccentric weight effect, conductor constraint effect)
- presence of retrofit devices (all kinds including interphase methods)
- angular orientation of ice *in the presence of wind*
- ratio vertical/torsional frequency for each mode, *in the presence of wind*

Many investigations have been performed to determine the non-dimensional groups of properties relating to the above factors which provide the best candidates for a general approach to galloping [Lilien and Dubois, 1988; Lilien et al., 1989; Rawlins, 1993; Wang, 1996].

Obviously, the mechanical and aerodynamic properties of the iced conductor are very important but they are properties over which the designer can generally exercise little control, except by the use of certain devices.

The current view on which dimensionless groups of properties form the most important parameters in the analysis of galloping is presented in Table 4.1. There are four such dimensionless parameters for single conductors and five for bundles.

Table 4.1: Galloping parameters

Parameter		**Range**	
		Single conductors	**Bundles**
Vertical / torsional frequency	ω_v/ω_θ	0.1 to 0.3	0.8 to 1.2
Conductor diameter/bundle diameter	d/a	Not applicable	0.03 to 0.13
Reduced wind velocity	$V/(\omega_v.d)$	15 to 1000	15 to 1000
Reduced ice inertia	$m_{ice}.d_{ice}/(m.d)$	0.01 to 5	0.01 to 5
Conductor span parameter	12.5d/f	0.01 to 1	0.01 to 0.12

d is the conductor diameter (m), f the sag (m), a the bundle diameter (m), d_{ice} is the distance between conductor centre and ice gravity centre (m), m_{ice} is the mass of ice p.u. length (kg/m), m the mass of conductor (kg/m) and V the wind velocity (m/s). ω_v and ω_θ are the circular frequency (rad/s) of the vertical and torsional mode under analysis (without wind or ice).

The conductor span parameter can be expressed in a number of ways: for example - with a constant factor difference - it is equal to the product of the catenary parameter (T/mg) and the torsional compliance (φ/L^2). These latter parameters occur in the stability criterion deduced from the galloping equations. The constant multiplier of 12.5 has been chosen so that the parameter has a maximum value of unity.

Good candidate parameters for analysing galloping amplitude in dimensionless form are the ratio of motion amplitude to conductor diameter or, from the product of this ratio with the span parameter, the well-known ratio of motion amplitude to sag.

4.5 Incidence of galloping

4.5.1 Summary of verbal galloping reports – 1988 to 2005

4.5.1.1 INTRODUCTION

This document summarises 192 verbal reports on galloping from 28 countries over the 20 meetings of TFG since 1988. North America was by far the most active with 38 reports followed by Norway with 18 reports, Belgium with 16 reports, the UK with 15 reports, Germany (East, West and United) with 14 reports and Japan with 12 reports. Other countries with a significant number of reports included Denmark, Holland, Italy, Japan, Russia (including USSR) and Sweden. Reports of 'no activity' were regarded as important in establishing the general pattern, however, 'no activity' simply means that nothing was observed or reported, not that galloping did not occur.

4.5.1.2 COUNTRIES REPORTING AT MEETINGS

Table 4.2: Galloping verbal report summary

O = No activity to report, X = Activity to report, - = No report

Countries reporting at meetings listed	Paris 9/88	Opatija 10/89	Paris 8/90	Oslo 5/91	Paris 8/92	Montreal 9/93	Evreux 8/94	Madrid 9/95	Paris 8/96	Sendai 10/97	Avignon 8/98	Chester 4/99	Sydney 10/99	Kolding 5/00	Quebec 5/01	Krakow 4/02	Moscow 5/03	Oslo 5/04	Bilbao 4/05	Rio de Janeiro 9/05
Austria	X	-	-	-	-	-	-	-	O	-	-	-	-	O	-	-	-	-	-	O
Belgium	O	X	X	X	O	O	X	X	X	X	O	X	-	-	O	-	X	X	X	-
Brazil	-	-	-	-	-	-	-	-	-	-	-	-	-	-	-	-	-	-	X	X
Canada	X	X	X	X	X	X	X	X	X	X	X	X	-	X	X	X	X	X	X	X
Chile	-	-	-	-	-	-	-	-	-	-	-	-	-	-	X	-	-	-	-	-
China	-	-	-	-	-	-	-	X	-	-	-	-	-	-	-	-	-	-	-	-
Croatia (Yugoslavia)	X	X	X	-	O	-	-	-	-	-	X	-	-	-	-	-	-	X	-	-
Denmark	-	-	-	O	O	O	-	O	X	-	O	O	-	O	-	-	-	-	-	-
Finland	-	-	-	-	-	-	-	-	-	-	-	-	-	-	-	-	X	-	-	-
France	-	-	-	-	-	-	-	-	-	-	-	-	-	-	-	-	-	-	-	O
Germany (East&West)	X	-	X	X	X	-	X	X	X	X	X	X	X	O	-	-	O	-	X	-
Greece	-	-	O	-	-	-	-	-	-	-	-	-	-	-	-	-	-	-	-	-
Holland	O	X	O	O	O	X	-	-	X	-	O	X	-	-	-	-	-	-	-	-
Iceland	-	-	-	-	-	-	-	-	-	-	X	-	-	-	-	-	-	-	-	-
India	-	-	X	-	-	-	-	-	-	-	-	-	-	-	-	-	-	-	-	-
Iran	-	-	-	-	-	-	-	-	-	-	-	-	-	-	-	-	-	-	-	X
Italy	X	O	-	-	-	-	O	O	-	-	O	O	-	-	O	X	-	-	X	O
Japan	X	-	-	X	X	X	X	X	X	X	-	-	X	O	X	-	-	O	-	-
New Zealand	-	-	-	-	-	-	-	-	-	-	-	-	-	-	-	-	-	-	X	-
Norway	X	X	O	X	O	X	X	X	X	X	X	X	-	X	-	X	O	X	X	X
Poland	-	-	-	-	-	-	-	-	-	-	-	O	-	O	O	-	X	-	O	-
Russia (USSR)	-	O	O	-	X	-	-	-	-	-	X	X	-	X	X	X	X	X	O	-
South Africa	-	-	-	-	-	-	-	O	-	-	-	-	-	-	-	-	-	-	-	-
Spain	0	-	-	-	-	-	-	-	-	-	-	-	-	-	-	-	-	-	X	-
Sweden	-	X	O	O	-	X	X	-	X	-	-	X	-	X	O	X	-	X	-	-
Turkey	-	-	-	-	-	-	-	-	-	-	-	-	-	-	-	-	-	-	X	-
UK	X	X	O	X	O	O	-	X	O	-	O	X	-	X	X	-	-	O	O	X
USA	X	X	X	X	X	X	X	X	X	X	X	X	-	X	O	X	X	X	X	O

4.5.1.3 SUMMARY BY COUNTRY

Where a galloping technique is referred in the following summaries, further information on the technique can be found in Section 6.

4.5.1.3.1 Austria (4 Reports)

Only one incident of freezing rain galloping on twin and quad lines was reported in 1979. No control devices were fitted.

4.5.1.3.2 Belgium (14 Reports)

Despacering of bundles was introduced on twin 220 kV lines in the coldest parts of Belgium with considerable success in the 1960s and galloping became a marginal problem which affected only smaller diameter conductors on lines with small clearances.

In the 1980s, the development of the network using larger diameter conductors and twin bundle 400 kV construction saw galloping reappear as a problem on lines with and without spacers.

Twin despacered bundles with both smooth and stranded conductors galloped in freezing rain conditions. Despacered bundles had also experienced damage due to heavy icing, which was thought to impose higher loads than on the equivalent spacered bundle.

Three- and four-loop galloping with amplitudes greater than the sag had caused damage on spacered bundles and one instance of galloping on a dead-end span was reported but interest in galloping was declining in the mid 90s.

A 150 kV line galloped and a trip resulted but no damage to the line itself was found. Galloping on the earthwire of a 220 kV line in hilly terrain was observed and a Stockbridge Damper fell off, although high frequency vibration typical of earth wires was thought to be a contributory factor.

Comparative trials on twin and triple bundles with Torsional Detuning Pendulums (TDP) and Torsional Detuning Dampers (TDD) showed that both devices were more or less effective compared to reference spans. Large tension variations were recorded during galloping. In a particular test on identical phases with twin horizontal bundles, the undamped phase galloped at large amplitudes with tension variations >40 kN, the phase fitted with TDPs galloped with limited amplitudes with tension variation up to 15 kN whilst the phase fitted with TDDs experienced very little movement with tension variations up to 5 kN.

The Villeroux test station in the Ardennes saw galloping events on many different bundle configurations, some events having large tension variations. However, in 2003, it was reported that the Ardennes test station had been closed and it was becoming increasingly difficult to obtain any information on galloping events.

4.5.1.3.3 Brazil (2 Reports)

A ground wire without ice but fitted with 4 Aircraft Warning Markers at 1/8, 3/8, 5/8 and 7/8 of span length exhibited a high amplitude, low frequency galloping like motion.

4.5.1.3.4 Canada (19 Reports)

Canada has experienced a high level of galloping activity and it was noted that a ‘mild’ winter by Canadian standards tends to increase the incidence of galloping. Co-operative field evaluations with Canadian utilities have been a feature throughout the period but the quality of data returned was often of a poor quality. The development of a galloping reporting form was intended to counter this but with mixed results. There was an attempt to develop a galloping monitor but the results were not reported.

Galloping in both one- and two-loop modes was reported over the period on distribution lines and single and bundled HV lines from 120 kV to 735 kV under ice (thickness ranging from 1 mm to 12 mm) and wet snow conditions. A number of trip-outs were reported and damage has included structures, conductors and the failure of an OPGW. Wind velocities of up to 50 km/h and amplitudes up to 3 m have been recorded. In the case of a twin 315 kV line, phases were twisted together under high wind velocities, gusting up to 100 km/h, but with no damage to conductors or fittings.

A 66 kV wood pole line in the Yukon experienced low frequency motion at temperatures between -30 and -40°C with hoar frost on the conductors.

Various galloping control methods have been trialed over the period. The 'T Foil' was found to be ineffective but the TDP was tested and was generally successful, offering the opportunity to reduce vertical clearances. In one case, however, a single, unenergised AAAC fitted with TDPs galloped with 6 mm of ice whereas an untreated, energised phase did not gallop. A 154 kV line fitted with flexible interphase spacers attached with AGS clamps galloped but no damage was recorded.

As in other countries, interest in galloping has waxed and waned over the period but in 2005, a project to produce a 'Design Guide to Control Galloping of Transmission Line Conductors' was announced.

4.5.1.3.5 Chile (1 Report)

A 230 kV single conductor line at 4000 m altitude in a mountainous area in Chile had galloped. The line was in service for less than one year and heavy icing conditions were experienced. No further data was available.

4.5.1.3.6 China (1 Report)

Extensive galloping and consequential damage was reported in the north and north east of China and a triple bundle, river crossing galloped with the failure of conductors and spacers and damage to suspension insulators. Control devices included spacer-mounted TDP.

No further reports were received but China seems to be an untapped source of experience.

4.5.1.3.7 Croatia {Yugoslavia} (6 Reports)

There was considerable pre-war interest in galloping in Yugoslavia and galloping with amplitudes up to 8 m peak-to-peak on a 400 kV twin line caused trip-outs and line collapse. This resulted in a trial site of one 300 m span of the operating line being equipped with various control devices including standard spacers, rotating clamp spacers, hoop spacers, Air Flow Spoilers (AFS), TDP and despacering. Activity was monitored by tension variation measurements.

Tentative results suggested that the despaced phase was least active whilst the rotating clamp spacers also performed well. The hoop spacers failed due to embrittlement of the plastic at high voltages and were replaced with TDPs.

Two galloping events were reported during the earlier period when 3 m peak-to-peak amplitudes were observed with 10 mm of radial ice and wind velocities of 25 m/s. No damage resulted.

After the break up of Yugoslavia, only one unquantified report of galloping was received. However, 7 to 8 Croatian lines were reported as having collapsed due to ice overload.

4.5.1.3.8 Denmark (8 Reports)

Early on in the period covered, it was reported that about 20% of line outages in Denmark were thought to be due to galloping but subsequently, a series of mild winters resulted in no reports of galloping. T2 conductor was strung, with some installation difficulties but no galloping was reported on the section of line involved.

One exception was the winter of 1995 when galloping resulted in a series of twin bundle trips, a broken insulator string, tower and spacer damage. Horizontal galloping, previously only observed in Holland and Japan, was also experienced. Horizontal galloping was also reported back in the 1970s by Mr. R. Brand of the (then) W. German utility PREAG.

4.5.1.3.9 Finland (1 Report)

The first report from Finland was received in 2003 and covered the galloping of an earthwire fitted with warning markers, which were thought to be a contributory factor. It was also reported that five spans of a 110 kV line were fitted with two interphase spacers/span.

4.5.1.3.10 France (1 Report)

No reports of galloping were received.

4.5.1.3.11 Germany {West & East) (14 Reports)

Reports suggested that many German lines were prone to galloping over the period and in 1999, for example, it was reported that forty-six lines had been affected by galloping with six cases of conductor damage.

Horizontal twin bundles on 220 kV lines experienced several galloping events over the period, including the 400 m span of the Buren test site, which galloped during a snowstorm. There was an observation of multiple-loop, ice-induced galloping on a twin bundle line with wind velocities of 12 to 14 m/s. Vertical twin bundles also galloped but there were fewer reports.

Activity on 400 kV quad bundles was also reported, with twenty-six events on one occasion in 1993/94 under snow and rain conditions at -1°C. On other occasions, one quad bundle galloped at 13 m peak-to-peak with ice and a wind velocity of 20 m/s whilst a 400 m quad span galloped at -5°C in an 8-loop mode with amplitude of 2.5 m peak-to-peak. Limited activity was also reported on triple bundles and single conductors.

In 1997, a triple circuit line fitted with two quad 380 kV circuits on the upper crossarms, each in a triangular configuration, and one twin 230 kV circuit on the lowest crossarm, experienced ice galloping- related trips. Horizontal interphase spacers were fitted on one of the quad circuits between the two lower bundles and this circuit did not gallop whereas the others did.

Six thousand porcelain interphase spacers were installed in eastern Germany, with some failures on twin and triple bundles in 1994. There was one reported event in western Germany of galloping of a line fitted with interphase spacers. A 600 m span of a quad line galloped and experienced subspan oscillation under freezing rain conditions whilst the other circuit fitted with interphase spacers was unaffected.

The availability of dedicated observers probably accounted for the high number of incidents reported although towards the end of the period, personnel changes led to a reduction of reports.

4.5.1.3.12 Greece (1 Report)

No activity reported

4.5.1.3.13 Holland (9 Reports)

As with other countries, a series of mild winters and no activity led to a decline of interest in galloping over the period. Galloping events on single conductors, twin bundle lines and earthwires were noted early in the period and in one case, a nylon rope wrapped on a 34 mm single conductor successfully mitigated galloping.

In 1992/3, attempts to predict galloping risk and to carry out a fatigue test at galloping loads on suspension clamps and conductors were mooted. It was also suggested that a new 400 kV line would be designed with larger clearances and antigalloping devices but nothing more was subsequently reported on any of these initiatives.

The worst galloping event was reported in 1996 when a twin circuit quad bundle line near the sea galloped with 2 to 3 mm of radial ice and wind velocities of 6 to 8 m/s. This was the first reported instance of such galloping and resulted in a dead-end failure due to the brittle fracture of a linkage. The cost of the incident was said to be $1 million.

Later in the period, a twin bundle galloped horizontally at 4 m peak-to-peak under wet snow and thin ice conditions and a wind velocity of 15 to 18 m/s at 45° to the line direction. Span lengths were 270 to 340 m.

4.5.1.3.14 Iceland (1 Report)

One galloping event was reported in 1998 but no details were available.

4.5.1.3.15 India (1 Report)

One event of galloping near New Delhi was reported in 1990 but no further information was available.

4.5.1.3.16 Iran (1 Report)

It was reported that seven regional electricity companies in Iran have experienced galloping, which appears to be fairly widespread. Between 20% and 30% of single conductor 63 kV lines in three companies were said to have galloped, including spans of 250 m and above. Similar percentages of bundle conductor lines at 132 kV, 230 kV and 400 kV have experienced galloping in five of the companies. Although 'severe load conditions' were reported, it is not known if any failures occurred. It is thought that some of the galloping incidents may, in fact, be ice shedding. Preventative solutions have included decreasing span lengths and increasing middle crossarm lengths to increase interphase clearances. Interphase spacers have been used where ice load and ice shedding is a problem.

4.5.1.3.17 Italy (10 Reports)

In 1988, it was reported that twin and triple bundle lines had experienced frequent outages and inter-bundle twisting. 40 km of the twin bundle and 20 km of the triple bundle were fitted with TDPs and no further outages were reported over the period, indicating that the TDPs appeared to be effective.

A 130 kV single conductor line galloped in the South of Italy and a tower collapsed but this was due to ice load rather than galloping.

In 2002, six galloping events were reported on other twin and triple bundle lines at four locations around Italy. TDPs were fitted at two locations with designs based on 6 mm of ice and single loop galloping. No galloping was subsequently reported and more data was being sought.

4.5.1.3.18 Japan (12 Reports)

Over the period, galloping activity was high and was regarded as a serious problem in Japan. There was considerable interest in monitoring and anti-galloping devices. The Tsurga test station was set up in an area prone to rime icing with devices to monitor galloping by torsional conductor movements and tension changes.

Early in the period, a single conductor 66 kV line galloped due to asymmetrical snow profiles caused by weights fitted to prevent conductor rotation during wet snow accretion. Midspan flashovers were noted and three interphase spacers were subsequently installed.

Galloping events were reported regularly throughout the period on quad lines with wet snow. In one case, flashover occurred on a 275 kV line on a 500 m span with a 13.5 m interphase clearance and in another, a 6-conductor bundle line galloped.

Eccentric weight control devices were generally successful in preventing galloping. Interphase spacers were also used but in one event, a 154 kV line fitted with interphase spacers experienced two-loop galloping and flashover on a dead-end span. There was also a report of a broken interphase spacer on a single conductor line.

4.5.1.3.19 New Zealand (1 Report)

One galloping event was reported but no details were forthcoming.

4.5.1.3.20 Norway (18 Reports)

Norway experienced a lot of galloping activity over the period and interest remained high. Lines running N/S along the coast and at high altitudes in the mountains experienced several events and damage. In 1993, it was reported that serious failures in the Norwegian grid system had been experienced due to ice galloping.

Single conductors, twin and triple bundles and earthwires at voltages from 132 kV to 420 kV were all affected and amplitudes up to 10-15 m peak-to-peak were reported. Damage included burned and broken earthwires at suspension clamps, broken conductors and damaged structures. In one case, a large single conductor replaced a twin bundle but twelve failures were experienced in one month alone in 1997. Interphase spacers were subsequently installed.

The most widely used control method is interphase spacers in both horizontal and vertical modes. These have been broadly successful but in 2002, damaged interphase spacers were found where the bolt connecting the insulating member to the clamp had broken.

TDPs were also used on a much smaller scale with some good results. In one case, a single 56 mm conductor in a 210 m span had galloped up to 15 m peak-to-peak. A remote camera based monitoring system was installed and TDPs fitted. In one event, TDPs reduced galloping by a factor of four, in another reduced the amplitude to zero but galloped in a third event whilst the untreated span was quiet.

One unusual case of a hollow, laminated wood 'H' frame structure vibrating severely with consequential damage to the phases was reported in 1991. In 2005, it was reported that a corona ring had been pushed to the top of an insulator by galloping.

A remote test site on a mountaintop experiencing high winds and ice up to 120 kg/m operated for several years but was closed in 2002 due to budgetary restraints.

Ground wires were also removed from galloping prone lines.

Broken ground wires were reported on a 420 kV line but may be due to ice load rather than galloping.

4.5.1.3.21 Poland (5 Reports)

Ice shedding was reported in 2003 but no further information was available.

4.5.1.3.22 Russia {USSR} (11 Reports)

In the period under review, reports from Russia started around 1998 and it soon became apparent that galloping was widespread and often severe.

In 1998, the collapse of a tower on 1000 kV 8-conductor bundle line was reported but no other information was available. The failure of a splice due to an earthwire galloping at about 1.5 to 2 m peak-to-peak was also reported.

Following the galloping of a 150 kV line in Siberia, reporting forms were distributed to utilities in an attempt to gather historical data.

Later reports covered the rime ice and freezing rain galloping of a 500 kV triple bundle line with span lengths of 380 m to 420 m at – 40°C to – 50°C in NW Siberia. One, two- and three-loop galloping was observed at wind velocities from 3 m/s to 8 m/s and insulator strings broke and the installation of TDDs was under consideration.

The galloping of a 220 kV with 50 mm of ice and wet snow resulted in conductor breakages and tower collapses over a 10 km section whilst in the Crimea, a 330 kV twin bundle line galloped with 50 mm of ice and up to 40 km experienced flashovers, broken insulators and conductors and tower collapses. In the last case, the use of ice melting techniques resulted in further flashovers due to phase 'bounce' as ice was shed.

Solutions are being sought.

4.5.1.3.23 South Africa (1 Report)

No galloping activity was observed.

4.5.1.3.24 Spain (2 Reports)

No reports of galloping were received. In 2005, it was reported that a line in a mountainous area at 600 m above sea level experienced the cascade collapse of 12 towers with ice accretions of up to 200 mm.

4.5.1.3.25 Sweden (11 Reports)

Sweden has experienced some galloping activity over the period, including the non-ice galloping of a 'figure of eight' optical fibre cable.

Freezing rain was said to be predominant in galloping events although one instance of wet snow galloping was reported on a 20 kV wood pole line with a 20 mm dia conductor on post insulators. The wind velocity was 15 m/s and three spans were affected with flashovers and an outage. Another 20 kV line experienced a broken seven-strand Aldrey conductor near a hand bind and it was thought that aeolian vibration might have been a contributory factor.

Other reports included that of a two day outage due to freezing rain galloping and outages due to the galloping of 132 kV and 400 kV lines. A 10 kV line with spans of 80 to 100 m on wooden poles with a triangular arrangement of 62 mm² conductors galloped with outages being reported.

The use of control methods were not widely reported but rotating clamp spacers were said to be effective under wet snow conditions but poor under freezing rain conditions.

4.5.1.3.26 Turkey (1 Report)

The first incidence of galloping was reported in 2005. A double circuit triple bundle line of Cardinal conductors at 470 mm spacing galloped in a two-loop mode in a 300 m span between two tension towers. The temperature was close to 0°C with wet snow and a strong perpendicular wind.

4.5.1.3.27 United Kingdom (15 Reports)

As in other countries, interest in galloping in the UK has declined over the period with milder winters and fewer resources being devoted to the problem by the utilities.

Early on in the period, a twin bundle line experienced wet snow galloping and AFS were installed on one circuit. A 400 kV quad bundle line experienced severe wet snow galloping with wind velocities of 30 to 40 m/s. Detuning pendulums were fitted based on North American experience but 20 flashovers were experienced in four hours and burn marks were evident on the conductors of the treated spans. A further event was reported in 1996 on a twin line of Zebra ACSR and Rubus AAAC when freezing rain galloping occurred for two and a half hours. The AAAC was damaged due to flashovers.

Experience with offset despaced twin bundles was generally good and such a line was quiet whilst a parallel quad line galloped with 15 to 24 mm of snow and winds of 20 m/s. However, bundle collapse was experienced on one despaced bundle due to a high current load so metallic hoop spacers were proposed as a solution.

AFS were used on UK distribution lines with success and an EHV version was developed for Norwegian trials.

Interphase spacers and TDDs had been installed in Scotland over the period but no reports were received regarding their performance. In the case of the TDDs, however, 30 incidents were reported in the year prior to their installation but no faults have been recorded since then.

4.5.1.3.28 USA (19 Reports)

Early in the period, a twin circuit triple bundle line in the Rockies experienced wet snow galloping. It was planned to install interphase spacers and TDPs, leaving one circuit untreated. Estimates of galloping were to be made using aluminium deflection indicators fitted on top of the insulator strings.

Over the period, a number of galloping events were reported associated with wet snow and ice storms. In the early 90s, a single conductor line on wooden 'A' frames galloped whilst a twin circuit line failed under wet snow galloping in Colorado and severe ice storms in NY state caused tower failures and protracted outages with up to 8 mm of radial ice. In a later event, a single conductor failed at the suspension clamp due to galloping.

In one case in 1992, a cascade failure of a line with flexible towers was thought to be due to galloping whilst in another in 1993, wide spread failure of distribution lines in the SE was associated with snow storms.

The use of 'T2' conductor and AFS increased over the period with good results. Two galloping events were reported on 'T2' conductor under heavy icing conditions and it was thought that the ice had 'swamped' the conductor's profile. In another case, a self-damping conductor galloped.

Three instances of galloping on a river crossing were reported. In 2004, a 220 kV twin bundle river crossing that had galloped in 1989, galloped again, resulting in a 48-hour outage. TDPs are to be installed. A galloping event in Texas was also reported.

In general, after 'liberalisation' of the US supply industry, galloping was not regarded as being very important and there was a subsequent lack of information although the demand for anti-galloping devices remains strong.

4.5.2 Detailed galloping observation summaries

Very few countries have well-informed staff available for the collection of detailed galloping information: thus, most galloping events go undetected or unreported. The following paragraphs, however, relate to a few exceptions where extensive collations of galloping data have been made.

Mr. C. Jürdens, a TFG member from Germany, actively pursued the collection and collation of galloping data on the German network over a 20-year period and provided the extensive information shown in Figures 4.6 to 4.8. These galloping events cover 110 kV (12 events), 220 kV (17 events) and 380 kV (17 events). Nine cases involved single conductor lines, 22 involved twin bundle lines and 16 quad bundle lines. All are Al/St conductors with a cross-section ranging from 185 to 340 mm². Most of the cases caused a short-circuit, implying that the galloping amplitudes were quite high. In four cases, permanent bundle collapse was sustained, caused by large torsional movement.

Japan's utilities have also provided interesting and detailed information, as shown in Figures 4.9 to 4.17. Table 4.3 lists the investigation period for each utility, which, in one case covers 30 years. A total of 776 cases of galloping were observed in Japan during these investigation periods: the locations of these events are shown in Figure 4.9. The subsequent figures show the number of incidents according to line voltage, conductor size, type of bundle, span length, altitude, wind velocity and wind angle to the line. These incidents have also been classified by ice shape and ice location on the conductor (table 4.4).

Another impressive set of data aimed mainly at establishing galloping amplitudes on conductors with or without anti-galloping devices has been collected in Canada and USA [Havard, 1996]. Those results are shown in section 6.2.1, entitled design against galloping.

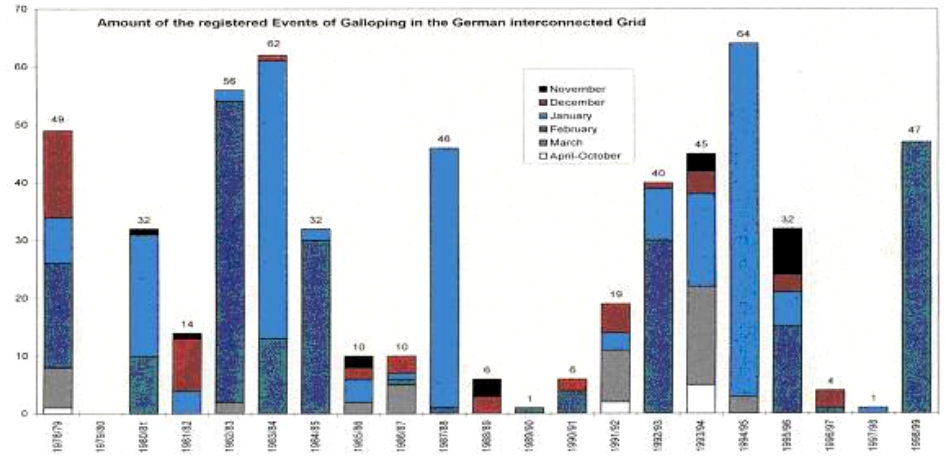

Figure 4.6: Number of recorded events of galloping on the German interconnected grid during 20 years (1979-1999) (Courtesy C. Jürdens)

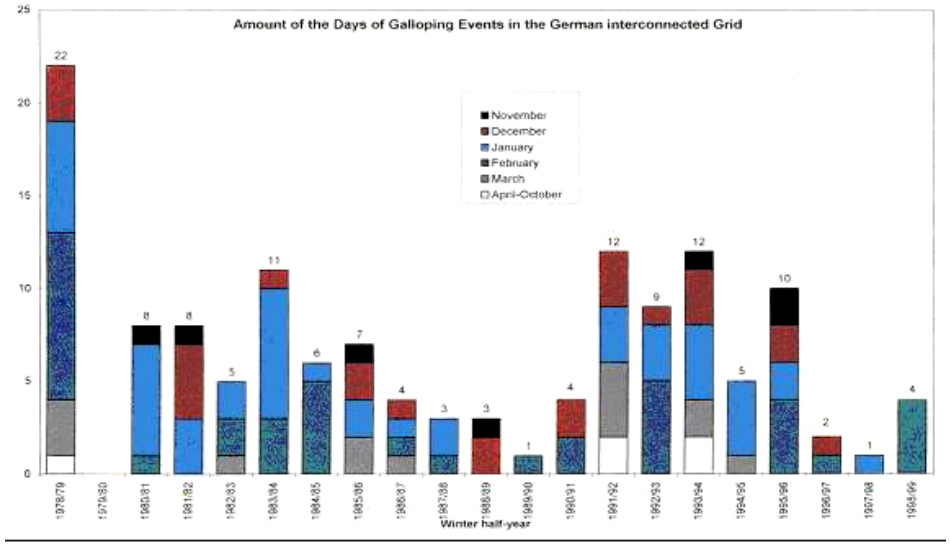

Figure 4.7: Number of days with galloping events in the German Interconnected grid during 20 years (1979-1999) (Courtesy C. Jürdens)

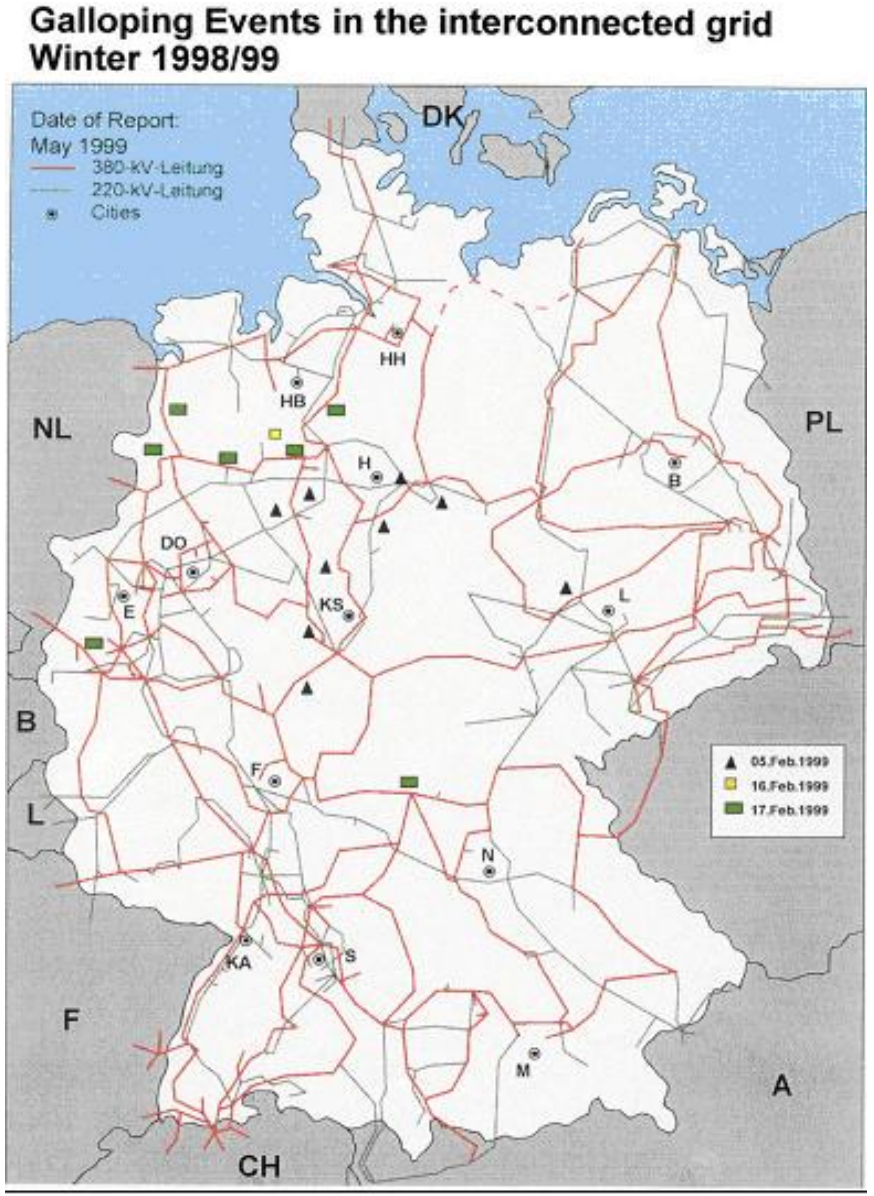

Figure 4.8: Locations of galloping events in Germany during winter 1998-1999 (courtesy C. Jürdens)

Table 4.3: Investigation period of Japan utilities

Name of utility	Investigation period
Hokkaido	1970 ~ 2000
Tohoku	1989 ~ 2000
Tokyo	1986 ~ 2000
Chubu	1993 ~ 2000
Hokuriku	1993 ~ 2000
Kansai	1972 ~ 2000
Chugoku	1986 ~ 2000
Shikoku	1977 ~ 2000
EPDC	1989 ~ 2000

Figure 4.9: Locations of galloping events in Japan

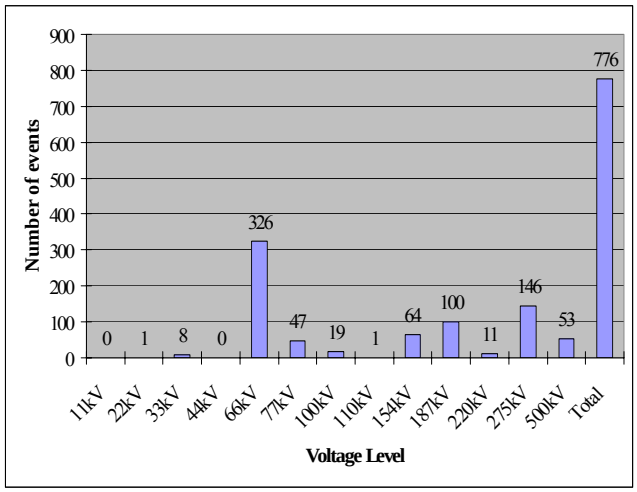

Figure 4.10: Number of galloping events vs voltage level in Japan

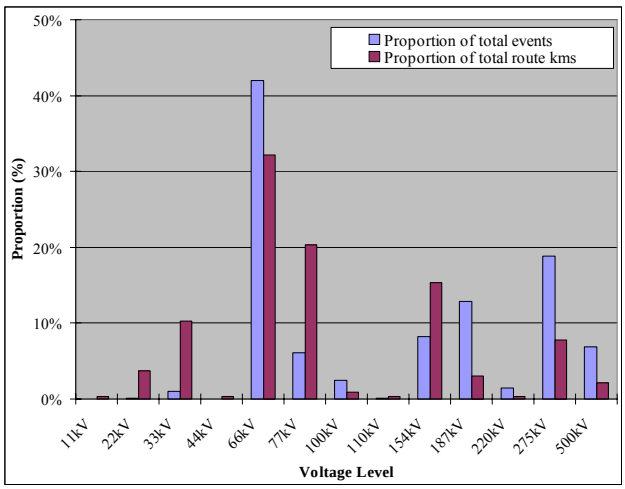

Figure 4.11: Incidental ratio and route length ratio vs voltage level in Japan

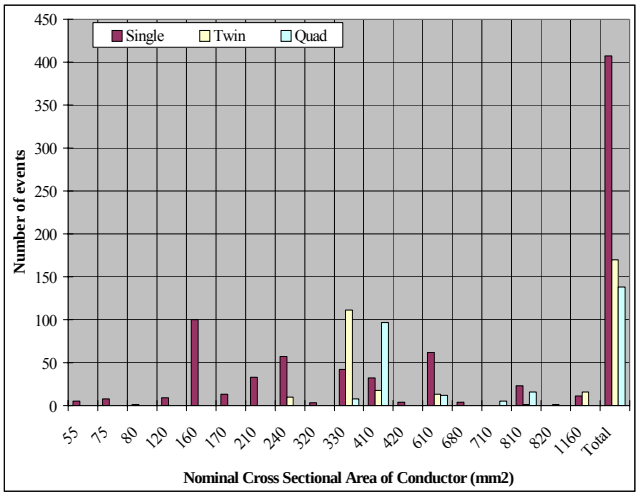

Figure 4.12: Number of galloping events vs conductor size and number in Japan

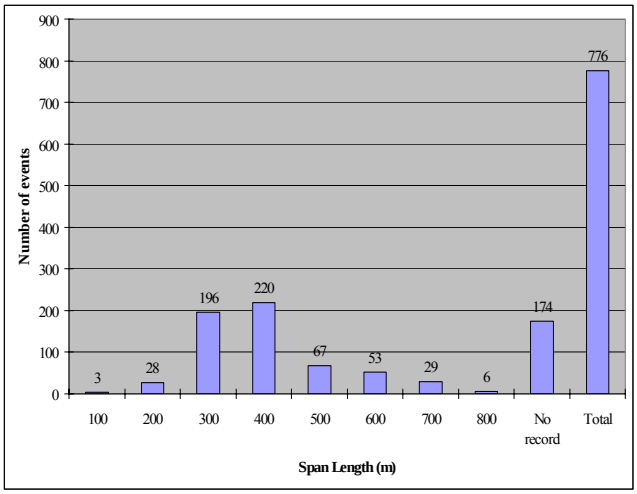

Figure 4.13: Number of galloping events vs span length in Japan

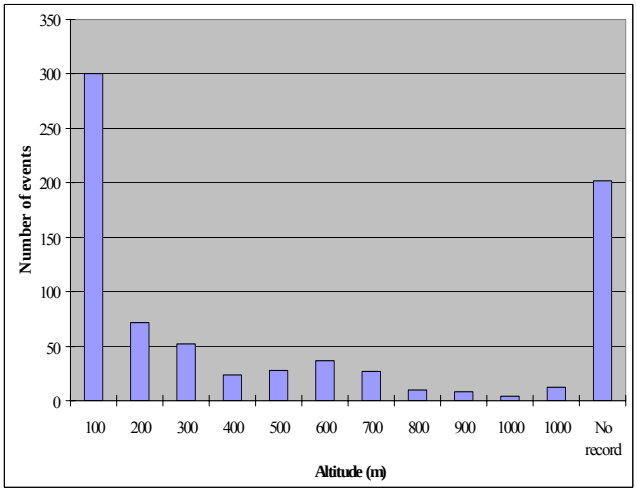

Figure 4.14: Number of galloping events vs altitude in Japan

In Figure 4.15 to Figure 4.17, the legend refers to the source of the quoted meteorological data as follows:

The Field: Measured on site during galloping observations.

Nearest Tower: Collected from nearest tower equipped with a meteorological data acquisition system (DAS).

Utility's Facility: Collected from nearest Company building equipped with a meteorological DAS.

AMeDAS: Collected from nearest Automated Meteorological DAS (AMeDAS) operated by the Japan Meteorological Agency (on average, every 17 km throughout Japan).

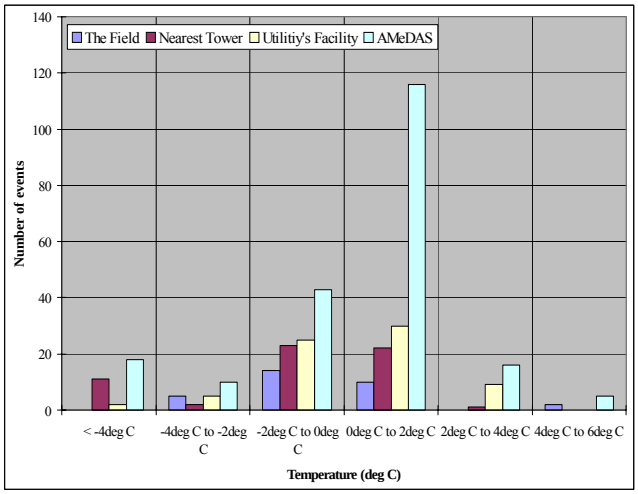

Figure 4.15: Number of galloping events vs temperature in Japan

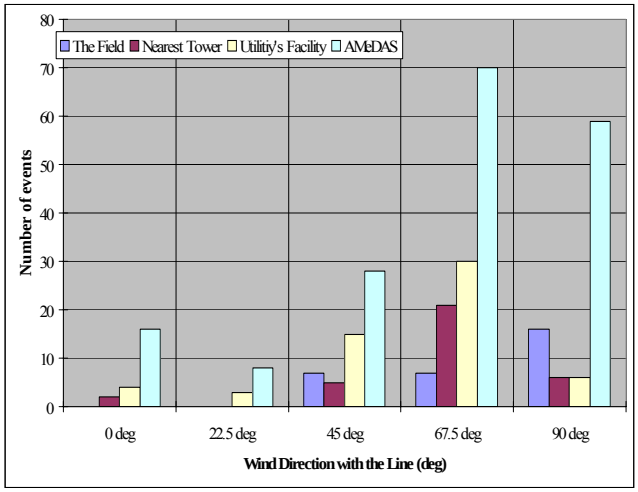

Figure 4.16: Number of galloping events vs wind direction in Japan

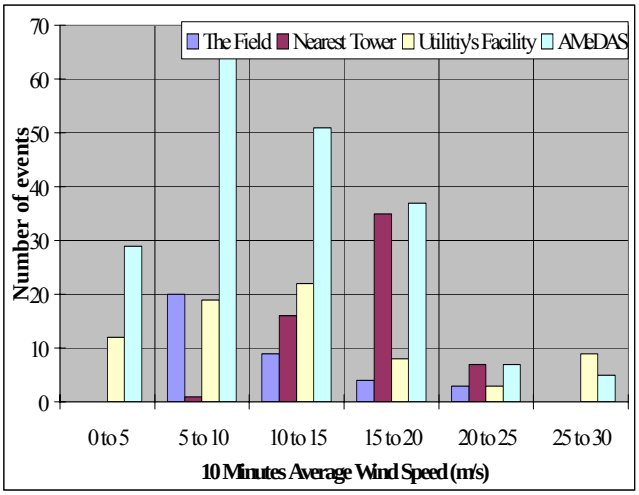

Figure 4.17: Number of galloping events vs wind velocity in Japan

In 124 cases of ice accretions on conductors, the thickness, shape and windward/leeward orientation of the accretion was recorded. The corresponding data are presented in Table 4.4.

Table 4.4: Number of icing events for each accretion category (courtesy M. Masataka)

Shape	Thickness of ice / conductor diameter							
	0 ~ 0.5		0.5 ~ 1.0		1.0 ~ 2.0		2.0 ~	
	windward	leeward	windward	leeward	windward	leeward	windward	leeward
Triangle	9	10	8	3	1	0	0	0
Triangle with tip round	3	1	34	2	4	0	0	12
Crescent	23	0	1	0	1	0	0	0
Others	7		0		1		4	

5. Galloping mechanisms, amplitude and resulting loads on towers

5.1 Mechanisms of galloping

5.1.1 Basic physics of galloping on overhead lines

A body immersed in a moving fluid experiences lift and drag forces which act through a point in the body known as the aerodynamic centre. In general, this will not be the same point as the centre of gravity and, a priori, its position will not be known [Binder, 1962; Blevins, 1990; Davison, 1939]. As the movement of the body in response to the fluid flow is restricted by the boundary conditions - for example, a conductor tensioned between towers - it is generally more convenient to consider the forces and moments acting at a known location, typically the shear centre in the case of a conductor. This requires the introduction of an aerodynamic pitching moment about the new location. The evaluation of lift, drag and pitching moment is usually done in a wind tunnel on a fixed, rigid cylinder on which the ice shape has been reproduced [Bokaian and Geoola, 1982; Chabart and Lilien, 1998; Koutselos and Tunstall, 1986; Koutselos and Tunstall, 1988; Nakamura, 1980]. However, there is still some concern about the evaluation of such forces and moments on a fixed wind tunnel model (quasi-steady approach) rather than a moving one. The quasi-steady hypothesis will be discussed later and its limitations clearly pointed out. All existing simulation models are based on the quasi-steady approach.

For the sake of simplicity, we will discuss only pure vertical + torsion movement. No horizontal movement is taken into account.

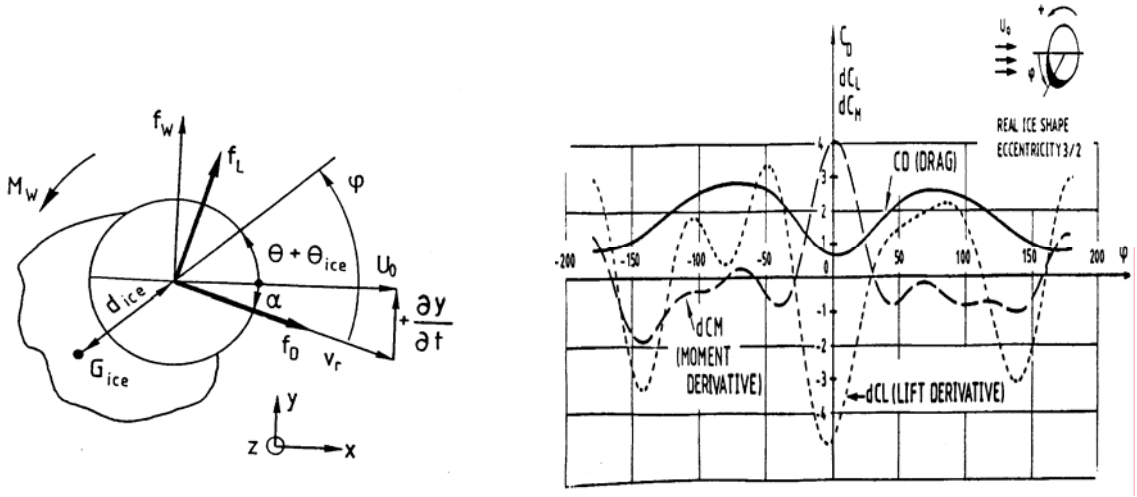

Figure 5.1: Aerodynamic Characteristics of an Iced Conductor

On the left in Figure 5.1 is shown a representation of the cross-section of an iced conductor as already shown in Chapter 4. The conductor, subject to a wind, U_0, is shown at a time, t, during vertical+torsional motion. Aerodynamic forces, f_L, and f_D, and moment, M_W, act at the shear centre. The conductor is assumed to move vertically upwards with a positive vertical speed. The initial ice position is Θ_{ice} and Θ is the actual rotation of the conductor; φ is the so-called 'angle of attack' and is positive anticlockwise. The drag force, f_D, is oriented in the direction of the relative wind speed, v_r (the combination of U_0 and the conductor's vertical speed). The lift force, f_L, is perpendicular to the drag force and positive upwards. The pitching moment is positive anticlockwise.

On the right in Figure 5.1 are shown the drag and derivatives with respect to φ of the lift and pitching moment for an assumed ice shape. The regions where the lift curve derivative crosses the drag curve are regions of possible Den Hartog instability (see just after, eq 5.9). It is remarkable that a small variation in the ice shape leading to a slightly asymmetric lift curve results in a Den Hartog instability region around -50º but not at +50º.

$$\left.\begin{aligned} f_D = k_D v_r^2 C_D(\varphi) \qquad f_L = k_D v_r^2 C_L(\varphi) \qquad M_w = k_M v_r^2 C_M(\varphi) \\ k_D = \frac{1}{2}\rho_{air} d \qquad\qquad k_M = \frac{1}{2}\rho_{air} d^2 \end{aligned}\right\} \qquad (5.1)$$

The lift (f_L) and drag (f_D) force per unit length (N/m) and pitching moment (M_W) per unit length (N.m/m) are given by the equations (5.1), where ρ_{air} is the air density at the corresponding altitude and temperature (about 1.2 kg/m^3) and d the conductor diameter (without ice). C_D as well as C_L and C_M derivatives are given by the measured values as shown in Figure 5.1 evaluated during wind tunnel testing.

To evaluate possible instabilities, the vertical force acting on the (moving vertically and torsionaly) conductor is calculated as follows (noting that α is negative):

$$f_w = f_L \cos\alpha + f_D \sin\alpha \qquad (5.2)$$

Where f_L is the lift force (proportional to the lift coefficient C_L given in Figure 4.4 (chapter 4) and depending on the angle of attack φ, as shown in equation 5.1) and f_D is the drag force (idem):

$$\varphi = \vartheta_0 + \vartheta - \alpha \qquad (5.3)$$

where

φ = total angle of attack to consider

θ_0 = initial ice position on the conductor (ice accretion angle)

θ = extra rotational component of the conductor (or the bundle) due to acting forces (pitching moment, inverse pendulum effect, inertial effect) in the dynamic movement

α = the part of the angle of attack which is due to vertical movement

Instability occurs in a vertical movement if a perturbation in vertical movement (thus creating a vertical speed) would see a change in applied force which would amplify the movement. For example, a positive vertical speed would generate an increase of vertical net force in the same direction, in other terms:

$\Delta f_w > 0$ unstable (5.4)

$\Delta f_w < 0$ stable (5.5)

To establish the variation of the force, we will make the simplified hypothesis that the drag coefficient is constant and also note that the angle α is very small.

$$\Delta f_w = \Delta f_L + f_D \Delta\alpha \qquad \Delta\alpha = -\frac{\Delta\dot{y}}{U_0} \qquad (5.6)$$

$$\Delta f_L = k_D \frac{\partial C_L}{\partial \varphi} \Delta\varphi = k_D \frac{\partial C_L}{\partial \varphi} (\Delta\vartheta - \Delta\alpha) \qquad (5.7)$$

$$\Delta f_w = k_D \left[C_D \Delta\alpha + \frac{\partial C_L}{\partial \varphi} (\Delta\vartheta - \Delta\alpha) \right] \qquad (5.8)$$

So that instability criteria are easy to predict, noting that Δα is negative for an upward movement, it depends on the torsion behaviour. Two cases have to be considered.

5.1.1.1 Case 1: no torsion (infinitely rigid)

$$\Delta\vartheta = 0 \rightarrow C_D - {\partial C_L}/{\partial \varphi} > 0 \text{ (also noted } C_D - C_{L\alpha} > 0) \rightarrow \text{The system is stable}$$

$$\Delta\vartheta = 0 \rightarrow C_D - {\partial C_L}/{\partial \varphi} < 0 \text{ (also noted } C_D - C_{L\alpha} < 0) \rightarrow \text{The system is unstable} \qquad (5.9)$$

Therefore the system may be unstable only for $C_{L\alpha} > 0$ and larger than C_D. This is the classical Den Hartog criterion [Den Hartog, 1932]. The unstable range of attack may be derived from Figure 5.1 (right), drawn with lift derivative: It may occur when the C_D curve crosses the $C_{L\alpha}$ curve (dotted line). Thus, only one narrow zone around -50º and another one around 180º may be unstable according to the Den Hartog criterion.

That criterion (equation 5.9) is often presented with a "+" instead of a "-". That is simply because of the sign convention chosen for clockwise or anti-clockwize angle of attack.

This criterion does not take into account conductor torsion. But, as we know, the torsion on overhead line conductors cannot be assumed to be null, in fact a several hundred of metres beam with a diameter of a few centimetre is obviously not rigid in torsion. A lot of investigation have been done in the literature on the subject, mainly by Nigol&Havard [Nigol and Clarke, 1974; Nigol et al., 1977; Nigol and Buchan, 1981] and Lilien&Wang [Lilien et al., 1989; Lilien et al., 1994; Wang and Lilien, 1998a], which covered, both single and bundle conductors.

For bundle conductors, the torsional stiffness depends on the mechanical tension in the subconductors and the spacing in the bundle as well as the number of subconductors and the spacers used. Bundle conductor torsional stiffness (several thousand of $N.m^2$) are two orders of amplitude larger than that of single conductor (a tenths to some hundreds of $N.m^2$). However, bundles have a resonance between vertical and torsional mode, which is not there for single conductors where the frequency ratio is about 3 to 10 (the torsional frequency being higher than the vertical one). This induces a completely different behaviour but in both cases, torsion during dynamic movement is easy to obtain.

Thus, a second case has to be considered; the most frequent one.

5.1.1.2 Case 2: torsion occurs

$$\Delta\vartheta \neq 0 \qquad (5.10)$$

→In presence of torsion, at least two cases must be considered:

5.1.1.2.1 $\Delta\vartheta$ in phase with vertical velocity (the case of single conductor)

$\Delta\theta = -\kappa.\Delta\alpha$

The criterion does not change compared to the Den Hartog criterion but the derivative of lift is increased by the coupling.

$C_D - C_{L\alpha}.(\kappa + 1) \leq 0$ The system is unstable

As above, for torsion to be in phase with velocity requires a forced movement with no inertial effects. This would need a large difference between vertical and torsional frequencies, which will be possible only for single conductors with very thin ice deposit.

5.1.1.2.2 $\Delta\vartheta$ in opposite phase with vertical velocity (may be one particular case of bundles)

The criterion is completely modified. Instability may occur even if $\partial C_L < 0$, but non only. In this case the phase shift (vertical/torsion) play an important role, this last being strongly related to torsional damping and the proximity of resonance. This last case is called "coupled flutter" or simply "flutter" galloping for electrical engineering.

This expands the range of instabilities to include *completely different mechanisms, as the derivative of lift no longer needs to be negative as is the case for the Den-Hartog instability criterion.*

These galloping cases are considered as "aeroelastic" (and not aerodynamic) as structural data (like the ratio vertical/torsional frequencies, inertial effect, torsional stiffness, damping) may interact strongly in the phenomenon. Not only aerodynamic properties (= lift, drag and moment aerodynamic curves) are important but also structural data play a major role.

Of course, many other situations are also possible (torsion not in phase with vertical velocity).

5.1.1.3 Discussion

We may complexify easily these developments by introducing horizontal movement, limit cycle frequency (which is close to the vertical one but not equal), etc. This can be managed by computer but experts have not found significant discrepancies with the theory explained above. Some new kind of instabilities (horizontal/torsion) may occur but the physics remain similar.

If both kind of instabilities (Den Hartog and flutter type galloping) are theoretically possible, very few ice shapes can produce Den Hartog instabilities. There are many discussions in the literature [Chabart and Lilien, 1998; Chadha, 1974a and 1974b; Davison, 1939; Den Hartog, 1932; Diana et al., 1991; Dubois et al., 1991; Edwards and Madeyski, 1956; Hunt and Richard, 1969; Keutgen, 1999; Lilien and Dubois, 1988; Nakamura, 1980; Nigol and Buchan, 1981; Novak, 1972; Otsuki and Kajita, 1975; Ottens, 1980; Parkinson, 1971; Richardson, 1979; Richardson et al., 1963; Wang, 1996] about that, especially a great concern about the liability of test performed with artificial D shape, which are easily unstable on the Den Hartog principle, but which are not at all close to any observed kind of ice shape. The few ice shapes producing aerodynamic properties in agreement with Den Hartog are some very thin ones [Chadha, 1974; Tunstall and Koutselos, 1988] (a very few mm thickness), such cases are unstable in a very narrow range of angle of attack (near zero °) which would lead to limited amplitudes, but increasing linearly with the wind speed (using a simplified approach).

There is another case of Den Hartog galloping possible on any arrangement: angle of attack close to 180° (see Figure 5.1, 6.28 and 6.29). It means that the wind would have to reverse its direction between the icing period and the galloping period which occurs seldom even if few cases have been recorded in the literature.

Bundle conductor configurations have a natural collapse of vertical and torsional frequencies as explained in the literature [Lilien and Dubois, 1988], a collapse which depends on wind speed and ice position. Such arrangements are obviously more prone to gallop under the second type of instability (flutter type).

Nevertheless there are still some concerns on single conductor. Some experts (i) would enhance the fact that torsional frequency (about 3 to 8 times the vertical frequency without wind or ice) may drop to resonance due to ice and wind. Some others (ii) do not agree with such theory which supposes that ice shape remains on the same position, independently of the wind speed level. The latter could not find any collapse of the frequencies for single conductor arrangements, taking into account that actual ice shape position cannot be maintained in a position which would be statically unstable.

The first theory (i) may allow coupled flutter on single conductor while the second (ii) won't.

The basic theory behind galloping is at the origin of retrofit methods. See later.

The following sections will detail some aerodynamic aspects of the phenomenon, to better understand the physics behind the Den-Hartog galloping, and to estimate validity of some hypothesis. It will also explain basic differences between some other aerodynamic phenomenon and galloping.

Remark : aerodynamicists and aeroelasticians, in general, have adopted the Den Hartog type instability as the definition of 'galloping' - in essence, a one-degree-of-freedom (dof) motion. Other forms of instability involving two or more dofs are classified as fluttter, a term coming from the original aircraft wing, aeroelasticity studies and subsequently applied to suspension bridge deckings, etc. However, as far as the overhead line world - and CIGRE - is concerned, the term 'galloping', covers all forms of large amplitude, low frequency oscillation, caused other than by turbulent buffeting. It is a term that conveys the visual impact of what lines do and it therefore includes vertical-torsional flutter, as well as the Den Hartog instability.

5.1.2 Aeolian vibrations and galloping of conductors

Conductors can be characterized aerodynamically as bluff bodies: the airflow in proximity of their surface separates and forms vortices shed downstream in their wake. Conductors are flexible structures with almost no internal or self-damping and will become prone to aeroelastic instabilities consecutive to this flow separation. The aeroelastic instabilities of major concern are the Aeolian vibrations, wake induced oscillations and galloping. Wake induced oscillations will not be detailed here.

The first, the Aeolian vibrations, is associated to the pressure fluctuations applied on the conductors' surface as the vortices are shed in the wake. These pressure fluctuations are present whether the conductors are in motion or not. In the case of a bare conductor (Reynolds number value, Re, of the order of 10^4), the boundary layer remains laminar from the point of stagnation to the point of separation located at an average angle of 91°. Ballengee & Chen [1971] have measured

an almost linear variation of the angle of separation with Reynolds number, from 91° at $Re=10^4$ to 83° at $Re=3.9*10^4$. The shear layer proceeding from the point of separation undergoes transition and rolls on itself to form a vortex that will be shed downstream the wake. Vortex shedding is then a fluctuating flow instability the frequency of which is linked, via the Strouhal number, to the oncoming flow velocity and the conductor's diameter only. Aeolian vibrations of the conductor onsets as the vortex shedding frequency approaches one of the conductor's resonance frequencies. In practice aeolian vibrations covers a range of wind velocities extending from 80% to 120% the value of the matching Strouhal wind speed. In this range of wind speeds, the conductor will vibrate and its steady amplitude of motion will depend upon an energy balance between the wind power input from the flow vortices and the damping ability of the line. The nature of vortex shedding is obviously altered as the amplitude of the conductor's motion increases. The amplitude (peak-to-peak /2) will seldom exceed one diameter (d) of the conductor.

Aeroelastic instability of concern, galloping, results generally from an ice accretion on the conductors' surface that modifies the shape of the conductors' cross-section and causes the flow to separate at some discontinuities of the ice layer. The shear layer proceeding from this imposed point of separation modifies the mean flow and consecutively the mean pressure applied on the conductor's surface. Since ice accretion remains a time dependant process, the shape of the conductor "seen by the wind" changes, as well as the location of its center of gravity. The asymmetry of the mean pressure distribution generates a net force on the conductor in addition to its displacement in the direction of the applied force. If, at the new position, the new mean pressure distribution still generates a net force in the same direction and larger than the combined restoring and damping forces, the conductor motion will persist and might reach very large amplitudes (up to 150 d). This description fits the case of the galloping of a soft oscillator. Galloping may be initiated by an initial perturbation: the latter, by displacing the shear layer about the conductor, modifies the mean pressure distribution that otherwise would generate a net force in the direction opposite to the motion. This case is defined as a hard oscillator.

In contrast to the aeolian vibrations originating from fluctuating flow instabilities, galloping is then an aeroelastic instability inherently linked to the motion of a bluff body, in this case the conductor more or less covered with a layer of irregular ice: the shear layer proceeding from the separation point are then displaced with the conductor's motion and the entire mean flow field and mean pressure distribution are modified.

5.1.3 The quasi-steady hypothesis and a non-linear model

In the case of a single elastic bluff body undergoing galloping, the frequency of oscillation can be sufficiently low relatively to the wind speed: under these conditions, the effect of the body motion will be equivalent to a modification of the relative velocity (vector sum of dy/dt and V) and the angle of attack of this body. The flow "seen" by the body in motion would be equivalent to that "seen" by the same body but stationary and at the modified angle of attack and relative wind velocity. The lift and drag forces acting on the bluff body in motion are then assumed identical to that of the stationary body under the same flow conditions. Its equivalent angle of attack is simply defined as:

$$\tan(\alpha) = \frac{dy/dt}{V} \qquad (5.11)$$

Using a polynomial fit (preferably Tchebichev polynomials for their properties) of the experimental data, it is then possible to evaluate the value of the transverse force at any position of the bluff body motion. The equation of motion is then non-linear and the aerodynamic contribution acts as a negative damping. The first non-linear modeling of galloping is the work of Parkinson & Smith [1964]. This modeling, later extended by Novak [1969] was quite successful in predicting double amplitudes and onset velocities even for cables covered with ice under smooth and turbulent flows [Novak, Davenport & Tanaka, 1978] as it will be seen.

Laneville & Parkinson [1971] and Novak [1971] have shown that the initial hypothesis and resulting non-linear theory can be extended to steady turbulent flows by using the mean oncoming flow velocity in the definition of the angle of attack and by using the stationary force data measured under the identical turbulent flows. These two conditions are prerequisite since the reattachment of the flow is influenced by the turbulence contained in the oncoming flow [Laneville, Gartshore and Parkinson, 1975]: small scale turbulence enters the boundary layer via the stagnation point and changes the properties of the shear layer.

5.1.3.1 VALIDITY OF QUASI-STEADY THEORY

The quasi-steady theory with steady aerodynamic force coefficients is generally applied in clarifying the fundamental mechanism of galloping phenomena of ice-accreted conductor transmission lines and in conducting their simulations, while its validity had not been carefully discussed for long time. Recently, however, some Japanese researchers [Kimura

et al., 1999; Kimura et al., 2000; Shimizu et al., 2004] have tried to experimentally investigate the characteristics of unsteady aerodynamic coefficients in order to check the validity of quasi-steady theory applied to the galloping problem of ice-accreted bundled conductors.

5.1.3.1.1 Measurement of unsteady aerodynamic forces in wind tunnel

The unsteady aerodynamic forces on a 1/2-scale section model of an ice-accreted four-conductor bundle in Figure 5.2 were measured using a newly designed apparatus that can forcedly oscillate the model with large amplitudes; ±500 mm for the vertical and ±55° for the rotational direction. A center of the rotational motion was chosen to be the center of gravity of the conductors. The measurements were made with the forced oscillation frequency between 0.3 and 0.4 Hz, and the corresponding wind speed for the prototype is approximately twice the experimental wind speed.

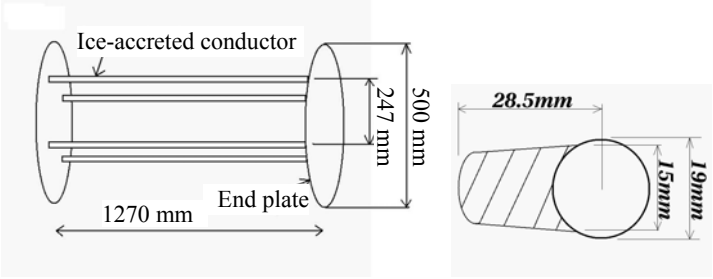

Figure 5.2: Half scale section model of conductors and accreted ice configuration.

5.1.3.1.2 Unsteady aerodynamic forces

The time series of the unsteady aerodynamic forces under the harmonic vertical forced motion (amplitude: ±350 mm, frequency: 0.3 Hz) are shown in Figure 5.3. The angle of attack was chosen to be 8° because the galloping occurred with elastically supported model when the mean rotational displacement became around this angle of attack. The model vertical displacement is also shown in the figure as the reference. The measured lift force generally agrees with the quasi-steady lift force, while the measured moment does not agree well with the quasi-steady moment.

The aerodynamic forces under the harmonic rotational forced motion (±40°, 0.4 Hz) are shown in Figure 5.4. The time series of the unsteady lift force seems to agree again with the quasi-steady lift force, while clearer difference between the measured and quasi-steady moments is observed in the time series where the phase of the unsteady moment is slightly behind the quasi-steady moment.

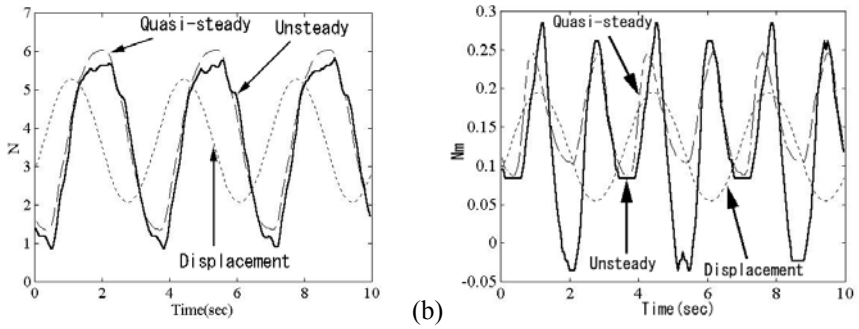

(a) (b)

Figure 5.3: Time series of (a) lift force (N) and (b) moment (Nm) under vertical oscillation: U = 8 m/s.

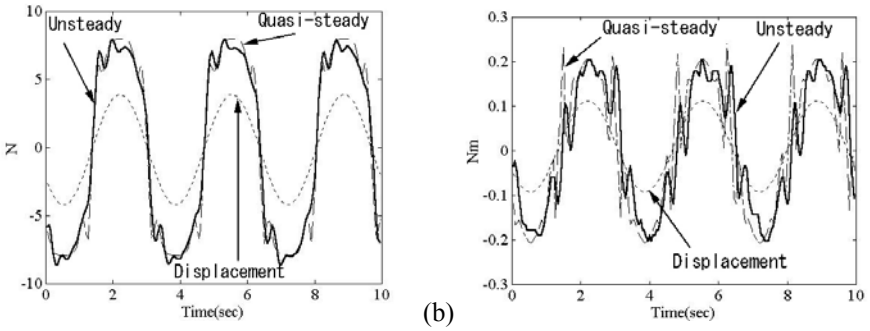

(a) (b)

Figure 5.4: Time series of (a) lift force (N) and (b) moment (Nm) under rotational oscillation: U = 8 m/s.

5.1.3.1.3 Unsteady aerodynamic force coefficients under rotational oscillation

For the rotational motion, the relative angle of attack cannot be defined and therefore the rotational velocity cannot be considered in the formulation of the quasi-steady forces. In order to clarify the effects of the rotational velocity on the unsteady aerodynamic forces, the unsteady force coefficients are plotted in 3-D figures with rotational displacement and rotational velocity as the parameters (Figure 5.5). The angle of attack is chosen to be 0° for this series of measurements.

Figure 5.5(a) shows the 3-D plot of the unsteady lift coefficient C_{Fz*} as the function of rotational angle q and reduced rotational angular velocity. The cross-sections in θ-C_{Fz*} plane of the plot are shown in Figure 5.6(a) and compared with the steady lift coefficient. The unsteady lift agrees with the steady lift coefficient, and the unsteady lift force is not affected much by the reduced angular velocity. For the unsteady moment coefficient, the 3-D plot is shown in Figure 5.5(b). The cross-section in θ-C_M plane of the plot does not agree with the steady moment coefficient even with the reduced angular velocity of 0 (deg), and the difference becomes larger with angular velocity, as shown in Figure 5.6(b).

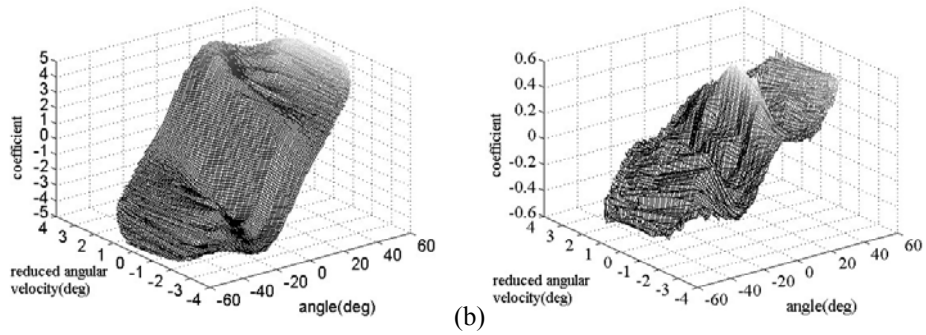

(a) (b)

Figure 5.5: 3-D plots of unsteady (a) lift and (b) moment coefficients under rotational oscillation: U = 13 m/s, f = 0.3–0.35 Hz.

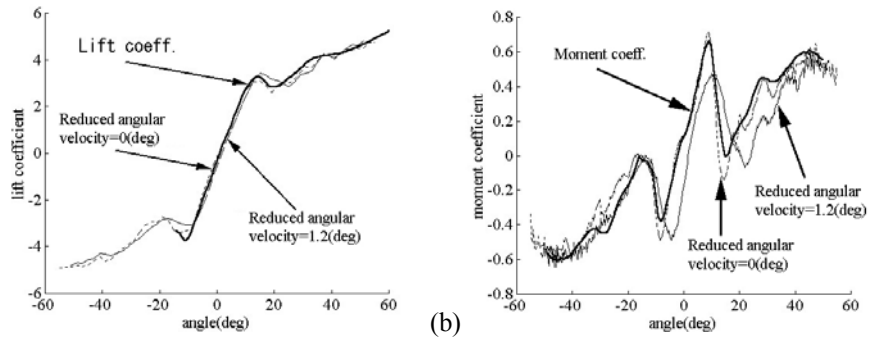

(a) (b)

Figure 5.6: Cross-section of 3-D plots in θ - C plane for unsteady (a) lift and (b) moment coefficients under rotational oscillation.

5.1.3.1.4 Characteristics of unsteady aerodynamic forces and validity of quasi-steady theory

The characteristics of unsteady aerodynamic forces are summarized as follows; 1) With the vertical motion, the unsteady lift agrees with the quasi-steady lift, while the unsteady moment differs from the quasi-steady moment considerably; 2) For the rotational motion, the unsteady lift is slightly different from the quasi-steady lift, and the unsteady moment differs significantly from the quasi-steady moment; 3) The effects of the angular velocity are not very significant for the unsteady lift, whereas considerable effects are observed for the unsteady moment.

The quasi-steady forces have been widely used to simulate the galloping, and it is necessary to clarify how much the simulation results are affected by the discrepancy in the formulation of the aerodynamic forces. Because the moment force sometimes plays important role in the galloping response, the difference pointed out above may be meaningful.

5.1.4 Galloping in turbulent flows

Turbulent flows are generally characterized by two criteria, the intensity (symbol i in Figure 5.7) and the macro-scale of turbulence, the former being defined as the ratio of the r.m.s. velocity fluctuations to the mean oncoming velocity and the latter as the correlation length. Figure 5.7, from Parkinson [1989], shows some effects of systematic variation of rectangular afterbody aspect ratio e/d (d/h in the Figure).

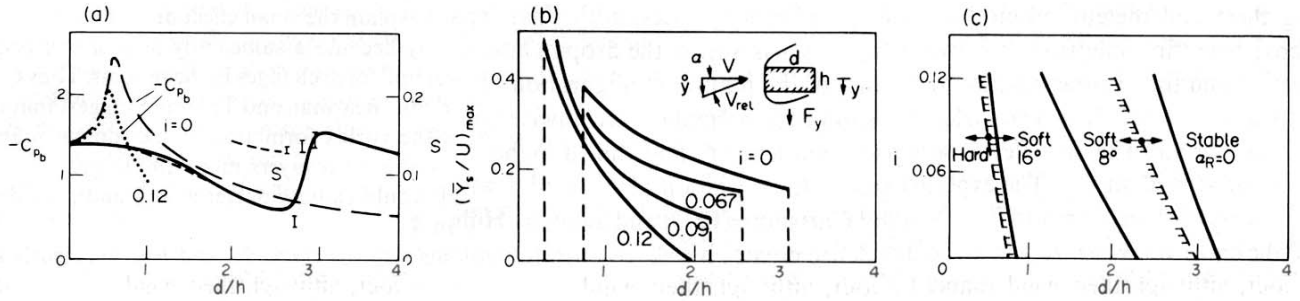

Figure 5.7: Effects of rectangular afterbody aspect ratio and turbulence intensity; (a) base pressure and Strouhal number, (b) soft galloping amplitude, (c) reattachment and galloping. Experimental data from [Brooks, 1960; Hoerner, 1965; Laneville and Parkinson, 1971; Nakamura and Tomonari, 1977; Novak and Tanaka, 1974; Smith, 1962; Washizu and Ohya, 1978]. Source: [Parkinson, 1989] Figure 2, page 173.

In Figure 5.7 (a), the variation of the base pressure coefficient is shown for the range of afterbody lengths $0 \leq e/d \leq 1$ in a turbulent flow of 12% intensity in addition to its variation and that of the Strouhal number in smooth flow. The intensity of turbulence, as suggested by Gartshore [1973], Laneville, Gartshore & Parkinson [1975], Laneville [1977] and Hillier & Cherry [1981], creates increased entrainment of fluid by the separated shear layers, thus thickening them and promoting firstly the interference between the shear layer and the trailing edge corner and secondly the reattachment of the shear layer at this trailing edge at lower values of e/d than for smooth flow. From these observations, the galloping behaviour in turbulent flow might be expected to be similar to that in smooth flow, but shifted as this is seen to occur in Figure 5.7 (b): as turbulence intensity in the oncoming flow is increased from i = 0 to 12%, a soft galloping profile becomes weaker and eventually stable while a hard galloping profile becomes soft.

Figure 5.7 (c) emphasizes the relationship between galloping, afterbody length, turbulence intensity and reattachment by superimposing curves of constant angles for reattachment (solid lines a_R = 0°, 8° and 16°) on an i-e/d map showing galloping zones (bounded by dashed lines). The a_R data are from shadowgraph experiments by Laneville [1973] on rectangular profiles tested in smooth and turbulent flows (two scales and three intensities). The right boundary of soft galloping, at which the profile becomes stable, is close to the curve a_R = 0°, but not coincident with it; it would rather coincide with a_R = 3°, perhaps indicating that in the case of profiles with $a_R \leq 3°$, the transverse exciting force becomes too weak for galloping to occur, even in a lightly damped structure. The left boundary of soft galloping, at which it becomes hard, so that a sufficient impulse is required to initiate galloping, lies close to the line a_R = 16°, the angle of reattachment in the case of a square profile in smooth flow.

The scale, or eddy size, of the incident turbulence does not seem important.

5.1.5 Possible control of galloping mechanism?

Against « Den Hartog » mechanism, we have first to say that, up to now, the vertical damping of the system was neglected. The vertical damping will impose a minimum wind speed for which galloping may occur. This is explained in detail in the

literature [Den Hartog, 1932; Richardson et al., 1963]. It is known by practice that a minimum of about 5 m/s is needed. Such a value applied on typical data of overhead lines would point out that the vertical damping at such low frequency (fraction of Hz) is around 0.5% of critical. A value which is extremely difficult to validate by test as most of existing data on damping are related to Aeolian vibration and are covering frequencies higher than 5 Hz. Recent studies (see sections 7.3.2 and 7.3.3) would like to point out that a measured damping on conductor only (need a very long span for testing) is far lower (at least one order of magnitude). Some experts explained the fact that end-span damping are becoming more important for low frequencies as bending mainly occur near the clamps for low frequencies, and suspension insulator may contribute as well as the tower itself in some cases. So that there are only three ways to go against Den Hartog instabilities : (i) increase vertical damping at low frequencies or (ii) avoid icing shape with the bad properties on the bad angle of attack or, more hazardous, (iii) to change ice shape.

Some devices have been proposed to mitigate galloping and are summarised in an ELECTRA paper [Cigre, 2000b]. Some of those methods are also described in Chapter 8.

As the condition is purely aerodynamic, all the modes are unstable, the lowest frequency mode shape will generally dominate in amplitude (because its critical wind speed will be the lowest) (as we know the lowest frequency can correspond to one- or two-loop modes, one-loop for multi-span (so called « up and down ») and two-loop for dead-end span), but of course depends of ice accretion on each span.

Against "coupled flutter" galloping, there are many new open roads to control galloping. In fact structural data are playing an important role in the phenomenon. (i) To limit torsion amplitude by detuning and (ii) to avoid 90° phase shift are two important factors. It is in fact easier to fight against torsion than to fight against vertical movement, because of the relative amount of energy in each movement. In other words, torsion is needed by the instability to inject energy into vertical movement, so that an appropriate action in torsion may avoid the phenomenon.

The devices used against coupled flutter have very limited action against Den Hartog kind of instabilities, except the fact that the increase of torsional stiffness is limiting torsional amplitude in such events, thus they do not desegregate the modified Den Hartog criterion.

Only some of the galloping modes (for which the tuning is strong enough) are participating to the movement.

Other spectacular galloping, even if rare (not so rare in Japan), is three DOF galloping driven by torsion but especially with large amplitude when horizontal swinging frequency is close to half of vertical frequency (this last being close to torsional frequency). In such case the galloping mode has a shape of number eight. This frequency ratio can be met more easily on some dead-end span.

There are theoretically many other coupling possible, like horizontal swing with torsion (also driven by torsion) but few or no observations have been made on such instabilities. All these cases can be analysed by theoretical approach.

Basically most of the dangerous galloping on bundle conductors are driven by torsion (2 and 3 dof galloping) an most of dangerous galloping on single conductors seems to be driven by pure Den-Hartog, means one degree of freedom galloping (even if torsion exist, it is just forced by vertical movement).

5.1.6 Equations of galloping

There are many papers dealing with all details in relation with galloping equations. The reader may found such information in [Hunt and Richard, 1969; Keutgen, 1999; Lilien and Ponthot, 1988; Lilien and Dubois, 1988; Lilien et al., 1989; Lilien and Chabart, 1995; Nakamura, 1980; Nigol and Clarke, 1974; Nigol and Buchan, 1981; Parkinson, 1974; Rawlins, 1979; Richardson et al., 1963; Wang and Lilien, 1994; Wang, 1996; Wang and Lilien, 1998b].

If it is relatively easy to write down these equations, it must be emphasized that we cannot neglect:

Self-damping of the conductors, even if very small. These data are relatively close to 0.5% of critical for the vertical movement and 2% for torsional movement. For horizontal movement it is really close to zero.

Aerodynamic damping is automatically included in the aerodynamic coefficient (drag mainly (always positive) but also the derivative of lift and pitching moment, these last could be negative values), no more is needed

Inertial coupling (the eccentricity of ice induce rotational inertial term in the vertical movement (readily negligible for most of ice shape) and vertical inertial coupling in torsional equation (not negligible), as the rotation is around the shear centre

So called "inverse pendulum effect" which is a static effect on torsional stiffness due to ice eccentricity weight (= $m_{ice}.g$)

The aerodynamic effects, which induce some important coupling (due to the derivative of lift and the derivative of the pitching moment) and seriously affect the torsional stiffness too.

The vertical frequency is strongly affected by tension variation (thus by amplitude of vibration), which cannot be considered as a constant (taut string model is not valid), as already explained in another chapter. This effect is only active for odd modes (1 and 3 mainly).

The torsional frequency is dependent on the torsional stiffness, which is very complex in case of bundle conductor (depending on the tension in each subconductor f.e. and also depending on torsional amplitude) [Wang and Lilien, 1998a]

The tension in the conductor (included in the vertical frequency) is not a constant and depends on the amplitude, the kind of modes shapes (several could be present at the same time). Fundamental effect is also that the tension in the conductor is the resultant of the whole section (all spans) movement at a given time. The tension is the variable through which all modes are interrelated and all spans in a section are depending from each other.

It is recommended to look for all these details in the literature, but we would like to present here a very simplified case which could be a good base to study the possible instabilities in a vertical-torsion movement.

As we are looking for instabilities only (thus not valid to estimate amplitudes), we may limit our investigation to very small movement and make e development limited to first derivatives.

For the sake of simplicity, we will also limit the case to one mode only (the mode at a frequency ω_v for vertical and the mode at ω_θ for torsion). Such a mode may be a section mode, as detailed in other chapters, including the movement in different spans. Let's choose an "up and down" mode for which tension variation is small enough.

The complete equations may be written down right a way, and the corresponding linearised terms are coming out, with our hypothesis. We just use the modal decomposition method to be tuned on one mode under investigation for each of the considered degree of freedom (vertical an torsion here), so that each of the term (including aerodynamic coefficients, $\sin\theta_0$, etc.; are in fact integral terms taking into account the repartition of these data all along the multi-span section) (symbols are defined in Appendix A):

$$\ddot{y} + \left[\frac{k_D U_0}{m} \left(C_D - C_{L\alpha} \right) + 2\xi_V \omega_V \right] \dot{y} + \omega_V^2 y = \frac{k_D U_0^2}{m} C_{L\alpha} \theta - \frac{m_{ice}}{m} d_i \sin\theta_0 x \ddot{\theta} \qquad (5.12)$$

$$\ddot{\theta} + 2\xi_\theta \omega_\theta \dot{\theta} + \omega_\theta^2 \left[1 - \frac{k_M U_o^2}{\omega_\theta^2 I} C_{M\alpha} + \frac{m_{ice} g d_i}{\omega_\theta^2 I} \sin\theta_0 \right] \theta = \frac{k_M U_0}{I} C_{M\alpha} \dot{y} + \frac{m_{ice} d_i}{I} \cos\theta_0 \ddot{y} \qquad (5.13)$$

There is one strong hypothesis on ice shape: due to lack of data (if known it would be possible to introduce actual data), the ice shape has to be supposed given all along all the spans and this is generally done by fixing a corresponding eccentricity of ice in no wind condition which is the same all along the section.

The instability analysis may be "easily" evaluated on such a simple non-linear two degree of freedom system. The solution of such analysis would be (complex eigenvalue analysis):

The frequency of the limit cycle, if any (if unstable, there exist a limit amplitude due to nonlinearities, mainly coming from aerodynamic coefficients, but not only). The frequency of the limit cycle is close to ω_v but not equal.

The modal shape of the limit cycle which is a combination of vertical and torsional amplitude.

For single conductor (torsional frequency being much larger than vertical frequency or $\omega_\vartheta >> \omega_v$), inertial term and damping term can be neglected in the torsional movement (as the galloping frequency is close to ω_v) , the torsion is forced by the vertical movement and is in phase with the vertical speed of the conductor, the amplitude being dependent of the pitching aerodynamic moment and some structural data.

For bundle conductor, the torsion is in resonance with vertical movement ($\omega_\vartheta \approx \omega_v$) so that phase shift between the two movements may cover all the range and the amplitude may be large.

All effects cited in this brochure are summarized on these two equations: limited to vertical movement only, the Den Hartog criterion is transcendent in the damping term of the vertical equation (the critical wind speed may be written directly). The coupling between torsion and vertical is obvious and the change of torsional stiffness with the ice pendulum effect and aerodynamic pitching moment is clearly established.

The block diagram of such closed looped system is readily established and the instability conditions can be clearly stated, in which the product $C_{L\alpha}.C_{M\alpha}$ is playing a major contribution which is also multiplied by the cubic power of the wind speed.

An interesting feature to consider is the fact that, if Den-Hartog criterion is not violated, both separate equations would have positive damping, but owing to the coupling between the two movements, the system may nevertheless become unstable as we already stated out.

5.2 Estimation of unstable conditions

Some parametric studies have been presented in the literature and generally are looking for the stability conditions (or reduced amplitude) drawing the envelope curves given by a constant parameter in the plane of two other parameters. Unfortunately it is very difficult to have a global overview of the influence of five parameters (see Table 4.1) plus self-damping, ice position and ice aerodynamic curves.

To get some sense, the analysis needs to be performed using the following sequence:

With a given wind speed and a given ice profile (means aerodynamic curves), all possible ice position around the conductor are studied (this need to study the static equation in torsion). Inverse pendulum effect as well as pitching moment are both fundamental to study such equilibrium position

All found possible static position of ice (in the presence of wind) (some are generally impossible at mid span for strong winds) are studied by stability analysis (complex eigenvalue) and the dangerous ice accretion angle are located, if any.

For the most dangerous cases, if suspected to be possible, limit cycle analysis is performed either by energy method (very quick but approximate as it is difficult to include tension variation in such methods, moreover such method are limited to one mode only) or by time response. This last may lead to long calculations (some few minutes on actual portable notebook) as all the section (multi-span generally) has to be analysed with all its modes in vertical, horizontal and torsion (some up-to-date simulation are able to limit the amount of modes par span to be studied).

It must be noticed that simple energy method may lead to discrepancies with time response analysis. This last may lead sometimes to the mixture of several modes.

Only time response analysis may give access to appropriate tension variation in the conductor as well as in the suspension insulator chain.

Only finite element methods may give access to appropriate interphase effects (in case of existing interphase spacers), these last cases have to include travelling waves and some local effect introduced by some retrofit methods. (See f.e. [Keutgen, 1999])

5.2.1 Example of typical analysis for galloping

Figure 5.8 is giving access to a stability analysis. Parameter P2: a/d (bundle separation), P3: $V/(\omega_v.d)$ (wind speed), P4: $m_{ice}.d_{ice}/(m.d)$ (reduced ice inertia) and P5: 12.5 d/f (conductor span) being given as well as ice eccentricity, the stability analysis is performed in the plane (torsional damping, angle of ice accretion) for different parameter P1: ω_v/ω_θ value (detuning). It is remarkable that more or less all position of ice may be unstable. But in fact actual torsional damping is around 2-4% depending on conductor type, spacers used and end span fixation. It results that unstable area for galloping are located around -50° for ice accretion in that case. It is also remarkable to notice that a detuning of 20% would completely remove all unstable area. The detuning may be obtained either with an increase or a decrease of the torsional frequency, both having some different actions. A too large detuning seems to create new unstable area close to 0° (ice facing the wind). The same curves are shifting to stronger galloping problem for higher wind speed as stated in the Figure on right (but the unstable area over -130° disappears).

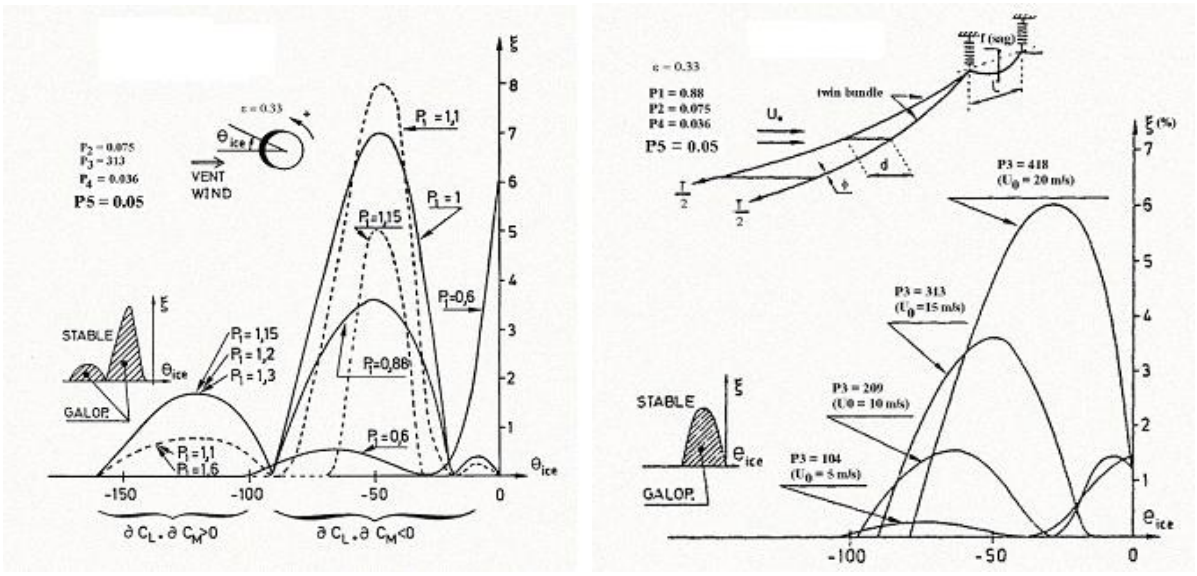

Figure 5.8: Typical instability analysis. Detection of galloping risk for a bundle conductor line. The specific wind speed are given for the case (d = 0.033 m; m = 1.7 kg/m; a = 0.45 m, T/2 = 35 kN; span length = 360 m (4 span section, equal length), sag f = 7.8 m; up and down 0.23 Hz vertical mode, ice thickness of 5 mm, ice density 900 kg/m^3)

5.3 Estimation of galloping amplitudes and ellipse shape

The amplitude reached during a Den-Hartog instability can be estimated by a very simple criterion: the range of angle of attack during a limit cycle is the one that annihilates completely the negative value of the Den Hartog criterion (area compensation). As an example, the Figure 5.1 (right) is showing a negative Den Hartog value around -50°. It is easy to evaluate (visual inspection) that the range of angle of attack needed to compensate the crossing area of C_D and $C_{L\alpha}$ is about 30° (+/- 15°) or 0.5 radians. That value is equal to the inverse of the reduced wind speed ($\omega_v.Y_{max}/U_0$) where Y_{max} is the half amplitude of the galloping, approximately. In that case, for a wind speed of 10 m/s and a vertical frequency of 0.3 Hz (1.9 rad/s), the half amplitude would be 2.6 m. It may seem peculiar that the output is independent of the span length and initial sag. But, obviously, non linear effects of the tension in the conductor (which depends on the span length and the initial sag) would seriously affect the amplitude if it reached about the sag. Only advanced method can easily treat such additional non-linear effect.

Such a simple approach is not applicable to flutter type galloping.

The scientific world has developed numerical and analytical tools to study the complete interaction between all the degrees of freedom, including every aspects of a multi-span line. So that we may say that the galloping is now completely covered by its equations which are well known and defined, but the complexity of so many interactions in a real problem make it very difficult to understand everything, even if it is possible to simulate any case. The practical problem is more related to solve galloping by appropriate retrofit method and not to be able to reproduce a specific observation. That is why it is a major concern to simplify equations reasonably to have access to the different kind of instabilities. Nevertheless, the numerical or analytical tools developed may help to estimate the efficiencies of the retrofit method used using typical ice shape and appropriate range of wind speed, for all possible ice accretion. The finite element method may even evaluate the efficiencies of interphase spacers as detailed in [Keutgen, 1999]. But no numerical tool can estimate properly the retrofit method based on ice shape modification, because of the lack of aerodynamic properties of the modified conductor shape all along the spans.

Figure 5.10 is giving access to a typical amplitude analysis. In this case the equi-amplitudes are drawn in the plane (wind speed, ice accretion angle), for all other parameters fixed.

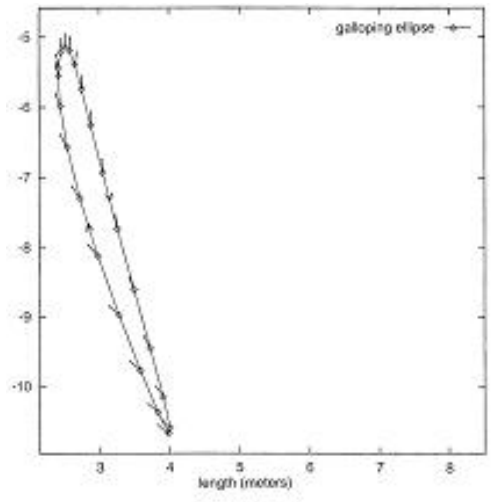

Figure 5.9: A typical galloping ellipse in a vertical plane at mid-span, due to coupled flutter, the straight line attached to each square point (all square being spaced by the same time between them, around 0.1 s) is giving access to ice position all around the limit cycle. (calculated by University of Liège using analytical tools).

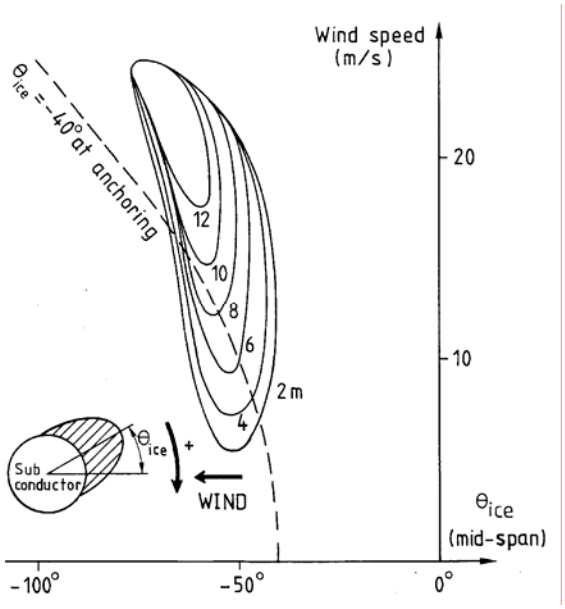

Figure 5.10: Typical amplitude analysis. Equiamplitude have been drawn in a plane (wind speed, angle of ice accretion) all other parameters fixed. In this case only a small range of ice accretion may lead to large amplitudes, in a narrow range around -20 to -50° at the anchoring level. It may be seen that there is a need a very particular data combination to get a dangerous galloping. For example a given ice (-40° location at anchoring level) may give a galloping of 8 m for wind speed around 10 m/s but would not give any galloping for wind speed higher than 15 m/s or lower than 5 m/s.

5.3.1 Galloping and/or gust response effects?

Galloping is not the only source of motion of transmission lines in their low frequency modes. The turbulence of the natural wind contains significant energy at these low frequencies and can cause a random amplitude, forced response of the lines, termed 'buffeting'. Thus the buffeting response cannot be overlooked in lines subject to high gust loads because of the high flexibility of transmission lines. Since the characteristics of galloping and of the gust response are entirely different, the way to control or minimize them would be different for a rational design approach to phase clearances and for the fault-free operation of transmission lines. In some circumstances it may, therefore, be necessary to identify galloping and gust responses separately by processing field data [Gurung et al., 2002; Gurung et al., 2003; Yamaguchi et al., 2003]. An example in which two methods are applied to some test line data is now presented.

5.3.1.1 Typical wind-induced vibrations

Several wind-induced vibration events of ice accreted Tsuruga Test Line were observed in Phase B (4-bundled conductor, semi-suspension span) and Phase C (6-bundled conductor, dead-end span). A typical Lissajous diagram measured at quarter span in Phase C is given in Figure 5.11(a), which is oriented obliquely at an angle of 45º with unsteady oscillation locus. Since the observed vibration is associated with large amplitude and with a relatively long period, there is a possibility of interpreting this event as oblique galloping. Such interpretation, however, could be misleading without analyzing the data to determine the contributions from galloping and the contributions from turbulent buffeting. In fact, the corresponding time series of vertical response in Figure 5.11(b) has very low-frequency fluctuation reflecting wind turbulence. Furthermore, the amplitudes of both the vertical and horizontal responses with this low frequency, shown in Figure 5.11 (d) (obtained by low pass filtering) and corresponding to a swinging type of motion caused by the quasi-steady response to the gusting of the turbulent wind, are comparable to those of the major galloping component identified in Figure 5.11 (c). This galloping component has a relatively high frequency, corresponding to a two-loop mode.

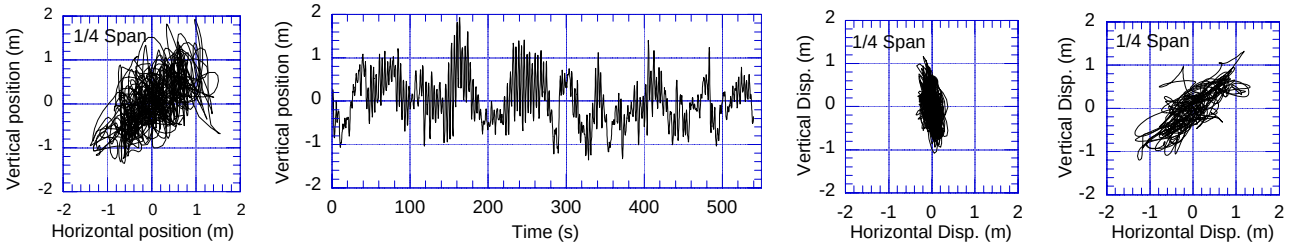

(a) Lissajous diagram (b) Time series of vertical response (c) Highpass filtered (d) Lowpass Filtered

Figure 5.11: A typical wind-induced vibration observed at quarter span in Phase C of the Tsuruga Test Line, Japan.

5.3.1.2 Prony's method for identification of galloping component

Prony's method is signal processing method which fits dots on complex exponential fit. This is giving access to both frequencies and damping.

After filtering the data with very low cut-off frequency to exclude the quasi-static response component, Prony's method is applied in piecewise fashion with respect to time, in order to find out a dominant harmonic component in the higher frequency component of responses. Forty seconds (approximately 10 times of the natural period of two-loops mode) long piece of record has been selected, and the harmonic components of each piece of record are identified at every two seconds by moving the starting point of each piece of records.

The results of the Prony-based analysis are shown in Figure 5.12. All the results are indicated by open dots (◦), while the dominant harmonic component in each 40 s piece, defined as the component with the maximum amplitude, is identified by a filled dot (•). Figure 5.12 (a) depicts the change in frequency composition of significant harmonic components in the vertical response at quarter span. There exist dominant harmonic components with fairly constant frequency with respect to time. The frequency is close to the natural frequency (0.27~0.29 Hz) of the in-plane, two-loops mode and independent of the excitation frequency in gusty wind. Thus, the correlated dominant harmonic components with time represent the major galloping component. The amplitude and damping ratio of the major galloping component can be estimated from Figure 5.12 (b) and (c), respectively. That is, the maximum amplitude of major galloping component is approximately 0.85 m, while the damping ratio varies randomly ranging from negative to positive one.

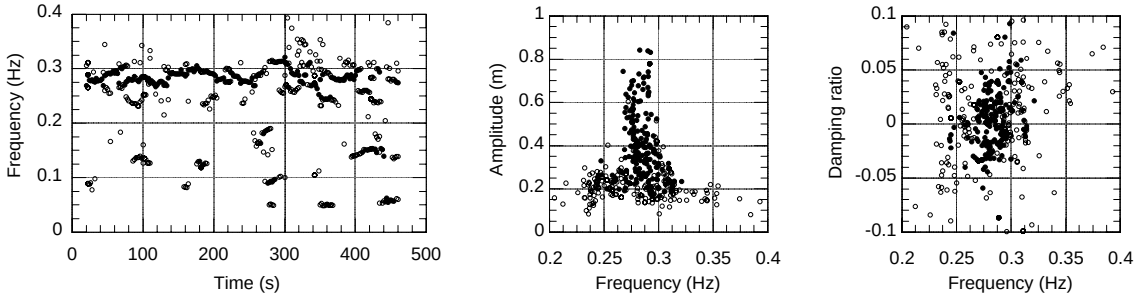

(a) Change in frequency composition (b) Amplitude of harmonics (c) Damping ratio of harmonics

Figure 5.12: Prony-based decomposition of vertical response at quarter span

5.3.1.3 Multi-channel modal analysis for galloping study and comparison with buffeting analysis

The multi-channel modal analysis is also applied to more precisely identify the galloping event by using the data of vertical, horizontal and torsional responses measured at different locations along the span. It should be noted that highpass filtering is applied to each response to remove the low-frequency, quasi-static response to turbulent gusts which is sometimes the dominant component of transmission line response but is unimportant for galloping studies. A result is shown in Figure 5.13, which clearly indicates that the oscillation envelope observed in the field is significantly influenced by the presence of the gust response due to wind turbulence.

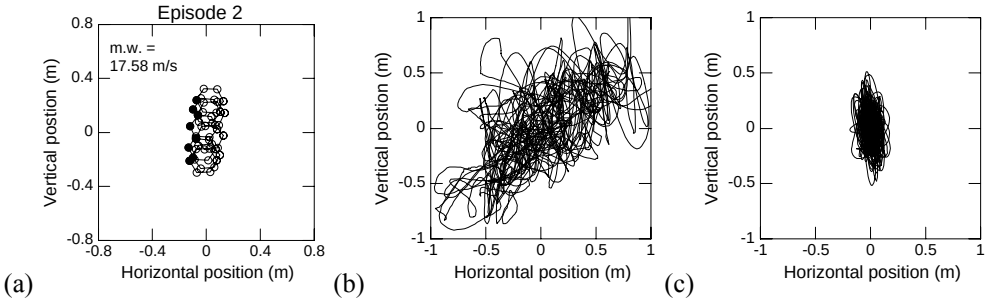

Figure 5.13: Lissajous diagrams at ¼ span: (a) galloping by modal analysis, (b) observed in the field and (c) galloping component obtained by using high-pass filter.

RMS of vertical fluctuation observed in the field is compared with corresponding value of expected buffeting response. Figure 5.14(a) and (b) depict RMS of vertical fluctuating component of response measured at field in Phases B and C, and corresponding value of analytically estimated buffeting response at ¼ span, respectively. The events, which are identified as galloping based on the multi-channel modal analysis, are depicted by filled symbols. As expected, augmenting action of motion-induced force in galloping response is clearly seen as shown in Figure 5.14 (b) with higher value of the galloping response than expected buffeting response. Response in these galloping events doesn't follow the trend of the buffeting response, which is parabolic with respect to mean wind speed.

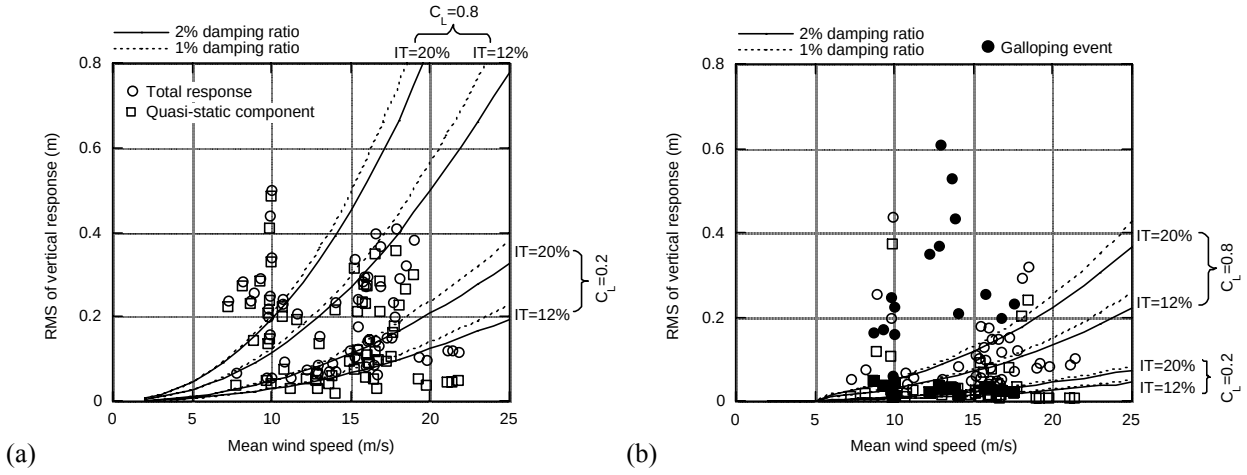

Figure 5.14: RMS of vertical fluctuation at ¼ span: (a) Phase B, (b) Phase C.

5.4 Resulting dynamic loads on towers

The dynamic load on tower is given by the tension variations around the initial value (equilibrium taking into account wind and ice as static load).

For the sake of simplicity in this demonstration, we will suppose that the tension is the longitudinal component of a levelled multi-span section, it is supposed constant all along the whole section. (in practice, this is not true because suspension insulator would not move in such situation). This helps to define a unique initial tension T0 for the whole section.

N.B. Such hypothesis is NOT used in any simulation method.

Tension variation (ΔT) may be obtained by the Hooke's law:

(E, the conductor young modulus (N/mm^2), A the cross section (mm^2), L, Δl are lengths and length variation and K the stiffness (see later))

$$\Delta T = \frac{EA}{L}\left(\Delta l - \frac{\Delta T}{K}\right) = K_{ev}\Delta l \qquad (5.14)$$

The change of length in the Hooke's is the conductor length change, so that we must subtract the end span movement, related to tower stiffness K (N/m) (the K here is the equivalent of the two end stiffness putted in series). The length to consider is the whole length of the section (all spans between two tension towers).

Where

$$L = \sum_{s=1}^{N_s} L_s \qquad (5.15)$$

and

$$\frac{1}{K_{ev}} = \frac{L}{EA} + \frac{1}{K} \qquad (5.16)$$

In order to find relationship between tension and galloping amplitudes, we have to express the same equation using, to write down Δl, the modal decomposition in "k" modes in each span "s" of the section.

$$\Delta T = K_{ev}\sum_{s=1}^{N_s} L_s \sum_{k=1}^{\mathrm{mod}\,es}\left(\frac{k\pi}{2L_s}\right)^2\left(y_{s,k}^2 - y_{s,k0}^2\right) \qquad (5.17)$$

the $y_{s,k0}$ is the modal contribution k to the initial sag in the span s.

$$y_{s,k0} = -\frac{4mgL_s^2}{(k\pi)^3 T_0} \qquad (5.18)$$

obviously only for k odd (and 0 for k even). The reader may easily verify that for infinite number of k modes, such formula tends to the classical expression of the sag.

To better feel the content of the equation (5.17), we will make some example:

5.4.1 Example 1: multi-span of equal length Ls and only one mode is considered.

$$\Delta T = K_{ev}\frac{\pi^2 N_s}{4L}\sum_s\left(y_s^2 - y_{s0}^2\right) \qquad (5.19)$$

or

$$\Delta T = K_{ev}\frac{\pi^2 N_s}{4L}\sum_s\left(2y_{s0} + \Delta y_s\right)\Delta y_s \qquad (5.20)$$

with

$$\Delta y_s = y_s - y_{s0} \qquad (5.21)$$

From such a formula the following evidence may be stated:

For the "up-and-down" mode we have the following relationship:

$$\left(\sum_{s} \Delta y_s = 0 \right) \qquad (5.22)$$

So that the second order terms remain (so called non-linear) and the frequency content would clearly be the double frequency of the observed vibration. There will be an offset of the ellipse compared to loaded sag. The tension variations are proportional to the square of t he amplitude.

For the up-up mode (all spans in phase) both single frequency and double frequency of observed displacement will be present. Tension variations are very large, even for low amplitudes. They are proportional to the amplitude and to the initial sag for limited amplitude level.

N.B. Due to non-linear coupling, most of the up-and-down mode are forcing up-up mode (even if limited in amplitude) which are generating large tension variation. So that most of the case generate both single and double frequency of the observed displacement.

5.4.2 Example 2: only a two-loop galloping is concerned (apparently) and all section has equal span length.

$$\Delta T = K_{ev} \frac{\pi^2 N_s}{4L} \sum_{span} \Delta y_s^2 \qquad (5.23)$$

So that only second order terms remain and the frequency content would be the double frequency of the observed vibration. The tension variations are proportional to the square of amplitude.

Remark:

A multi-span section may have gallop in only some spans. Nevertheless all tension variations are applied to end span tension towers. So that observers may not see anything moving significantly at some location despite huge tension variations measured on the tower.

The evaluation of tension difference between adjacent spans needs to write down equilibrium equation at suspension span and this would include the displacement of suspension insulator. This has been done in [Wang, 1996] and is obviously automatic in finite element simulation as insulator is modelled separately. The frequency content of suspension chain insulator is more complex as it includes the content of both displacement of adjacent spans and conductor tension.

It is quite interesting to evaluate the effect of tower stiffness on tension variations. Clearly, all formulas are showing a direct proportionality of tension variation with Kev. defined in equation (5.16). So that tower stiffness (order of amplitude 10^6 N/m at transmission level) may have some influence if in the same range as EA/L, L being the *section* length. Generally tower stiffness has very limited effect, except for extreme cases (and at least for distribution level).

Last, but not least, we neglect the dynamic behaviour of the tower (order of amplitude 1 Hz for transmission level), which may not be discarded in some cases. But we have never observed such case.

5.4.3 Order of amplitudes of tension variations

There are some interesting published papers on the subject, including measurement on site. Obviously we must be cautious about the main differences existing between dead-end cases and multi-span cases [Anjo et al., 1974; Cigré WG11-TFG, 1989; Havard, 2002; Keutgen, 1999; Lilien and Ponthot, 1988; Lilien, 1991; Lilien et al., 1994; Wang, 1996].

Tension changes are generally considered by reference to a given tension value at appropriate temperature (so called here after "initial static value"), wind speed and ice load (static). Ice load during galloping has been considered as limited in most of the cases. Thus the tension with no ice load can be used as initial value before galloping. Wind speed is not considered in that reference value and temperature is chosen at 0°C. Of course particular locations have to be considered with different hypothesis.

Equation (5.20) is giving access to the maximum theoretical value reached for one-loop in a dead-end arrangement with amplitude equal to the sag (neglect tower stiffness) ($\Delta y_s = y_{s0}/2$)

$$\Delta T = K_{ev} \frac{\pi^2 N_s}{4L} \sum_s (2y_{s0} + \Delta y_s) \Delta y_s \qquad (5.24)$$

Which would be equal to 1.2 times the initial static value for amplitude equal to the sag (means roughly ($\Delta y_s = y_{s0}/2$). Such a value has in fact been observed.

In all summarized cases, the following *tension variation* has been observed:

Anchoring level: up to 1.2 times the value without wind

Suspension level: up to 1.7 times the value without wind

When the variation is very large, the movement may slightly overpass the sag level, as can be seen on some joined videos and the tension may be completely relaxed at the upper position. But most of the times the tension is not relaxed in multi-span arrangement, even during extremely high amplitude, because up and down exist and the tension in the conductor reflect, as detailed, the whole section length changes, which is never relaxed for all span together, except may be for some dead-end span.

Concerning suspension insulator, they have to sustain stronger vertical loads, but they are also submitted to dynamic horizontal loading (due to tension variation in the span). The tensioned insulators have a specific eigenfrequency which may be excited by these horizontal excitations. Such effects may lead in dramatic movement. Some can be seen in the joined videos).

Some corollas of the above evaluations can be stated:

- Is that the longitudinal loads on tension towers, during galloping events may reach 2.2 times the load existing without wind (but with ice). Ref. [Havard, 2002] shows available measurements in the literature on such tension variations (peak-peak/static) and observed factors up to 2.2 on ¨standard¨ high voltage lines, but observed for short span lengths (80 m long) in Iceland some extreme cases going up to a factor of 2.8 on test spans.
- The vertical load on crossarms (an thus existing in the suspension insulators) due to galloping may reach 2.7 times the load without wind. The same reference as cited above has also analysed such loads detailed in the literature and found out dynamic peak factor always lower than 2.
- As there is no reason for synchronism or asynchronism of galloping loads in each phases, both extreme may be reached at different time in the events, so that some tension towers with two circuit in vertical arrangement may be submitted to torsional loads induce by a quasi-relaxation on one circuit and the maximum values in each phases of the second circuit.

as a conclusion on dynamic load factors, we would recommend, in the absence of detailed simulation able to point out particular cases, to choose the following design values:

- anchoring level: tension variation during galloping: from 0 to 2.2 times the static value (with ice, no wind);

- suspension level: vertical load: from 0 to 2 times the static value.

The risk of tension tower torsion has to be analysed as well as the risk in suspension tower related to unbalanced vertical loads between the left and the right hand side of towers (triangle arrangement or double circuit).

6. In the field and laboratory observations

6.1 Introduction

Data on conductor galloping may be collected by three different means:

- By doing field observations on existing lines subjected to conductor galloping (see also section 2.5 Incidence of galloping);
- By reproducing conditions propitious to conductor galloping using artificial ice shapes on a full scale test line, or;
- By characterizing aerodynamically different ice shapes through wind tunnel measurements and determine the cable response using a mathematical model.

Tests of galloping behavior in full-scale spans exposed to natural winds are normally directed at improved understanding of the phenomenon, at testing theories of galloping or at evaluation of proposed protection schemes. Certain test programs are carried out on spans fitted with artificial ice of some shape. Others are organized on spans of operating lines on which icing is anticipated.

Tests motivated by research and development are usually performed on spans equipped with artificial ice, whereas tests aimed at assessing effectiveness of protection methods that are in an advanced state of development are ordinarily carried out on operating lines. Use of artificial ice permits much more rapid testing and better control of test variables.

The use of a mathematical model allows its user to predict the behaviour of a line regarding conductor galloping. It will predict galloping amplitudes, forces transmitted to towers or dynamical conductor tensions. It may also be used to better understand the effect of a change of geometry on a given line. However, as with every model, the answer is only as good as the modelisation and the input. Since the aerodynamic forces depend on the conductor ice accretion which in turn varies from one galloping event to the other, one cannot expect exact answers. Even with their limitations, models are still very useful to generalize results obtained through field observations.

Those different approaches are described with more details in the following sections.

6.2 Testing with natural ice

Tests involving natural galloping of spans in operating lines are usually aimed at validating the effectiveness of proposed protection methods. They are also conducted to better understand the phenomenon (kind of icing events, wind speeds, torsional behaviour, range of tension variations, shape of galloping, amplitudes) and to validate simulation tools. Test programs entail the selection of spans in areas that are likely to experience glazing conditions and provision of means for determining the behavior of the spans when icing occurs.

The main advantage of testing protection methods under natural icing conditions is that it is realistic. The interpretation of results does not depend upon theoretical assumptions about which even experts may disagree. In addition, environmental effects found in actual service, such as icing-up of moving parts, are present. Retrofit systems based on aerodynamic control devices or torsional control devices must be validated with natural icing or artificial ice with natural shapes or else the interaction mechanism will not be proven adequately. Normally, one or some of the phases of the spans under test are not protected against galloping in order to provide a comparison basis.

There are several disadvantages. The most serious is the low productivity of such test programs. Glazing conditions conducive to galloping occur so infrequently, are so localized and have such random geographical distribution that a given test area may produce useful data only once in several years.

The large number of variables that influence galloping behavior aggravates this disadvantage. A protection method may be used with confidence only if it is known to be effective throughout the range of wind conditions that is anticipated and against the variety of ice shapes, thicknesses and postures that are likely to occur. Thus a large number of episodes of galloping are required in order to properly evaluate a protection system.

A second disadvantage concerns acquisition of data. The low productivity of individual test areas makes it difficult to justify automatic data recording equipment. Such equipment can sense motion at only one support point (tension recording). Remote control is sometimes possible, but costly. However, nowadays internet facilities may help a lot with the possibility of using Webcams on a test site. The measurement of tension and other parameters are not an easy task due to awful meteorological conditions during which most of galloping occurs. Even though a test area may experience galloping, on most occasions all spans or even phases do not participate in it, and when they do, they do not participate to the same degree. Recording at only one location thus provides only a narrow sample of the activity occurring in the area

where it is located. Because of this situation, the most effective method for data acquisition is through observer teams who visit test areas when glazing occurs. The observers are able to cover all phases of a line over a length of several miles. In fact, the first galloping observed were seen by lineman who reported to their chief such huge amplitude. Nobody believed them until the first video had been taken. There are also some famous cases, like the one in U.K. in 1986 where galloping was observed during about four days on quad bundle lines. Many videos have been taken and some can be seen on the joined CDrom.

The most classical real time detection of galloping remains the recurrent circuit-breaker operation, several times in a few minutes, due to clearance problems in the galloping phases. Some unexplained consequences can clearly be the output of some galloping, like bundle twist, abnormal insulator failure, tower legs troubles, spacer failure, conductor damages (up to breakage).

Some temporary installation may also be installed in windy regions, like the experience explained in [Lilien and Vinogradov, 2002]. Some rare operating lines (some sections) are (were) under permanent supervision, like in Belgium in the Ardennes (Villeroux) where a 400 kV four spans section have been recorded for more than ten years with different bundle line arrangements [Lilien et al., 1998; Rogier et al., 1998].

As mentioned earlier, most testing conducted with natural ice aims at the validation of antigalloping devices, which are covered in Chapter 6. However, more general results were gathered through such tests that are worth mentioning here.

Japanese researchers have been especially active in the field of galloping experimental tests. Yutaka et al. [1998] summarized observations, measurements, and studies conducted in Japan. The authors found that their country has 10 to 100 galloping cases annually. Galloping happens at sea level as well as in high-altitude areas. Galloping with ice accretion is caused chiefly by strong winds. Galloping with snow accretion is identified with a wide range of wind speeds.

At the Mt. Kasatori test line, observed oscillations, as shown in Figure 6.1, were:

- one loop, or more correctly, pseudo-one loop mode
- mixed one loop “up and down” and two loops
- three loops per span.

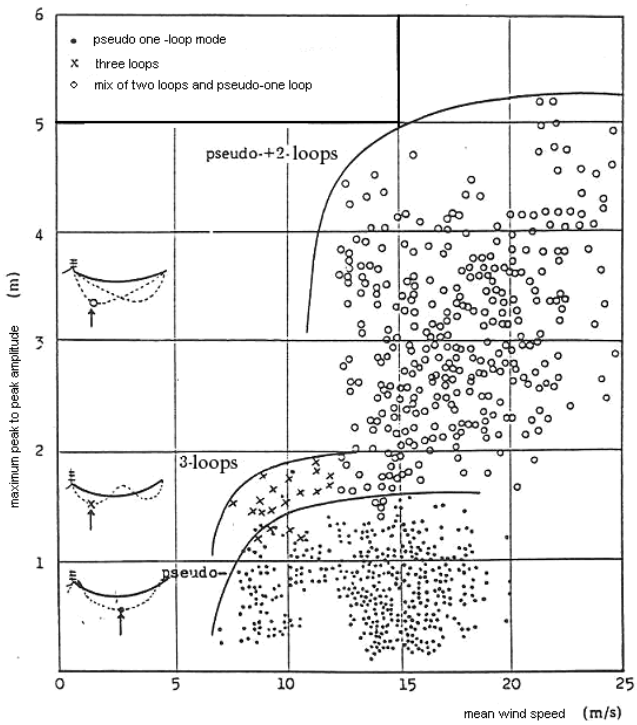

Figure 6.1: Maximum observed galloping amplitudes versus 30-sec mean wind speed at the Kasatori-Yama test line [Anjo et al., 1974]. Bundle of 4 x 410 mm^2 ACSR, two-span section, span lengths 312 and 319 m, conductor mass = 6.7 kg/m, subconductor diameter 26 mm, tension 123 kN/phase, sag at 0°C = 6.5 m. Pseudo-one loop frequency at 0.36 Hz, twoloop frequency close to 0.46 Hz and three-loop frequency close to 0.68 Hz. Conductor span parameter 0.05.

It was found that large-amplitude oscillation occurs when prevailing modes overlap. The dominant locus drawn by the oscillations was a vertical oval shape. The oscillation amplitude increases with wind speed, and it was observed that the oscillation amplitudes tended to reach a plateau at a certain wind speed.

At the Tsuruga test line, large-diameter bundled lines of six conductors were tested, and unusual horizontal oscillations were observed (Figure 6.2).

Studies at the Mt. Sanpo test line found that super-large bundled lines had a lower galloping frequency and smaller oscillation amplitude than conventional quad-bundle lines [Morishita et al., 1984].

Other tests conducted on the Tsuruga test line [Gurung et al., 2003] have confirmed that galloping of bundle transmission lines involves significant coupling of vertical and torsional motions. On bundles, the most likely galloping mode in deadend spans is the two-loop mode and large amplitudes of galloping occur when the torsion and vertical oscillations are in-phase.

Furthermore, deadend span line sections are more prone to galloping than semi-suspension spans. According to Matsuzaki et al. [1991], observations have shown that galloping occurs even in conditions that are stable according to the Den Hartog criterion, and it is considered that this phenomenon is closely linked to the fact that the twisting of conductors creates an unstable area.

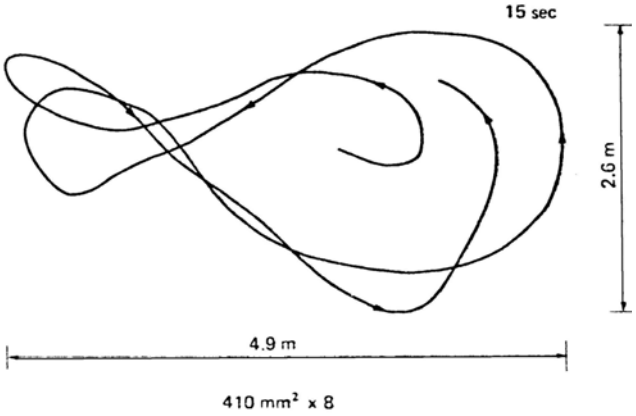

Figure 6.2: Orbit shape obtained on an eightconductor bundle during galloping due to wet snow with a wind velocity of 18 m/s (40 mph) [Morishita et al., 1984]

Hokuriku Electric Power Company experienced galloping [Kasima et al., 1996], and they found that galloping occurred with wet snow and most of the time at temperatures of -1 to +2ºC. Most galloping occurred at a wind velocity of 5 to 7 m/s (16 to 23 ft/s), and the highest wind velocity corresponding to galloping was 14 m/s (46 ft/s). Galloping occurred on spans located at an altitude below 100 m (328 ft) above sea level, but some galloping was also observed at altitudes up to 700 m (2297 ft). Based on the ratio of number of spans experiencing galloping over the total number of spans, it seems that bundles are more prone to galloping than single conductors.

In Norway [Halsan et al., 1998; Fikke, 1999], a monitoring system using video cameras was installed in a remote location to monitor galloping. Motion of the image of the conductor across the video screen was detected by optical sensors and used to trigger permanent recording of the motions for subsequent analysis. It was noted that several galloping events occurred without immediate impact on the operation of the lines, especially on a horizontal circuit. In fact, galloping, being comprised of mostly vertical motions, did not result in any interphase faults, although galloping events were observed. The authors concluded that the dynamic forces associated with these galloping events might contribute to progressive deterioration of the line due to fatigue from the large cyclic motions.

It is important to mention also that extensive field trials were carried out on operating power lines, mainly in North America, including systematic observation of motions of the overhead conductors during galloping occurrences. The main purpose of those tests was to validate the efficiency of detuning pendulums. The field sites were set up to include identical spans of conductors with and without the galloping controls subject to the same conditions of ice or wet snow and wind. The program generated an extensive database on galloping motions with and without the control devices [Havard and Pohlman, 1984; Havard, 1996].

6.2.1 Galloping observations by measurement and data analysis

Instrumented test lines and instrumented sections of operating lines are particularly valuable in advancing the understanding of galloping, since they produce numerical records. Galloping can occur in a number of different modes, and these often appear in combination. Recorded data on the variables that are involved in galloping can be used to

determine which modes were present in particular galloping events, and can often permit estimates of galloping amplitudes, even if amplitude was not directly recorded. Doing this requires detailed knowledge of the modes that can occur in the span or line section involved.

In Belgium, a two-circuit 400 kV/220 kV operating line in the Ardennes has been equipped for galloping detection, including instrumentation to record tension variations. This section of the line is composed of one deadend span and four suspension spans. The recording system was used between the 1980s until end of the 1990s. Some interesting events have been recorded and detailed in the literature and internal reports, and some are detailed in this section. The dynamic tensions during the galloping events were measured on twin horizontal bundles [Lilien et al., 1998]. Large tension variations of up to 100% peak-to-peak of the sagging tension were recorded. Despite the fact that the span was a deadend span, galloping occurred mainly in single loop. Many observations were made at different times, including some with the four spans of the section galloping in one loop, some with two-loop galloping located in only one span of the section, etc.

Analysis of the possible normal modes of the section was carried out using the procedures of Rawlins [2001]. These modes are determined based on linear elastic behavior, and several are pictured in Figure 6.3, identified by their frequencies. It should be noted that the motions that occur in natural galloping are not strictly identical to the undamped free normal modes obtained from the procedures of Rawlins [2001], since aerodynamic forces are not taken into account. However, those aerodynamic forces are small compared with the inertial and elastic forces at work in the conductors. Thus, they cause only small perturbations in the gross features of the normal modes—i.e., the frequencies and amplitudes of motion and tension variations. The free normal modes provide a good, if imperfect, representation of the major features of actual galloping.

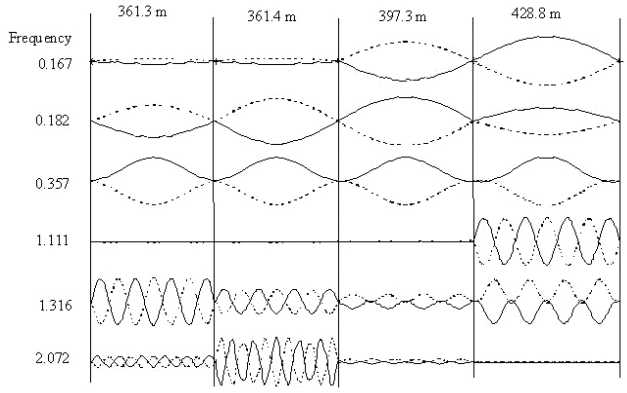

Figure 6.3: First six possible eigenmode shapes and frequencies for the four-span test section at Villeroux.

In February 1997, an interesting galloping case occurred on the deadend span of the 400 kV line. Figure 6.4 shows the wind speed component perpendicular to the line extracted from measurements taken during that galloping event. The galloping observed was a typical occurrence with large vertical amplitude, and was recorded under 25% turbulent wind. Galloping occurred with amplitudes around 6 m peak-to-peak, in a single loop on a dead-end span, at around 710 minutes and another significant event occurred around 830 minutes. The temperature was close to 0°C with a strong wind and freezing rain precipitations. Tension variations up to 25 kN peak-to-peak were recorded (Figure 6.5). One of the two events, for which only tension recordings were available, has been reconstructed as shown in Figure 6.6.

Another typical case of galloping event occurred on March 4, 1986 on the 220-kV line. The galloping occurred on a twin horizontal bundle of normal stranded conductors, 2 x 620 mm^2 AMS, all aluminium alloy conductor, with standard spacers. The subconductors diameter was 32.4 mm (1.3 in.) and their spacing was 0.45 m (1.5 ft).. The tension at 0°C was 35 kN per subconductor (sag 7.7 m). There were load sensors at the same deadend tower on five different arrangements of reference conductors or conductors with galloping controls, with one sensor per subconductor.

The wind speed during the galloping event was between 3 and 5 m/s (10 to 16 ft/s), measured at 10 m (33 ft) from ground level. The wind direction was not purely perpendicular to the line, but precise data was not available. The temperature was rising from -2.9°C up to -1.8°C during the event. The precipitation was freezing rain.

There were several separate periods of galloping during the episode. Tension records were obtained during two of them. In the first, the maximum tension variation in one subconductor observed was 27 kN peak-to-peak at a frequency of 0.36 Hz during 15 minutes. It was very similar in the other subconductor of the same bundle. Much lower tension oscillations were observed in the other phases, with a maximum of 4 kN in one phase and 14 kN in another.

The period of strong tension variations lasted for about 50% of the galloping period. The second period of galloping occurred with a maximum tension variation of 18 kN/subconductor but lasted for 30 minutes.

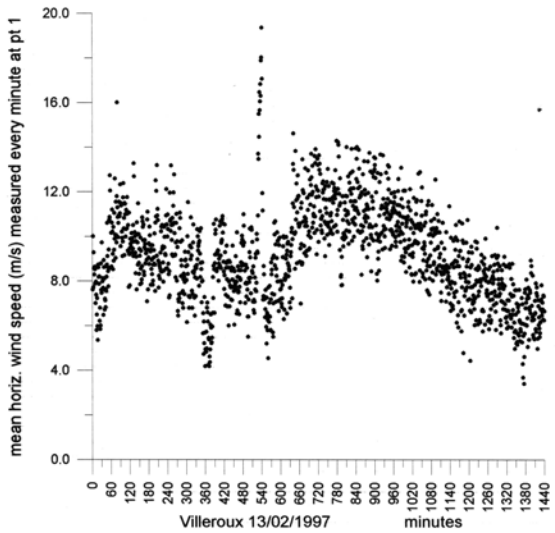

Figure 6.4: Mean wind speed measured as a function of time at the Villeroux line during the whole day of February 13, 1997. Recordings were made at one-minute intervals. Turbulence was quasi-constant around 25%.

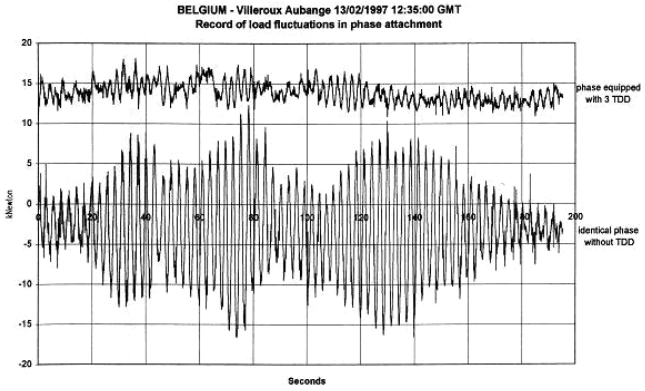

Figure 6.5: Typical tension variation at an anchor tower during actual galloping on untreated phase and phase with galloping control device, as measured on an actual twin-bundle 400-kV line at the Villeroux test station in Belgium. Upper trace: ±5 kN peak-to-peak for the phase with antigalloping devices. Lower trace: ± 25 kN peak-to-peak, in the reference phase during the same period of observation.

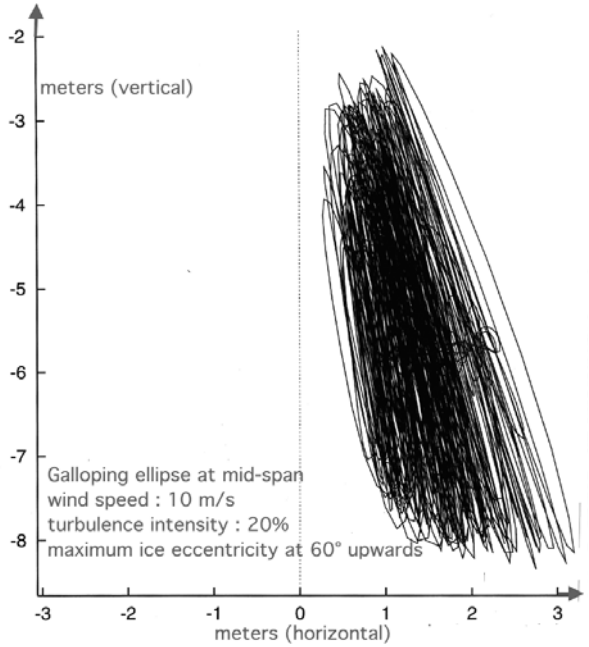

Figure 6.6: Galloping orbits at mid-span, recreated by simulation (10-minute records) based on tension recordings.

The buildup of galloping at the strongest value was in two steps, as illustrated in Figure 6.7:

1. A period of about 10 minutes with limited amplitude, 10 kN peak-to-peak, with some beating phenomena.

2. The last "beat" wave was a little bit higher in amplitude, 12 kN, and then it started to grow again, with no further beating. It reached the maximum amplitude of 27 kN in 5 seconds and stayed at that amplitude for a long time, 20 minutes, without any beating.

The frequency was the same (0.36 Hz) throughout the observed oscillations.

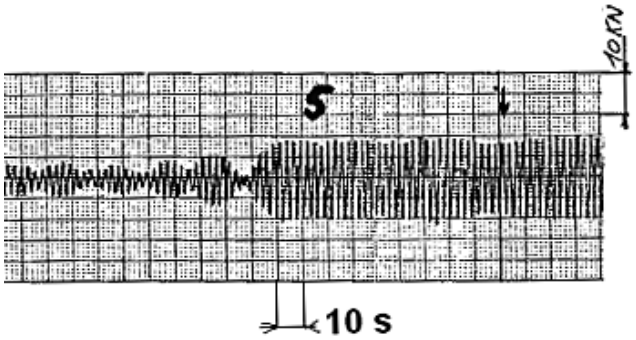

Figure 6.7: A recorded initiation of galloping at the Villeroux test station (courtesy Laborelec, Belgium) on March 4, 1986 with natural icing. The figure shows changes of tension over time in one subconductor at an anchoring tower. The main frequency observed is 0.36 Hz.

A third galloping event recorded at the Villeroux test station will be treated here. It was measured in the same 220 kV four spans section equipped with horizontal twin-spacered bundle. The FFT (Fast Fourier Transform) of the signal is reproduced in Figure 6.8. The recorded variable was the conductor tension at one of the deadends of the four-span section. The spectrum shows 12 major peaks, suggesting that 12 different oscillation modes were active. This is not the case as explained below.

Analysis of the possible normal modes of the section was carried out using the procedures of Rawlins [2001]. As already mentioned, several of these modes are pictured in Figure 6.3, identified by their frequencies. Table 6.1 lists the major spectral peaks of Figure 6.8, and associates many of them with eigenmodes of the section. Some of these peaks reflect the tension variations that are synchronous with the galloping motion, such as the eigenmode at 0.357 Hz, and those at 1.111, 1.316, 1.406, and 2.072 Hz. Other peaks reflect tension variation due to nonlinear effects. When galloping amplitude becomes large enough, stretching of the conductor at its extreme displacements causes increases in tension twice at each cycle. This introduces a tension variation at twice the frequency of the eigenmode. For example, the peaks at 0.66 and 0.74 Hz arise from autonomous two-loop galloping in the 397.3 and 361.4 m (1303 and 1186 ft) spans, which had resonant frequencies of 0.341 and 0.375 Hz, respectively. The eigenmode at 1.316 Hz causes a peak at 1.31 Hz directly, and one at 2.63 Hz due to nonlinear effects.

The peaks at 1.53 and 1.89 Hz are not associated with eigenmodes of the recorded phase. A 1.89 Hz peak was present in the tension spectrum of another phase, and probably caused motion in the deadend structure that was reflected in the signal leading to Figure 6.8. The 1.53 Hz peak has the same frequency as subspan resonance in another phase. It also corresponds to the longitudinal resonance of the four-span section [CIGRE, 1989; Lilien et al., 1998]. The peak may be associated with this coincidence.

Detailed knowledge of the eigenmodes associated with the spectral peaks permits calculation of the galloping amplitudes from the spectrum ordinates. Table 6.1 shows these estimated amplitudes reported as the maximum peak-to-peak amplitude in the section. Note that the source of the 0.36 Hz peak is ambiguous. That peak may mean either 2.5 m (8 ft) in the 0.182 Hz eigenmode, or 0.19 m (0.6 ft) in the 0.357 Hz eigenmode. It would require additional information, such as from an insulator swing transducer, to distinguish between the two possibilities. Fortunately, on-site observers were present during the galloping and could not have failed to see the 0.182 Hz mode. Thus, the tension peak at 0.36 Hz must have been from the 0.357 Hz eigenmode directly. The observers did report seeing, and filmed, two-loop galloping in the 361.4 m span with an amplitude of 3 m (10 ft). This is consistent with the 2.91 m (9.5 ft) calculated from the tension spectrum.

The combination of recorded data from an instrumented test line, supported by observer reports, with detailed analysis of the possible galloping modes permits greater insight into the complexity of galloping in nature. In the example described here, there are three different modes with amplitudes larger than 2 m (6.5 ft) simultaneously present. The picture that emerges highlights the challenge faced by on-site observers in attempting to describe galloping events verbally and the great value of a video record of the event.

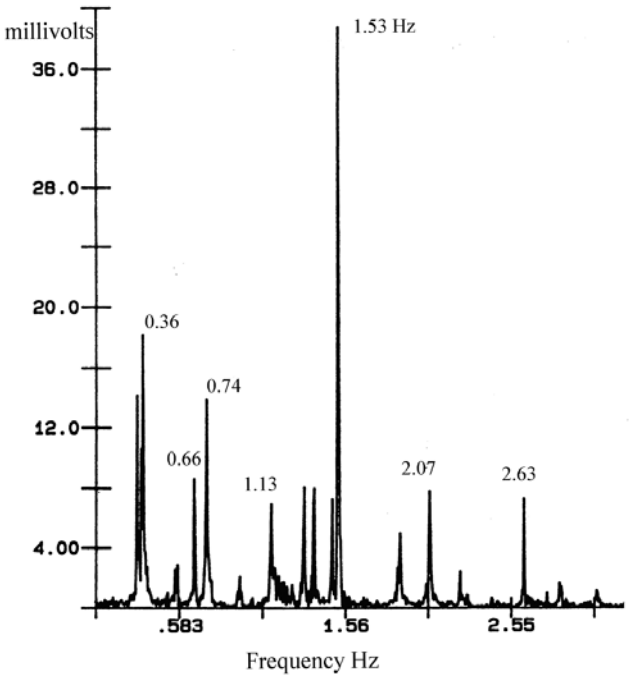

Figure 6.8: Spectrum of conductor tension, Sensor 4, Villeroux, April 4, 1989.

Table 6.1: Correlation of Spectral Peaks with Eigenmodes

Measured conductor tension peak frequency (Hz)	**Corresponding conductor displacement eigenmode frequency**	**Effect on tension**	**Estimated maximum conductor displacement (m peak-to-peak)**
0.33	0.167 Hz	Nonlinear	2.42
0.36	0.182 Hz	Nonlinear	2.49
0.36	0.357 Hz	Direct	0.19
0.66	2 loops in 397.3 m span	Nonlinear	2.38
0.74	2 loops in 361.4 m span	Nonlinear	2.91
1.13	1.111 Hz	Direct	0.40
1.31	1.316 Hz	Direct	0.15
1.38	1.406 Hz	Direct	0.014
1.53	Subspan gallop in another phase?		
1.89	Transfer from another phase.		
2.07	2.072 Hz	Direct	0.64
2.63	1.316 Hz	Nonlinear	0.27

6.2.2 How to collect field data

Providing trained personnel for the above purpose, during a period when service continuity is being challenged, is a hardship for utilities, but appears at present to be the most widely used method for acquiring data. There has been a clear trend toward programs spanning several utilities in order to speed field evaluations. A significant illustration of this trend has been EPRI's Research Project 1095, which involved 24 utilities and about 56 test areas, and the Canadian Electrical Association's similar field programs on control of galloping on distribution lines and on bundle conductor lines. These projects aimed at concentrating enough testing effort on a few devices at a time to permit their speedy evaluation. It appears that programs involving such wide involvement are necessary if in-service testing is to achieve useful objectives.

For participating utilities, programs of the above type encompass the following elements, given the choice of one or more protection systems to be evaluated.

Site Selection

The most important criterion in selecting a test area is the expected incidence of galloping. Past experience is the best guide. Smooth, unobstructed terrain is quite desirable. Additional factors are: accessibility from observer crew bases; number of circuits within an area that a crew can reasonably cover; and availability of a series of similar spans in similar terrain. The last of these is important because adjacent suspension spans in the same phase are coupled through support point movements longitudinal to the line. A protection method should be applied in a series of four or more spans, unless deadends permit isolation of the test section from adjacent spans.

Installation

The particulars of device installation depend upon the device involved, and supplier recommendations should be followed if possible. A short length of pipe or of conductor should be hung parallel to the line from one tower near ground level so that, later, ice thickness and shape can be measured. This sample will not reflect the effect of resistance heating of the conductors or of conductor rotation due to the eccentricity of the deposit, but will probably provide the best available basis for estimating what is on the conductors. Sags should be checked. If targets are to be installed to aid in estimating amplitudes and modes, it is convenient to do that at the same time devices are installed. Convenient observation points should be noted, along with reference dimensions of the line that might be useful in estimating galloping amplitudes. Choice of these locations may be influenced by whether or not targets are employed. If local inhabitants are to be recruited to report the existence of galloping, it may be most convenient to show them the test area at this time.

Observer Training

Observers should be provided with suitable report forms, camera and tripod to produce a film record that can be scaled, thermometer, and wind meter; they should also be trained in obtaining the information that is requested. The details of reporting forms vary from case to case. Some or all of the following information may be requested:

- Identity of observer
- Date and time
- Identity of line, circuit, and phase
- Voltage
- Location in the line by tower number
- Weather conditions, including precipitation, temperature, and wind speed and direction
- Mode of galloping: standing loops or traveling wave; one mode or several; number of loops; adjacent spans moving synchronously or not; subspan motion in bundles or in spans divided by interphase spacers or other devices
- Amplitudes of galloping: vertical, horizontal, and torsional, for bundles and for singles fitted with targets; shape of galloping ellipse
- Support point motions longitudinal and lateral to the line
- Location in the span where adjacent phases came closest
- Frequencies of observed modes of motion
- Shape and thickness of ice coating on conductors
- Behavior of nearby circuits

If the crew can make a video recording of the galloping, the form should include a map of the test area so that camera positions can be noted. The form may provide for later entry of line current and occurrences of trip-outs.

The most valuable form of report is a film of the galloping motion, and the observers need to receive guidance on where to stand and point the camera. An effective record of each of the directions of motion requires a different position, and the crew must be encouraged to take all film from a tripod and to expose film that can be scaled to determine amplitudes after the fact.

The most difficult items of requested information pertain to modes, amplitudes, and frequencies. It is advisable to use films of past galloping episodes in training observers to assess these items. Modes are most easily classified when viewing along the line where the entire span falls within a narrow field of view, and adjacent phases can be more readily distinguished. Amplitudes are easier to estimate from a broadside position because the middle of the loop can be more

accurately located. In addition, known line dimensions, such as insulator string lengths, can be more easily employed because effects of perspective are minimized. One useful technique (Hydro Electric Power Commission of Ontario) is to stand about one span length to the side of the line, hold a pencil vertically at arm's length, and mark off with the thumb a distance on the pencil that corresponds to panel height, insulator string length, or phase spacing. The pencil is then swung, still at arm's length, to line up with the middle of the galloping loop, and amplitude is estimated with reference to the known line dimension.

Classification of modes is rendered difficult when several are present simultaneously. When observed motions are too confusing, classification can sometimes be achieved by associating each discernible frequency with its amplitude. Later calculation permits the modes corresponding to the several frequencies to be identified. Even when motions are simple and easy to classify as to mode, frequency should be counted, since it permits the loaded sag of the conductor to be calculated.

A methodology for collecting data from a galloping event has been carefully described in a report prepared by a CIGRÉ task force [CIGRÉ, 1995]. Some parts of that document—including examples of galloping mode shapes, how to measure galloping ellipses, and how to install cameras during galloping observations—are shown in Figure 6.9, and galloping reporting forms are shown in Figures 6.10 to 6.12.

Since galloping instability depends not only on ice shape, aerodynamic force coefficients, and wind conditions, but also sometimes on structural characteristics, it is particularly important to evaluate them adequately. A review of methods and systems for collecting icing data has been completed recently [Fikke, 2003]. Moreover, there is still some additional information that might be gathered during or after the galloping event, such as the possibility to collect ice samples that have fallen from the cables. In rare cases, because the line collapsed and the cables lie on the ground, the ice samples may be still on conductors. In either case, security of the personnel must be considered first, but this will not be covered here. It should be noted that the orientation of the ice samples remains problematic in either case.

When collecting ice samples, the following procedure should be followed:

- Identify the conductor or ground wire or OPGW from which the ice sample comes.
- Identify the span number.
- Measure the distance from the nearest tower, since the ice shape may vary along the span due to the variation of torsional rigidity of the cable.
- Cut a section of the ice section and take a photograph with an object of known dimension (a rule is ideal for that purpose).
- Make a sketch of the ice sample section with its main dimensions, indicating the orientation of the ice section relative to the horizontal plane.
- Put the ice sample in a plastic bag to prevent loss by sublimation and keep it in a cold place.
- As soon as possible, measure the mass of the ice sample to deduce its mass per unit length.
- Prepare plaster molds of the ice samples for future aerodynamic characterization in a wind tunnel.

Galloping observed on operating lines in the field often shows variation between responses of apparently identical phases under the same conditions of ice and wind. Table 6.2 shows the report of one event on one of Ontario Hydro's test sites during a freezing rain occurrence in 1977. The test site includes two parallel circuits. One circuit has one phase with detuning pendulums installed and two phases with no devices, while the other circuit has no devices. The report shows that in a 30-minute period some phases with no devices remain still while others gallop with amplitudes between 0 and 3 m (10 ft). In the same time period some phases have single loop motion, while others undergo two-loop galloping.

Although most testing on operating lines is conducted through observer crews, remote sensing has been used in a few areas experiencing a high incidence of galloping. A system was developed by Ontario Hydro in connection with early detection of conductor icing [Kortschinski, 1968]. It employs a load cell in series with the suspension string at a selected tower. The signal from the load cell is telemetered to the system control center.

The arrangement at the support is shown in Figure 6.13. The load cell is restrained against movement lateral to the line, so only the vertical load at the tower is measured. The system is sensitive enough that as little as 1 mm (1/32 in.) of radial ice thickness can be detected. As originally conceived, it served the same purpose as monitoring carrier loss: detection of icing to permit timely ice melting. However, it was found that the dynamic loads caused by galloping in spans either side of the support could be detected and recorded on an oscillograph in the control center. With several load cells located in the same area of high galloping incidence, it was possible to make comparisons between protected and unprotected phases, without dispatching observers.

In Norway [Halsan et al., 1998; Fikke, 1999], a monitoring system using video cameras was installed in a remote location to monitor galloping. Motion of the image of the conductor across the video screen was detected by optical sensors and used to trigger permanent recording of the motions for subsequent analysis.

Table 6.2: Sample Report on a Galloping Field Observation (extract from Ontario Hydro Research Division Report No. 78-75-K, [Chadha et al., 1978])

GALLOPING OBSERVATION REPORT								
Observed by: PB & AV		Temperature: -1ºC		Conductor size: 795 kcmil		Date: Dec 18, 1977		
Location: Minden line		Wind direction:		Weather: Freezing rain		Voltage: 230 kV		
Time	Circuit & tower numbers	Wind speed estimate	Phase	Control device	Gallop mode	Peak to peak amplitude estimate	Electrical load	Comments
12:25	M9R 959-956	15-20 mph 24-32 km/h	Top	None	1 loop	1.8 m (6 ft)	88 MW	Ice thickness – 1/16 inch ~ 1.6 mm
			Middle	None		0		
			Bottom	None		0		
12:25	M9R 959-956	15-20 mph 24-32 km/h	Top	None	1 loop	1.8 m (6 ft)	88 MW	
			Middle	None	1 loop	0		
			Bottom	4 x 11.3 kg pendulums		0		
12:50	M9R 959-956	15-20 mph 24-32 km/h	Top	None	1 loop	1.8 m (6 ft)	88 MW	
			Middle	None	1 loop	1.5 m (5 ft)		
			Bottom	4 x 11.3 kg pendulums		0		
12:55	M9R 959-956	15-20 mph 24-32 km/h	Top	None	1 loop	1.8 m (6 ft)	88 MW	
			Middle	None	2 loop	3 m (10 ft)		
			Bottom	None		0		

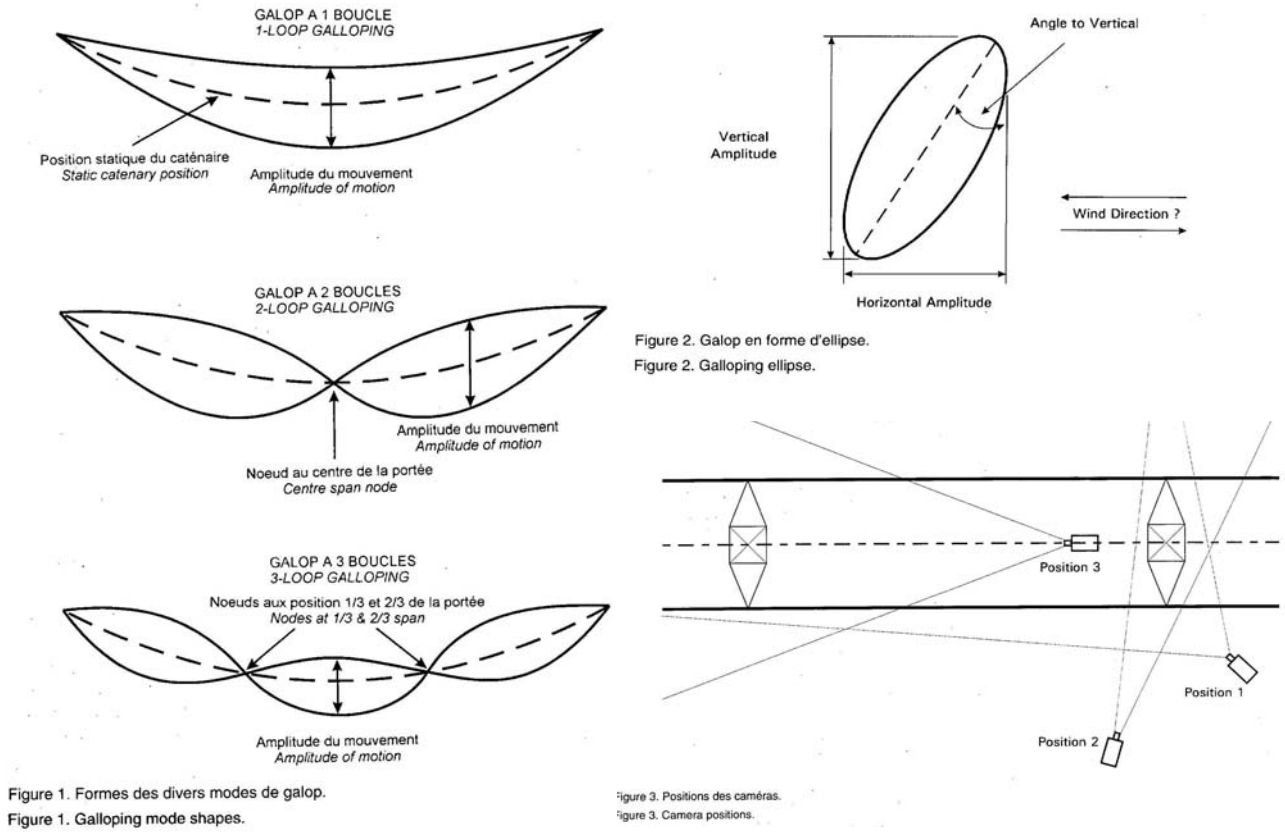

Figure 6.9: Field observations of overhead line galloping, ref. [Cigre, 1995]

Event No.	Sheet No.

CIGRE GALLOPING REPORTING FORM 1: ON-SITE OBSERVATIONS

Utility Name: Section Name: Date of Event:

Span Number	1.	2.	3.	4.	5.	6.	7.	8.
Circuit Identifier								
Phase Identifier or G/W								
Time								
Vertical Amplitude (m) *								
No. of Loops (1,2,3, etc)								
No. of Cycles in 1 min.								
Elliptical Motion? (yes/no)								
Horizontal Amplitude (m)								
Angle to Vertical (°) *								
Inclination								
Torsional Motion? (yes/no)								
No.of Loops (1,2,3, etc)								
Angular Amplitude (°)								
No. of Cycles in 1 min.								
Wind speed (m/s)								
Angle to Line (°)								
Air Temperature (°C)								
Type of Control Technique								

Type of Icing (tick type)	
Rime (freezing cloud/fog)	Glaze (freezing rain)
Wet Snow	Other (describe over)

Give basis for sketch: e.g. fallen ice, tower icing, line observation, conductor sample, etc.

Video/Movie made? (yes/no)	

Flashovers (ccts and phases)

Damaged Items (tick)	
Conductors	Towers
Insulators	Fittings

Other Observations: e.g. duration of galloping (continue overleaf)

Form completed by:	

* See illustration overleaf

Figure 6.10: Galloping reporting forms, ref. [Cigre, 1995]

Event No.	Sheet No.

CIGRE GALLOPING REPORTING FORM 2: LINE AND SITE INFORMATION

Utility Name: **Line Section:** **Date of Event:**

Circuit Identifier	1.	2.	3.	4.
Voltage (kV)				
Conductor Type and Stranding				
Conductor Dia. (mm) / Weight (N/m)				
Cond. Tension (kN) at Galloping Temp.				
Number of Conductors per Phase				
Bundle Size and Format (sketch)				
GW or OPGW Type and Stranding				
GW or OPGW Dia. (mm) & Wt. (N/m)				
GW or OPGW Ten. (kN) at Gal. Temp.				

Sketch of Line Section	
Show span lengths and control device locations.	Mark spans that galloped (G) or flashed over (F).

Details of Control Techniques
Type, dimensions, weights, etc. Service problems, etc.

Sketch of Typical Tower
Show tower type, phase separations,heights, etc.

Details of Terrain	
Flat Rolling Hilly Mountainous	Rural Coastal Wooded Urban

Form completed by:	

Figure 6.11: Galloping reporting forms, ref. [Cigre, 1995]

Event No.	Sheet No.

CIGRE GALLOPING REPORTING FORM 3: DAMAGE AND COSTS

Utility Name: **Circuit Section:** **Date of Event:**

Electrical Faults		
No. of Flashovers:	MVA Interrupted:	Total Duration:

Mechanical/Electrical Damage		
Component	**Type of Damage**	**No.**
Conductor	Burns	
	Breakages - location and type of damage	
	Fatigue at suspension clamp	
	Wear at spacer	
	Jumper failure	
	Other (specify)	
Insulator (identify type)	Detached	
	Broken	
	Other (specify)	
Spacers	Loosened clamps	
	Broken arms	
	Other (specify)	
Stockbridge dampers	Loosened clamps	
	Broken messenger cables/loss of weights	
	Other (specify)	
Linkages	Worn	
	Broken	
	Distorted	
	Other (specify)	
Suspension Clamps	Worn	
	Burnt	
	Other (specify)	
Towers or Poles	Loss or failure of bolts	
	Distortion of members, hole enlargement	
	Fatigue failure of members	
	Collapse (partial/total)	
	Loosening of poles	
	Other (specify)	

Costs of Galloping Event ($k)			
Repairs		Loss of Energy Supplied	
Remedies (e.g. control methods)		Replacement Generation	

Other Consequences (e.g. road closures, public complaint, etc.)

Form completed by:	

Figure 6.12: Galloping reporting forms, ref. [Cigre, 1995]

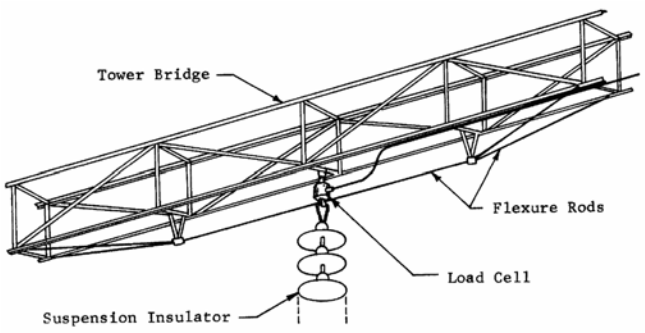

Figure 6.13: Arrangement for sensing vertical load in insulator string [Kortschinski, 1968].

6.3 Tests using artificial ice

As mentioned previously, to obtain galloping test results in a relatively short time and with a well defined test set-up, it is possible to install artificial ice shapes on the conductor of a full scale test line. There are few such lines in the world. The two most well known still in service, are installed in Japan (where many such sites exist, the most famous one being Mogami test line) and in Canada (IREQ facilities - total length of 1.6 km). These installations may have up to three suspension spans under testing. Japan researchers are conducting such tests for more than thirty years [Anjo et al., 1974].

6.3.1 Description of artificial ice shapes

Different artificial ice shapes have been used to induce galloping on test lines. The most common artificial ice shapes used on test lines are the D, crescent, triangular and D-modified shapes. Reproductions of natural ice shapes have also been used and the crescent shape is one of those. However, on those tests, the same shape is used along the span while on a real accretion it varies according to the torsional stiffness of the cable which decreases as it goes further from the tower. The wind speed also varies along the span and with the height of the cable and may also influence the amount and shape of ice accretion.

The square prism which induces galloping in wind tunnel [Parkinson and Smith, 1964] was tested at IREQ test line during four weeks. The use of such a prism would have been advantageous since it would have induced galloping with winds coming from both sides of the test line. However, on a 27.8 mm ACSR conductor, it induced only torsional instability with a vertical displacement limited to an amplitude of the order of the conductor diameter. This difference of behaviour was explained by the low torsional stiffness of the conductor compared with the wind tunnel model. However, Edwards [1966] obtained 0.5 m galloping amplitude with such a shape but it was much less prone to galloping on their test line than a D-shape.

Section 6.4 shows the aerodynamic characteristics of some typical ice shapes, including the “D” shape, which has been used frequently in galloping studies. D shapes (Figure 6.14 and Figure 6.15) and some “aerodynamically-similar” profiles (Figure 6.16) are found to be very unstable when their vertical face is facing the wind, even when the wind is not necessarily perpendicular to the span. These shapes show a very different aerodynamic behavior compared to triangular or crescent-type eccentricity (Figure 6.17, 6.22, 6.23), particularly when the ice is located on the windward side of the conductor.

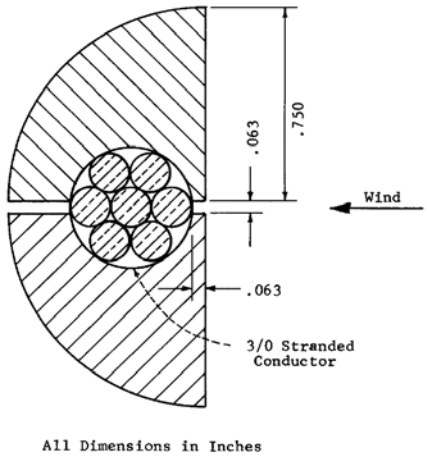

Figure 6.14: Simulated ice section employed by Tornquist and Becker [Tornquist and Becker, 1947].

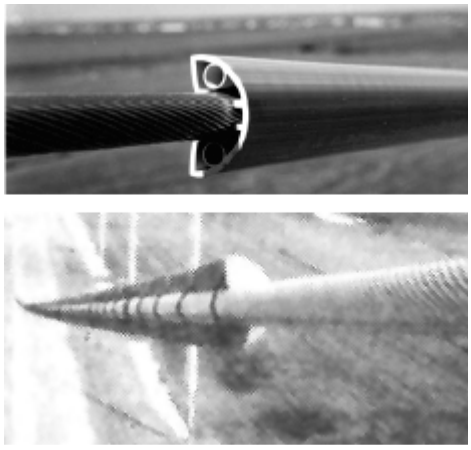

Figure 6.15: Typical artificial D-shapes (courtesy Hydro Québec)

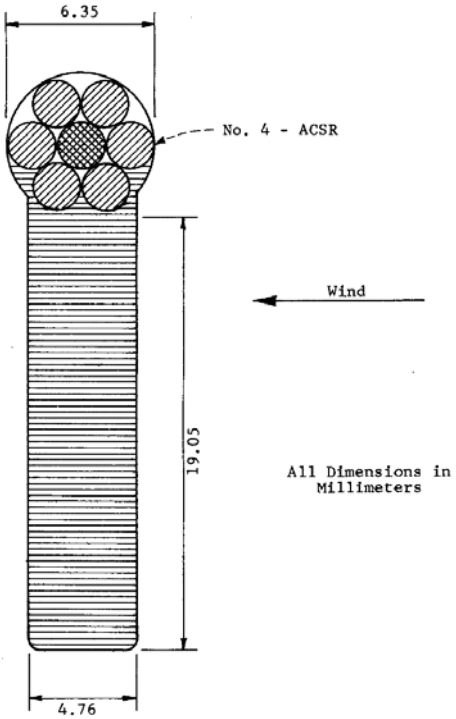

Figure 6.16: Simulated ice section employed by D.C. Stewart [Stewart, 1937].

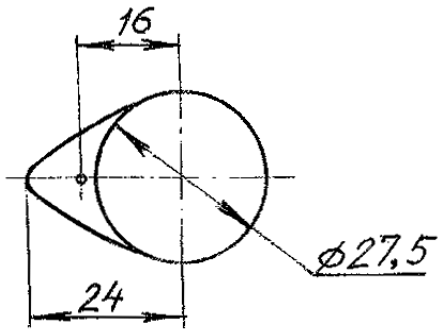

Figure 6.17: Typical triangular-type artificial airfoil employed by Vinogradov [Lilien and Vinogradov, 2002].

It is more difficult to create galloping-type instabilities when testing with artificial, triangular or crescent-shaped profiles. Only particular angles of attack would allow significant galloping amplitudes, and the specific angle of attack may be dependent on structural properties. But actual ice shapes are more close to these triangular or crescent-shaped profiles.

Galloping can be strongly dependent on structural properties, such as torsional stiffness, moment of inertia, natural frequencies, the ratio between frequencies in different directions of movement, etc. Test spans need be designed to

reproduce these properties, which is not always easy. For example, testing on a single deadended span will not be able to account for important influences, especially span-to-span motions at suspension insulator strings. For that reason, most of the existing test arrangements have at least two spans in the test section.

Tests with artificial ice are usually viewed as not providing strong enough validation to support confident use of proposed protection schemes. In-service testing is required. Antigalloping devices that modify or interfere with the galloping mechanism—which is practically all of them, except perhaps, interphase spacers—should be tested on lines with different conductor sizes and span lengths and in different locations, and over a certain period of time, since they may perform differently with different densities and shapes of ice accretion.

To circumvent this limitation, some researchers have decided to spray water on conductors of a test line during cold, windy days [Egbert et al., 1984]. However, this method is tedious and time consuming. It must also be repeated until the anti-galloping device has been exposed to different shapes of ice that the researcher feels that they are representative of what is expected to happen in the field and to different line geometries.

The artificial ice shapes, or airfoils, are generally reproduced in plastic, silicone rubber, or metallic foil in lengths of about 1 to 2 m. These airfoils are fixed on the conductor in a way that their orientation is sufficiently constant on a significant part of the span as shown on Figure 6.18 using the air-foil of Figure 6.17. This is particularly difficult on single conductors on long spans because conductors tend to rotate during installation. It must be noted that airfoil weight and center of gravity may be of dramatic importance on instabilities, as shown in Section 6.4. Consequently, on single conductors, it is easier to install artificial ice shapes having their center of gravity coincident in a horizontal plane with the center of the conductor. Because of the high torsional stiffness of bundles, a D-modified shape which has its center of gravity outside the conductor may be used on it.

As the instability may be limited to a small range of angles of attack, it may be very cumbersome to change airfoil all along the span(s) and then to wait for an appropriate wind speed(s) and orientation. Some test stations use rotational devices at the support points to permit rotation of the conductor, whether single or bundle, on the whole span.

Galloping is readily obtained with many shapes, when the airfoil is installed at an angle of attack of about 180°—that is, on the downwind side of the conductor. The result is the Den Hartog type of galloping under conditions that are rare on real lines, because it would need a reversal of the wind speed compared to that present during ice accretion. This is of limited practical interest in evaluating the performance of antigalloping devices.

To reproduce actual galloping conditions, it is strongly recommended to install a crescent-shaped airfoil on the windward side of the conductor. Generally, but not always, unstable positions are found at about 0° and 90°, both upwards and downwards. Figure 6.19 shows the zones of instability of a twin-bundle span using the airfoil shown in Figure 6.17 and Figure 6.18.

It can also be very useful to install a D-shaped airfoil because galloping would occur at lower wind speeds and may be observed during more hours, which helps to measure and to observe many details. Such testing procedure would, nevertheless, not be useful to test antigalloping devices based on the torsional mechanism. But it would be valid to evaluate, for example, interphase spacers or mechanical damping devices.

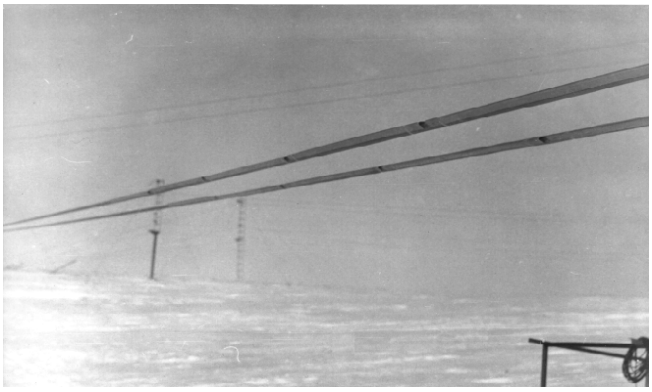

Figure 6.18: Artificial airfoil installed on twin bundle at Talasker test station [Lilien and Vinogradov, 2002].

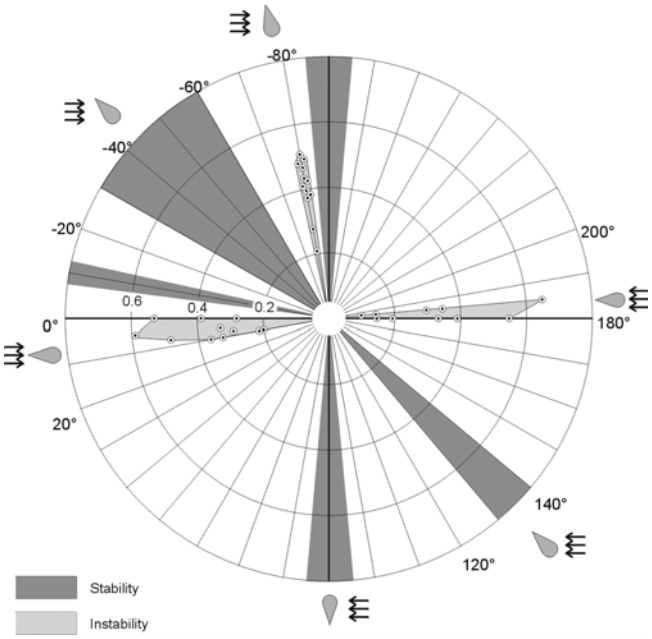

Figure 6.19: A polar representation of zones with no instabilities observed, dark grey, and the three narrow zones where instabilities were observed, light grey with dots, on a twin-bundle span using an airfoil shown in Figure 6.17. The radius coordinate indicates the ratio of galloping amplitude/sag [Lilien and Vinogradov, 2002].

6.3.2 Tests on Single-Conductor Lines with Artificial Ice Shapes

The need to use simulated ice, in order to permit year-round controlled testing for research purposes, was evident to early investigators. The first successful test span using artificial ice was apparently that described by D.C. Stewart of Niagara Mohawk [Stewart, 1937].

Stewart erected a single 32 m (104 ft) span of No. 4ACSR (6/1) in 1936, and attached to it the wax section shown in Figure 6.16. The span galloped in one loop. The trajectory of the conductor was elliptical, with the major axis vertical. Maximum amplitude was about 1 m (3 ft). The motion that occurred included considerable rotation of the conductor, more than 180° over the course of a cycle of motion.

Stewart utilized the span for fundamental investigations, including an assessment of the energy balance of the span during limit cycle motions.

In 1947, Tornquist and Becker of the Public Service Company of Northern Illinois reported results of tests on two test lines equipped with artificial ice [Tornquist and Becker, 1947]. 3/0 copper conductor was employed in both lines. The first line had a single 76 m (250 ft) span, which was deadended through springs at eachend. The "ice" shape employed is shown in Figure 6.14, and was chosen on the basis of extensive wind tunnel model tests. The wooden sections were about 76 cm (30 in.) long and were fastened to the conductor with iron tie wire. The span galloped in two, four, and six vertical loops, generally without significant accompanying torsional motion. Galloping occurred only when the wind struck the flat side of the section, and then only when wind direction was more than 10° off perpendicular to the span. There was no one-loop galloping.

Tornquist and Becker's second line had four 76 m (250 ft) spans and three phases. The middle three supports were in suspension. The same "airfoil" was employed as in the first line.

The line galloped in one loop (Figure 6.20), in two loops (Figure 6.21) and in a combination of these modes. Amplitudes as great as 2.3 m (7.6 ft) were achieved. Apparently significant torsional motion did not occur.

One of the important problems in tests using artificial ice concerns how well the behavior obtained represents that occurring under conditions of natural icing. The presence or absence of torsional motion, and its role in natural galloping, is one of the central issues involved. Stewart had torsional motion. Tornquist and Becker, in general, did not, using the D-section. In an AIEE paper [Edwards and Madeyski, 1956] reported use of the D-section in a span at Ontario Hydro's Port Credit test line. The conductor was 336.4 kcmil ACSR (30/7) in a 126 m (412 ft) span. They obtained only very small amplitude galloping of the span when torsional motion was absent, but large amplitudes when torsional motion occurred. In certain tests, the torsional frequency was tuned to coincide with vertical natural frequencies, and this had the effect of broadening the conditions under which spontaneous galloping would occur. They interpreted the failure of the span to

display torsion-free galloping as an indication that terrain in the vicinity of the Port Credit test line was too obstructed to permit the smooth winds on which D-section galloping was predicated.

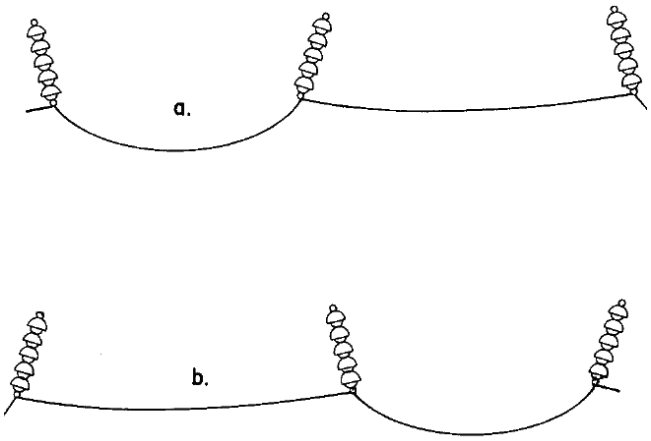

Figure 6.20: Coupled one-loop galloping of adjacent spans [Tornquist and Becker, 1947].

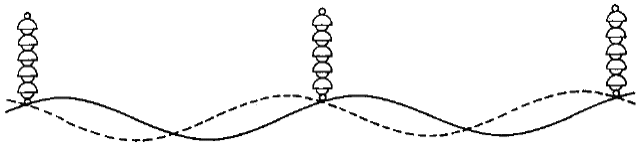

Figure 6.21: Two-loop galloping [Tornquist and Becker, 1947].

Binder reported similar experience with D-sections in a 1962 article in Electric Light & Power [Binder, 1962], but drew a different conclusion. He had fitted six 76 m (250 ft) spans of 3/0 and 300 kcmil copper conductor with wooden D-sections and found, like Edwards and Madeyski, that torsional tuning to encourage torsional motion was needed in order to obtain high-amplitude galloping. He concluded that such tuning does occur on occasion with natural ice coatings, and is responsible for the galloping that actually takes place. He investigated use of torsional dampers for preventing galloping.

However, Ratkowski [1963] also reported work on a short outdoor model span, demonstrating torsion-free galloping using the D-section. Ratkowski's "conductor" was a flat steel strip 8.7 m (28.6 ft) long with wooden quarter-rounds attached to its upper and lower surfaces to form the "D." He concluded that conductor rotation is not required in galloping of iced conductors.

Meanwhile, continued investigation at Ontario Hydro pointed toward the damping effect of the wooden airfoils used by Edwards and Madeyski as the explanation for the Port Credit test span's failure to gallop in the absence of torsional motion. In 1966, Edwards [Edwards, 1966] reported use of D-section airfoils of extruded polyethylene on a test line at Scarborough, Ontario. The plastic airfoils caused considerably less damping than had the wooden airfoils. The test line, comprising nine 335 m (1100 ft) spans of 795 kcmil ACSR, displayed frequent high-amplitude galloping, without the need for torsional tuning. Amplitudes as great as 3 m (10 ft) peak-to-peak were obtained in the two-, three-, and four-loop modes. A square-shaped section was also tried, with more limited success. The test line has been used extensively in evaluating proposed systems for controlling galloping.

More recently, at the Hydro-Quebec test line, Van Dyke and Laneville [2004] observed that the D-section (Figure 6.15) was more prone to gallop with winds having an angle of about 45º from perpendicular to the conductor. They concluded that, in that case, the wind flows around an effectively thicker D-section—that is, it has a different aspect ratio. For example, for a direction of about 50º from the perpendicular to the line, the apparent aspect ratio of the D-section becomes 0.78 instead of 0.5. Based on research by Nakamura and Tomonari [1980], who have measured the aerodynamic characteristics of D-sections with different aspect ratios in a turbulent flow, D-sections with aspect ratios above 0.73 will experience galloping that starts spontaneously from a resting state. This result emphasized the fact that a mathematical model based on aerodynamic coefficients corresponding only to the direction perpendicular to the section considered will not provide adequate results for other wind directions.

During the same tests, they also found that conductor galloping may induce large bending amplitudes in the conductor [Van Dyke and Laneville, 2005]. They measured bending amplitudes as high as 3.0 mm (0.1 in.) peak-to-peak in the conductor adjacent to a metal-to-metal clamp corresponding to fy_{max} values as high as 1.2 m/s (4 ft/s) peak. Those results are covered with more details in Section 6.3.1 on conductor fatigue.

The D-section's apparently fickle behavior has roused considerable debate among researchers concerned with galloping. However, the D-section can be quite energetic once it gets going, and the galloping behavior that then occurs is very

similar to that observed in natural galloping. This is a considerable virtue because, for a number of years, the "D" was one of the few artificial sections that enjoyed that distinction (square sections had also performed well in a few tests). Attempts to produce high-amplitude galloping with shapes more representative of natural ice had been largely unsuccessful [Edwards and Madeyski, 1956; Alcoa laboratories].

In the 1970s, renewed efforts at Ontario Hydro to obtain high-amplitude galloping with sections similar in shape to natural ice have produced more fruitful results. Nigol and Clarke [1974] made silicone rubber casts of actual ice shapes taken from conductors (Figure 6.22) and, based on them, had the extruded plastic shapes shown in Figure 6.23 manufactured. The sections were fitted to conductors in a test line at Kleinburg, Ontario, having three 244 m (800 ft) spans, the middle one supported in suspension. Extra care was taken to simulate natural conditions, by applying ballast slugs to the span to make up for the smaller density of the plastic shapes relative to natural glaze.

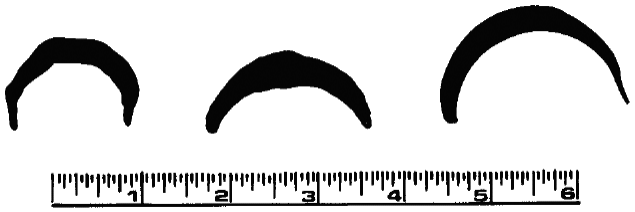

Figure 6.22: Silicone rubber casts of sections of ice removed from conductor [Nigol and Clarke, 1974].

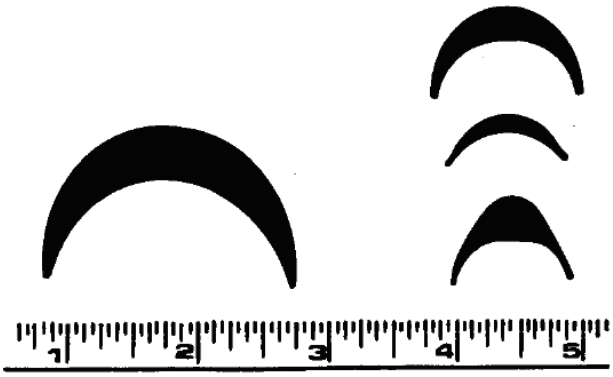

Figure 6.23: Plastic test foils used to simulate natural ice deposits [Nigol and Clarke, 1974].

Nigol and Clarke obtained high-amplitude galloping similar to that of naturally-iced spans for certain ranges of foil orientation (angle-of-attack). Galloping occurred in one-, two-, and three-loop modes and in higher modes. One-loop amplitude as great as 3.7 m (12 ft) was obtained. The galloping always involved torsional motion.

Nigol and Clarke viewed their experience with these shapes as supporting the hypothesis that torsional motion is required when natural galloping is to occur. They, and later Nigol and Havard [1978], have pursued development of devices to control the torsional motion in such a way as to prevent high-amplitude galloping.

Tests with shapes not typical of natural ice [Tornquist and Becker, 1947; Ratkowski, 1968; Edwards, 1966; Alcoa laboratories] have shown that torsion is not in principle necessary. Analyses of films of natural galloping [Edwards and Madeyski, 1956] have shown that torsion does not always occur. However, the results of Nigol and Clarke [1974] indicate either: that the most commonly-observed ice shapes require torsional participation; that Nigol and Clarke's models still do not represent natural ice sufficiently well; or that some important factor is not yet comprehended in existing galloping theory or testing. Most workers pose the question in terms of the percentage of occasions in which torsional motion is crucial to instability. While some have expressed the opinion that the answer is "rarely," and others that the answer is "always," objective evidence permitting resolution of the question does not appear to be available. This situation significantly limits the usefulness of tests with artificial ice for evaluating protection methods for single conductors.

It seems that more or less all observations, except those with tuning between vertical and torsional frequencies, cited in this subsection on single conductor, are related to Den Hartog type of galloping:

- either with a significant ice eccentricity, thus with significant torsion, clearly the case of Figure 6.17, but also to a lesser extent with Figure 6.23, thus with significant contribution of inertial effect, inverse pendulum effect and pitching moment effect, or
- with a very limited eccentricity, Figure 6.14, thus with limited torsion.

In addition, Nigol and Buchan [1981] have observed that some ice shapes showing Den Hartog conditions in the quasi-static aerodynamic coefficients have not generated instabilities during dynamic testing. This observation tends to prove that, in some cases at least, the quasi-steady theory used in all modeling today cannot be considered as valid in all cases.

6.3.3 Tests on Bundle Conductor Lines

In the case of bundled conductors, there is wide agreement that torsional motion accompanies vertical galloping all or most of the time [Anjo et al., 1974; Liberman, 1974; Nigol and Havard, 1978; Matsubayashi, 1977]. Problems of properly modeling natural ice are of significance even in the case of bundles. Anjo et al. [1974] found that torsional motion led vertical motion in phase during an episode of galloping with natural ice, but lagged it during galloping with artificial ice having a shape related to the D-section. They were testing a four bundle of 950 mm^2 ACSR at the Mt. Kasatori test line, in a series of two spans 310 and 315 m (1017 and 1033 ft) long.

This observation is not a definitive claim against D shape testing, as many parameters influence the phase shift between torsion and vertical movement, e.g. ice shapes, torsional damping, ratio between vertical and torsional frequencies. Nevertheless it clearly shows the vast field of possible galloping on actual lines, some of them being easily observed by particular ice shapes, such as the D shape. But these are not necessarily the shapes to be controlled as they are special cases different from actual observed ice profiles.

A modified D shaped artificial ice has also been used on bundle conductors. Tsujimoto et al. [1983] conducted tests using such an artificial ice accretion at the Juoh test line to compare the galloping behavior of eightbundled and quad-bundled conductors.

Additional tests were also conducted on the eight-bundled conductors with natural ice accretion at the Tsuruga test line. The tests demonstrated that the fluctuations of mechanical tension for eight-bundled conductors were similar under both artificial and natural ice conditions. The amplitude of the fluctuation in tension, for eight-bundled conductors, increased less rapidly than for quad-bundled conductors. Furthermore, the ratio of tension fluctuation over static tension for eight-bundled conductors was about 80% of the value for the quad-bundle. The maximum wind velocity reached during those tests was 20 m/s (65.5 ft/s).

Asai et al. [1990] performed galloping tests on a deadended test line having a span length of 162 m (531 ft), using modified D artificial ice accretions on a twin bundle. With an average wind velocity of 15 m/s (49 ft/s), they obtained a ratio of maximum dynamic tension variation over static tension of the conductor of 2.6. It has to be noticed that the variation in tension is not symmetrical with respect to the average tension. The same configuration was tested with one interphase spacer in the span, and the ratio decreased to 2.0. Oura et al. [1995] obtained the same ratio of dynamic conductor tension over static tension of 2.6.

Using a triangular-type artificial ice shape, Ozaka et al. [1996] obtained peak-to-peak galloping amplitudes as large as about 6 m (19.5 ft) on the Mogami test line. Furthermore, horizontal large-amplitude, figure eightshaped galloping was observed. Variation of peak-to-peak dynamic conductor tension during galloping reached a maximum of 1.2 times the static tension.

6.3.4 Observations, Measurements, and Recordings

The procedures employed in conducting tests on spans fitted with artificial ice vary with the purpose of the test and the productivity of the span. Some testing employs simple visual observation for acquiring data. Amplitudes are estimated with reference to known line dimensions, frequencies are timed with a watch, and wind is measured with hand-held anemometers. More often, suitably chosen transducers and recording systems are employed.

Conductor motions have been sensed by attaching a string to the conductor, the string being supplied from spring-loaded reels at ground level. A multiturn potentiometer coupled to the reel shaft makes an electrical signal representing vertical amplitude available for recording. This method was developed by A. S. Richardson and was utilized by Alcoa Laboratories.

Accelerometers have also been used for sensing vertical, horizontal and torsional amplitudes [Edwards and Madeyski, 1956; Nigol and Clarke, 1974]. The conductor displacement along the span may be inferred from two accelerometers signals [Van Dyke et al., 2006]. Bending amplitude recorders of the type normally utilized in aeolian vibration testing have been applied on occasion for galloping recording. It should be noted that some of these bending amplitude recorders have a lower limit to the range of frequencies recorded, which may preclude their registering normal galloping motions.

The amplitude of galloping, or its severity, can be inferred from support point load variations and insulator string deflections if conductor tension is known. Clinometers may be added on the insulator string of suspension towers to calculate the components of force transmitted to the tower.

In addition to instrumentation of the above types, Anjo et al. [1974] employed an optical tracker for studying orbits of motion and for determining the space swept by a conductor during an extended episode of galloping.

Finally, to relate the galloping recordings to mathematical models, it is important to measure the wind velocity and direction as well as the temperature.

6.4 Testing in wind tunnel

The basic mechanism of galloping, described by Den Hartog [1932], was outlined in Section 3.1. Analysis of a model constrained to move solely in the vertical plane led to the criterion that galloping may occur if:

$L_\alpha + D \leq 0$ with clockwise reference for positive angles (4.1)

$D - L_\alpha \leq 0$ with anticlockwise reference for positive angles (4.2)

Where

α: Angle of attack of the wind on the iced conductor

D: Drag force acting on the iced conductor

L: Lift force acting on the iced conductor

$L_\alpha = dL/d\alpha$: Slope of the lift Vs angle of attack curve

Those expressions known as the Den Hartog criterion may also be expressed as a function of the aerodynamic coefficients of lift and drag and their derivatives:

$C_{L\alpha} + C_D \leq 0$ (clockwise) (4.3)

$C_D - C_{L\alpha} \leq 0$ (anticlockwise) (4.4)

Tornquist and Becker pointed out that this criterion had actually been derived as early as 1919 in connection with autorotation of airfoils [Tornquist and Becker, 1947]. Later on, based on aerodynamic coefficients of a square section obtained in a wind tunnel, Parkinson and Smith [1964] added to this criterion the effect of system damping on the onset of galloping, or the minimum wind velocity at which galloping occurs. Other modelisations have then been derived to take into account the effect of conductor torsion, line geometry, etc. However, one constant remains in these modelisations, it is the fact that aerodynamic coefficients of the iced conductor drive conductor galloping.

The fluid forces acting on an iced conductor shape can be measured in wind tunnels on stationary models assuming the quasi-steady theory is valid (see section 3.1.3). Thus, efforts have been made to verify the analyses against tests in wind tunnels and on full-span test lines. On the whole, correlation has been good where theory has been tested against experiment in wind-tunnel simulations. However, correlation has been less evident where full-span galloping in natural wind is involved.

Many teams have worked around the world to obtain aerodynamic properties of ice shapes. For these measurements, static wind-tunnel tests are performed by installing the conductor with its ice shape supported rigidly within a wind tunnel with sensors to measure the lift, drag, and moment for the chosen wind speed. The support system can rotate the conductor allowing the measurement of the aerodynamic properties at different angles of attack. The conductor support must be designed to enable measurement of the appropriate pitching moment.

Some of these teams were trying to reproduce actual ice shapes due to wet snow or freezing rain. To obtain these shapes, two methods were used:

- Collect ice shapes fallen from the line following galloping events. Then they reproduced the ice shape by creating a mold, using low-temperature curing silicone rubber, and further creating replicas of the ice shape using that mold, which were then attached to a simulated conductor for use in the wind tunnel [Nigol and Buchan, 1981].
- Create ice accretions in an icing wind tunnel in which samples of conductors are placed across the wind tunnel, and freezing rain or snow is deposited on the conductors during a given time. The conductor samples are installed with end supports having a torsional stiffness equivalent to that of the in-span conductor [Chan et al., 1992; Fujikura personal communications; Nigol and Buchan, 1981].

It is useful to note that the aerodynamic lift, drag, and moment coefficients are, in principle, reasonably independent of the particular conductor diameter of the sample tested in the wind tunnel. Only the ratio of ice thickness over conductor diameter and the geometric shape of the ice layer are important. Any other ice profiles that can be obtained by using a scale factor would have the same aerodynamic coefficients.

6.4.1 Aerodynamics of some ice coatings and corresponding potential incidences of the Den Hartog instability condition

Many investigations have been described in the literature regarding the aerodynamic properties of replicas of actual ice shapes. These shapes were obtained during galloping observations, usually as pieces of ice shed from the line (Figure 6.24 to Figure 6.26), or in a wind-tunnel experiment simulating natural icing conditions. This last procedure used a piece of conductor fixed in the vertical and horizontal directions but able to rotate with appropriate torsional stiffness. Snow or ice was injected into or created in the wind tunnel to produce the ice accretion shapes, which are dependent on temperature, wind speed, duration of the icing event, and conductor torsional stiffness. Afterward the ice shapes were reproduced and the aerodynamic forces measured in a classical wind tunnel. Most of these complex tests were performed in Japan [Otsuki and Kajita, 1975] and Canada [Buchan, 1977].

As a general conclusion based on such tests performed during the last thirty years, the results can be summarized as follow:

- Ice accretions having a shape similar to an airfoil with significant eccentricity are more susceptible to experience Den Hartog instability; those shapes occur mainly on bundle conductors (Figure 6.24 and Figure 6.25). The eccentricity ε is defined as the ratio of ice thickness over conductor radius. For example, in Figure 4.5, 11 mm (0.4 in.) of ice on 32.4 mm (1.28 in.) diameter conductor gives ε = 0.67.
- Ice shapes on single conductors which can generate galloping are more related to thin glaze ice (Figure 6.26).
- The D-shape type of ice almost never occurs.

It has been shown by laboratory testing (e.g., Tunstall and Koutselos [1988]) that extremely thin deposits behave, near the zero angle of attack, differently than for thicker accretions. Their lift curves have opposite slopes with derivatives greater than the drag indicating potential Den Hartog instability, similar to the D-shape but in a much more restricted range of angle of attack.

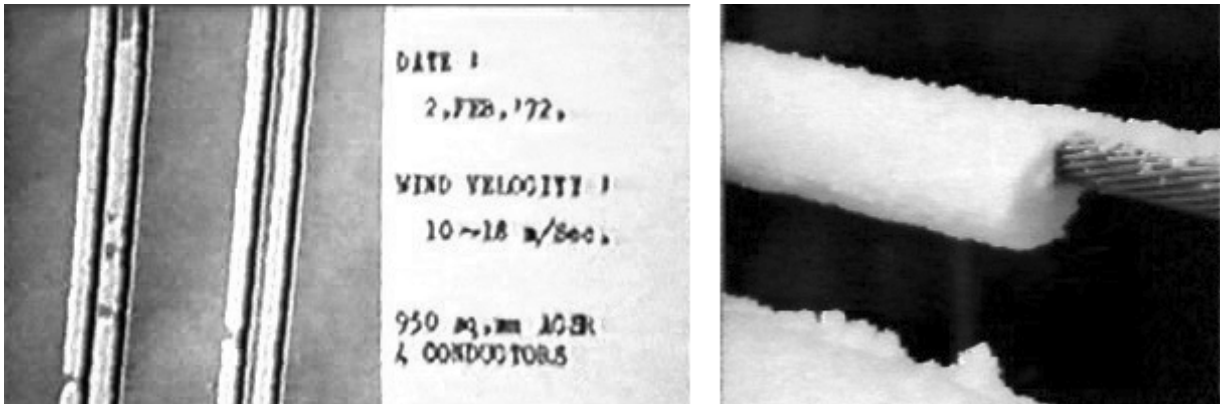

Figure 6.24: Actual ice shapes causing galloping. *Left:* on a quad bundle, as observed in Japan [Anjo et al., 1974] extracted from a video record from the Kasatori- Yama test line. *Right:* ice accretion on a rigidly reinforced bundle conductor, with eccentric mass.

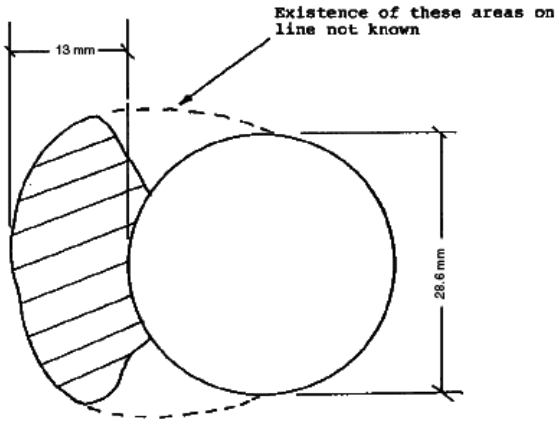

Figure 6.25: Freezing rain ice shape fallen from quad bundle line during a galloping event in the United Kingdom in 1986 (courtesy M. J. Tunstall, CEGB, Corech meeting, September 1987).

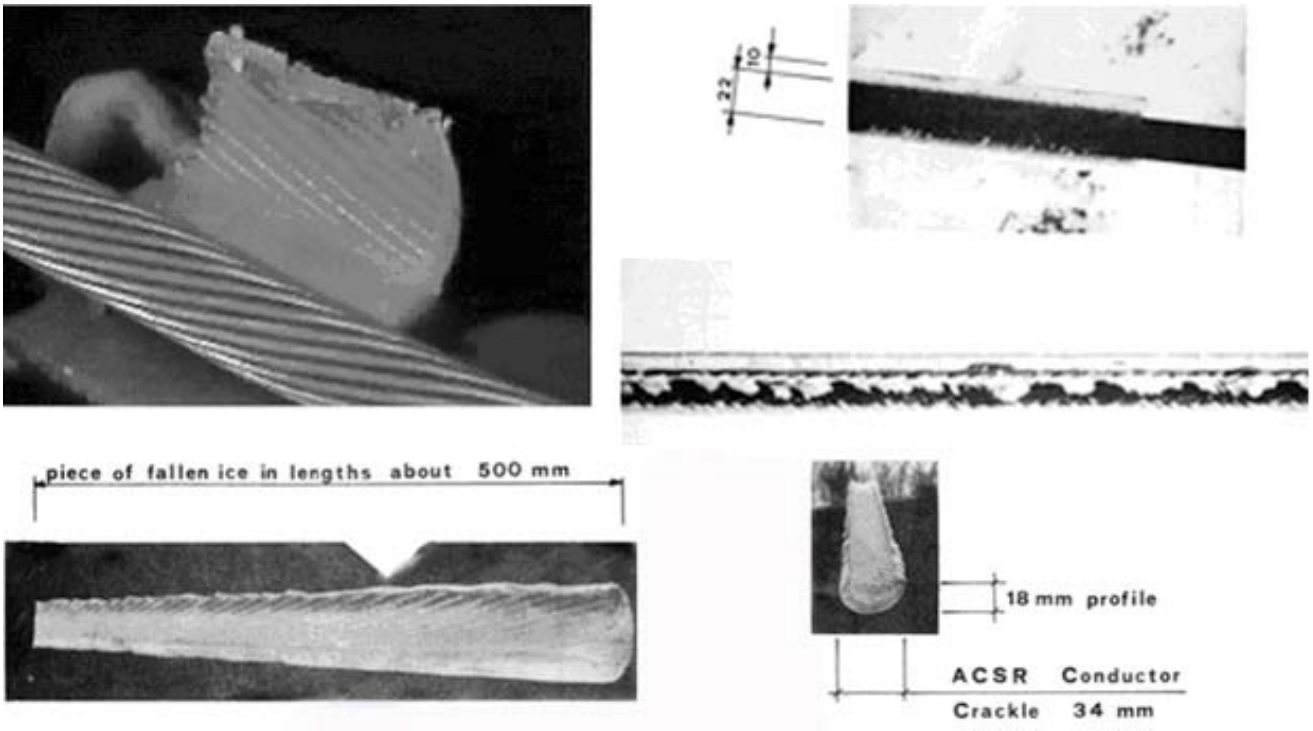

Figure 6.26: Ice layers on ACSR conductors. *Upper Left:* Groningen, diameter 22 mm (0.87 in.). *Below:* Grackle, diameter 34 mm (1.34 in.), during a galloping event (courtesy P.H. Leppers, Corech meeting 1979).

The aerodynamic curves shown in Figure 6.27 to Figure 6.30 have been obtained by the methods described above. Ranges of angles of attack with Den Hartog instability zones are highlighted by a thicker line on the abscissa. The angle of attack is measured in the anticlockwise direction for all curves presented.

The figure on the left shows lift and drag, and the figure on the right side shows drag and derivative of lift. The Den Hartog instability zones occur when the latter curves cross, due to the choice of the anticlockwise sign convention. All curves are smoothed using a high-bandpass Fourier filter with 42 harmonic components.

It must be noted that a conductor with a "classical" crescent-shaped ice coating with different eccentricities, such as those shown in Figure 6.27 to Figure 6.29, have similar aerodynamic lift curves but with different amplitudes. There is little or no Den Hartog instability zone, except at 180°, which means that the wind must blow from the side opposite to the ice coating.

The D-shape (Figure 6.30) has a large range of instability near the zero angle of attack [Nakamura and Tomonari, 1980]. Figure 6.15 shows artificial D-shapes used in test stations.

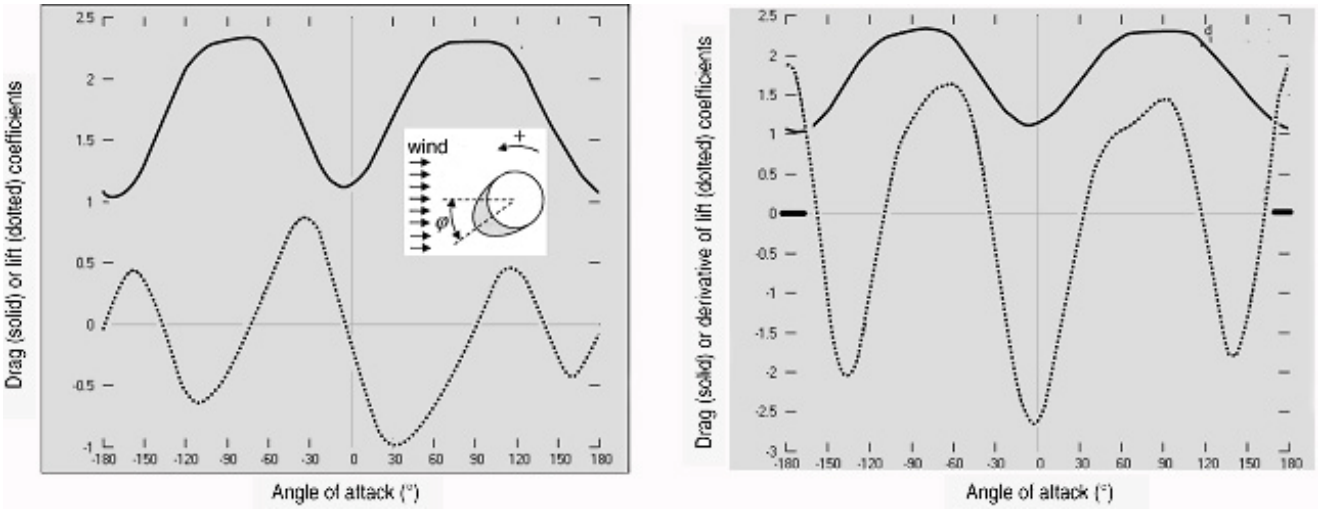

Figure 6.27: Aerodynamic properties of a conductor with ice eccentricity 0.33 [Buchan, 1978]. There is only one small range of Den Hartog instability zone near 180°.

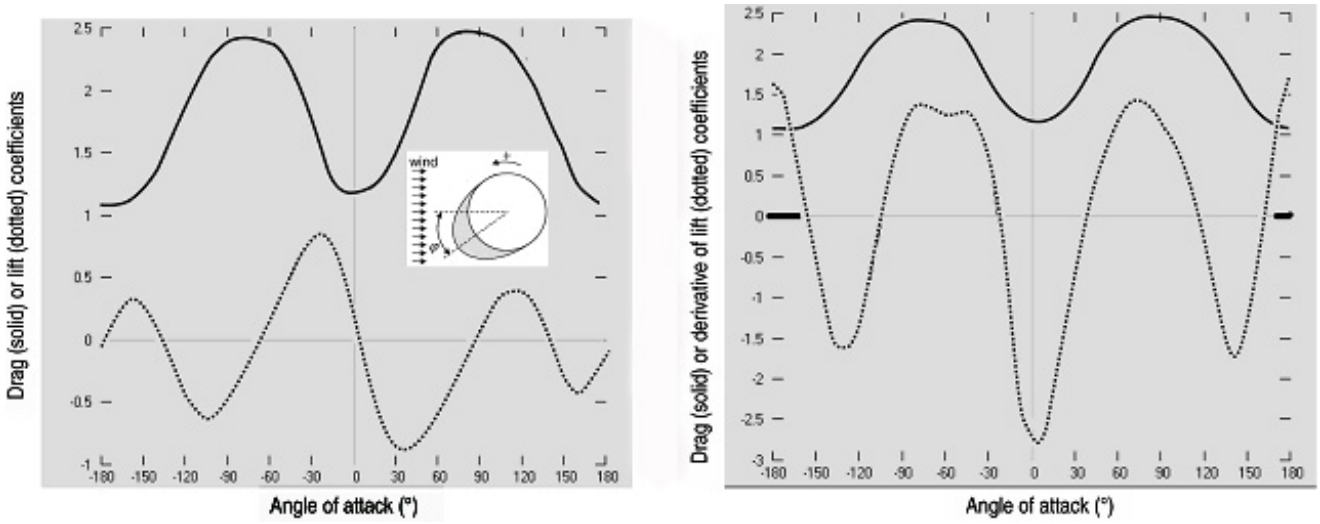

Figure 6.28: Aerodynamic properties of a conductor with eccentricity 0.82 [Chan et al., 1992]. There is only one small range of Den Hartog instability zone near 180°.

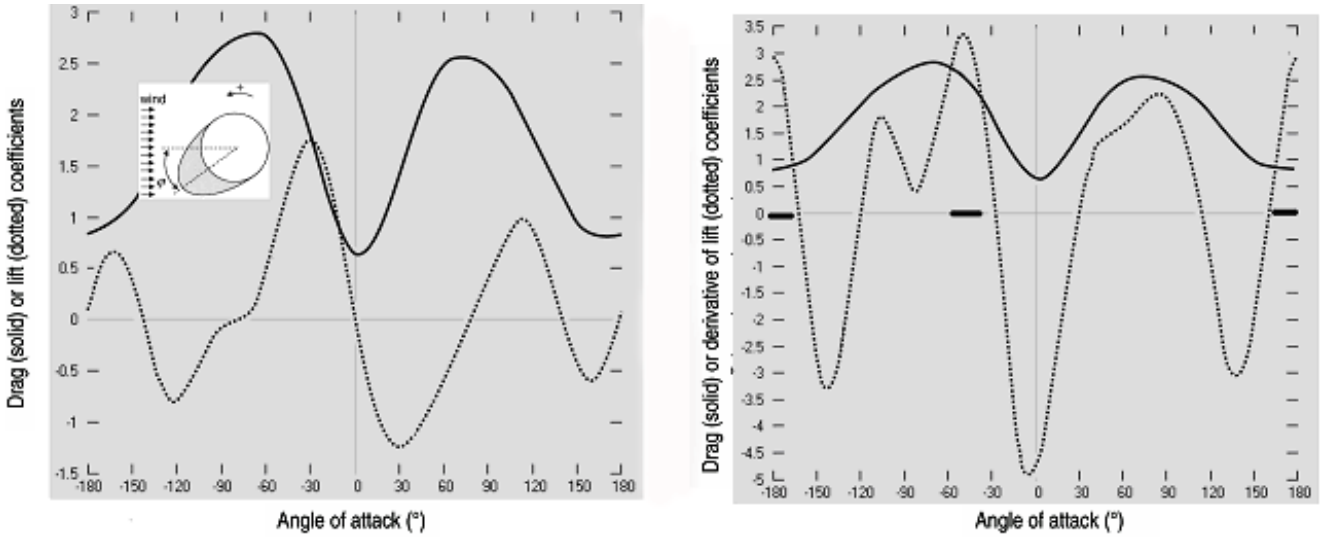

Figure 6.29: Aerodynamic properties of a conductor with eccentricity 1.39 (source: Fujikura, courtesy T. Oka). There is one small range of Den Hartog instability zone near 180°, plus one asymmetric instability zone near -40°.

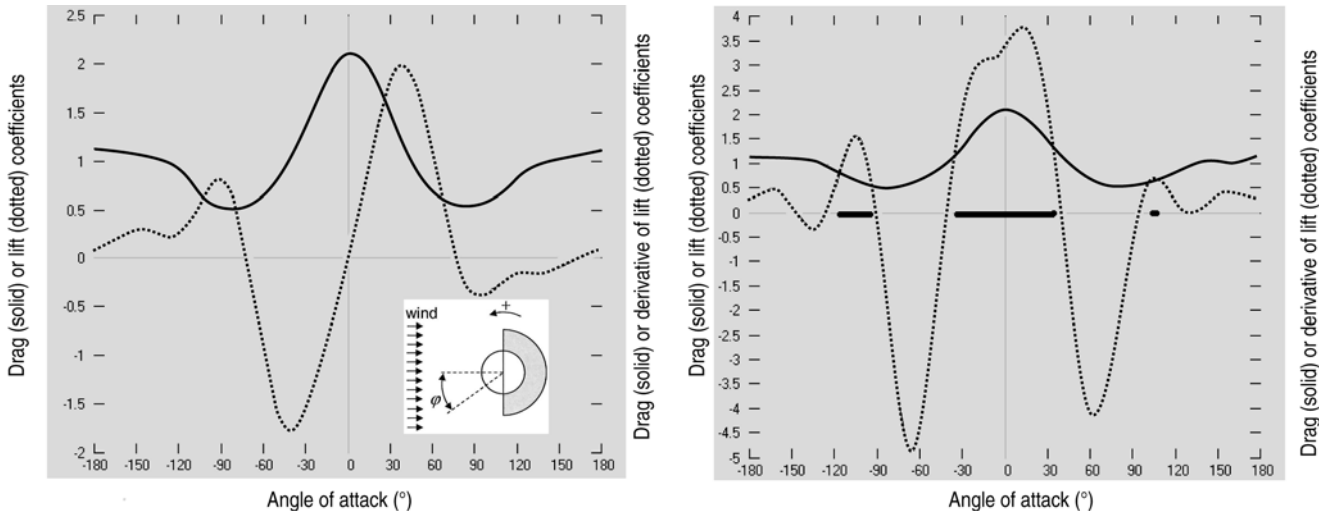

Figure 6.30: Aerodynamic properties of a conductor with a D-Shape accretion (courtesy University of Liège, 1999). There is a large range of Den Hartog instability zone near zero and 90° angles of attack.

6.4.2 Galloping in a wind tunnel

It is possible to recreate a portion of the span inside a wind tunnel by means of a support and springs (Figure 6.31) that will be tuned to the appropriate horizontal, vertical and torsional resonant frequencies in order to reflect the modes under investigation. In the case of bundles, the appropriate number of rigid tubes may be installed in parallel. Keutgen and Lilien [2000] have used this kind of setup to induce galloping inside a wind tunnel. They have obtained a coupled flutter with the displacements described in Figure 6.32 to Figure 6.34.

The frequencies of the three movements are the same, 0.89 Hz, which corresponds to the galloping frequency (reduced wind speed of 335). The trajectory of one point of the sample in the x-y plan is called the galloping 'ellipse'. It was interesting to note that the same parameters with a slightly different wind speed have induced quite different galloping ellipses (Figure 6.35).

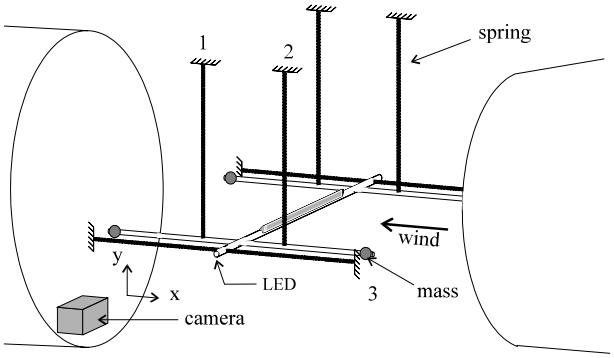

Figure 6.31: Diagram of the dynamic system in the wind tunnel.

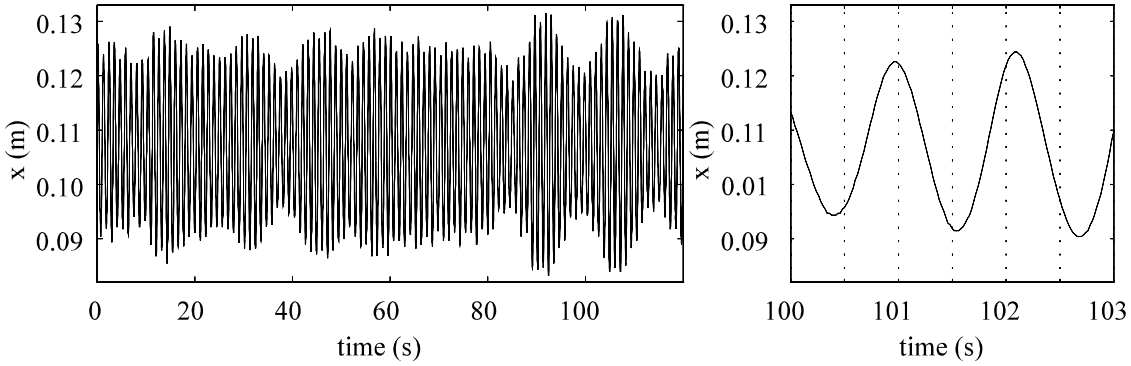

Figure 6.32: Horizontal displacement, U_0 = 9.7 m/s, θ_0 = -30°, f_v/f_θ = 0.98, $U_0/(fd)$ = 335.

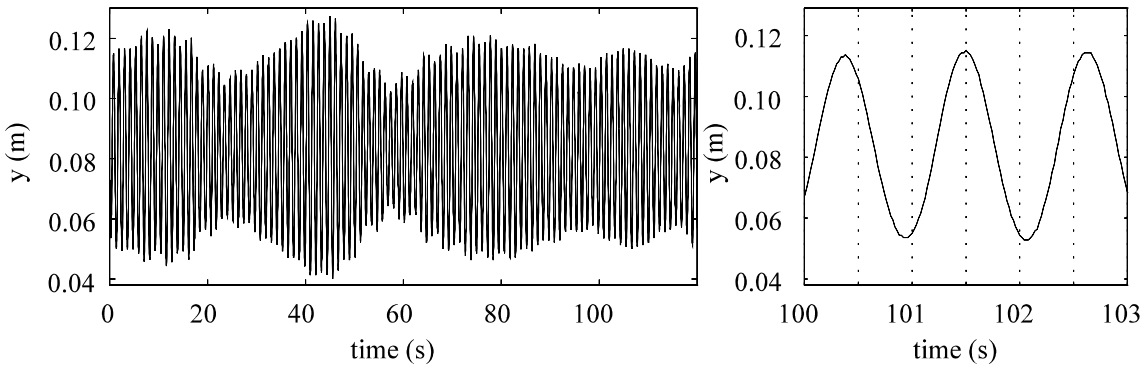

Figure 6.33: Vertical displacement, U_0 = 9.7 m/s, θ_0 = -30°, f_v/f_θ = 0.98, $U_0/(fd)$ = 335.

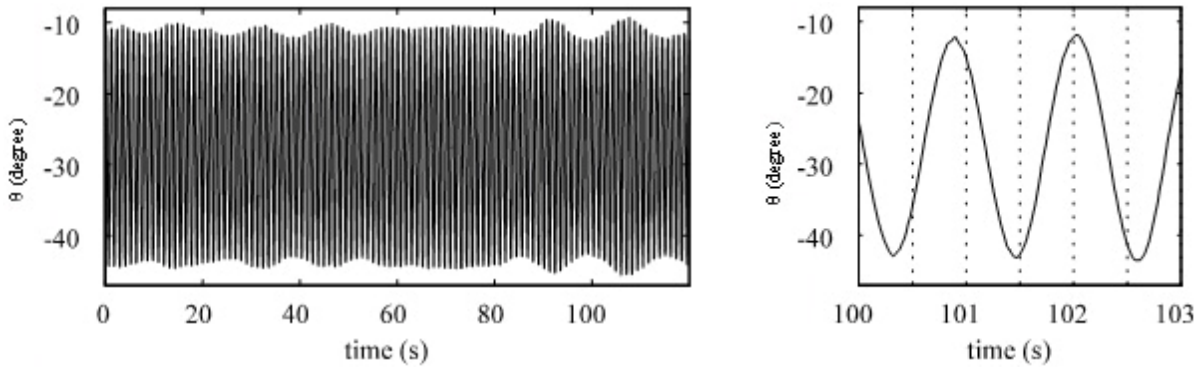

Figure 6.34: Angular position of the ice, U_0 = 9.7 m/s, θ_0 = -30°, f_v/f_θ = 0.98, $U_0/(fd)$ = 335.

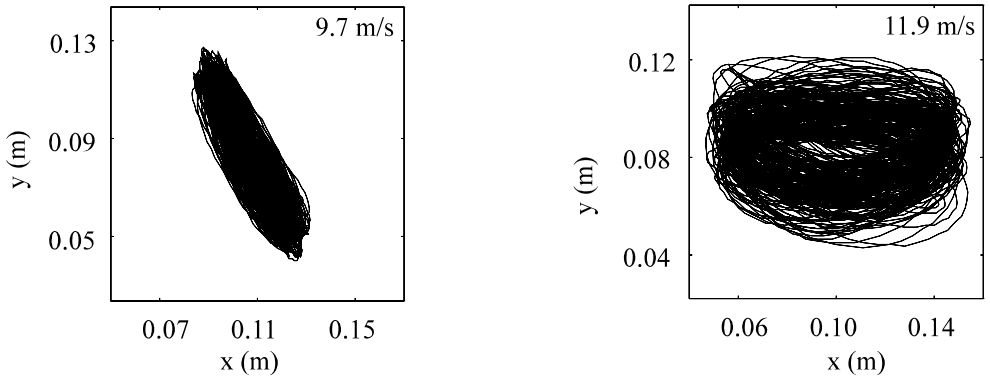

Figure 6.35: Galloping 'ellipse' for different wind speeds, θ_0 = -30°, f_v/f_θ = 0.98. Typical coupled vertical-torsion galloping.

The following case shows a Den-Hartog instability on another arrangement having a detuning (torsional frequency corresponding to about twice the vertical frequency), obtained with a wind blowing in the direction opposite to the ice accretion (ice accretion at 180°).

The rotational amplitude at the end of the recording was less than 3° peak-to-peak. The frequencies were not the same for each movement. It was 0.85 Hz for the vertical displacement, the horizontal movement was not easily detectable and 1.71 Hz for the rotation (twice the vertical frequency).

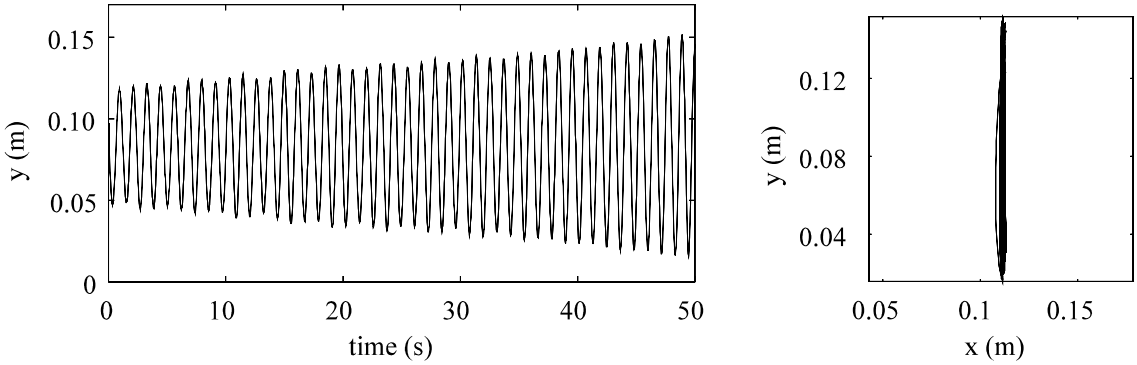

Figure 6.36: Vertical displacement and galloping 'ellipse', U_0 = 8.5 m/s, θ_0 = -180°, f_v/f_θ = 0.55, $U_0/(fd)$ = 308. Typical pure Den-Hartog galloping.

6.5 Effects of terrain on propensity of galloping

It is certain that galloping only occur in specific locations. That is because of the necessity, for the power line to be located in region where:

- Having cold temperature (most of galloping occurred near 0°C, but some cases have been observed at much lower values) (we are speaking about conductor temperature, which must be able to accrete ice/snow/rime). Ice may easily transfer calories, so that small wind velocities are able to dissipate significant amount of calories from the conductor heat losses. Of course high electrical loads will limit the risk, this is an easy calculation to be done on conductor and wind data.

- The power line must be more or less perpendicular to dominant wind speed (range over 5 m/s) during winter time.

- To have a wind acting similarly on most of the span(s) of the same section (in the same direction) with no significant obstacle in the close vicinity (which would induce turbulence in a part of the span). Of course very flat area like desert, rice field, large river crossing, and tundra are very sensitive.

- Of course a "section" may be reduced to one span (especially for distribution lines), in that case a span by span risk analysis may be necessary.

- Environment which favours wind acceleration and/or driving wind in a direction close to perpendicular of the power lines may be very sensitive, like fjords, power lines down a hill from which transverse wind may arrive from the top of the hill over a forest for example, power lines on a top of hills subject to tranverse wind are one of the worst conditions, plateau in mountainous area with enough distance (several hundreds of metres) for the wind to "re-arrange" before arriving on the power lines.

- Never forget that winter conditions may drastically change from summer conditions as some obstacles may be hidden by the snow.

- Near water lines (lakes, rivers, seas, and oceans) perpendicular to dominant winds, which are locations very prone to power lines icing together with significant wind coming from the water side or the ground depending on the season.

Of course the observation is depending on power lines cable altitudes, a power line in a city may be subjected to galloping if conductors are over the boundary layer of high turbulence created by buildings, etc.

Some moving power lines cable in strange location, not prone to galloping, may be induced by a real galloping in other spans of the section. So that a galloping risk evaluation must look for the whole section length.

7. Influence of supports, fittings, phase geometry, and conductors on galloping

7.1 Supports

Although support points are nominally rigid, they are not entirely so. There is a small amount of compliance (the reciprocal of rigidity), due to the flexibility of the structure and perhaps in its junction with the earth. This compliance can include some hysteretic damping. Sample measurements of support point damping at Alcoa's outdoor test spans in Massena, NY have shown that this damping is small and often negligible.

Hysteretic damping at an elastic support is represented by the equation,

$$D = 2\pi\varepsilon \cdot \frac{1}{2} \cdot \frac{F^2}{k}, \qquad (7.1)$$

where ε is the loss factor or loss tangent, F is the amplitude of the applied force, and k is the spring constant representing the rigidity of the support. The factor ε / k is called the loss compliance of the support. When it is known, damping energy resulting from any applied force can be calculated from equation (7.1).

When ε is not too large, damping can be determined from decrement tests through the relation,

$$D = 2\delta U_{os}, \qquad (7.2)$$

where δ is the logarithmic decrement and U_{os} is the stored energy of the oscillating system that supplies the force. It can be shown that

$$\frac{\varepsilon}{k} = \frac{\delta}{\pi K}, \qquad (7.3)$$

for a spring-supported mass system, where K is the constant of the supporting spring. For a pendulum system,

$$\frac{\varepsilon}{k} = \frac{\delta}{\pi} \cdot \frac{L_p}{mg}, \qquad (7.4)$$

where L_p is the length of the pendulum, m is the pendulum mass and g is gravity.

The results of the sample measurements are shown in Table 7.1.

To illustrate, the 100 m span of Drake ACSR, galloping in one loop with 2 m peak-to-peak amplitude would have 64.2 Joules of stored energy. Using equation (7.2), the dissipation per cycle for the wood H-frame east phase would be 0.0061 J, which is clearly negligible.

Damping due to longitudinal loading at tangent structures arises from longitudinal swinging of the suspension string. The value of F depends upon the angle of swing and the tension in the string. These in turn depend upon the span arrangement in the galloping section, and on the section eigenmode and its amplitude. For illustration, information pertaining to a galloping test to be described below has been used to calculate structure dissipation due to longitudinal loading for the 138 kV structure of Table 7.1. The mode shape was calculated according to the method of Rawlins [2001]. Dissipation per cycle was found to be 7.8 J. The total kinetic energy stored in both spans of the system was 983 J. Thus, D was less than 1% of U, and was again negligible.

Table 7.1: Loss compliance of transmission structure support points - ε / k (meter/Newton)

Test Point	Loss compliance (m/N)	
	Vertical	Longitudinal
Wood H-Frame Structure – East Phase	$2.90 \cdot 10^{-7}$	$2.12 \cdot 10^{-5}$
Wood H-Frame Structure – Centre Phase	$1.05 \cdot 10^{-7}$	
138 kV Double-Circuit Steel Lattice Tangent Structure	$5.00 \cdot 10^{-9}$	$1.06 \cdot 10^{-5}$
110 kV Double-Circuit Steel Lattice Tangent Structure	$1.22 \cdot 10^{-8}$	$7.30 \cdot 10^{-6}$

7.2 Phase geometry

This chapter deals with structural data having an effect on galloping, other than the contribution of wind and ice. It is understood however that the presence of wind and ice may contribute to these changes, either positively or negatively.

As galloping of single conductor is mainly driven by Den Hartog's criterion, there are few structural options available to control it (except the increase in vertical damping). There is however one exception to this statement: the use of retrofit methods (see section 7.2.2) changing the structural properties of single conductors considerably, making them more sensitive to coupled-flutter type galloping and using appropriate structural changes to control it.

Galloping on bundle conductors may easily be driven by coupled flutter-types of instabilities. As we already discussed, such type of galloping is strongly influenced by structural properties.

Most of the simple structural remedial actions possible are in relation to the torsional behaviour related to the change of torsional stiffness, as well as to the moment of inertia of the bundle, to a lesser degree. The ways to increase or decrease the torsional stiffness are discussed below.

7.2.1 Single conductor

The torsional rigidity of a single conductor and its influence on galloping is presented in section 7.3.5. The following section discusses this property for bundle conductors.

7.2.2 Bundle conductors

The torsional stiffness of bundled conductors is quite different compared to single conductors. It is at least one order of magnitude larger. In addition to the intrinsic individual torsional stiffness of each sub conductor (which is a minor part of the whole torsional stiffness) there are the bundling effect, which is related to the tension in each sub conductor and to the bundle diameter, as well as the spacers which maintain such diameter constant when possible, along the span. This phenomenon has been first analysed by Nigol et al [1977], then completed later on by a generalized approach by Wang & Lilien [1998]. This last reference showed the influence of tension differences between each sub conductors in a bundle, which has a major effect on its torsional stiffness. A factor of two can be obtained between the two conditions - equal or unequal tension in each sub conductor. It also discusses the various concepts applicable to the design of suspension and dead-end strings with such conditions.

In bundle conductors, the effects of spacers are multifold. Both the sub span length and conductor spacing have a significant influence on torsional stiffness. The method of conductor fixation to the spacer is also important. If the conductor is rigidly attached to the spacer, it will allow the intrinsic sub conductor stiffness to influence the bundle torsional stiffness. For example the so-called “rotating clamp spacer” is designed to suppress the contribution of the conductor's intrinsic stiffness to the bundle stiffness, if the rotation of the clamp is not impeded by ice. The spacer's offset weight, which is the centre of gravity of the spacer compared to centre of gravity of the bundle, is acting like a pendulum.

The bundle orientation also has some significant effect on the torsional frequency because the tension in sub-conductors changes during rotation, so that a vertical twin bundle is not as "stiff" as a horizontal one. In addition, the yoke plate of sub conductor fixation plays a major role in the bundle's stiffness, as detailed in Wang & Lilien [1998]. Two examples are illustrated below (Figure 7.1 and Figure 7.2), one of a dead end arrangement and one of a suspension arrangement. Both cases increase the torsional stiffness of the bundle.

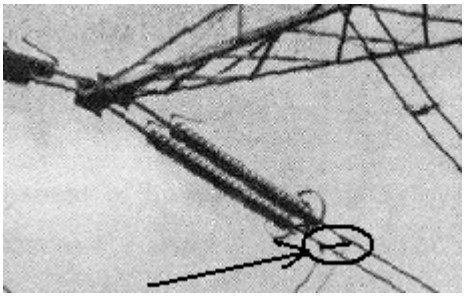

Figure 7.1: Rigid Anchoring Attachment

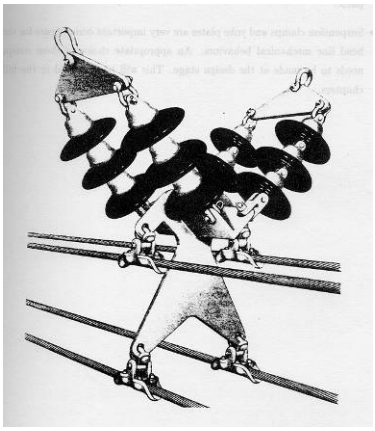

Figure 7.2: "Rigid" suspension arrangement

Experience with wet snow accretion

Experience in the Netherlands, Germany and Belgium, as well as other European countries where winter precipitation occurred mainly in the form of wet snow, was that small to medium sized single conductors were virtually gallop free while bundle conductors galloped severely, leading to sporadic occurrences of serious damage. The difference in behaviour is attributed to the ability of long spans of single conductor to twist under the weight of the accretion, and for the ice to form in a smooth profile with smaller aerodynamic lift forces. This twisting action is not possible in short single conductor spans, in bundle conductors due to the restraint of the spacers, or in large single conductors due to their inherent much higher torsional stiffness. For these spans the accretion will build up on one side of the conductor and develop into a more pointed profile, with higher aerodynamic lift forces.

Modifications to the design of bundle conductors were investigated in order to allow the sub conductors to rotate under the weight of the accretion, thereby acting more like spans of small single conductors [Leppers et al, 1978]. The modifications generally involved moving the sub conductors to different heights, and the removal of spacers from the spans. Figure 7.3 shows samples of suspension arrangements for two-, and four-conductor bundles developed for this purpose, and applied to transmission lines operating at 150, 220 and 380 kV in the Netherlands, Belgium and Germany. The height differentials were introduced so that during swing-out under buffeting winds the sub conductors do not clash, and also to reduce the wake effects in bundles, which contribute to an increase in wind energy transfer to the conductors. The applications were on lines with sub conductors in the 18 to 22 mm diameter range.

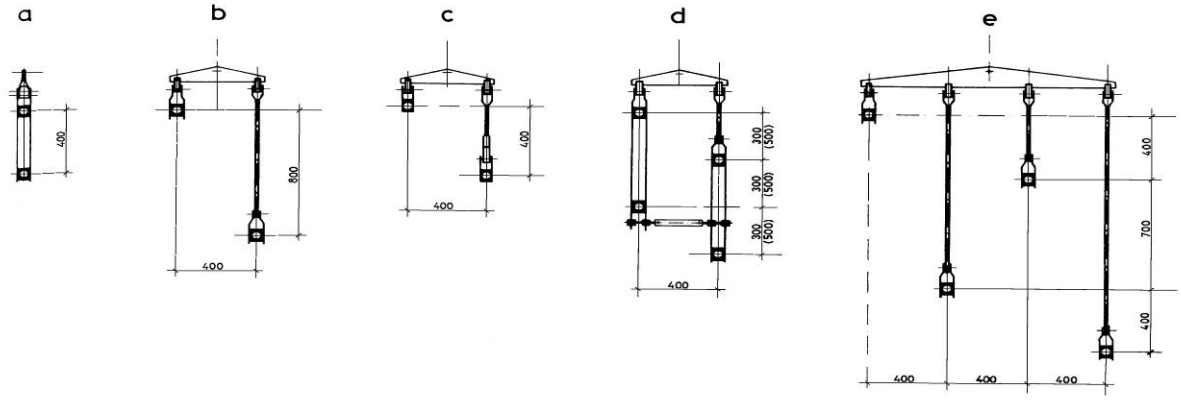

Figure 7.3: Alternative arrangements of bundles without spacers [Leppers et al, 1978]

The initial development was simply removal of spacers, but adverse behaviour was experienced during emergency current conditions in which there are high electromagnetic forces of attraction between the sub conductors causing the bundle to collapse inward. These forces are inversely proportional to the spacing between sub conductors, so the bundle will remain in its collapsed state even when the current is reduced to normal operating levels. The current must be reduced to zero to restore the bundle geometry.

A new design of spacer was developed to allow free rotation of the sub conductors, while preventing the collapse of the bundle. This is the "hoop" spacer, and a sample design is shown in Figure 7.4. Hoop spacers are shown installed on an experimental section of a 150 kV twin bundle line in the Dutch Utility system (PLEM) in the Netherlands in Figure 7.5. The left hand circuit is despacered, as shown in diagram "a" in Figure 7.3, and top and bottom phase suspension strings are replaced by "V' strings to limit excursions of the phases during galloping. The right hand circuit has the top two phases despacered as in diagram "a" of Figure 7.3 and the hoop spacers are mounted on the bottom phase only, which remains in its original horizontal configuration. This line was monitored by line patrols during galloping events and on two occasions the sections with conventional spacers were seen to gallop while the sections without spacers were quiet. The patrols also reported that the ice coatings were eccentric and pointed on the conventionally spacered section, and fell off quickly after the temperature rose. On the other hand, the despacered section was covered with a smoother ice coating, which persisted for a longer period.

Figure 7.4: Hoop spacer used to maintain separation of sub conductors in despacered bundles [Hoffman & Tunstall, 2003]

In Belgium, UNERG implemented the despacered vertical twin bundle configurations shown in Figure 7.3 "a" and "c". The lines were initially at 150 kV and were later up rated to 220 kV. The lines run through the Ardennes mountain range, and had a history of galloping problems. The effectiveness of the spacer removal program was monitored by a remote sensing station established by LABORELEC, the Belgian electrical industry research laboratory. The station instrumentation measured the dynamic loads on a dead end span. All six phases of the double circuit line were monitored to facilitate comparison of the despacered vertical and standard horizontal bundle configurations with different types of spacers. As shown in Figure 7.6, these measurements indicated dynamic tension variations up to 60 percent of the static conductor tension at 0°C on the horizontal bundles at a frequency corresponding to the galloping motion. On the despacered phase the loads were much smaller and irregular, indicating that the load variations were not due to galloping conductors, but due to the reactions of the towers and cross arms to the galloping motions on the other side of the tower.

Initial trials of despacering in the German utility PREAG were on a twin bundle 220 kV line, and the arrangement shown in Figure 7.3 "b" was used. Due to numerous repair sleeves and resulting uneven sags in this galloping prone section of the line, the 80 cm vertical separation was applied. The previous poor performance during the winters was eliminated with this modification.

When PREAG applied the spacer removal approach to 380 kV quad bundles, rearranged as shown diagrams "d" and "e" of Figure 7.3, there were increases in electric field, radio interference, and audible noise. Subsequently, such modifications were limited to uninhabited areas only. An alternative method of achieving the free rotation of sub conductors was then developed, illustrated in Figure 7.7. This is the "rotating clamp spacer", and consists of two shells around each conductor,

one clamped to the sub conductor and one attached to the hinged link forming the spacer. The two shells are designed to rotate freely one within the other, and care is required to ensure that the sub conductors are at the same tension, to facilitate rotation. Also one metre long, wind driven "vane drives" were added to the conductor to effect continuous movements and keep the sliding surfaces free.

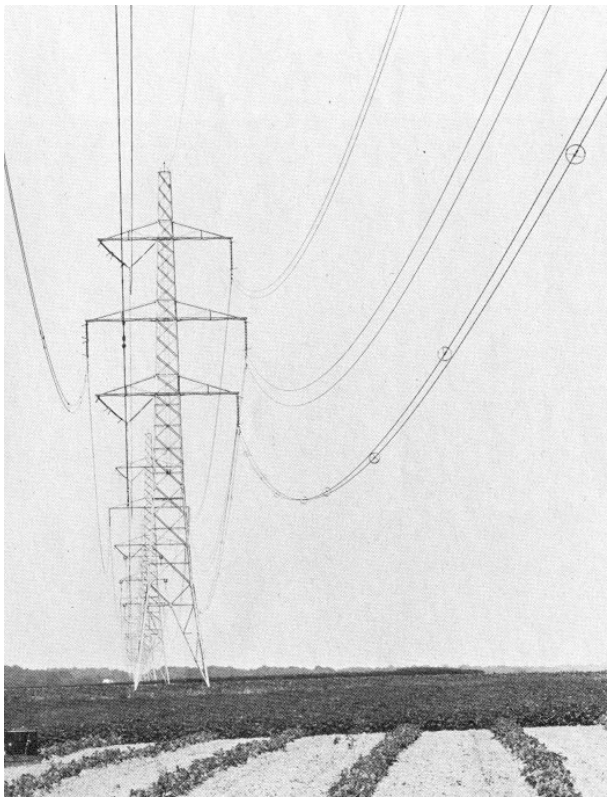

Figure 7.5: Despacered vertical twin bundle 150 kV transmission line with hoop spacers on lower phase of right circuit [Leppers et al, 1978]

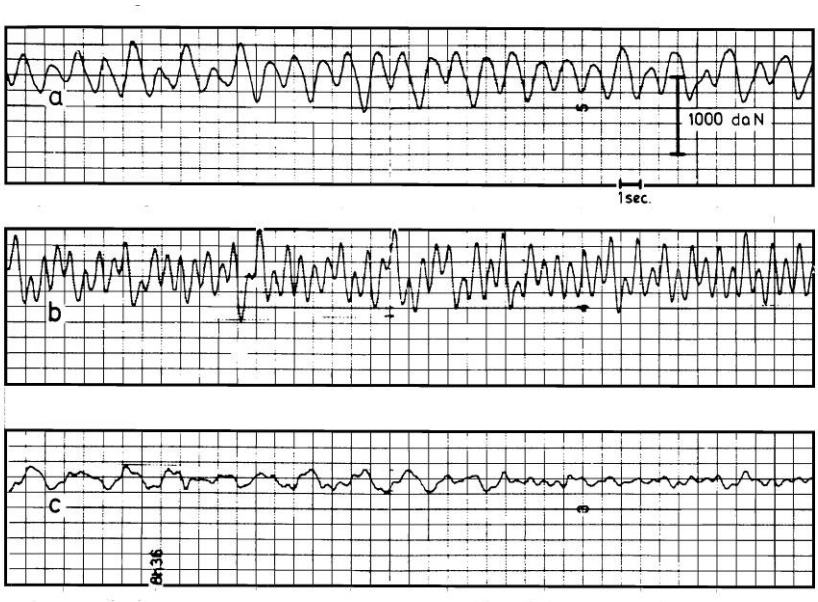

Figure 7.6: Load measurements during galloping on a twin bundle in Belgium (Leppers et al. 1978)
(a) horizontal bundle with standard spacers
(b) horizontal bundle with heavy spacers
(c) vertical bundle without spacers

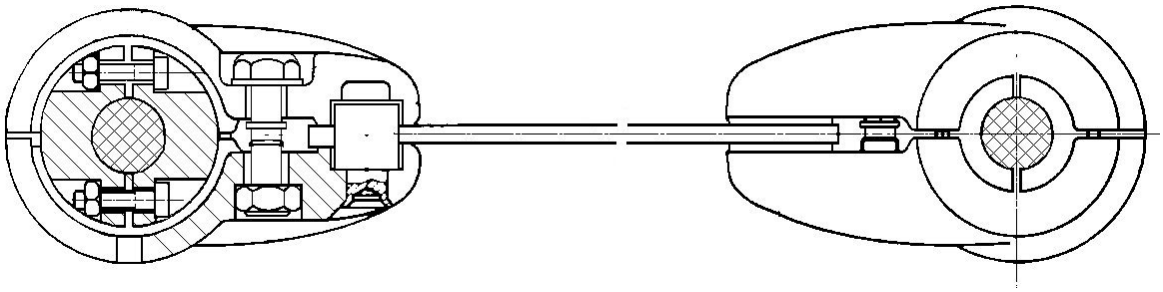

Figure 7.7: Rotating clamp spacer to allow sub conductor twisting during ice and wet snow accretion [Leppers et al, 1978]

7.2.3 Bundle moment of inertia

The bundle moment of inertia plays a major role in instability criterion. The galloping stability equations found in Chapter 3 demonstrate that such value is the denominator of the coupling term between vertical and torsional equation.

The bundle moment of inertia's main contributors are the sub conductor mass and bundle diameter, which is an important factor for galloping. Most of the time, the diameter of the bundle is fixed by other considerations (corona effect and manufacturer standardization), but there are some exceptions. In theory, an increase of bundle moment of inertia decreases the risk of instability. But the same cannot be said concerning the amplitude, if instability criterion remains violated.

An increase in sub conductor spacing increases both the moment of inertia of the bundle and its torsional stiffness. In the absence of any anti-galloping device however, these two increases unfortunately compensate each other so that the effect on torsional frequency is insignificant.

7.3 Conductors

7.3.1 Ice and icing of conductors

The types of ice and snow that may accrete on conductors are rime ice, glaze ice, frost, dry snow and wet snow [Poots, 1996]. Rime is an ice deposit caused by the impaction of supercooled droplets and their freezing onto a substrate. When air temperature is well below 0°C, supercooled droplets possessing small momentum will freeze upon hitting the substrate, creating air pockets between them in the process. This type of deposit is known as *soft rime*. When the droplets possess greater momentum, or the freezing time is greater, a denser structure known as *hard rime* is formed. *Glaze* ice will form when the droplet freezing time is sufficiently long to let a film of water form on the accreting surface. The latter type of ice accretion has the highest density and the strongest adherence to conductors. *Frost* is formed when water vapour in the air sublimates on a substrate of temperature below 0°C. Ice load due to frost is insignificant and rare. *Dry snow* has low density and accretes at sub-freezing temperatures. Dry snow rarely accumulates and only when wind speed is very low, below 2 m/s. *Wet snow* accretion is observed when air temperature is between 0°C and 3°C, and may occur under any wind speed. Wet snow is made up of a matrix held together by capillary forces and ice bonding. The adhesion of wet snow to conductors may be strong, and its accretion may be quick, causing its liquid water content to increase to such a level that the aerodynamic and gravitational forces eventually overcome the internal cohesive forces [Admirat et al, 1988]. Above this level the snow sleeve breaks up and means no further danger for the transmission line.

The relation between accretion type and air temperature and wind speed, is shown in Figure 7.8 (based on [Tattelman & Gringorten, 1973; Sakamoto, 2000]).

Formation of ice and snow on conductors may come from cloud droplets, raindrops, snow or water vapour. Cloud droplets are a constitutive part of fog, while raindrops and snowflakes are associated with freezing rain and snow falls, respectively. Cloud droplets are very small, their diameter ranging between 10 μm and 40 μm. Freezing rain droplets are significantly larger, with diameter as great as 500 μm. Snowflakes have the largest size; they may grow up to 1 cm, although it is difficult to describe their size by a single value, because they are usually not spherical [Poots, 1996].

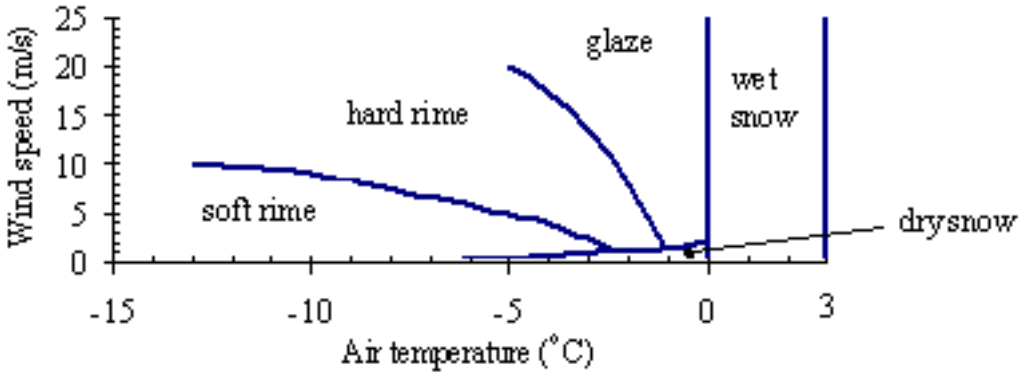

Figure 7.8: Relation between accretion type and some meteorological conditions

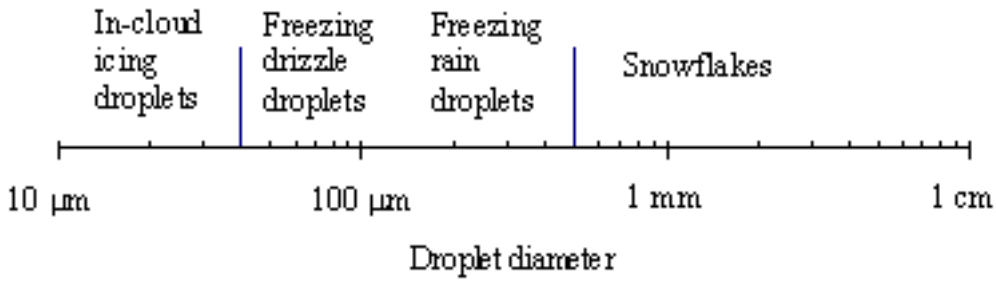

Figure 7.9: Size spectrum of different droplets

Transmission line cables are highly flexible and tend to rotate following asymmetrical ice building-up on the surface. The cable surface position facing a supercooled water flux tends to shift constantly due to that rotation, resulting in an evenly distributed and circular-shaped ice mass over the cable surface. Figure 7.10 shows ice shapes obtained experimentally by Personne *et al*. [1988]. The averaged conditions of accumulation were as follows: Refrigerated natural wind tunnel, Liquid water content (LWC): 0.3 g/m^3, wind velocity (V): 10 m/s, droplet diameter (d): 15x10^{-9} m, Temperature (T): -15ºC, accretion duration (t_{acc}): 7h20.

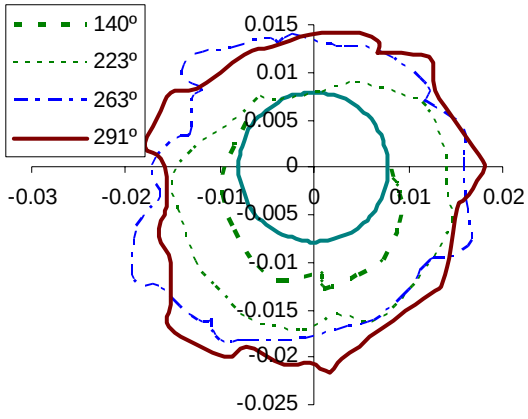

Figure 7.10: Ice shapes obtained from experimental studies (based on [Personne et al, 1988]).

Rigidity of the cable has a direct influence on ice shape as shown in Figure 7.11. After 180 minutes of simulation time, a total rotation of 130° was found for the rigid cable and 280° for the soft one. Ice accretion on the soft cable exhibits a perceivably circular shape while the one on the rigid cable is asymmetrically distributed. The averaged parameters of accumulation were as follows: LWC: 1.1 g/m^3, V: 8 m/s, d: 30x10^{-9} m, T: -15ºC, t_{acc}: 3h00.

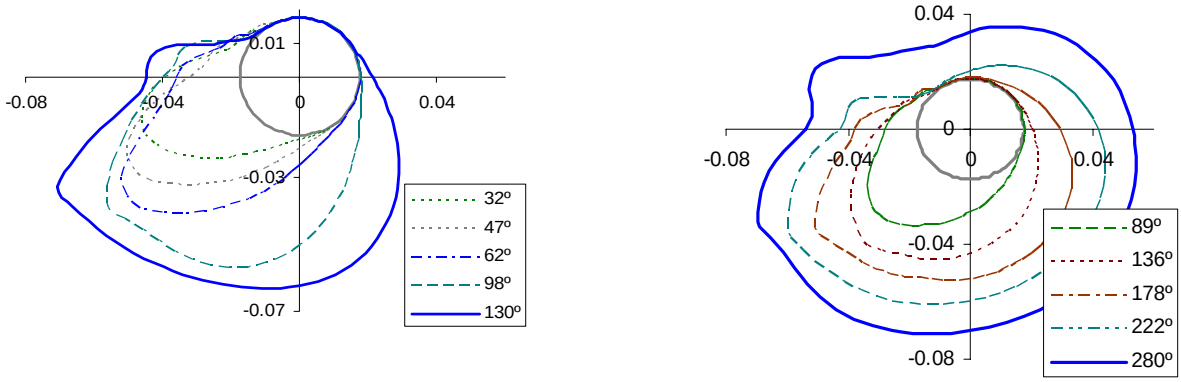

(a) (b)

Figure 7.11: Simulated ice shapes for cables with finite torsional rigidity (adapted from [Fu and Farzaneh, 2006])
(Parameters: diameter 0.035 m, duration 180 min, temperature -15ºC)
(a) Predicted ice shapes for a rigid cable (torsional rigidity: 100 Nm^2)
(b) Predicted ice shapes for a soft cable (torsional rigidity: 351 Nm^2)

Increasing wind speeds may result in thicker and broader ice mass in the windward direction and, consequently, in a significant ice-load growth. Figure 7.12 shows the simulated ice accumulations obtained by applying varied wind speeds while maintaining the other conditions constant.

Conductors with any noncircular cross-section are prone to galloping. Principally, both the lift and drag coefficients determine if galloping will occur. These coefficients basically depend on shape, angle of attack, and Reynolds number. For any noncircular cross-section, there exist angle of attack ranges where galloping may occur. These ranges and the minimum wind speed which initiates galloping, however, vary to a great extent with the shape of the cross-section [Blevins, 1990].

(a) (b)

Figure 7.12: Comparison of ice shapes (based on [Lozowski et al, 1983])
(a) Case 1: air speed 5 m/s
(b) Case 2: air speed 10 m/s

7.3.2 Self-damping

The amplitudes of galloping that actually occur are determined by energy balance between the net energy supplied through aerodynamic action, including effects of aerodynamic dampers if any, and mechanical dissipation in the galloping system. Mechanical dissipation arises mainly from self damping in conductors, hysterisis at span supports, and dampers and damping spacers. Dampers and spacer-dampers are discussed elsewhere in this report. The remaining sources of dissipation, self damping and supporting structure damping have little if any effect on the energy balance because their contribution is negligible. While torsional self damping can influence the conditions where torsion-coupled instability occurs, the energy loss is not significant to the overall energy balance.

7.3.2.1 Self Damping in transverse movement

For transverse vibration, self damping is small at all but the highest aeolian frequencies, and negligible at galloping frequencies. A basically elastic solid cannot dissipate more energy during a loading-unloading cycle than is stored in it at the time of maximum loading. It is common to refer to the loss coefficient of a solid, $\eta = D/2\pi U$, where *D* is the energy actually dissipated in a full cycle and *U* is the maximum stored energy of strain. Noiseux has evaluated η in several ACSR sizes in connection with self damping in aeolian vibration and found values consistently less than 10^{-3} [Noiseux, 1992]. For conductors, *U* is the energy required to flex the conductor against its bending rigidity *EI*. There is so little conductor curvature involved in galloping that *U* is negligible and *D* turns out to be miniscule.

For a conductor vibrating in sine-shaped loops, the bending energy can be shown to be,

$$U_f = \frac{\pi^4}{4}\frac{EI}{L^3} y_{\max}^2 . \qquad (7.5)$$

where *L* is the loop length. The energy per cycle lost to bending hysterisis is

$$D_f = 2\pi\eta U_f . \qquad (7.6)$$

In steady vibration, the maximum stored energy of strain, not just bending but tensile as well, must be equal to the maximum kinetic energy, which is given by,

$$U_k = \frac{1}{4} m c^2 \frac{\pi^2}{L} y_{\max}^2 . \qquad (7.7)$$

Where ***c*** is the wave velocity. To illustrate, for Drake ASCR at 20% RTS tension in a 100 m span galloping in one loop, it turns out that $U_f / U_k = 2.84 \cdot 10^{-5}$. Using the largest value of η suggested by Noiseux, 0.001, $D_f / U_k = 1.78 \cdot 10^{-7}$. Longer spans would yield even lower values.

7.3.3 Field Tests

The purpose of the following tests was to verify the amount of mechanical sources of damping, and determine if it is negligible in regards to galloping.

2-span section of Drake ACSR at a low tension

This galloping test was carried out at Alcoa's outdoor test spans. The test system was a 2-span section of Drake ACSR at a low tension. The middle support was a single insulator string, 2.8 m long, and was located on the same tower as that where ε / k was measured for Table 7.1. The test procedure involved "pumping up" galloping motion of the two-span system by pulling on ropes hung from the middle of each span and then recording the decay of motion with transducers. It was expected that aerodynamic damping would be the dominant source of dissipation. This damping is strongly influenced by the force of the wind on the conductor, and can be calculated from theory.

One set of test results is shown in Figure 7.13. Aerodynamic damping was calculated for the actual mode shape, using a drag coefficient of 1.15. The results show that aerodynamic damping comprised virtually all dissipation. The difference between that damping and the measured damping was consistent with the predicted support point structural damping, and confirmed that mechanical sources of damping were negligible.

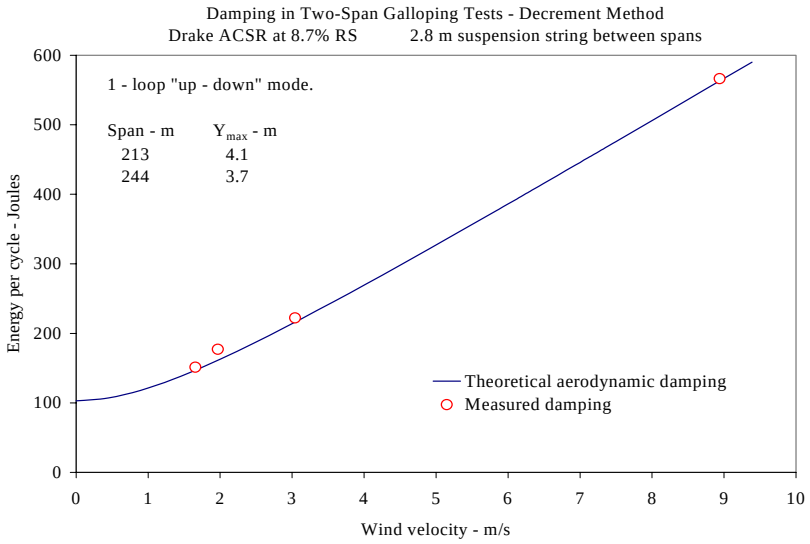

Figure 7.13: Energy dissipation during pumping up tests on a two span ACSR Drake single conductor.

3-span section of ACSR twin bundle conductor

This test was performed in a test span at Kazakhstan Scientific Research Power Institute, situated 200 km west of the city of Almaty. Kurdai Highlands have a sort of wide gate. This region is known as a site where high winds appear frequently. The three-span experimental set-up, located in an open terrain site, was erected during the summer of 2004. Its profile is adapted to the landscape (Figure 7.14). The bundled conductor type was a 394 mm^2/51 mm^2 (54/7) ACSR, mounted in the spans. Two dead-end assemblies and two suspension assemblies are used in the fixing points. The length of the main span is 292 m, and the lengths of the two anchor spans is 78 and 84 m respectively. The set-up consists of two anchor supports and two portal structures supporting the double-conductor bundle (Figure 7.15). The bundle runs from south to north at an angle α = 30º to the East of the line South – North. The diameter of the conductors in the bundle was 27.5 mm. The horizontal spacing between the sub-conductors 400 mm. The tension on the conductors was 29 kN. The results obtained are shown in Table 7.2 and in Figure 7.16 to Figure 7.18.

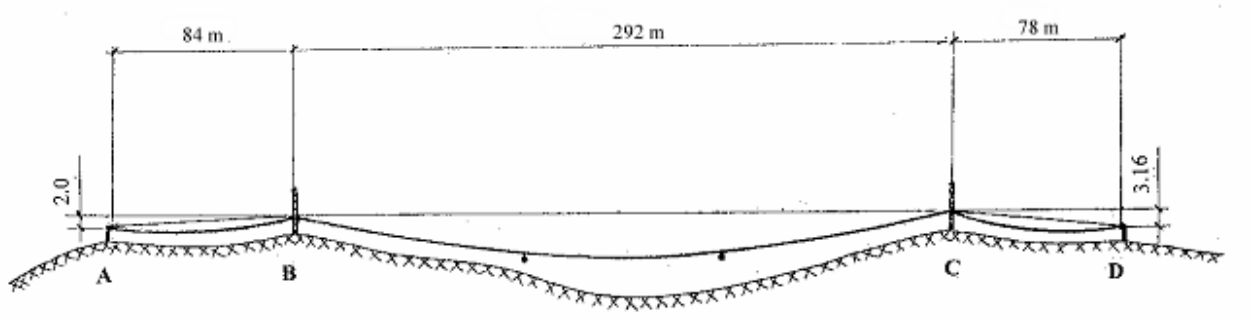

Figure 7.14: Side view of the set-up (horizontal and vertical scales are different).

Figure 7.15: Portal structure

Table 7.2: First two measured frequencies (one and two loops) on the Kazakhstan test span

Test No.	Excitation point	Number of loops n	Vertical Oscillation Hz
1	L/2	1	0.33
2	L/4	2	0.46

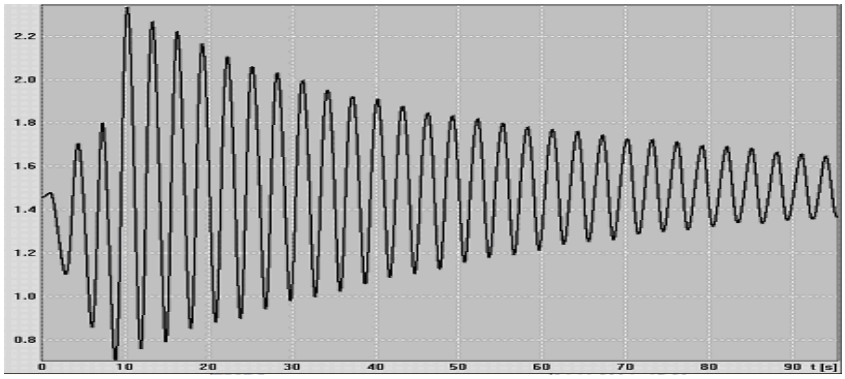

Figure 7.16: Free vertical oscillation under excitation at L/2 (f = 0.33 Hz)
test performed by ESSP, Russia

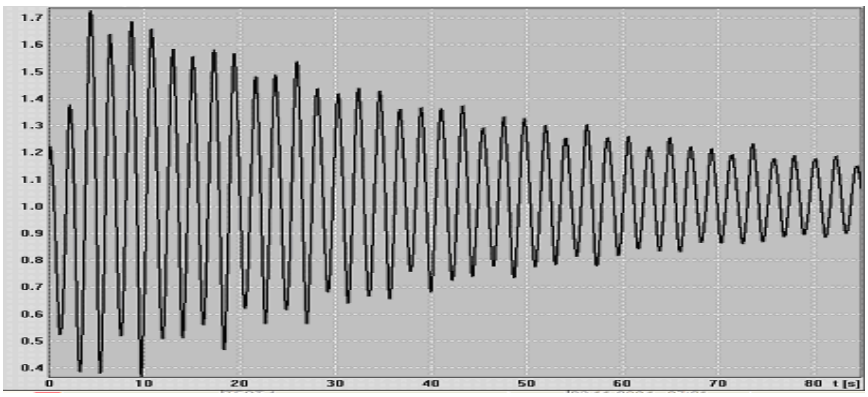

Figure 7.17: Free vertical oscillation under excitation at L/4 (f = 0.46 Hz)
The conductors were fixed at L/2 to create a node

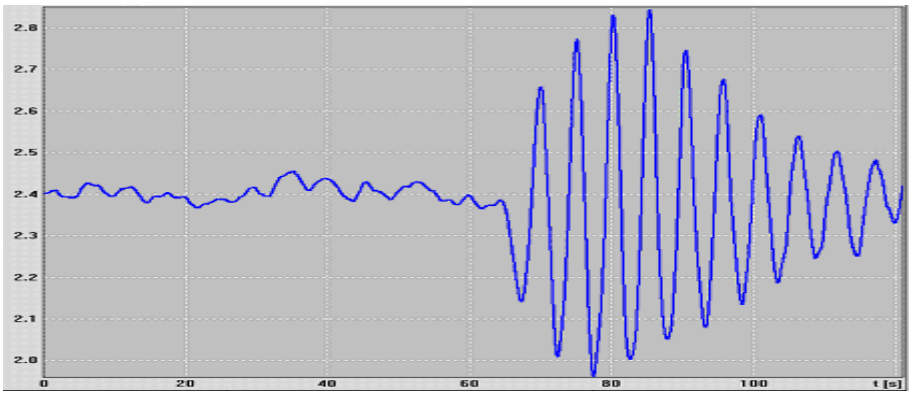

Figure 7.18: Free horizontal oscillation under excitation at L/2 without streamliners[1] (f= 0.19 Hz)

Based on the log decrement calculated from these figures, we may estimate the percentage of critical damping for these movements:

Table 7.3: Bending mode, percentage of critical damping

Mode 1 (vertical):	0.5% (Figure 7.16)
Mode 2 (vertical)	0.4% (Figure 7.17)
Mode 1 (horizontal):	0.4 % (Figure 7.18)

The aerodynamic damping may be calculated from the vertical equations of the movement. It can be demonstrated that the equivalent percentage of critical damping due to the drag effect follows equation (7.8):

$$\xi_{eq} = \frac{k_D.U_0.C_D}{2m.\omega_v} \qquad (7.8)$$

where

$$k_D = \frac{1}{2}\rho_{air} d \qquad (7.9)$$

ρ_{air} density of air, taken as 1.2 kg/m^3
d sub-conductor diameter, m
U_0 wind speed, m/s
C_D conductor drag coefficient at the appropriate wind speed
m sub-conductor mass per unit of length, kg/m
ω_v modal pulsation of the observed eigenmode (rad/s), = $2\pi f_v$

The wind velocity during the test was approximately between 2 to 5 m/s as the area is very windy.

[1] Streamliner: Artificial ice shape clipped on the conductor.

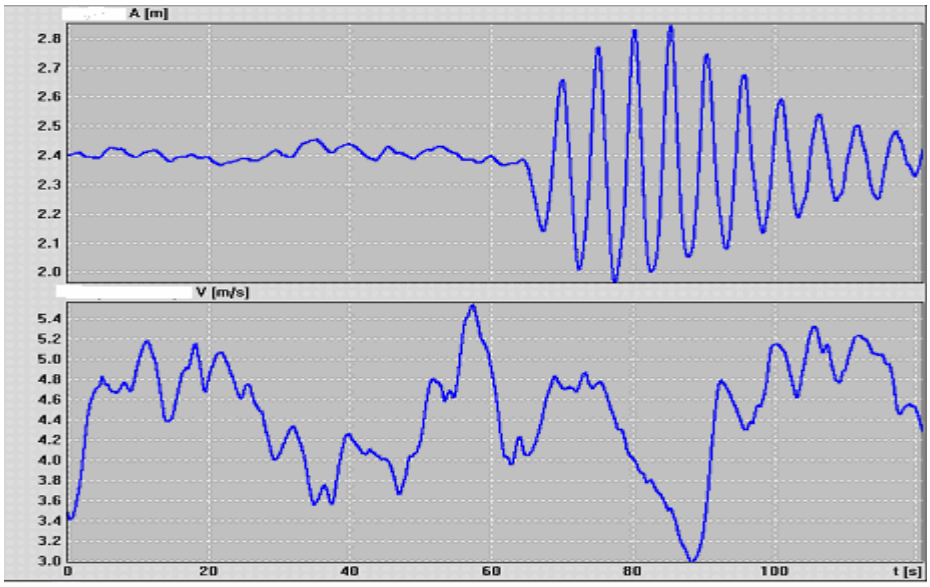

Figure 7.19: Synchronous measurement of forced horizontal one loop oscillation together with wind speed.

For a drag coefficient of 1.2, a conductor mass of 1.2 kg/m and diameter of 0.0275 m, at a mean wind velocity of 4 m/s and an observed frequency of 0.33 Hz, equation (7.8) gives an equivalent percentage of critical damping close to 1.6% which is in itself four times larger than the measured value from the graph.

We may estimate the power dissipation during one cycle at a given amplitude, say 0.4 meter zero-to-peak value as shown in Figure 7.19:

$$E_D = \xi_\vartheta . I . \pi . L . b^2 . \omega_\vartheta^2 \quad E_D = \int_0^{\frac{2\pi}{\omega_v}} dt \int_0^L k_D . U_0 . C_D . \left(\frac{dy}{dt} \right)^2 dz \qquad (7.10)$$

which, for a *pure* sine wave both in space and time, with an amplitude zero to peak of "a" on a span length of L (m) yields:

$$E_D = k_D . U_0 . C_D . \frac{\pi}{2} . L . a^2 . \omega_v \text{ (Joules)} \qquad (7.11)$$

Assuming the above mentioned values, this equation yields 12 Joules.

In conclusion, transverse vibration damping at low frequencies, typical of galloping phenomenon (generally 0.1 to 1 Hz), have negligible mechanical damping. The portion of the damping due to the tower or insulator string is also negligible. Most of the energy dissipation is coming from the drag coefficient and the wind speed (from as low as 2 m/s) which are generating larger energy dissipation than any mechanical source. Since damping has negligible effect on galloping amplitude, it is often modelled with no mechanical source of damping in the transverse movement (horizontal and vertical). However, as stated in Chapter 2, mechanical damping will influence the wind velocity at which the onset of galloping will occur.

Self damping in torsion

Despite a significant amount of the critical damping being in torsion, the amount of energy in a torsional movement remains very low. It can be estimated by the torsional equation of movement in a similar way as for vertical movement:

$$E_D = \int_0^{\frac{2\pi}{\omega_v}} dt \int_0^L 2\xi_\vartheta . I . \omega_\vartheta . \left(\frac{d\vartheta}{dt} \right)^2 dz \qquad (7.12)$$

$$E_D = \xi_\vartheta . I . \pi . L . b^2 . \omega_\vartheta^2 \text{ (Joules)} \qquad (7.13)$$

Where:

b: zero-to-peak amplitude (in radians)

I: moment of inertia per unit length (kg·m^2/m)

For a single conductor, the moment of inertia is extremely low (in the order of 10^{-3} kg.m^2/m) and much higher for bundle (close to about 0.2 kg.m^2/m). The frequency in torsion (mode 1) is close to 1 Hz for single conductors, and 0.2 Hz for bundles, which is similar to the vertical frequency. Consequently, the energy dissipated in torsion for about 0.5 radian zero-to-peak amplitude (which is quite high), is approximately 5 Joules for the structures detailed in section 5.3.3 and illustrated in Figure 7.14.

Such a small amount of energy is sufficient however to drive flutter type galloping on bundle conductors, as in this type of galloping, the only way for the energy of the wind to be transferred to vertical motion is through torsion. This explains why there is a trend for anti-galloping devices to use the torsional energy to control flutter type galloping.

The torsional modes are largely influenced by the ice eccentricity and aerodynamic pitching moment. This is discussed in Section 3.1.6.

For pure torsional modes (single conductor), there is no contribution of the wind on self damping, the only source of damping being mechanical. On the other hand, for bundle configuration, there is a small vertical component of the movement that, if limited in amplitude, would have a negligible impact. Spacers may have some effect on damping, even for galloping type modes. In fact most of the spacers are rigidly connected to the sub conductors and no rotation inside the spacer clamp is permitted.

Some basic testing has been done in laboratory and in the field, but the basic physical mechanism of damping in torsional modes are not well understood. It is obviously related to interstrand friction, as for vertical modes, but in a different type of interaction. This is why the basic values obtained in vertical modes cannot be extrapolated to torsional modes.

Test on single conductor line

During the development of torsional devices for control of galloping, Ontario Hydro operated an outdoor test facility near Kleinburg Ontario. This was described in a CIGRE report [Cassan & Nigol, 1972]. That outdoor facility consisted of three spans, each 800 feet in length, on which various conductors could be supported and tensioned.

Among the tests conducted was the measurement of the fundamental vibrational properties of the span, and with a particular focus on the torsional behaviour. This was reported in detail in an IEEE paper [Nigol & Clarke, 1974]. Figure 7.20, reproduced from that paper, shows the natural vertical vibration of the span of bare 795 kcmil Drake ACSR conductor, supported in an 800 foot span, under a tension of 8000 pounds. The natural frequency is 0.288 Hz.

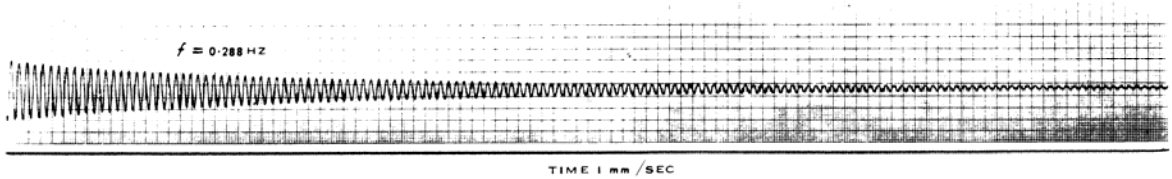

Figure 7.20: Frequency and decay curve in vertical oscillation for a 800 foot span of “Drake” 795 kcmil ACSR conductor vibrating in first mode. Frequency is 0.288 Hz.

Figure 7.21shows the equivalent natural frequency and decay in the first torsional vibration mode of the same span. The natural frequency is 2.4 Hz, some eight times as high as the vertical mode. The figures include the decay of the vibration in both modes, illustrating a much faster decay in torsion than in vertical motion. The rates of decay are 2.7 per cent per cycle in vertical mode and 7.9 per cent per cycle in torsional mode. It is worth noting that this higher level of torsional damping

was documented by Tebo [1941], and used in the development of the Tebo-Buchanan torsional damper for control of aeolian vibration.

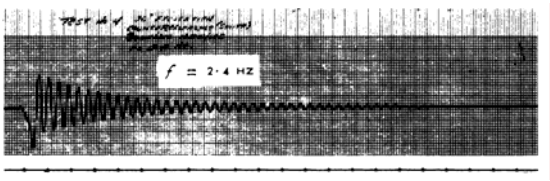

Figure 7.21: Frequency and decay curve in torsional oscillation for a 800 foot span of "Drake" 795 kcmil ACSR conductor vibrating in first mode. Frequency is 2.48 Hz.

Test on bundle conductor line

These test have been performed on the same set-up depicted in Figure 7.14 and 5.15.

The vertical amplitude during these tests was limited to 0.08 m peak-to-peak but torsional amplitudes were close to 0.5 radian peak. The corresponding percentage of critical damping can be deduced from the following curves (Figure 7.22 and Figure 7.23) and is close to 2%.

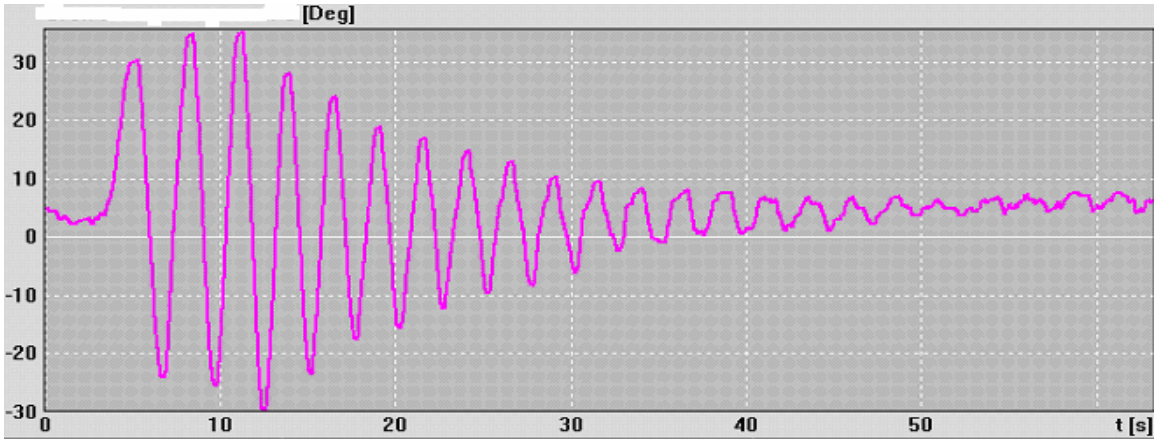

Figure 7.22: Angle of rotation of a twin bundle for a free torsional one loop mode (0.40 Hz)

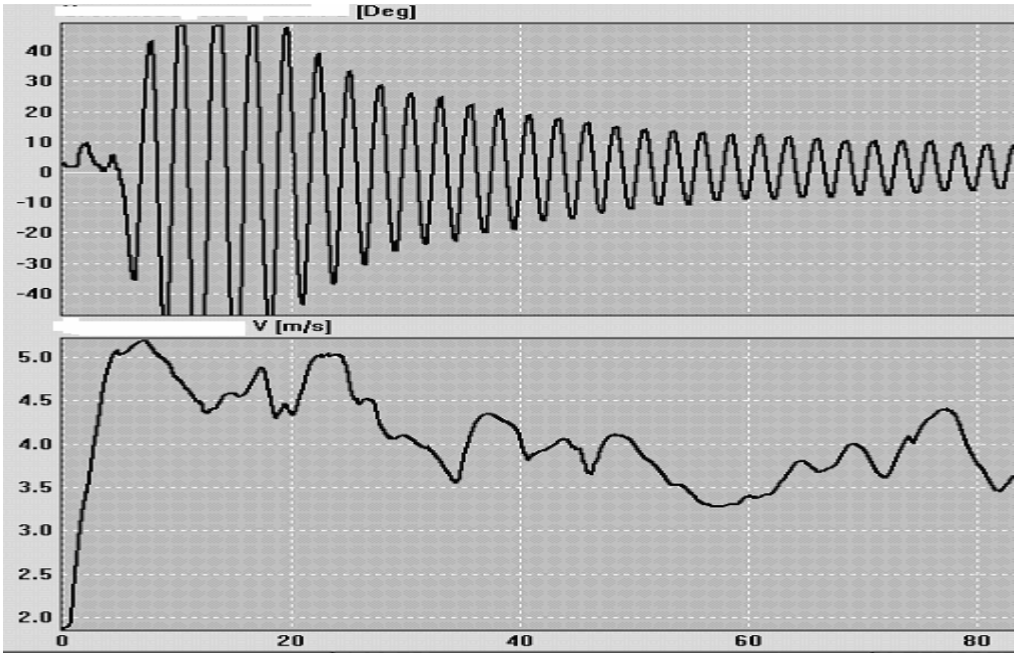

Figure 7.23: Free oscillation test for one loop torsional movement for a twin bundle (0.40 Hz) with synchronous measurement of wind speed

In conclusion, for torsional vibration, self damping of overhead conductors at galloping frequencies is small, but not always negligible. Despite the small amount of energy in torsional modes, it has a drastic impact on some galloping instability and therefore of prime importance to model it in appropriate ways, more specifically by its contribution in damping. It is reasonable to include about 2% of critical value of mechanical source of damping in a model, for the torsional movement, either for single or bundle conductor.

7.3.4 Anti-galloping conductors

Conductor manufacturing may affect galloping risks as they may change significantly the following characteristics:

- Ice accretion

  Depending on the type of ice, (rime, glaze or wet snow), the deposit may be altered either by the conductor surface (smooth, stranded), or its torsional stiffness. For example, Z-shaped conductors (Figure 7.24) are known to have, for diameters larger than 25 mm, a torsional stiffness more than two times that of round wire conductors, which influences the rotation of the conductor and hence the shape of the ice deposit. The same assumption can be made about compact conductors.

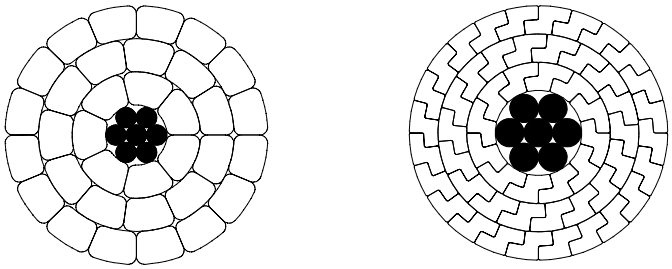

Figure 7.24: Compact and "Z" shaped conductor cross-sections

- Self-damping

  Some manufacturing may significantly increase self-damping at low frequencies which may help increase critical wind speed above which galloping occurs and even change stability conditions in coupled flutter instability for increased torsional damping.

– Aerodynamics

Some conductors, designed to limit aeolian vibration by changing its profile along the line (called "twisted pairs") may affect the aerodynamics of the conductor with ice, thus changing stability conditions of such conductors in presence of wind and ice (Figure 7.25). This is creating a kind of permanent air flow spoiler similar to some anti-galloping devices. Wind-tunnel tests have been performed to evaluate such risks [Douglas & Roche, 1981].

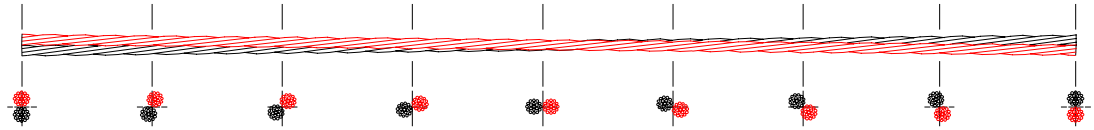

Figure 7.25: Twisted pair – varying profile

7.3.5 Torsional Rigidity

The expression of the torsional stiffness for a single conductor has been discussed manifold in the literature. The most detailed accounting of this has been published by Wang & Lilien [1998] and has set the following formula (applicable to conventional new conductors with round wires, AAAC or ACSR, from best fit of 87 different tests all around the world):

$$GJ = 0.00028\ \phi^4 \qquad (7.14)$$

where GJ is given in Nm^2/rad if the conductor diameter ϕ is given in mm.

Significant differences may occur for old conductors. The torsional stiffness has been measured on a number of different ACSR conductors [Nigol & Clarke, 1974], many when they were new, and others after some years of aging in service, and the measured values obtained are included in Table 7.4.

Table 7.4 - Measured torsional stiffness of sample ACSR conductors (per [Nigol & Clarke, 1974])

CONDUCTOR SIZE mm^2 **(kcmil)**	**DIAMETER** **mm (in)**	**AGE** **years**	**TORSIONAL STIFFNESS** Nm^2/rad **(**ft^2 **lb/rad)**
170.5 (336.5)	18.3 (0.721)	new	24.9 (60.3)
170.5 (336.5)	18.3 (0.721)	45	58 (140.3)
241.7 (477)	21.8 (0.858)	new	54.3 (131.4)
402.8 (795)	28.2 (1.110)	New	164 (396.8)
402.8 (795)	28.2 (1.110)	33	432 (1045.3)
472.6 (932.7)	30.5 (1.200)	new	289 (699.4)
604.3 (1192.5)	34.0 (1.349)	7	400 (967.9)
934.0 (1843.2)	40.7 (1.602)	new	455 (1101)
934.0 (1843.2)	40.7 (1.602)	11	2070 (5008.8)
1182.0 (2332.8)	45.7 (1.800)	7	1370 (3315)

The use of non-conventional conductors may also lead to some spectacular improvements (compact conductors have higher torsional stiffness, the largest measured increase being by a factor of 2.5 on aero-Z 620 mm^2).

It is important to note that the bundle torsional stiffness remains proportional to the fourth power of its diameter, making the torsional frequency independent of the conductor diameter.

The torsional stiffness of single conductors is easily modified by some simple devices, like eccentric masses (pendulum). Generally such devices also modify the moment of inertia of single conductors, which is basically very low. Global effect must be evaluated for galloping.

8. Risks, prevention, anti-galloping devices and design guide

8.1 Protection methods

The reader who would like to have access to more detailed discussion may go back to a recent publication published by the CIGRE TFG into ELECTRA [Cigre, 2000b].

We reproduce here the conclusions:

- The complexity of galloping is such that control techniques cannot be adequately tested in the laboratory and must be evaluated in the field on trial lines. This testing takes years and may be inconclusive.
- Analytical tools and field test lines with artificial ice are useful in evaluation of galloping risk and appropriate design methods.
- No control method can guarantee it will prevent galloping under all conditions.
- Interphase spacers virtually ensure galloping faults will not occur, but do not necessarily prevent galloping. Their usage is growing and their design is undergoing further development.
- Mechanical dampers to stop vertical motion are still being pursued but to only a very limited extent.
- Torsional devices, which either detune or increase torsional damping or both, are being pursued and actively evaluated.
- Techniques which disrupt either the uniformity of ice accretion by presenting a varying conductor cross-section or the uniformity of the aerodynamics by inducing conductor rotation are being actively pursued.
- Methods of ice removal or prevention are not widely used as specific anti-galloping practices.
- Despacering or using rotating-clamp spacers is still used extensively in a number of parts of Europe subject to wet snow accretions.
- For bundled conductors, the influence of the design of suspension and anchoring dead-end arrangements on the torsional characteristics of the bundle and on the occurrence of vertical/torsional flutter type galloping has been recognized.

8.1.1 Galloping control methods for existing lines

A survey of the various known galloping control methods was recently completed under the aegis of CIGRE and published in ELECTRA [Cigre, 2000b]. The various control approaches were classified as “retrofit” or “design” systems. This chapter will provide descriptions of “retrofit” devices. The ELECTRA paper also includes a list of discontinued methods. This chapter will focus on control devices which are considered to be practical, and in use, at least on a trial basis, on operating lines. Whenever possible, practical issues relating to ease of installation and side effects attributable to the devices will be summarized. A table forms the final section of this chapter, combining the key information about the application of each of the devices in current use. The devices will be discussed in this chapter including, where possible, the following aspects:

• For which type(s) of weather exposure and line construction has each device been tested and applied.

> Galloping can be caused by a range of different conditions, namely the type, density and adhesion of the ice, be it glaze, wet snow, or hoar frost, and the speed, direction, and turbulence of the wind. Most of the North American experience is with galloping due to wind acting on glaze ice accretions. Galloping due to wind acting on wet snow has received more attention in Japan and parts of Europe. The type of icing under which each device has been evaluated will be included along with known practical details. It is also different on small versus large single conductors, on bundle conductors versus single conductors, and on dead–end spans versus suspension spans.

There are even rare conditions, with wind but without ice, in which other mechanisms create galloping-like motions. The common feature of all galloping is the excitation of the lowest natural frequencies of the spans and the resulting large amplitude, low frequency motions.

• What are the proper locations for each galloping control device.

The number of devices required for control, or the physical design of the devices, or the manner of application of the devices may also differ according to the expected type of ice accretion and the physical details of the conductor span. Where there are alternative practices, these are identified. While application practices for some of the devices are public knowledge, for some devices these are considered proprietary by the suppliers.

• What are the limitations and precautions required with each galloping control device.

The performance of a control device may be acceptable in one range of sizes of conductor while less acceptable in another size range. Also the effectiveness in one weather condition may or may not indicate effectiveness in a different form of icing.

• Observed motions without and with each control device.

Data from tests on scaled or full size test lines, sometimes with airfoils to represent ice are included where available. More weight should be given to information obtained from observations on actual operating lines, especially where there are systematic trials including untreated phases similar to the phases with the control devices, and such results are included where possible. When galloping does occur in a span of an overhead line, the individual conductors are frequently moving at different amplitudes and in different modes under nominally the same exposure to ice and wind. During an ice storm the galloping amplitudes change as the speed and direction of the wind, as well as the amount of ice deposited changes. This randomness and variability are inherent in the galloping phenomenon. Conclusions on the overall performance of a device need to be based on a number of separate galloping events. The greatest confidence can be placed on the devices that have been the subjects of the widest exposure and evaluations. At the same time the control device needs to be installed on one or more phases in the same span as nominally identical phases without controls. Galloping motions on all the phases needs to be documented to enable proper statistically supportable conclusions on performance of the control devices to be obtained.

8.1.2 Interphase spacers

The most widely use galloping control device is the interphase spacer. Stiff and flexible interphase spacers have been used on 115, 230 and 500 kV lines since the 1970s [Edwards and Ko, 1979]. The earliest stiff spacers were assembled from ceramic insulator sections joined with an aluminum tube, and attached to the conductors using standard suspension clamps. These spacers were heavy and difficult to handle and install (Figure 8.1). Some early rigid spacers suffered breakages of the insulating sections due to the high compressive forces occurring during galloping, and there were failures of the welded joints at the ends of the central aluminum tube. Later polymeric insulators were substituted for the ceramic sections creating a lighter and more manageable, but still rigid, assembly (Figure 8.2). Flexible clamps were also used, but special means were needed to avoid arcing at the sliding surfaces. More recently armor grip suspension (AGS) clamps have also been used to reduce local stresses in the conductors at the points of attachment. Subsequent designs were made more flexible through joints within the length of the spacers, initially retaining the metal middle section (Figure 8.3). Later designs substituted silicone rubber covered fibreglass rods for the metal sections. These changes effectively created a chain of insulated links between the phases. Figure 8.4 and Figure 8.5 show designs of such interphase spacers used at 230 kV and 500 kV respectively, in the CEA sponsored field trials of galloping controls for bundled conductors [Pon and Havard, 1994]. The joints are bridged with flexible metal bonding straps to eliminate arcing from movements of the loose joints. Corona rings are mounted at the high voltage ends of the sheds of the polymeric insulators to reduce the electric field gradient and minimize arcing damage to the sheds. A sample installation of a flexible interphase spacer on a Manitoba Hydro 500 kV triple bundle line is shown in Figure 8.6.

While most of the applications are to vertical or near vertical circuit arrangements, interphase spacers have also been applied to horizontally arranged circuits with galloping problems. One such design for a two conductor bundle line in northern Norway which has experienced frequent winter damage, is shown in Figure 8.7. This rigid design uses composite insulators and has a tubular steel central section. It is underslung to ensure that the bundle stays in its normal orientation. Some cases of damage to interphase spacers have occurred with this design.

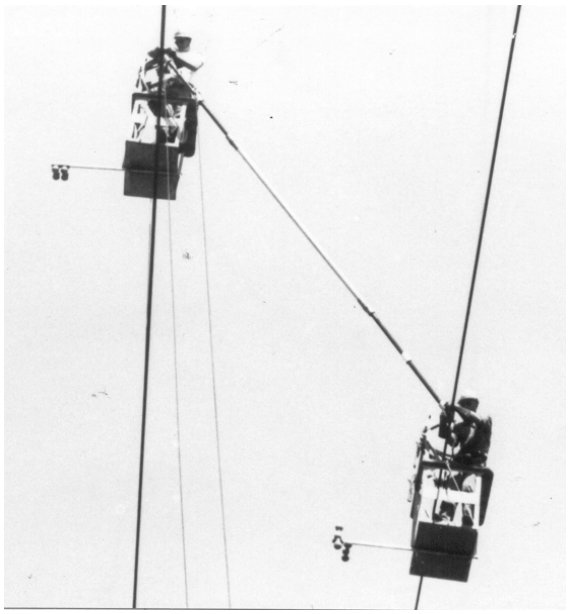

Figure 8.1: Installation of a rigid interphase spacer [Havard, 1978]

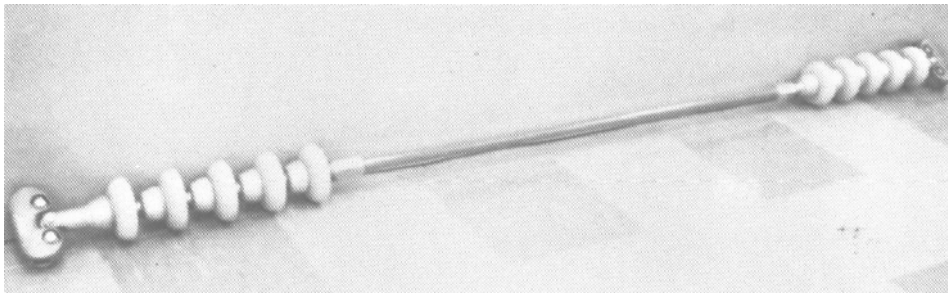

Figure 8.2: Stiff hybrid spacer for 115 kV lines [Pon et al., 1982]

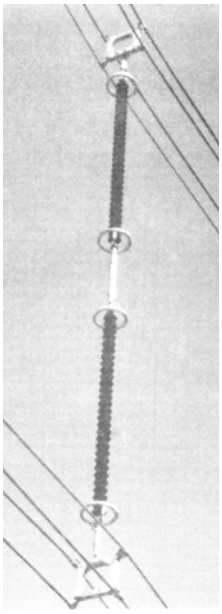

Figure 8.3: Flexible spacer for use at 500 kV [Pon et al., 1982]

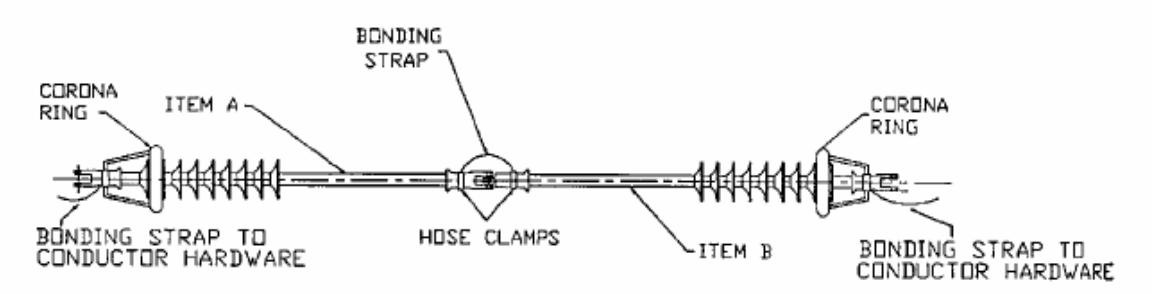

Figure 8.4: Flexible polymeric interphase spacer for use at 230 kV [Pon and Havard, 1994]

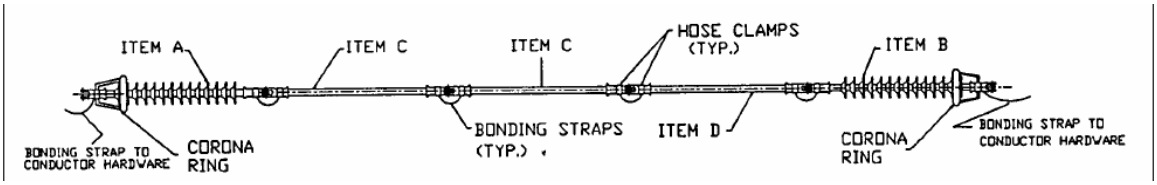

Figure 8.5: Flexible polymeric interphase spacer for use at 500 kV [Pon and Havard, 1994]

Figure 8.6: Flexible polymeric interphase spacer installed on a triple bundle 500 kV line in Manitoba Hydro [Pon and Havard, 1994]

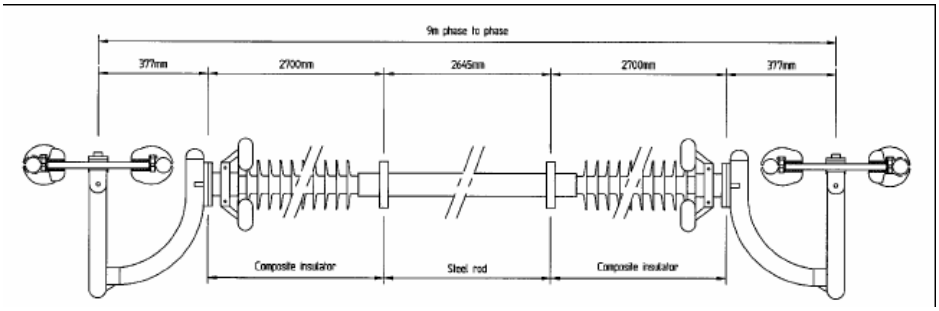

Figure 8.7: Rigid interphase spacer for a horizontally aligned two conductor bundle circuit in northern Norway [Loudon, 2003]

The proper location scheme for the interphase spacers in the span is important to ensure that the flashovers due to conductor clashing are avoided. Some interphase spacers have been installed at the point of largest galloping amplitude, namely the mid point of the spans. While this should avoid clashing and reduce the motions during single loop galloping, this point has the least impact on two-loop galloping.

Overhead line circuits in Germany can be vertical, horizontal or in a delta configuration. Interphase spacer location schemes, that are intended to be economical while still establishing an adequate level of control, have been proposed for each of these circuit designs [Schmidt and Jürdens, 1989]. The scheme for the delta circuit arrangement is shown in Figure 8.8. This spacing scheme was installed on over 100 spans of a twin bundle line in southern Germany, but the report does not include any field experience during galloping events. They also note that spans which include a transition from one configuration to another, or which serve to rotate the phases for electrical load balance, are at particular risk of flashovers during galloping. They recommend use of interphase spacers at the closest point of approach of the conductors.

Figure 8.9 illustrates recommended use of two or four interphase spacers per span of a vertically oriented circuit [Edwards and Ko, 1979]. In either of these arrangements the interphase spacers could be effective in both the single and two-loop modes. These arrangements were used in the field evaluations, but the alternative using four spacers is preferred, because there is still a possibility of contact between the phases at the quarter points in the span during mixed mode galloping with only two spacers. A diagram of this type of mixed mode motion, observed during a galloping event on Ontario Hydro lines, is shown in Figure 8.10. The upper and lower phase conductors are moving in a single loop mode, while the middle phase is in a two-loop mode. The middle phase conductor can approach the other conductors at the top of the left hand and at the bottom of the right hand interphase spacer.

Figure 8.11 shows a double exposure of a more usual type of galloping motion on a span of a vertical circuit fitted with four interphase spacers. This shows that galloping motion can occur but the spacers maintain the phase separation and minimize the likelihood of phase to phase contacts.

Field trials of interphase spacers were in place on Ontario Hydro lines during the 1970s [Pon et al., 1982]. In that period a number of manufacturers' products were installed, and most of the installations were on single conductor lines with stiff spacers. The field results from single conductor lines only are presented in summary form in Table 8.1.

The field data from single conductors are also presented graphically as a plot of peak-to-peak amplitude versus the fraction of the observations in Figure 8.12. The x-axis scale is based on the Weibull statistical analysis of values of extreme events (such as flood levels of rivers), and allows linear projection to give predictions of behavior beyond the plotted data. The figure includes all values of peak-to-peak amplitude on the untreated phases and all those with interphase spacers recorded during 10 separate galloping events. This figure shows that there is, on average, a reduction in the reported galloping amplitudes, but there are still large amplitudes of motion on the lines with interphase spacers.

In Figure 8.13 the same data are divided by sag and plotted against number of data points on the same scale as in the previous figure. This form of presentation compares directly with the design guides in which the galloping clearance envelopes are scaled to the sag of the conductor. The maximum amplitude is reduced from 0.52 x sag to 0.38 x sag, a reduction of 27%.

Results from Ontario Hydro's trials of interphase spacers on bundled conductors are included in Table 8.2, as part of the results of the CEA field trials.

The CEA field trials of galloping control devices for bundled conductor lines [Pon and Havard, 1994] included four sites with flexible interphase spacers on twin, triple and quad bundle lines. Figure 8.6 shows an installation on a 500 kV triple bundle line in Manitoba Hydro from that field program.

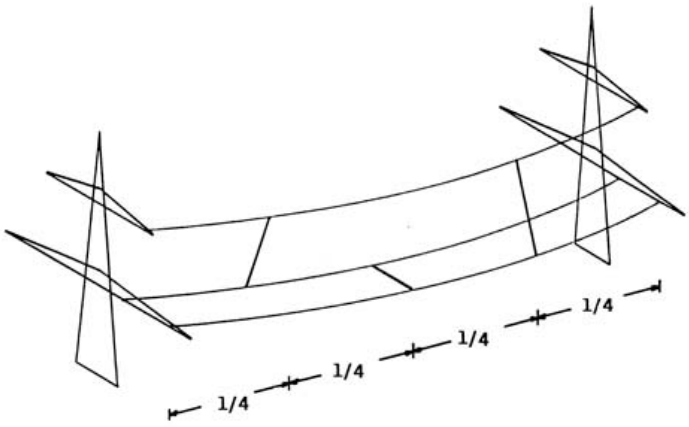

Figure 8.8: Mounting scheme for interphase spacers on a delta circuit [Schmidt and Jürdens, 1989]

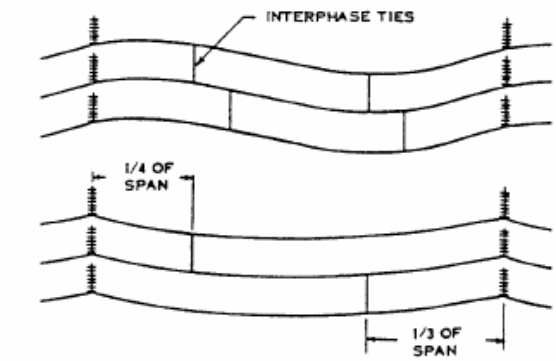

Figure 8.9: Alternative arrangements of interphase spacers in a span of a vertical circuit [Edwards and Ko, 1979]

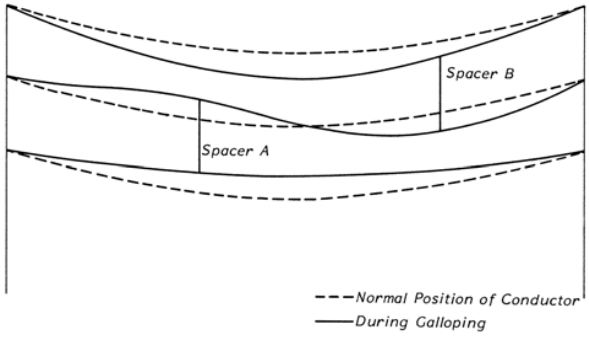

Figure 8.10: Forced motion of the middle phase conductor during mixed mode galloping with two interphase spacers [Pon et al., 1982]

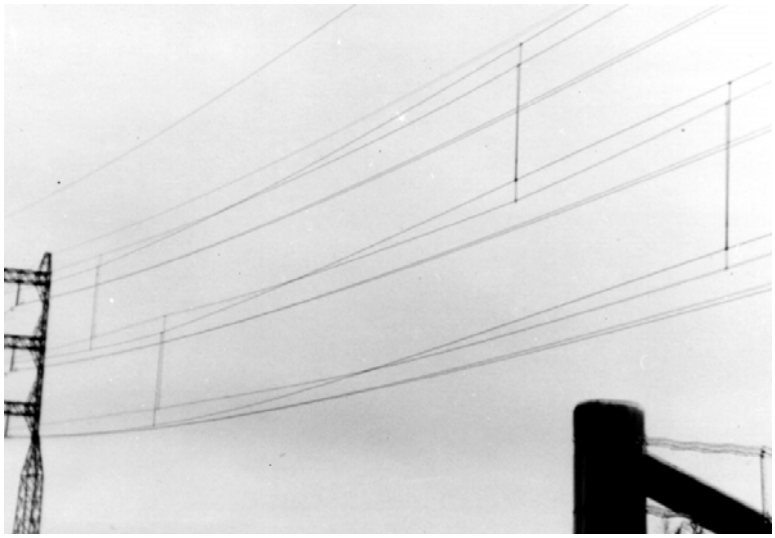

Figure 8.11: Double exposure photo of a span equipped with rigid interphase spacers during galloping showing two-loop motion [Pon et al., 1982]

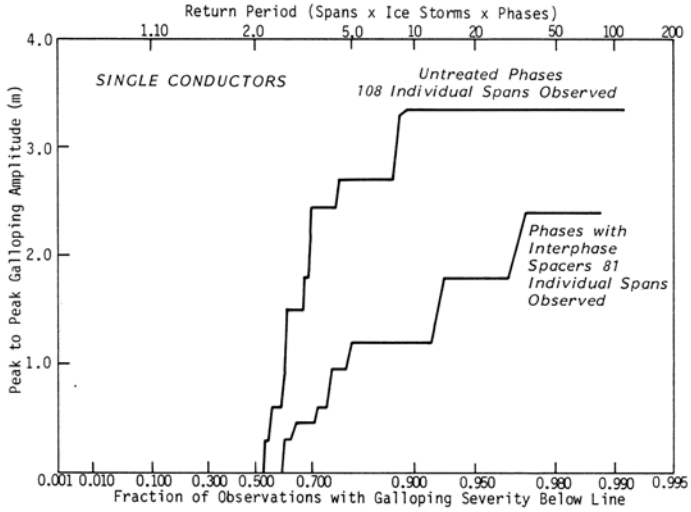

Figure 8.12: Effect of interphase spacers on peak-to-peak galloping amplitude based on 10 observations on single conductors [Pon et al., 1982]

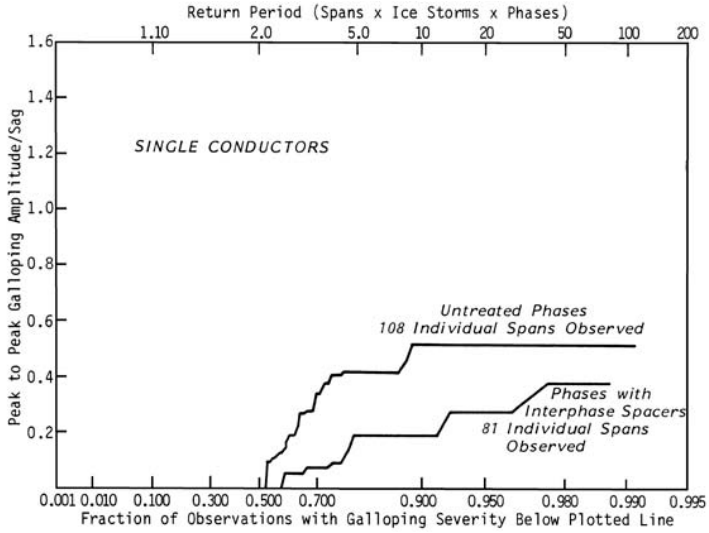

Figure 8.13: Effect of interphase spacers on peak-to-peak galloping amplitude/sag based on 10 observations on single conductors [Pon et al., 1982]

Table 8.1: Summary of performance of interphase spacers during eight galloping events on Ontario Hydro's single conductor lines [Pon et al., 1982]

LOCATION & VOLTAGE	CONDUCTOR DATA	AVERAGE PEAK-TO-PEAK GALLOPING AMPLITUDE WITH INTERPHASE SPACERS (m)	AVERAGE PEAK-TO-PEAK GALLOPING AMPLITUDE WITHOUT INTERPHASE SPACERS (m)
Kleinburg - Richview 230 kV	2332.8 kcmil ACSR 45.7 mm diam 190 m (620 ft) span	2	0
Kleinburg - Richview 230 kV	2332.8 kcmil ACSR 45.7 mm diam 259 m (850 ft) span	1.5	0
Kleinburg - Richview 230 kV	2332.8 kcmil ACSR 45.7 mm diam 259 m (850 ft) span	0	2.2
Kleinburg - Richview 230 kV	2332.8 kcmil ACSR 45.7 mm diam 259 m (850 ft) span	2.7	1.4
Major Mackenzie – Nashville 230 kV	2332.8 kcmil ACSR 45.7 mm diam 213 m (700 ft) span	0	4.8
Kleinburg – Richview 230 kV	2332.8 kcmil ACSR 45.7 mm diam 259 m (850 ft) span	1	1.7
Kleinburg - Richview 230 kV	2332.8 kcmil ACSR 45.7 mm diam 259 m (850 ft) span	1.4	2.1
Kleinburg - Richview 230 kV	2332.8 kcmil ACSR 45.7 mm diam 259 m (850 ft) span	1.7	1.5

The field trials of interphase spacers on bundled lines produced four documented galloping observations and these are summarized in Table 8.2. The results include three events in which there were no visible motions on the phases linked by the interphase spacers and small amplitude motions on the reference untreated phases. One event included significant motions on both the treated and untreated phases. These four results were not considered sufficient to draw conclusions about the overall performance of these devices under the range of ice and wind conditions conducive to galloping.

A world wide survey in the 1990s [Cigre, 1992] showed data from 32 utilities in 13 countries with nearly 13,000 installed interphase spacers. The survey reported that these are used on lines at voltages from 11 kV to 420 kV. The questionnaire investigated the opinion of the utilities with regards to both performance as a control device during galloping, and the experience with respect to damage and maintenance required of the interphase spacers.

Table 8.2: Summary of performance of interphase spacers during four galloping events on bundled conductor lines [Pon et Havard, 1994]

LOCATION & VOLTAGE	CONDUCTOR DATA	AVERAGE PEAK-TO-PEAK GALLOPING AMPLITUDE WITH INTERPHASE SPACERS (m)	AVERAGE PEAK-TO-PEAK GALLOPING AMPLITUDE WITHOUT INTERPHASE SPACERS (m)
Manitoba Hydro 500 kV	3 x 1271 kcmil ACSR 35.1 mm diam 377 m (1237 ft) span	6.1	7.6
Ontario Hydro 500 kV	4 x 585 kcmil ACSR 24.1 mm diam 255 m (837 ft) span	0	1.5
Ontario Hydro 500 kV	4 x 585 kcmil ACSR 24.1 mm diam 274 m (899 ft) span	0	1.5
Ontario Hydro 500 kV	4 x 585 kcmil ACSR 24.1 mm diam 274 m (899 ft) span	0	0.6

Solely from the performance point of view the survey indicated:

• Many survey responses indicated that there were no phase to phase or phase to ground flashovers after installing the interphase spacers

• Some low amplitude galloping was seen after spacer installation, but large amplitude motions appear to be eliminated

• Clashing was prevented but galloping continued at a lower level

• Wear and conductor damage occurrences were reduced

Reported side effects of using the interphase spacers included:

• Some mechanical damage to the insulator sections of the spacers in the form of cracking of the sections with sheds

• Electrical and mechanical breakdown in some urban areas, due to tracking attributed to pollution.

• A few cases of compression failures during galloping

• Some spacers damaged by birds pecking at the insulator sheds

• Some porcelain insulator sections were replaced by polymer insulators.

Spacers have proved effective at eliminating phase to phase contacts during galloping but there can still be conductor motions and dynamic loads on the support structures.

Recently, studies of interphase spacer behaviour during simulated galloping have been carried out at IREQ, Hydro Quebec's research facility [Van Dyke and Laneville, 2004]. A "D' section foil was attached to the conductors to produce galloping at any time of year providing the winds were adequate. Tests were conducted on full scale test line with a vertical conductor arrangement simulating a 120 kV line with and without interphase spacers. Interphase spacers were efficient in preventing conductors from coming close together, however, higher galloping amplitudes were reached with it.

It contradicts some observations from the field which indicate that conductors are generally less prone to galloping when equipped with interphase spacers. This may be attributed to the fact that in the field, the natural ice accretion may be different on each conductor and one conductor may act as a damper while the other one alone would experience severe galloping. Moreover, when there are no interphase spacers, conductors tilt under the effect of drag. Consequently, instead of remaining vertical, the initial angle of incidence on the D-section varies between 0º and 20º, depending on the perpendicular component of the wind speed. This may explain why the amplitude does not increase much with the wind speed when there are no interphase spacers since the angle of incidence exceeds the range of galloping instability. However, when there are interphase spacers, even for high wind speed, the conductors will remain mainly vertical because they are linked together at two points along the span. The D-sections were installed vertically and their initial angle of incidence remained the same regardless of wind speed. The higher torsional flexibility of the configuration without interphase spacers may facilitate the initiation of galloping but it may also set a lower bound for galloping amplitudes since the conductor torsion added to the apparent angle of attack (ratio of conductor speed over wind velocity) may bring the conductor out of its range of instability at lower amplitudes. Since the range of instability (in term of angle of attack) of a natural ice accretion is not necessarily located around the at-rest position of the conductor, its susceptibility to gallop may also be reduced by interphase spacers while it was increased for the D-section.

In summary, the interphase spacers have a good track record for eliminating flashovers during galloping but they do not prevent the galloping motions. Observations in the field show that motions still occur with interphase spacers in place, especially when the galloping conditions are such that high levels of motion can occur. The side effects of galloping such as high loads on the support structures and damage to the conductors at the suspension clamps can still be a problem with interphase spacers. Interphase spacers are also subject to breakage if they are not designed well enough for the dynamic loads applied to them.

8.1.3 Aerodynamic control devices

8.1.3.1 Air Flow Spoilers

Galloping can be suppressed by modifying the aerodynamics along the line with alternating profiles, as by the air flow spoiler and the twisted pair conductor described earlier. The standard Air Flow Spoilers are mainly used on single conductors up to 230 kV [Douglas and Roche, 1985; Whapham, 1982]. Above 230 kV, the standard PVC material can degrade in the high electrical gradient. For bundled conductors above 230 kV, a special PVC material is used to survive the high electrical gradient. The air flow spoiler is comprised of a circular cross section, ultra violet light resistant, PVC rod with a diameter almost as large as the conductor and length of 4.3 m (14 feet). It is formed to create gripping sections at each end and the middle section is wrapped around the conductor as shown in Figure 8.14. The air flow spoilers amounting to about 25% of the span length are applied in two groups around the quarter and three quarter points in the spans.

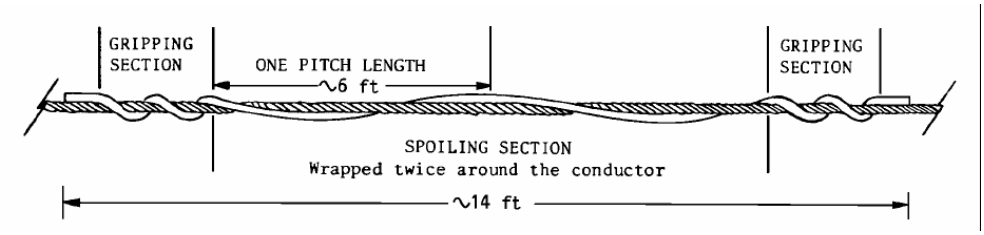

Figure 8.14: Air flow spoiler for galloping control on smaller conductors and overhead ground wires [Whapham, 1982]

Field trials of the air flow spoiler were conducted in the 1980-1986 period and these showed that galloping could be suppressed except when the ice covering is excessive and overwhelms the shape effect of the twisted profile. The field data obtained are summarized in Figure 8.15. This figure contains plots of field records of peak-to-peak galloping amplitude divided by sag versus percent of the data, using the Weibull extreme values probability scale. The left figure is from conductors without the air flow spoilers, and the right figure is from identical conductors with air flow spoilers within the same spans of operating lines. Division by sag allows comparisons with the galloping ellipses sizes used in design of clearances between conductors in structure profiles. The observations were obtained by field staff of cooperating US and Canadian utilities, during 31 different galloping events. They show that the air flow spoilers reduce the maximum galloping amplitudes from 1.3 to 0.5 times the sag, a reduction to 38 percent. The figures also show that there were no observable galloping motions during 20 of the 31 events when the air flow spoilers were installed.

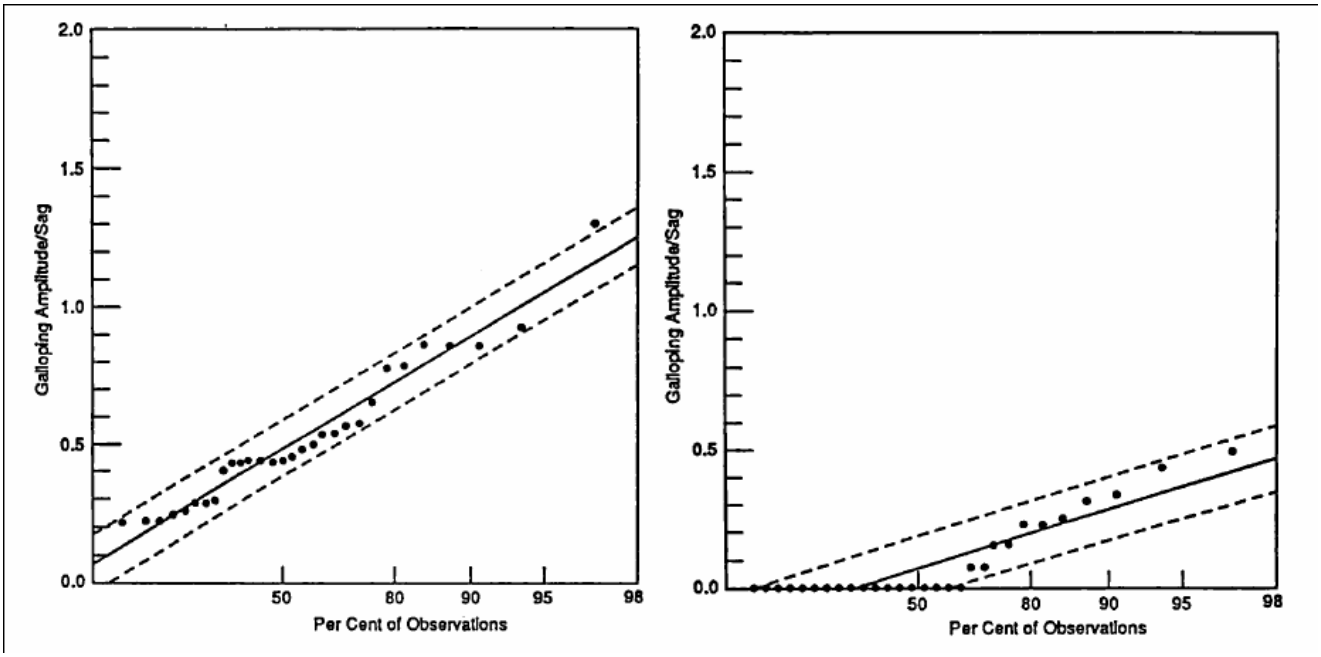

Figure 8.15: Extreme value plot of peak-to-peak galloping amplitude / sag versus per cent of observations on small conductors from 31 galloping events including fitted mean and 90% confidence limit lines. Left untreated conductors and right with air flow spoilers [Pon and Havard, 1993]

8.1.3.2 Eccentric Weights and Rotating Clamp Spacers

Galloping may be reduced when the ice profile is smooth and less eccentric. This review includes two devices that are together designed to encourage oscillation of the conductor during an ice storm to create a smoother ice profile with lower level of aerodynamic lift and moment. Figure 8.16 and Figure 8.17 show the devices used to apply this principle, namely the eccentric weights (GCD) and the rotating clamp spacers, which are for bundled conductors [Otsuki and Kojima, 1981].

The rotating clamp spacers allow the subconductors of the bundle to rotate and behave more closely to single conductors, which do not gallop as frequently as bundled conductors in Japan. This behavior is characteristic of regions where wet snow is more common than glaze ice. The eccentric weights are about 20 kg, and are mounted horizontally in alternating directions on the subconductors, and then any galloping motions that occur twist the weights around the subconductors and a smooth ice profile with lower aerodynamic lift is created. The system of rotating clamp spacers and eccentric weights has also been applied to quad bundles [Otsuki and Kojima, 1981].

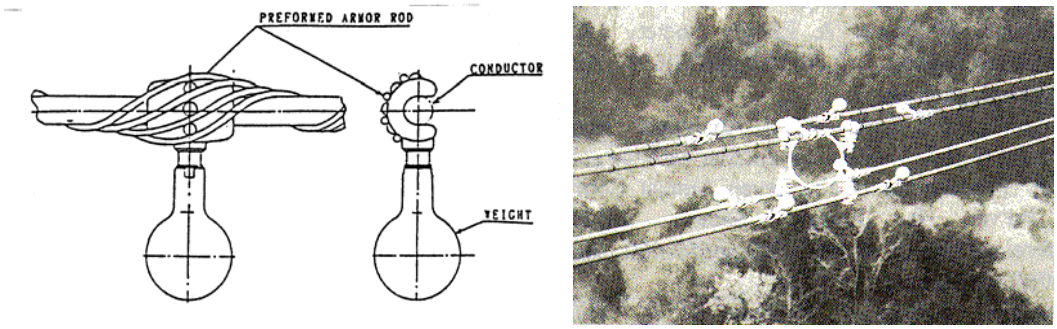

Figure 8.16: Eccentric weight (GCD) for galloping control [Otsuki and Kojima, 1981]

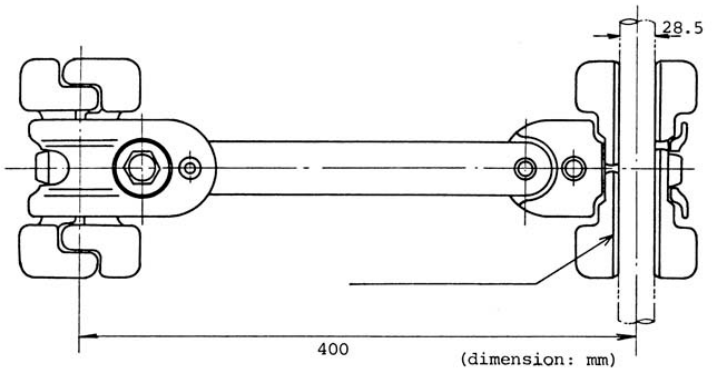

Figure 8.17: Rotating clamp spacer [Otsuki and Kojima, 1981]

The effectiveness of this device has been assessed from measurements of conductor tension changes during galloping events on an operating line. The dynamic tensile loads in the conductor were reduced by a factor of the order of 60 percent as indicated in Figure 8.18.

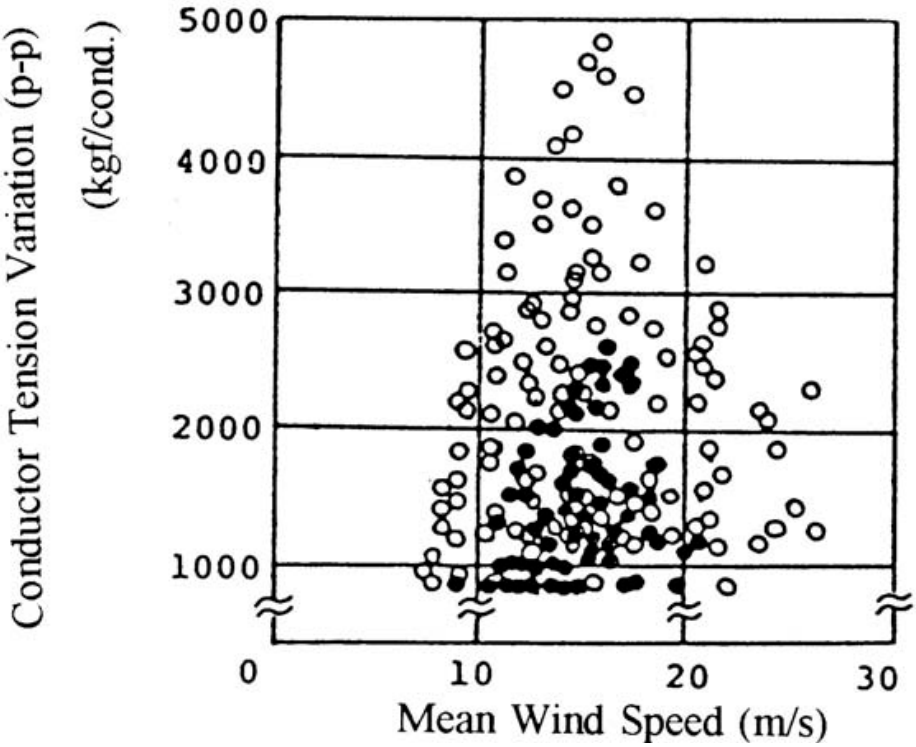

Figure 8.18: Variations of conductor tension versus wind speed during galloping events on bundled conductors. Open circles without GCD. Filled circles with GCD [Fujii et al., 1997]

8.1.3.3 AR Twister

The second device based on the principle of creating a smooth ice profile, but for single conductors, is the AR twister [Richardson, 1989]. This device is a weight attached rigidly to the conductor by a standard conductor clamp (Figure 8.19). The individual weights are about 3.6 kg (8 lb). The AR Twister is installed vertically above the conductor at mid-span, and the total weight and number of devices is chosen to rotate the conductor through between 90 and 140 degrees. During galloping the rotational oscillations are enhanced, so that the ice deposit forms on a greater area of the conductor, and a smoother profile is obtained. The aerodynamic lift is thereby reduced and galloping is less likely to occur. There do not appear to be any documented field evaluations of this device.

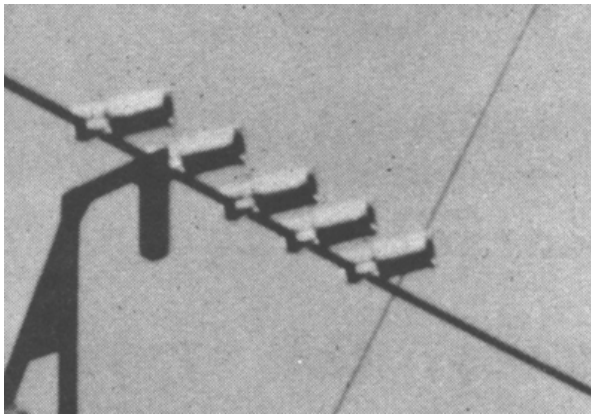

Figure 8.19: Installation of five AR twister devices on a steel guy cable [Richardson, 1989]

8.1.3.4 AR Windamper

The final aerodynamically based device, the AR Windamper, employs smoothing the ice profile and increasing both aerodynamic drag and the aerodynamic damping of the conductor. It is similar in some ways to the aerodynamic tee foil, which was used on distribution lines in the CEA field trials, but was also originally intended for use on larger conductors [Liberman, 1974]. The AR Windamper, Figure 8.20, is designed to provide a rocking motion due to the wind to create the smooth ice shape, and through its increase of area to the wind, adding aerodynamic drag and damping [Richardson, 1979]. There are versions for lower voltage lines, without the corona reducing end treatments, shown in the figure. There do not appear to be any documented field evaluations of this device.

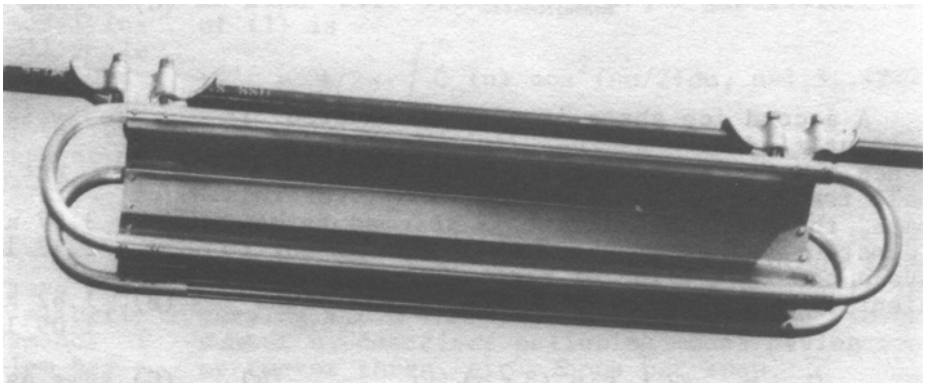

Figure 8.20: Aerodynamic drag damper [Richardson 1979]

8.1.3.5 Modified Drag Damper (MDD)

The Windamper was investigated at Ontario Hydro and subjected to analytical studies, and wind tunnel modeling. As well as confirming the available drag and damping effects, the findings included the discovery that under high winds the device would swing away from the vertical position and become aerodynamically unstable. These studies led to a version of the device termed the "modified drag damper" or MDD, Figure 8.21. The modified design has a slight change of angle of the two concave surfaces to optimize the aerodynamic characteristics. To stabilize the behavior under high wind, the addition of a second, heavier and geometrically similar, device was suggested for each span. This modified version was installed with both heavy (45 kg or 100 lb) and light (14 kg or 30 lb) designs in each span, and this control system was included in the field trials conducted on Ontario Hydro's operating lines [Havard, 1978].

The field trials that followed used at least two devices of different weights in each span. The devices were evaluated under galloping conditions on single and bundle operating lines in the same manner as the devices described earlier. The effectiveness was measured by comparing the peak-to-peak amplitudes of motion on nominally identical untreated conductors with those on the conductors with the MDDs in the same span. The results obtained on single conductors after eight galloping events are summarized in Figure 8.22. This plot uses the field data from every individual span of conductor recorded, as opposed to averages on the treated and untreated phases, which is statistically more valid. The peak-to-peak galloping amplitudes are divided by the sag to provide comparisons of spans of different lengths and with standard

clearance ellipse design procedures. The plot indicates that the MDD reduced the maximum amplitudes from 0.85 times to sag to 0.22 times the sag. This is an improvement of about 75 percent.

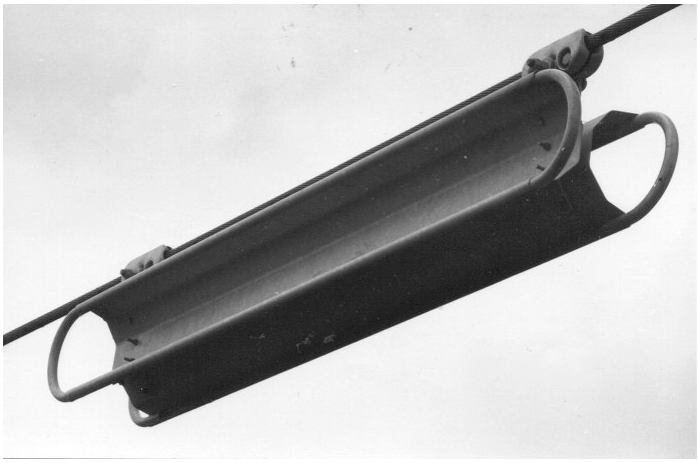

Figure 8.21: Modified Drag Damper used on Ontario Hydro field test sites [Havard, 1978]

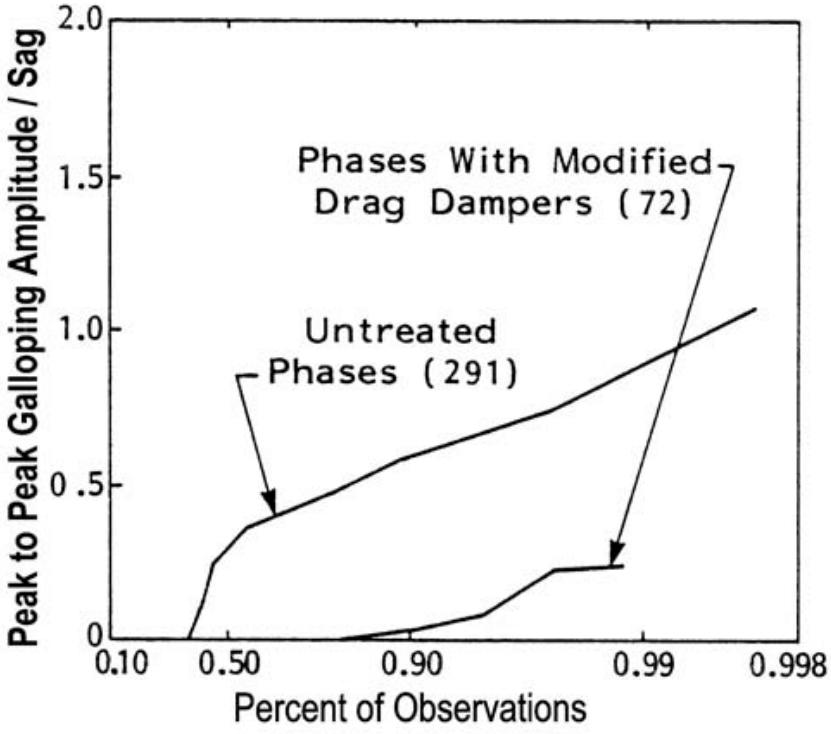

Figure 8.22: Observed amplitudes of galloping normalized by dividing by sag, on untreated single conductors and single conductors with modified drag dampers during 8 galloping events [Havard and Pohlman, 1981]

8.1.3.6 Aerodynamic Galloping Controller (AGC)

Another similar galloping control device recently introduced to the market by Engineering and Technology Solutions Inc., is the AGC or "Aerodynamic Galloping Controller", Figure 8.23. The claims for this device include improved aerodynamic effectiveness, applicability to all conductor types and span lengths, lower weight, better clamping systems, computer based calculation of installation locations, and ease of installation. There do not appear to be any published data on the field performance during actual galloping events.

Figure 8.23: Aerodynamic Galloping Controller (Engineering and technology solutions, promotional flyer, 2005)

8.1.4 Torsion control devices

Since the torsional mechanism of galloping was suggested [Nigol and Clarke, 1974], several add-on galloping controls have been developed and evaluated through field testing. These devices variously add damping of the torsional motion, or change the torsional behavior of the span.

8.1.4.1 Torsional Control Device (TCD)

An early device for controlling galloping of twin bundle conductors, that recognized and used the torsional motions, is the TCD or "torsional control device" [Sasaki et al., 1986]. The TCD damper is a tuned torsional spring and inertia system and is illustrated in Figure 8.24. Two or three of these devices are mounted in each bundle conductor span. The torsional natural frequency of the damper is made to coincide with the either first or second mode torsional frequency of the span with a typical ice load on the subconductors. There is no damping element. Under galloping-inducing conditions the damper oscillates preferentially to the bundle and reduces the overall galloping amplitude. Preliminary results are encouraging.

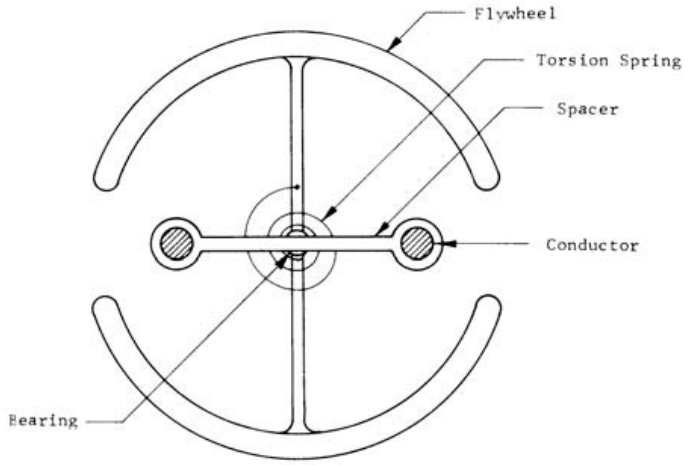

Figure 8.24: Torsional control device (TCD) for controlling galloping on twin bundle conductors [Sasaki et al., 1986]

8.1.4.2 Galloping Control Device (GCD)

Several forms of tuned torsional galloping control devices have been developed in Japan [Fujii et al., 1997]. Figure 8.25 shows another design named the galloping control device (GCD) in which a bundle of steel wires provides the elastic member attached to the inertia arm.

This approach has been extended to large bundles and an example installed on a bundle of six subconductors is shown in Figure 8.26 [Yanagisawa et al., 1990]. An example of its effectiveness on the 360 m (1181 feet) long, Oku-Nikko UHV, instrumented test span in a mountainous region of Japan, during a wet snow induced galloping event, is shown in Figure 8.27. This figure shows the orbits of movement on the two phases, one with the galloping controls shown in Figure 8.26, and the other without any controls. The figure shows oscillation of 4.2 m (13.8 feet) vertical and 1.2 m (3.9 feet) horizontal on the untreated phase, and 1.1 m (3.6 feet) vertical and 0.3 m (1 foot) horizontal, on the phase with the galloping control. The corresponding dynamic tensions were also documented. The measurements show that the tension in each subconductor were reduced from 1900 kgf (4180 lb) on the untreated phase to 500 kgf (1100 lb) on the phase with the galloping controls.

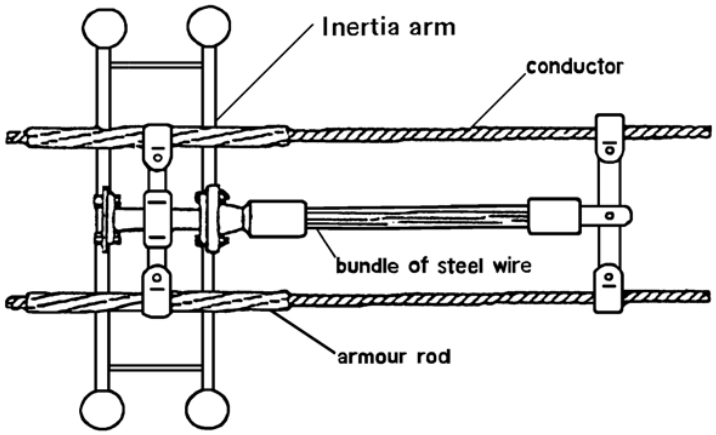

Figure 8.25: Galloping control device (GCD) for controlling galloping on twin bundle conductors [Fujii et al., 1997]

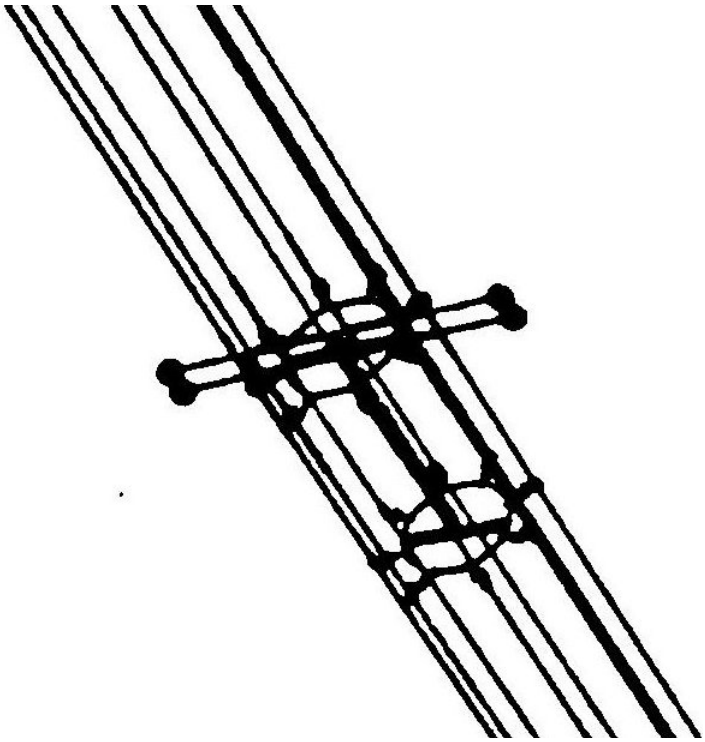

Figure 8.26: Galloping control device installed on a six conductor bundle test span [Yanagisawa et al., 1990]

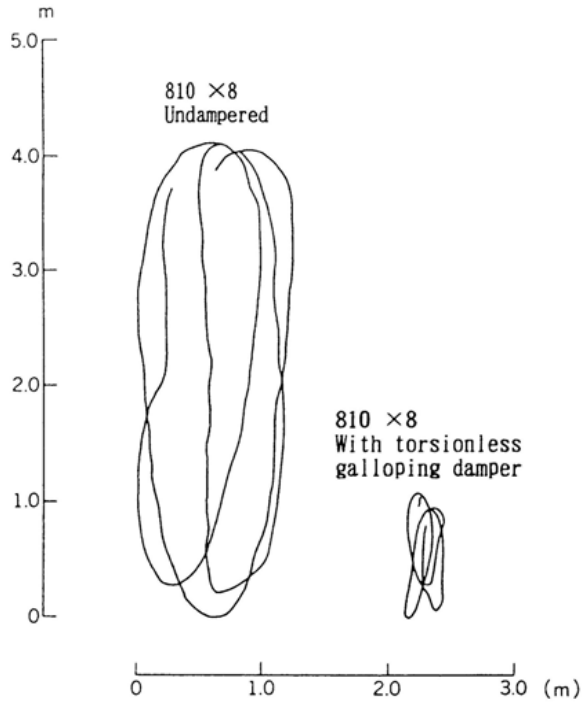

Figure 8.27: Orbits of conductor motion during galloping of a six conductor bundle test span. Left untreated span, Right with galloping damper [Yanagisawa et al., 1990]

8.1.4.3 Detuning Pendulums for Large Single Conductors

The earliest attempt to apply the torsional theory to controlling galloping of single conductors under glaze ice conditions in Canada, [Nigol and Clarke, 1974], involved adding torsional dampers. Initial trials on a test span and on operating lines were successful, but changes to the frictional properties of the sliding surfaces over time reduced their effectiveness.

Subsequently devices were designed to control the torsional oscillation frequency of the span and to keep it separated from the vertical natural frequencies during icing events. The most successful of these is the detuning pendulum (Figure 8.28). An early IEEE paper included the theoretical basis for designing detuning pendulums to suit each span [Nigol and Havard, 1978].

Figure 8.29 shows a typical configuration of an iced single conductor, illustrating the weight and wind forces acting on the cross section. The additional forces when a pendulum is added are included Figure 8.30. The key properties required in the selection of the parameters for the detuning pendulums are the natural frequencies of the span in vertical and torsional oscillation with ice and wind applied. The following two equations assume that the ends of the span are fixed. They also assume that the ice and wind forces and the stabilizing moment due to the pendulums, are constant across the span. The tension is the calculated value at the temperature of the galloping, including the effect of the weight of the ice and the pendulums.

The fundamental vertical natural frequency is given by:

$$f_{v1} = \frac{1}{2L}\sqrt{\frac{T}{m + m_{ice} + \frac{M}{L}}} \qquad (8.1)$$

Where:
L is the span length,
T is the conductor tension,
m is the mass per unit length of conductor
m_{ice} is the mass of ice per unit length of conductor, and
M is the total mass of all pendulums in a span

The fundamental torsional frequency of a span, f_{t1}, with pendulums of arm length R and total mass M, is given by:

$$f_{t1} = \frac{1}{2L}\sqrt{\frac{4s - 2m_{ice}gdL^2\cos(\theta+\theta_0)}{\pi^2} - \frac{dM_\alpha}{d\alpha} + MgRL\cos\theta}{d^2(\frac{m}{2}+m_{ice}) + \frac{\pi^2 MR^2}{L}} \qquad (8.2)$$

Where:
s is the torsional stiffness of the conductor,
g is the gravitational constant,
d is the diameter of the conductor,
M_α is the aerodynamic moment per unit length of conductor, and have the significance indicated in Figure 8.29 and Figure 8.30.

From these equations the vertical and torsional natural frequencies of an iced conductor span without pendulums are initially separate as shown at the left edge of Figure 8.31(a). The torsional frequency is higher than the first three modes of vertical oscillation. As the moment due to ice and wind builds up, the frequencies change as shown and at a certain level of ice and wind moment, circled, there is a near coincidence of frequencies and galloping can readily occur. After pendulums are added the frequencies change with increasing ice and wind as shown in Figure 8.31(b). With low values of ice and wind there is still a separation of torsional frequency from the vertical frequencies, but as ice and wind moment build up, the separation is sustained by the resistance to overturning of the pendulums. This separation of frequencies is maintained to a higher value of moment than without the pendulums as shown by comparing the ice levels for galloping, i_g, in Figure 8.31 (a) and (b). With pendulums attached, galloping is delayed to a higher level of ice and wind than without the detuning pendulums.

To ensure that they are effective in the various modes of galloping, three or four similar pendulums are attached at uneven spacing across the span. The arm length is between 150 and 450 mm (6 and 18 inches) and is chosen to control the torsional natural frequency so that it is at least twice the vertical frequency under the design ice load. The amount of mass per span is typically between 34 and 68 kg (75 and 150 lb), depending on conductor size and span length. The amount of mass is chosen to sustain the difference in frequencies up to a preselected amount of overturning moment from the ice weight and wind force, based on experience with applications on operating power lines.

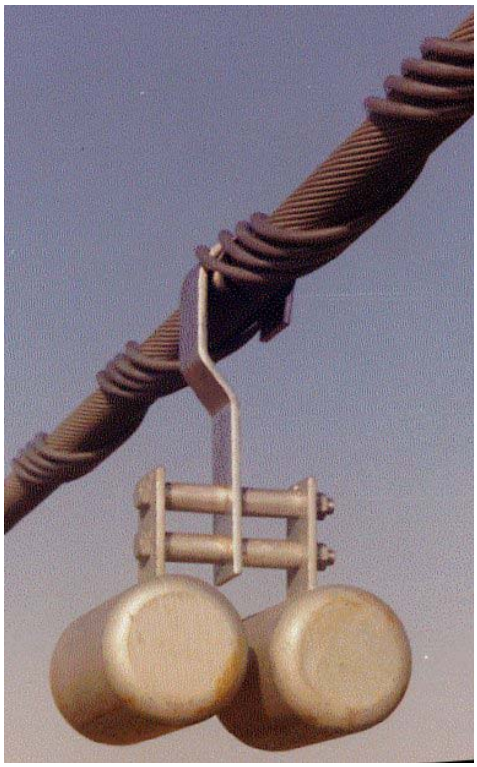

Figure 8.28: Detuning pendulum for single conductors [Havard, 1997]

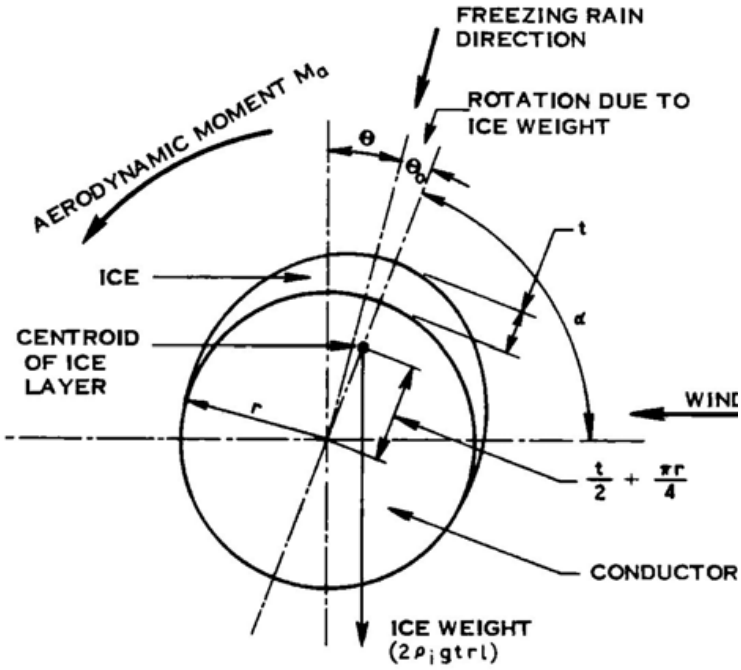

Figure 8.29: Schematic presentation of weight and wind forces an iced conductor [Havard, 1979b]

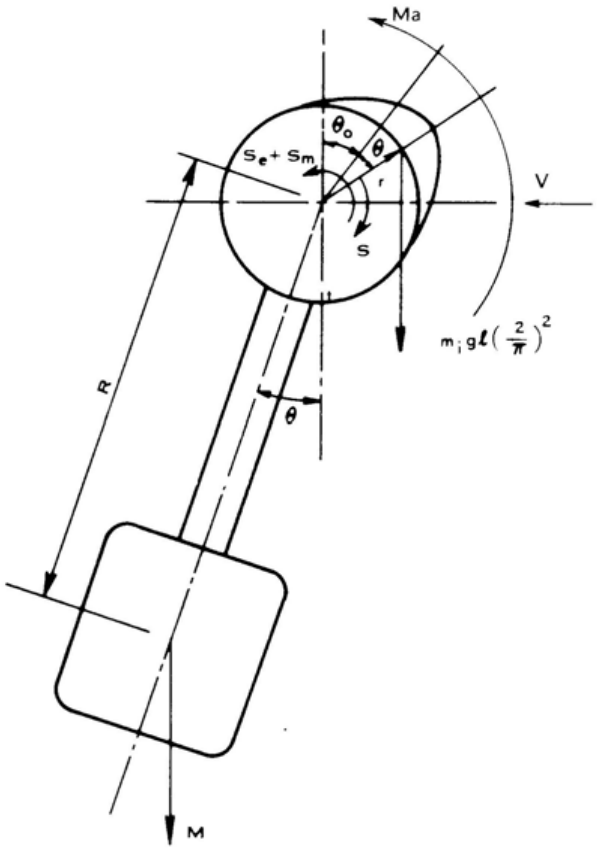

Figure 8.30: Schematic presentation of weight and wind forces on an iced conductor with a detuning pendulum attached [Havard, 1979b]

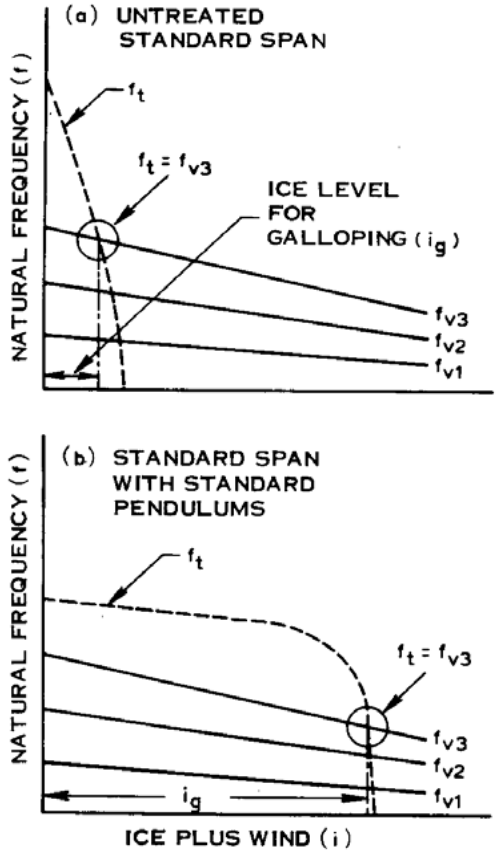

Figure 8.31: Variation of torsional and vertical oscillation frequencies of a single conductor span (a) without and (b) with detuning pendulums [Havard, 1979b]

These devices were used on a range of sizes of conductors in the same field trials as interphase spacers described earlier [Havard and Pohlman, 1979; Havard and Pohlman, 1984; Havard, 1996]. Figure 8.32 shows the results obtained on large single conductors, between and 25 and 50 mm (1 and 2 inch) diameter on spans between nominally 100 and 400 m (300 and 1200 feet), from 43 different glaze ice galloping events. Both parts of the figure show the fitted mean line and 90 percent confidence limits on the data. This figure allows comparisons of the peak-to-peak amplitudes divided by sag with and without the detuning pendulums. The figure shows that, at the 99 percentile level, the mean peak-to-peak galloping amplitude is 1.18 times sag without and 0.42 times sag with the detuning pendulums, a reduction of 64 percent. Also the untreated lines were seen to gallop in 41 of 43 ice storms while the pendulums were still in 24 of the 43 ice storms monitored.

An unusual property appears in the equations of torsional frequency, and cannot be readily found in conductor tables, and that is the torsional stiffness, s. This is the resistance to twisting of a length of conductor and it is determined through a simple test. A length, l, of the conductor is clamped at both ends and a twisting moment, T, is applied at the centre. The angle of rotation, , at the middle per unit of applied moment is calculated and the torsional stiffness, s, is determined from the following relationship.

$$s = \frac{\ell T}{4\theta} \qquad (8.3)$$

The torsional stiffness has been measured on a number of different ACSR conductors, many when they were new, and others after some years of aging in service, and the measured values obtained are included in Table 8.3.

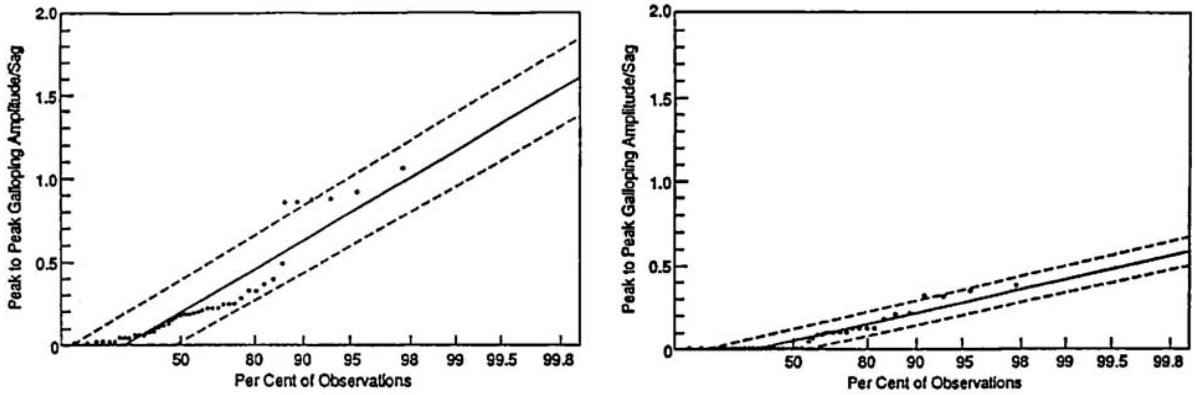

Figure 8.32: Comparison of peak-to-peak galloping amplitude / sag on large single conductors from 43 different galloping events. Showing fitted mean line and upper and lower 90 per cent confidence limit lines. Left without detuning pendulums, Right with detuning pendulums [Havard and Pon, 1990]

Table 8.3: Measured torsional stiffness of sample ACSR conductors [Nigol and Clarke, 1974]

CONDUCTOR SIZE kcmil	DIAMETER mm (in)	AGE years	TORSIONAL STIFFNESS Nm^2/rad (ft^2 lb/rad)
336.5	18.3 (0.721)	new	24.9 (60.3)
336.5	18.3 (0.721)	45	58 (140.3)
477	21.8 (0.858)	new	54.3 (131.4)
795	28.2 (1.11)	New	164 (396.8)
795	28.2 (1.11)	33	432 (1045.3)
932.7	30.5 (1.20)	new	289 (699.4)
1192.5	34.0 (1.349)	7	400 (967.9)
1843.2	40.7 (1.60)	new	455 (1101)
1843.2	40.7 (1.60)	11	2070 (5008.8)
2332.8	45.7 (1.80)	7	1370 (3315)

8.1.4.4 Detuning Pendulums for Distribution Lines

The detuning pendulums were also included in the field trials on distribution lines as described earlier [Pon and Havard, 1993]. These are smaller devices with a typical mass of 4.5 kg (10 lb), and arm lengths between 178 and 381 mm (7 and 15 inches), Figure 8.33. They were installed at several points along the span in a similar manner to the applications on the larger single conductors. The pendulums were attached using preformed spiral rods over a rubber lined saddle clamp.

The field trials generated a total of 15 sets of observations during mainly glaze icing events. The conductors were between 11.4 and 23.5 mm (0.45 and 0.93 inch) in diameter and span lengths were between 39.6 and 185 m (130 and 607 feet) in length. These are summarized in Figure 8.34 using the same type of presentation as before. The figure shows that, at the 98 percentile level, the mean peak-to-peak galloping amplitude is 1.76 times sag without and 0.93 times sag with the

detuning pendulums, a reduction of 47 percent. Also the untreated lines were seen to gallop in 11 of 15 ice storms while the pendulums were still in 8 of the 15 ice storms monitored.

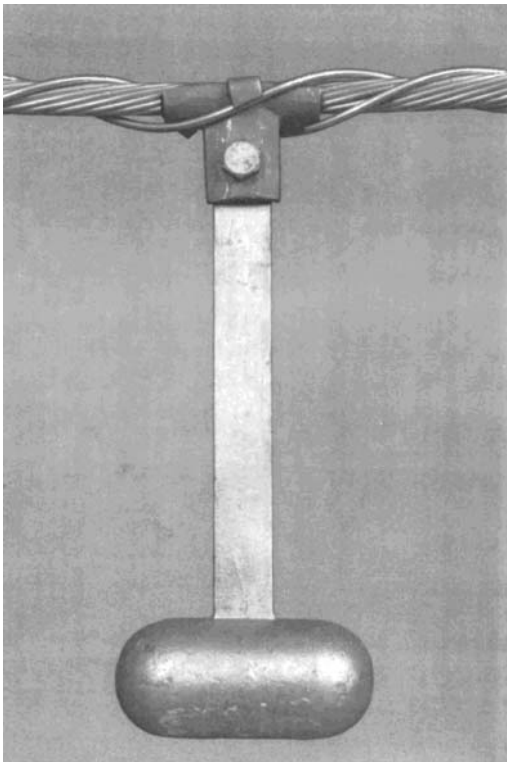

Figure 8.33: Sample detuning pendulum used in field trials on distribution lines [Pon and Havard, 1993]

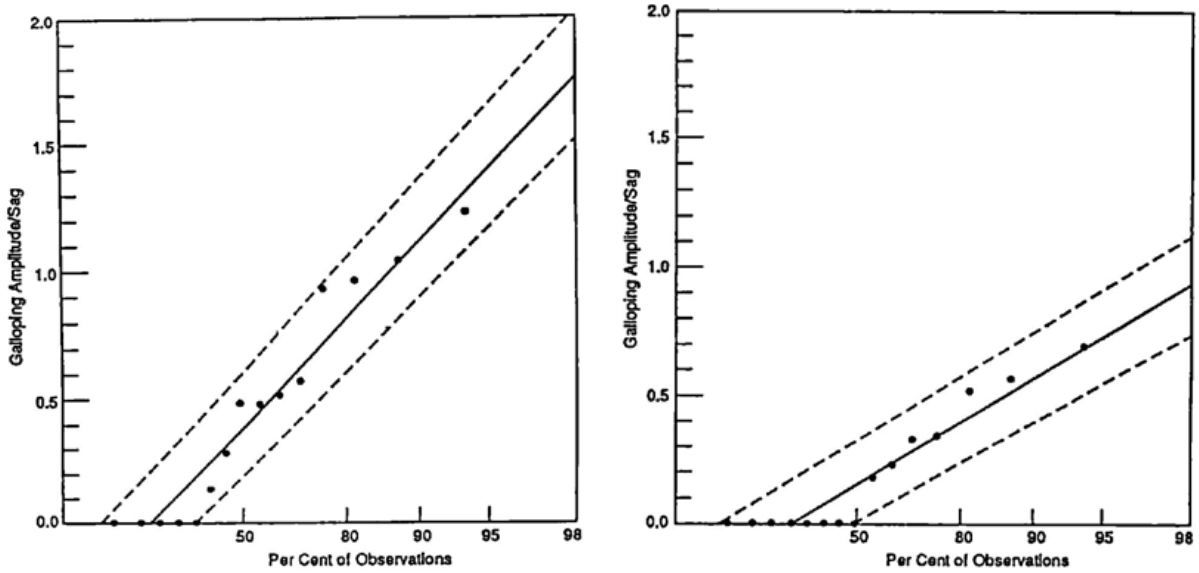

Figure 8.34: Comparison of peak-to-peak galloping amplitude / sag on small single conductors from 15 different galloping events. Showing fitted mean line and upper and lower 90 per cent confidence limit lines. Left without detuning pendulums, Right with detuning pendulums [Pon and Havard, 1993]

8.1.4.5 Detuning Pendulums for Bundle Conductors

The cooperative field trials also included sites for galloping control devices on twin, triple, and quad bundle operating overhead lines in USA, Europe and Canada. Figure 8.35, Figure 8.36, and Figure 8.37 show samples of the hardware used.

As for single conductors, the key properties required in the selection of the parameters for the detuning pendulums are the natural frequencies of the span in vertical and torsional oscillation during galloping combined with ice and wind. The major difference between the behavior of bundle conductors versus single conductors is that the conductor tension

contribute to the torsional stiffness and torsional natural frequency. The assumptions involved in developing the basic equations for bundles are the same as for the single conductors. The ends of the span are assumed to be fixed. It is also assumed that the ice and wind forces and the stabilizing moment due to the pendulums, are constant across the span. The tension is the calculated value at the temperature of the galloping, including the effect of the weight of the ice and the pendulums. With all symbols having the same significance as before and n_c being the number of subconductors in the bundle, the fundamental vertical natural frequency for a bundle is given by:

$$f_{v1} = \frac{1}{2L}\sqrt{\frac{T}{m + m_{ice} + \frac{M}{n_c L}}} \qquad (8.4)$$

The fundamental torsional frequency of a bundled span, f_t, is given by:

$$f_{t1} = \frac{1}{2L}\sqrt{\frac{Td^2\cos\theta + 4s + \frac{MgRL\cos\theta}{n_c} - \frac{2m_{ice}gdL^2\cos(\theta+\theta_0)}{\pi^2}}{d^2(m+m_{ice}) + \frac{\pi^2 MR^2}{n_c L}}} \qquad (8.5)$$

From these equations the vertical and torsional natural frequencies of an iced conductor span without pendulums are initially relatively close together, separate as shown at the left edge of Figure 8.38(a). The separation is greatest for single loop and is progressively closer in two-, three-, and four-loop galloping modes. As the moment due to ice and wind builds up, the frequencies change as shown and at a certain level of ice and wind moment, i_g in the figure, there is a near coincidence of frequencies and galloping can readily occur. This coincidence is circled for the two-loop galloping mode.

After pendulums are added, the frequencies change with increasing ice and wind as shown in Figure 8.38(b). With low values of ice and wind there are larger separations of torsional frequency from the vertical frequencies, than without the pendulums. But as the ice and wind moment builds up, the separation of the frequencies is sustained by the resistance to overturning of the pendulums. This separation of frequencies is maintained to a higher value of moment than without the pendulums as shown by comparing the ice levels for galloping, i_g, in Figure 8.38 (a) and (b).

The theoretical basis for both single and two-conductor bundle response was checked against the behavior of a full-scale test span, without and with pendulums added, at Kleinburg, Ontario [Nigol and Havard, 1978]. That test program also led to initial guidelines on the number of pendulums to be applied to conductors of different size and span length, in subsequent field trials on operating lines.

In the later field trials there were enough observations to provide statistically reliable data on performance of detuning pendulums on twin- and quad-bundles but not on triple bundles [Pon and Havard, 1994]. Figure 8.39 and Figure 8.40 show the data from 24 galloping events involving two conductor bundles, and 32 events on four conductor bundles, respectively. From the plot of data from galloping events on twin bundles, Figure 8.39, at the 99 percent point of the mean fitted line, the mean value of peak-to-peak galloping amplitude without control devices was 0.64 times the sag, while the corresponding mean peak-to-peak galloping amplitude was 0.18 times the sag with the detuning pendulums. This is a reduction of 72 percent.

From the plot of data from galloping events on quad bundles, Figure 8.40, at the 99 percent point of the mean fitted line, the mean value of peak-to-peak galloping amplitude without control devices was 0.67 times the sag, while the corresponding mean peak-to-peak galloping amplitude was 0.15 times the sag with the detuning pendulums. This is a reduction of 78 percent.

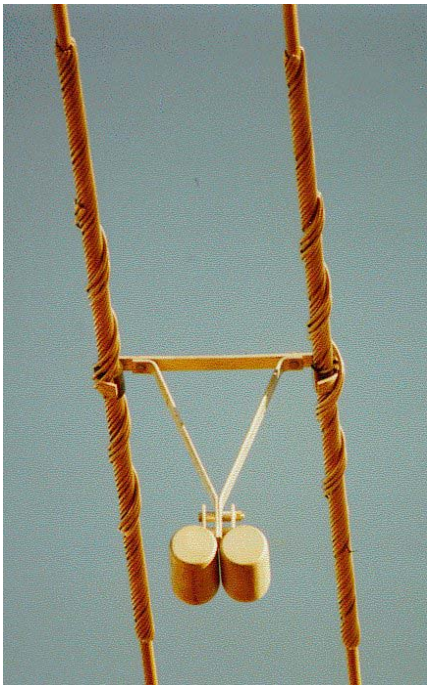

Figure 8.35: Detuning pendulum installed on a twin bundle conductor in Nebraska [Pon and Havard, 1994]

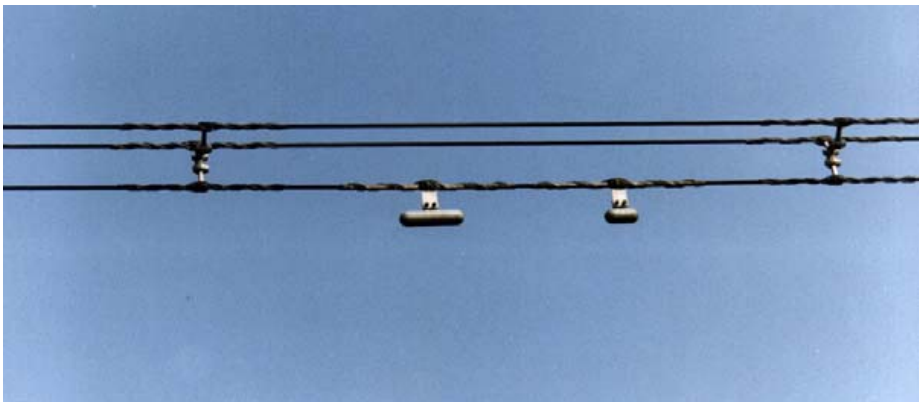

Figure 8.36: Detuning pendulum installed on a triple bundle conductor in Slovakia [Pon and Havard, 1994]

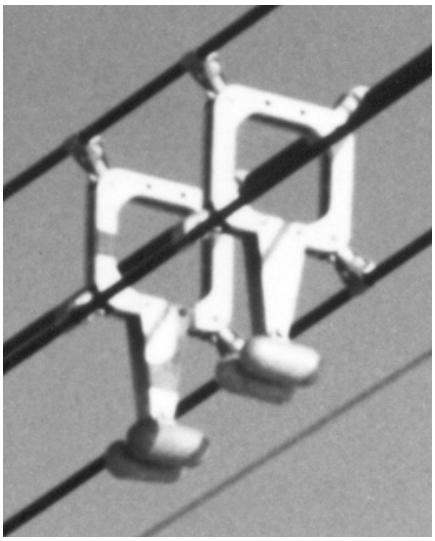

Figure 8.37: Detuning pendulums installed on a four conductor bundle line in Ontario [Havard and Pon, 1990]

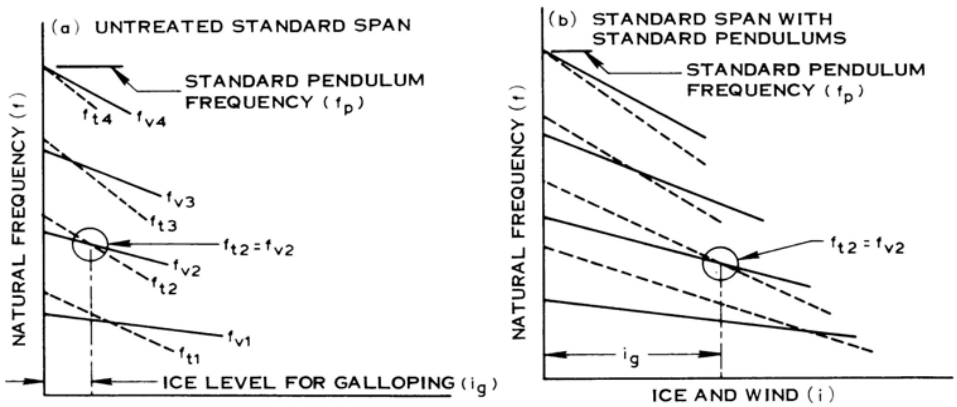

Figure 8.38: Variation of torsional and vertical oscillation frequencies of a bundle conductor span (a) without and (b) with detuning pendulums [Havard, 1979c]

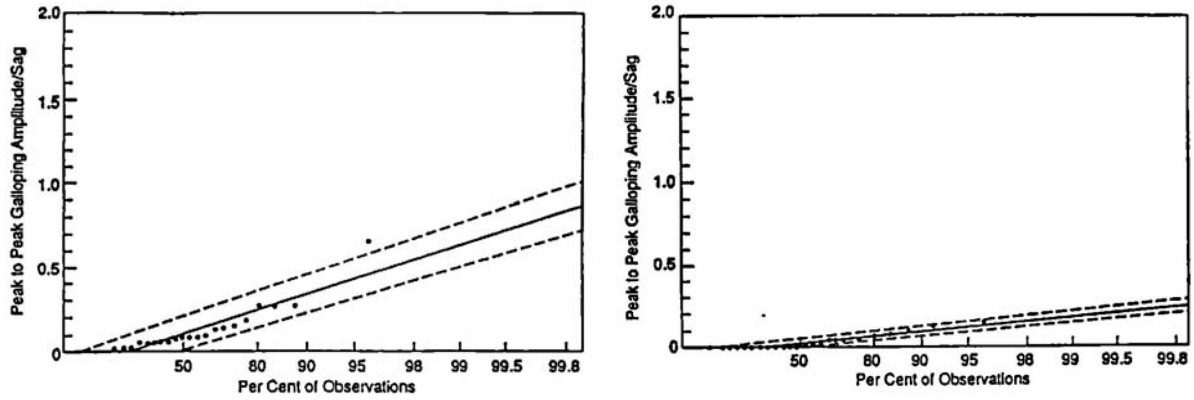

Figure 8.39: Comparison of galloping amplitudes on two-conductor bundles without and with detuning pendulums from 24 field observations showing fitted mean and upper and lower 90 percent confidence limit lines [Pon and Havard, 1994]

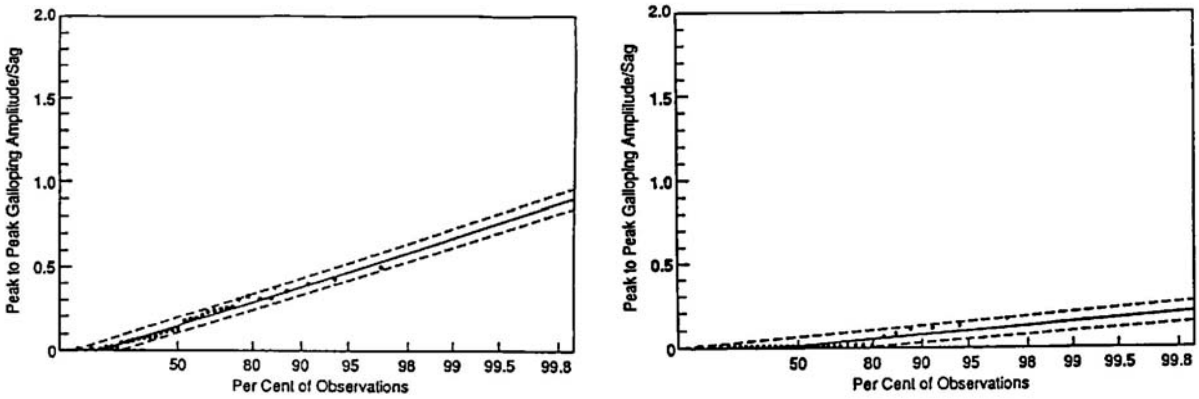

Figure 8.40: Comparison of galloping amplitudes on four-conductor bundles without and with detuning pendulums from 32 field observations showing fitted mean and upper and lower 90 percent confidence limit lines [Pon and Havard, 1994]

8.1.4.6 Torsional Damper and Detuner (TDD)

Figure 8.41 shows a diagram of the Torsional Damper and Detuner (TDD) galloping control device that has been designed to make use of the torsional motion of a bundle conductor during galloping to activate damping [Keutgen and Lilien, 1998]. The devices are tuned to oscillate at the fundamental galloping frequency and shift the resonant frequency of the span away from that frequency. The device is attached to a twin bundle with metal clamps. An inertial arm with a concentrated mass at each end rotates about a bearing 505 mm (19.9 inch) below the bundle. The centroid of the device is below the bundle and so it also acts as a pendulum. The damping is generated by twisting the butyl rubber cylinders

installed within the horizontal tubes, that are situated below the line. The device weighs about 30 kg (66 lb) and its center of mass is about 350 mm (13.8 inches) below the bundle.

Preliminary trials of prototypes of the device were carried out on a 310 m (1017 feet) long instrumented span of a 380 kV, 2 x 620 mm^2, operating line. This was located at an elevation of 550 m (1800 feet) above sea level, in the Ardennes region of Belgium, and the tests continued over a two year period [Lilien et al., 1993]. The span was equipped with two TDDs tuned to the first and second natural galloping frequencies. This trial produced data from one galloping event, during which the tensions in a phase with the TDD and that of a similar untreated phase were measured. The maximum peak-to-peak tensions were 10 kN without the TDD and reduced to 1.3 kN with the TDD.

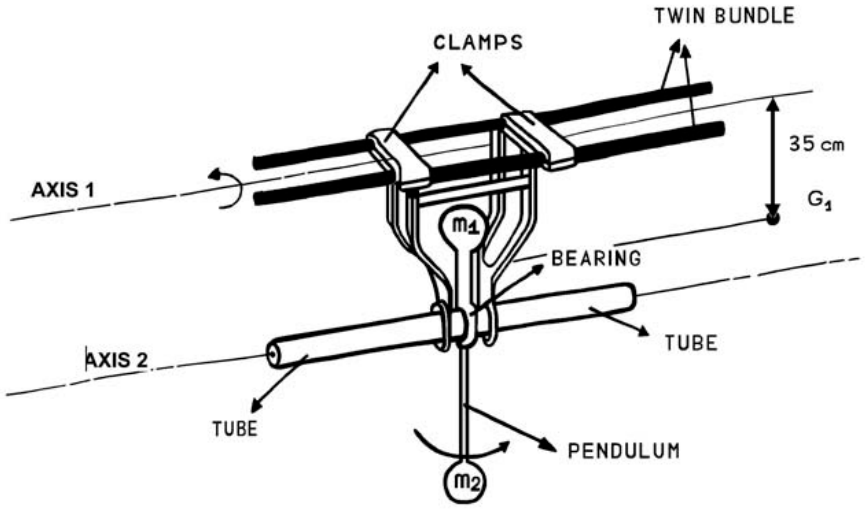

Figure 8.41: Diagram of the torsional damper and detuner (TDD) [Keutgen and Lilien, 1998]

Further field trials of the current design of the TDDs, Figure 8.42 have been performed in an open terrain site prone to strong winds in Kazakhstan [Lilien and Vinogradov, 2002]. These were carried out on an instrumented, three span, single phase, unenergized experimental line with span lengths of 84, 292 and 78 m (276, 958, and 256 feet). The conductor is a twin bundle of 451 ACSR conductor, with a diameter of 27.5 mm (1.08 inch). An ice coating was simulated by pointed airfoils on both subconductors, which could be rotated to change the angle of attack. The measurements were carried out sequentially on the middle span without TDDs, with two TDDs, and again without TDDs. Five combinations of wind direction and conductor tension were evaluated. The wind speed was typically in the 6 to 10 m/s (13.4-22.4 mph) range. Galloping was successfully achieved without the TDDs in place, reduced significantly by the addition of the TDDs, and restored to the previous levels when the TDDs were removed. The TDDs showed reductions of vertical amplitude between 86 and 92 percent.

Figure 8.42: Photograph of the torsional damper and detuner (TDD) installed on a twin (left) or triple (right) bundle line [Lilien and Vinogradov, 2002]

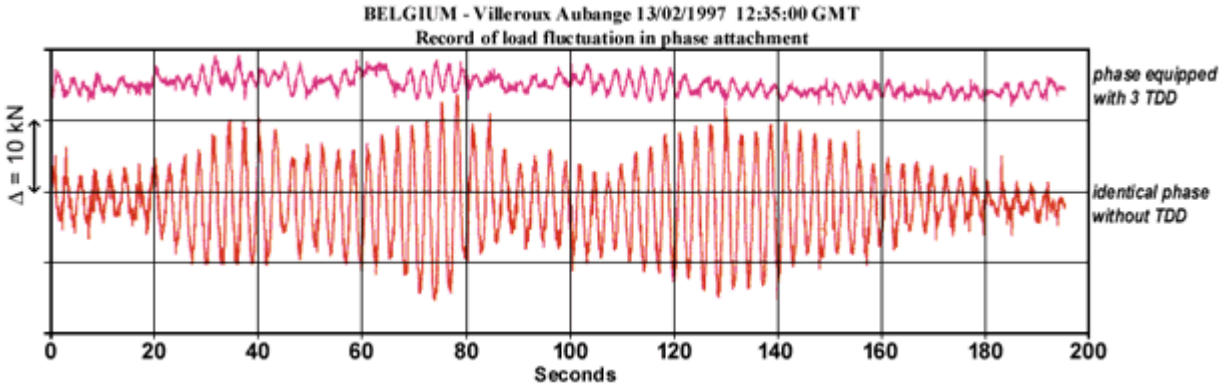

Figure 8.43: TDD efficiency as observed on operating 400 kV line in Belgium

8.1.5 Summary of galloping control devices

Table 8.4: Summary of Galloping Control Devices

NO	DEVICE NAME	APPL'N	WEATHER CONDITION		LINE CONSTRUCTION			COMMENTS
			Glaze	Wet snow	Dist'n	Single trans'n	Bundle	
1	Rigid Interphase Spacer	Widely used	Yes	Yes		Yes	Yes	Prevents flashovers, reduced galloping motions
2	Flexible InterphaseSpacer	Widely used	Yes	Yes		Yes	Yes	Prevents flashovers, reduced galloping motions
3	Air Flow Spoiler	Widely used	Yes		Yes	Yes	Yes	Covers 25% of span Limited by voltage Extensive field evaluation
4	Eccentric Weights &Rotating Clamp Spacers	Used in Japan		Yes		Yes	Yes	Three per single span one per spacer per subconductor
5	AR Twister	Used in USA	Yes			Yes	Yes	Two per span
6	AR Windamper	Used in USA	Yes			Yes	Yes	Two per span
7	Aerodynamic GallopingController (AGC)					Yes		Number based on analysis
8	Torsional Control Device (TCD)	Used in Japan		Yes			Yes	Two per span
9	Galloping ControlDevice (GCD)	Used in Japan		Yes			Yes	Two per span
10	Detuning Pendulum	Widely used	Yes		Yes	Yes	Yes	3 or 4 per span. Uses armor rods if tension is high. Most extensive field evaluations
11	Torsional Damper and Detuner (TDD)	Experi mental	Yes	Yes	No	No	Yes	2 or 3 per span

8.1.6 Cautions to be observed when applying in-span galloping control devices

In-span hardware, including galloping control devices and aircraft warning markers, are concentrated masses, which can act as reflection points of traveling waves of aeolian vibration. This vibration due to wind can occur in the sections of the conductors or overhead ground wires between the in-span devices and these sections of the span are isolated from any

vibration damping systems, which are most often applied to the ends of spans. For spans of conductors with low tension this does not cause any problems. However extra precautions are needed for spans with tensions approaching the safe tension limits with no dampers [CIGRE, 1999]. The precautions required are to reduce the stress concentrations at the metal clamps attaching the hardware to the conductors. Two alternatives for reducing these stresses are installing armor rods under the metal clamps or replacing the metal clamps with elastomer lined clamps [Van Dyke et al., 1995]. A further option is to add vibration dampers within each subspan between the in-span hardware.

A second aspect requiring caution applies to galloping control devices based on the control of torsional motions. These are custom designed based on the parameters of the conductor span. They are designed to ensure that the torsional natural frequency, after adding the devices and a chosen amount of ice and wind, falls within a range necessary for the proper function of the control device. The caution required for this is that the actual parameters of the line need to be known, and that may necessitate a line survey to confirm that the line is installed according to the design. In particular the tension of the conductors has been found to deviate from the as designed values, especially in regions where ice loads have occurred increasing the sag, or where repairs have been made in the spans. There are ratios of torsional to vertical oscillation frequency that make a span more likely to gallop. Consequently, it is possible to misapply the devices if they are designed with the wrong input parameters, or if the resonant behavior is not avoided by proper choice of device dimensions. It is therefore highly recommended that the design of galloping controls be carried out by experienced practitioners.

8.2 Design against galloping (clearances)

A database of 166 observations of galloping on single, twin, triple and quad bundle lines has been analyzed. The database is sufficiently detailed to define the variation of maximum amplitudes of galloping motion for single conductors in 50 to 450 m spans, and for twin and quad bundles in 200 to 450 m spans. Conventional design expectations are exceeded, for maximum galloping motions on short spans, and through the existence of single loop galloping on long spans.

The CIGRE TFG experts have approved the next formulas estimating the maximum galloping motions for spans without galloping controls. The best fit numerical model for single conductors uses the peak-to-peak galloping amplitude over conductor diameter versus “conductor span parameter“, the conductor diameter over the sag. The best-fit model for bundle conductors uses the peak-to-peak galloping amplitude over subconductor diameter as a function of the “conductor span parameter”.

The following proposal has been deduced from cases in the following range of data:

sag/span ratio in the range 1-5%

conductor diameter 10-50 mm

single and bundle conductors (two different formulas)

span length 50-450 m

More details of the database are presented in [Lilien and Havard, 2000].

8.2.1 The conductor span paramater

The approach employs the *reduced amplitude,* which is the ratio of peak-to-peak galloping amplitude ($A_{pk\text{-}pk}$) over conductor diameter (d), both in m:

$$\frac{A_{pk-pk}}{d} \qquad (8.6)$$

This reduced amplitude has a range between 0 and 500.

The conductor *span parameter* is a combination of the catenary parameter with the ratio of conductor diameter (d) over the square of the span length (L), which can also be expressed as the ratio of conductor diameter over the sag (f). The conductor span parameter is dimensionless:

Conductor span parameter: $100\frac{Td}{mgL^2} = \frac{100d}{8f}$ (8.7)

The conductor span has already been defined in Table 4.1 and has been denominated as **P5**.

Due to its definition and practical data, the conductor span parameter is in the range:

- For single conductor: 0 to 1

- For bundle conductor: 0 to 0.12

The observed values have been completed by simulated cases to fulfill missing zones of observation.

This parameter has a range of 0 to 1.1 with tension in N, mass in kg/m, span length, sag and diameter in m.

For single conductors, the fitted curve to the maximum amplitude over conductor diameter, which is included in Figure 8.44, is given by:

$$\frac{A_{pk-pk}}{d} = 80 \ln \frac{8f}{50d} \quad (8.8)$$

This is valid only in the 0-1 range of the conductor span parameter, which corresponds to the data base range.

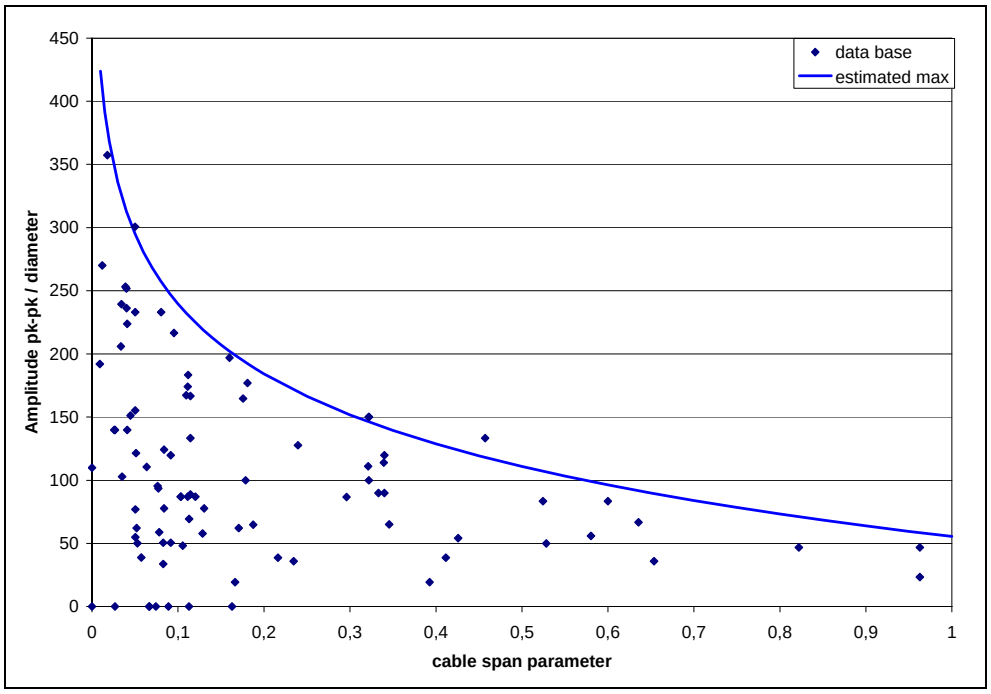

Figure 8.44: Variation of observed maximum peak-to-peak galloping amplitude/diameter on single conductors as a function of the conductor span parameter (defined in equation (8.7)).

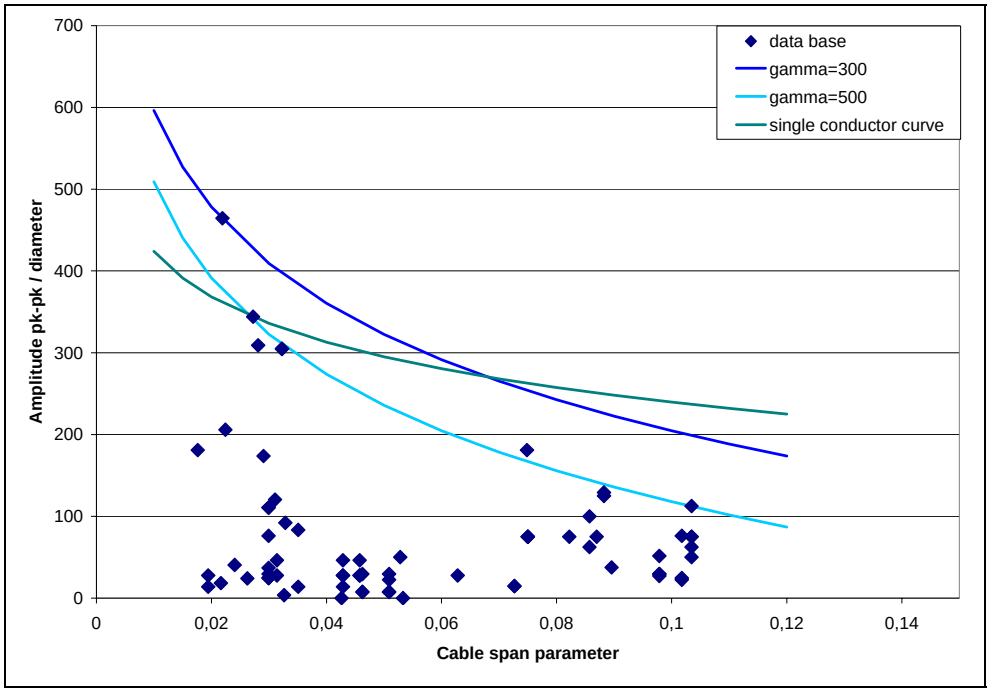

Figure 8.45: Variation of observed maximum peak-to-peak galloping amplitude/diameter on bundle conductors as a function of the conductor span parameter (defined in equation (8.7)). (gamma is defined in (8.9))

The observed values (all for wind speed lower than 10 m/s) are completed by many simulations coming from different aerodynamic curves (4 different) and for wind speed covering up to 15 m/s, means bigger than in observed cases.

As the difference (between observed and calculated) is much larger than on single conductor, more observations would be needed, especially for higher wind speed before coming to a conclusion.

Actually, we will recommend the fitted curve based on observed data only.

For bundle conductors, the corresponding fitted curve, which is reproduced in Figure 8.45 as the estimated maximum, is given by the denominator γ factor and could be 300 or 500 following the chosen curve fit on Figure 8.45:

$$\frac{A_{pk-pk}}{d} = 170 \ln \frac{8f}{\gamma \cdot d} = 170 \ln \frac{8f}{500d} \qquad (8.9)$$

This is valid in the range 0-0.15 of the conductor span parameter.

It may be noted that the expressions have the same form, but single conductors have up to about 2.5 times larger values of galloping amplitude/diameter for values of the conductor span parameter between 0.015 and 0.10.

It should be noted that the observed galloping amplitude on single conductors can reach up to 5 times the unloaded sag. In the context of distribution line conductor spans and sag, this indicates much larger galloping motions than conventionally considered in design [Dienne et al., 1985]. Also the data show a significant number of single loop galloping events on long spans, which is at variance with the above design guide.

The observed galloping amplitude on bundle conductor was limited to the unloaded sag in the observed cases.

A more detailed analysis of that database is available on [Lilien and Havard, 2000].

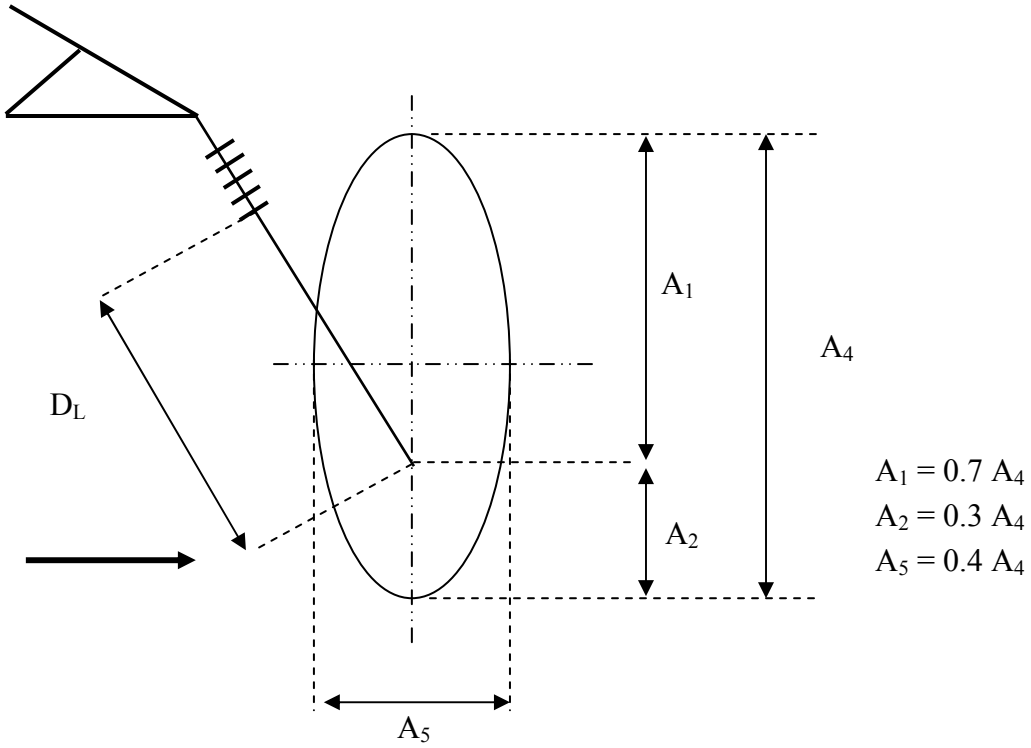

Figure 8.46: Proposed ellipse for clearance design against galloping for power lines

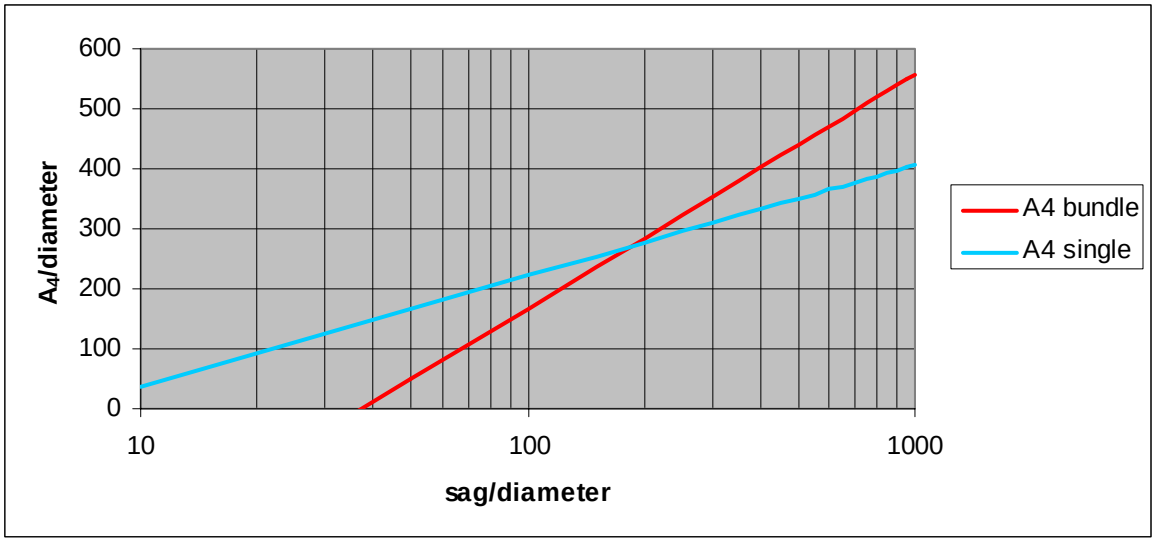

Figure 8.47: Proposed curves for galloping maximum peak-to-peak amplitude (all data in metres)

8.2.1.1 Range of application for given curves:

Span length between 30 m and 500 m

Sag/span ratio between 0.5% and 5%

Diameter of the conductor between 0.01 m and 0.05m

Data obtained from 166 observations and complementary simulations.

Data only based on classical bundle (symmetric 2,3 and 4 bundle conductor up to 0.6m bundle diameter)

Maximum design wind speed against galloping taken as 15 m/s.

Only realistic data considered, don't try a bundle with conductor diameter 0.01 m and 1 m sag.

This approach cannot be easily compared to BPA curves [Winkelman, 1974] or any other approach because of the dependence with the diameter and the sag.

Nevertheless we may apply both methods in a given case.

Let's imagine a multi-span 400 kV line, with span length close to 350 m, and having a twin bundle (45 cm bundle diameter). Initial loaded sag about 8 m (sag/span ratio 2.3 %)

Evaluation following BPA curves:

A4 = about 70% of the sag = 5.6 m

Evaluation following our method (need diameter data):

A4 = 10 m (diameter 32 mm); 8.5 m (diameter 22 mm), 5.6 m (diameter 11 mm)

Evaluation following KEMA method (B. Rhebergen, presented in Chester)

A4 = 8.5 m

The fact is that corresponding line in Belgium is a 32 mm conductor.

We do need more observation data which would include diameter as information needed to validate the new proposal. We do think that the proposed approach is completely valid for single conductor line but need more information for bundle conductors, as stated in [Rawlins, 1979]. The bundle curve reproduced here as already integrated numerous added data coming from simulation for wind speed up to 15 m/s because data base observations were mainly limited to 10 m/s.

8.3 Conductor and insulators fatigue induced by galloping

8.3.1 Conductor fatigue induced by galloping

Recent measurements on a full scale test line (Van Dyke and Laneville, 2005) have shown that during galloping events, fy_{max} , which is a measure of conductor bending amplitude, may reach amplitudes as high as 1.2 mm/s peak. Knowing that ACSR's endurance limit is 0.12 m/s peak [Rawlins, 1979], it shows that conductors may be severely stressed by galloping. Fortunately, such conditions happen seldom and the number of cumulated cycles may not be sufficient to damage the conductors. Consequently, the possible hazard associated with those events must be evaluated on a probability basis. More details are given hereafter.

Galloping tests were performed at the Hydro-Québec test line in Varennes on a single Condor conductor where the performance of different suspension clamps was compared regarding conductor fatigue (Van Dyke and Laneville, 2005). D sections were attached to the conductor in the middle span only to induce conductor galloping without being dependent on the temperature and precipitations. Their mass per unit length was 1.0 kg/m for the first test and 3.0 kg/m for the second test. When covered with D-sections, the mechanical tension of the conductor increased to 41 and 55% RTS for the first and second tests, respectively.

An elastomer lined clamp (made of helical rods, an elastomer insert and a clamp housing) and standard metal-to-metal clamps were installed on the same conductor at each end of the middle span where galloping was induced. The severity of vibrations was assessed using the fy_{max} values where f is the frequency (Hz) and y_{max} (m peak) is the maximum amplitude reached along the span. This product is frequently used to indicate bending stress levels at the end of the span.

The first test lasted 38 days during which time the wind conditions provided about 58 hours of galloping. There was no conductor damage during this test and the fy_{max} values recorded are shown in Figure 8.48. For the second test, the D-section mass was increased to 3.0 kg/m and, consequently, the conductor tension increased to 55% RTS. After six days of testing corresponding to 5 hours of galloping, a visual inspection revealed that the first aluminum layer of the conductor

was broken at the outlet of the metal-to-metal clamp in the middle span (Figure 8.51). There was no apparent damage at the elastomer lined clamp. The fy_{max} values recorded during those first six days are shown in Figure 8.49.

The conductor was cut on each side of the metal-to-metal clamp and a 20-m section was replaced with a new conductor using compression joints before continuing the test. The fy_{max} values recorded for the remaining 46 days of the test, corresponding to 30 hours of galloping, are shown in Figure 8.50. At the end of the test, the clamps were removed and six broken wires were found under the metal-to- metal clamp (Figure 8.52), while there was no damage under the elastomer lined clamp. The performance of the elastomer lined clamp shows that it is possible to choose an appropriate clamp that will withstand such stress when it is justified by the galloping exposure of the line.

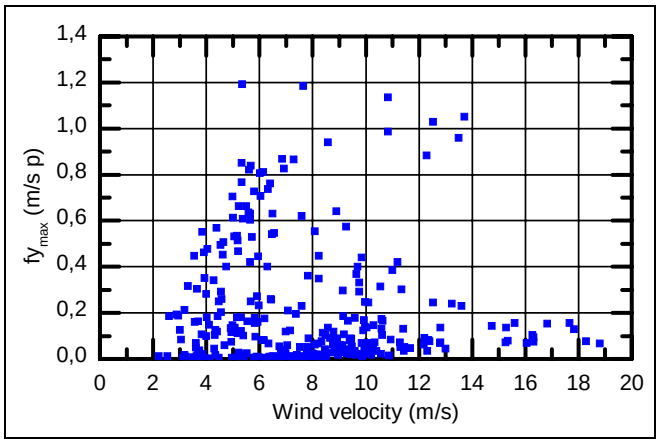

Figure 8.48: fy_{max} at 41% RTS after 38 days of the first galloping test

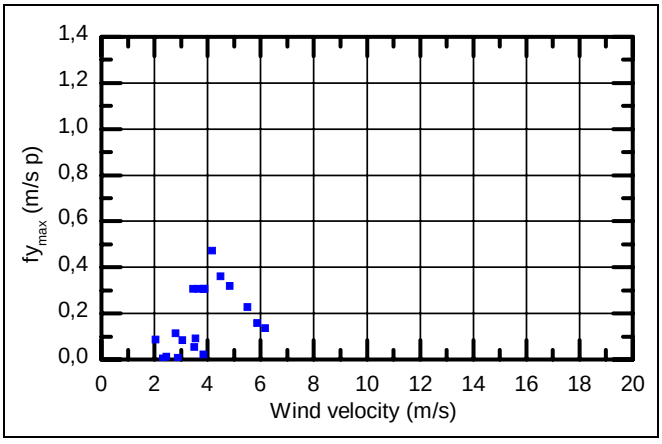

Figure 8.49: fy_{max} at 55% RTS after six days of the second galloping test

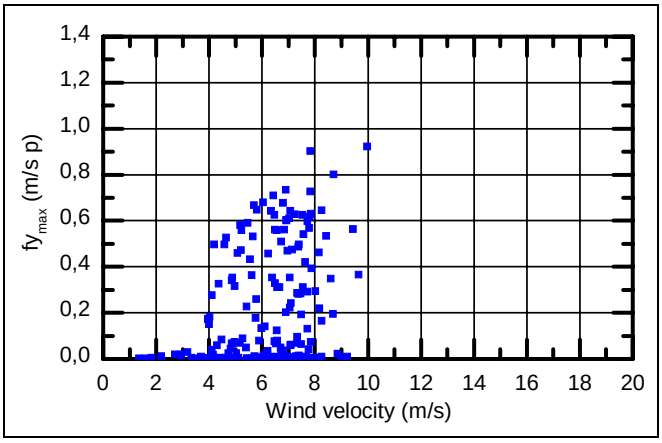

Figure 8.50: fy_{max} at 55% RTS for the 46 remaining days of the galloping test

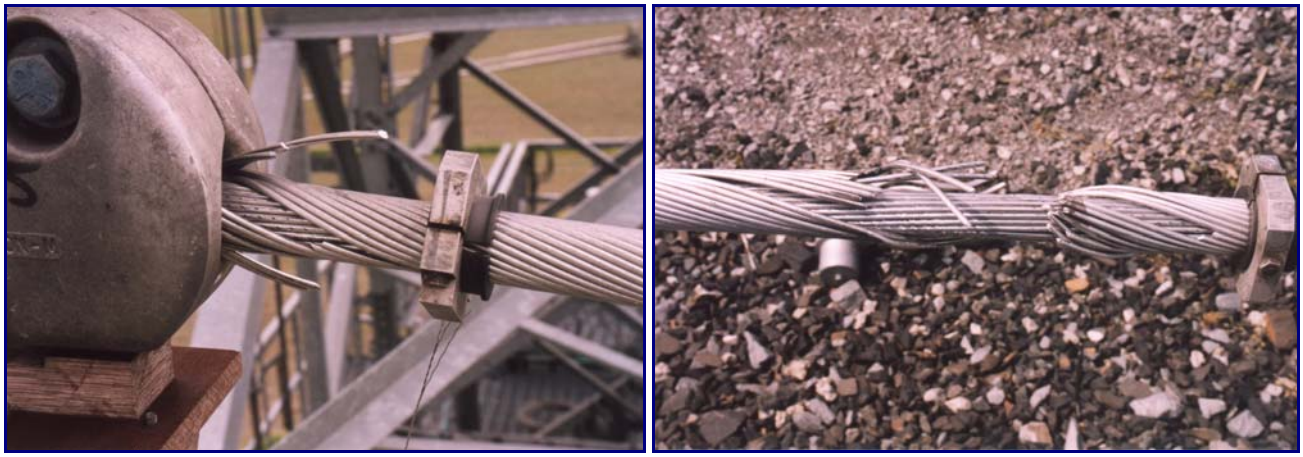

Figure 8.51: Damaged conductor under the metal-to-metal clamp in the 450-m span after six days of the second galloping test

Figure 8.52: Damaged conductor under the metal-to-metal clamp in the 450-m span at the end of the second test

8.3.2 Insulators fatigue induced by galloping

Dynamic loads resulting from galloping have been covered in section 5.4 and it was concluded that the maximum dynamic loads are of the order of 1.2 times the static value at dead-ends and 1.7 times the static value at suspensions. In areas subjected to ice loads, suspension insulators everyday loads are normally very low compared to their tensile strength; the ratio being of the order of one to nine. Consequently, the effect of galloping cyclic loads is normally of no consequence. For instance, fatigue tests conducted on porcelain insulators [Matsuura et al., 1990] have shown that they can withstand two million cycles at the following loads: average load of 25% of their M&E rating (mechanical and electrical rating), with a peak-to-peak load of 10% M&E. Their fatigue results showed also that the allowable no of cycles decreases with the dynamic loads. In areas experiencing only sporadic ice loads, the ratio between insulators everyday loads and their tensile strength may not be as high and the utility engineer should refer to the insulator manufacturer for fatigue data and compare with the dynamic loads and no of galloping cycles expected. Dynamic tests have also been conducted on composite line post insulators [de Tourreil and Kuffel, 1998] and showed also that the allowable no of cycles decreases with the dynamic loads.

However, on distribution lines where pintype insulators are used, tie wire failures due to galloping happen occasionally. Where clamptop insulators are used, cement failure of the porcelain insulators due to the bending moment applied on it during galloping has also been observed.

Finally, damages to insulators have been observed during galloping events when the insulator string was clashing on the tower arm. However, those damages are not related to a fatigue phenomenon.

9. References

Admirat, P., M. Maccagnan, and B. De Goncourt¨. 1988. “Influence of Joule effect and of climatic conditions on liquid water content of snow accreted on conductors,” *Proc. of the 4th International Workshop on Atmospheric Icing of Structures*, Paris.

Anjo, K., S. Yamasaki, Y. Matsubayashi, Y. Nakayama, A. Otsuki, and T. Fujimura. 1974. *An Experimental Study of Bundle Galloping on the Kasatory-Yama Test Line for Bulk Power Transmission*. CIGRE report 22-04. Paris.

Asai, S., H. Oura, S. Matsui, S. Torimoto, and D. Usami. 1990. “Design and Application of Phase-to-Phase Spacers for Overhead Transmission Line in Snowy Areas.” Proceedings of International Workshop on Atmospheric Icing of Structures. Tokyo, Japan. Paper B4-11. pp.1-5. October/November.

Ballengee, D.B. and C.F. Chen, 1971. “Vortex shedding from circular cylinders in an oscillating freestream.” AIAA journal, Vol. 9, No. 2, February.

Binder, R.C. 1962. “Galloping of Conductors Can Be Suppressed.” *Electric Light* & *Power.* Vol. 40, No. 9. May.

Blevins, R.D. 1990. “*Flow Induced Vibration.*” Van Nostrand Reinhold. New York. Second Edition.

Bokaian, A. and F. Geoola. 1982. “Wake induced galloping of two interfering circular cylinders,” J. Fluid Mechanics, Vol. 146, pp. 383-415.

Brooks, N.P.H., 1960. “Experimental Investigation of the Aeroelastic Instability of Bluff Two-Dimensional Cylinders,” M.A.Sc. Thesis, University of British Columbia, July.

Buchan, P.G. 1977. *The Artificial Deposition of Ice on Transmission Line Conductors: A Study of Profile Shape*. Ontario Hydro Research Division Report 77-387-K. Also distributed at Corech 83-45, 1983.

Callahan, F.B. 1973. “Curbs for Galloping Conductors.” *Transmission and Distribution.* October. pp. 66-8.

Cassan, J.G. and O. Nigol. 1972. “Research on compact transmission lines in Ontario”, Cigre report No 31-07.

Chabart, O. and J.L. Lilien. 1998. “Galloping of Electrical Lines in Wind Tunnel Facilities.” *Journal of Wind Engineering and Industrial Aerodynamics*. Vol. 74-76, pp. 967-976.

Chadha, J. 1974a. *A Study of the Mechanisms of Conductor Galloping and Its Control.* Hydro-Electric Power Commission of Ontario Research Division Report. No. 74-2124. June 12.

Chadha, J. 1974b. “A Dynamic Model Investigation of Conductor Galloping.” IEEE Winter Power Meeting. Paper 74 59-2.

Chadha, J.A., D.G. Havard, and A.T. Edwards. 1978. *Observations of Performance of Galloping Control Devices December 18, 1977*. Ontario Hydro Research Division Report. No. 78-75-K. February 18.

Chan, J.K., A.H. Shah, and N. Popplewell. 1992. *Modelling of Conductor Galloping*. Report CEA R&D. Project 321 T 672.

CIGRE. 1989. *An Observation of Galloping on Despacered Thick Conductor Bundles at the Villeroux Test Site*. CIGRE Document WG 22-11 (TFG) 89-12, October 5.

CIGRE. 1992. “Results of Questionnaire on Interphase Spacers.” CIGRÉ SC22 WG11. *ELECTRA.* Vol. 143. August. Convenor A. Berg.

CIGRE. 1995. CIGRE Study Committee 22. Working Group 11. Task Force 04. “Field Observations of Overhead Line Galloping: Galloping reporting forms.” Electra No 162, October, Convenor M. Tunstall.

CIGRE. 1999. “Safe Design Tension with Respect to Aeolian Vibration–Part 1: Single Unprotected Conductors.” *ELECTRA.* Vol. 186. October. CIGRÉ Committee B2 WG11 TF4. Convenor Claude Hardy.

CIGRE. 2000a. Guidelines for Field Measurement of Ice Loadings on Overhead Power Line Conductors. TB (Technical Brochure) 179. TF 22.06.01 August. Convenor S.M. Fikke.

CIGRE. 2000b. CIGRE Study Committee 22. Working Group 11. Task Force 04. “Review of Galloping Methods.” Electra No 191. August, Convenor M. Wolfs.

Davison, A.E. 1939. “Ice-Coated Electrical Conductors.” *Bulletin Hydro-Electric Power Commission of Ontario*. Vol. 26, No.9. September. pp. 271-80.

Den Hartog, J.P. 1932. “Transmission Line Vibration due to Sleet.” *AIEE Transactions.* Vol. 51. pp. 1074-6.

De Tourreil, C. and E. Kuffel. 1998 “Comportement des isolateurs composites rigides à socle soumis à des charges mécaniques dynamiques,” Canadian Electrical Association, Report No 004D877, December.

Diana, G., F. Cheli, A. Collina, A. Manenti, P. Nicolini, and F. Tavano. 1991. “Sensitivity Analysis of Bundled Conductors to Ice Galloping.” CIGRE symposium, Compacting Overhead Transmission Lines. Leningrad (USSR). June 3-5.

Dienne, G., R. Brand, M. Couvreur, P.H. Leppers, and M.J. Tunstall. 1985. “Present-day Experience from Four European Regions Concerning the Galloping of Overhead Transmission Lines.” Paper 85E 110.2. UNIPEDE. Athens Congress. June.

Douglass, D.A. 1981. *“Anti-galloping Potential of a New Twisted-Conductor Design.”*

Douglass, D.A. and J.B. Roche. 1985. “T2 Wind Motion Resistant Conductor.” *IEEE Transactions on Power Apparatus and Systems.* Vol. PAS-104, No. 10. October. pp. 2879-2887.

Dubois, H., J.L. Lilien, and F. Dal Maso. 1991. *A New Theory for Overhead Lines Vertical and Torsional Frequencies Computation*. Revue AIM (Belgium). No. 4.

Edwards, A.T. and A. Madeyski. 1956. “Progress Report on the Investigation of Galloping of Transmission Line Conductors.” *AIEE Trans, PAS*. Vol. 75. pp. 666-686.

Edwards, A.T. 1966. “Ontario Hydro Full-Scale Galloping Test Line.” Addendum 8, Summary of Proceedings of Conference on Conductor Galloping. Ontario Hydro W. P. Dobson Research Laboratory. Toronto. September.

Edwards, A.T. and R.G. Ko. 1979. “Interphase Spacers for Controlling Galloping of Overhead Conductors.” IEEE Symposium on Mechanical Oscillations of Overhead Transmission Lines. Vancouver, B.C. July.

Egbert, I.R., H.M. Snyder and C.G. Thomann. 1984 “*Development and operation of a galloping conductor test facility*” Second International Workshop on Atmospheric Icing of Structures, Trondheim Norway, June 19-21.

Eliason, A. J. Private correspondence to Dave Havard.

EPRI. 1979. *Transmission Line Reference Book*: *Wind-Induced Conductor Motion.* Electrical Power Research Institute. Palo Alto, California.

Fikke, S.M. 1999. “Electronic Eyes Monitor Remote Sites.” *Transmission & Distribution World*. September, pp. 60-68.

Fikke, S.M. 2003. *Methods and Systems for Collecting Icing Data and for Real-time Monitoring of Ice Storms*. CEATI Report No. T023700-3311B. October. 46 pages.

Fu, P. and M. Farzaneh. 2006 “Simulation of the ice accretion process on a transmission line cable with differential twisting.” accepted for publication in the *Canadian Journal of Civil Engineering*, 2006.

Fujii, Y., T. Koyama and T. Sawamoto. 1997. “Countermeasures Against Conductor Galloping.” Paper 11. Colloquium Environmental Impact of OHL in Japan. CIGRE SC22. Sendai Meeting.

Gartshore, I.S. 1973. “*The effects of free stream turbulence on the drag of rectangular two-dimensional prisms*.” Boundary Layer Wind Tunnel Laboratory 4-73, University of Western Ontario.

Gurung, C.B., H. Yamaguchi and T. Yukino. 2002. “*Identification of large amplitude wind-induced vibration of ice-accreted transmission lines base on field observed data”* Engineering Structures, 24, pp. 179-188.

Gurung, C.B., H. Yamaguchi, and T. Yukino. 2003. “Identification and Characterization of Galloping of Tsuruga Test Line Based on Multi-channel Modal Analysis of Field Data. *Journal of Wind Engineering & Industrial Aerodynamics*. Vol. 91, Issue 7. June. Pp. 903-924.

Halsan, K.A., D.G. Havard, S. M. Fikke, and A. Gerezgiher. 1998. “Galloping Studies at Statnett Using Remote Monitoring.” CIGRE SC22, WG11 meeting. Graz, Austria. Paper No. 22-98.

Havard, D.G. 1978. “Status of Conductor Galloping Research at Ontario Hydro.” Second Canadian Workshop on Wind Engineering. IREQ Varennes, Quebec. September 28-29.

Havard, D.G. and J.C. Pohlman. 1979. “Field Testing of Detuning Pendulums for Controlling Galloping of Single and Bundle Conductors.” Paper A79 499-5. IEEE Symposium on Mechanical Oscillations of Overhead Transmission Lines. Vancouver, Canada. July.

Havard, D.G. 1979a. “Detuning for Controlling Galloping of Single Conductor Transmission Lines.” Paper A 79 500-0. IEEE Symposium on Mechanical Oscillations of Overhead Transmission Lines. Vancouver, Canada July.

Havard, D.G. 1979b. “Detuning Pendulums for Controlling Galloping of Bundle Conductor Transmission Lines.” Paper A 79 501-8. IEEE Symposium on Mechanical Oscillations of Overhead Transmission Lines. Vancouver, Canada. July.

Havard, D.G. 1979c. *Galloping Control by Detuning*. EPRI Research Program RP-1095. Progress Report No. 2. Ontario Hydro Research Division Report No. 79-619-K. November.

Havard, D.G. and J C. Pohlman. 1981. “The Economics of Galloping Control.” CEA International Symposium on Overhead Conductor Dynamics. Toronto.

Havard, D.G. and J.C. Pohlman. 1984. “Five Years’ Field Trials of Detuning Pendulums for Galloping Control.” *IEEE Transactions on Power Apparatus and Systems*. Vol. PAS-103, No 2. pp. 318-327. February.

Havard, D.G. and C.J. Pon. 1990. “Use of Detuning Pendulums for Control of Galloping of Single Conductor and Two- and Four-Conductor Bundle Lines.” Fifth International Workshop on Atmospheric Icing of Structures. Tokyo.

Havard, D.G. 1996. “Fifteen Years Field Trials of Galloping Controls for Overhead Power Lines.” IWAIS ’95. 7th International Workshop on Atmospheric Icing of Structures. Chicoutimi, Canada. June 3-6.

Havard, D.G. 1997. “Analysis of Field Data on Galloping of Single and Bundle Conductors with and without Control Devices.” Paper 16, International Seminar on **C**able Dynamics. Tokyo. October.

Havard, D.G. 2002. “Dynamic Loads on Transmission Line Structures During Galloping.” Presented at The International Workshop on Atmospheric Icing of Structures. Brno, Czech Republic.

Hillier, R. and R.J. Cherry. 1981. “The effect of stream turbulence on separation bubbles.” *Journal of Wind Engineering and Industrial Aerodynamics*, v. 8, pp. 49-58.

Hoerner, S.F. 1965. “Fluid dynamic drag,” published by the author, New York, pp. 415.

Hoffman, S. P. and M. J. Tunstall. 2003. “A Review of the Service Performance of National Grid Transco’s Conductor Systems.” CIGRÉ Study Committee B2 Colloquium on “UK Transmission & Distribution—An Era of Change.” Edinburgh. September.

Hunt, J.C.R and D.J.W. Richard. 1969. “Overhead Line Oscillations and the Effect of Aerodynamic Dampers.” *IEEE Trans on PAS.* Vol. 116. No. 11. November. pp. 1869-74.

Kasima, H., Y. Nishimura, and Y. Sakamoto. 1996. “Galloping Events and Associated Meteorological Condition Experienced in Hokuriku Area.” 7th International Workshop on Atmospheric Icing of Structures. Chicoutimi, Canada. June 3-7. pp. 306-311.

Keutgen, R. and J.L. Lilien. 1998. “A New Damper to Solve Galloping on Bundled Lines. Theoretical Background, Laboratory and Field Results.” *IEEE Trans. On Power Delivery*. January. Vol. 13. No.1. pp. 260-266.

Keutgen, R. 1999. *Galloping Phenomena. A Finite Element Approach*. Ph.D. Thesis. Collection des publiciations de la Faculté des Sciences. Appliquées de l’Université de Liège. No. 191. Pp. 1-202.

Keutgen, R. and J.L. Lilien. 2000. “Benchmark Cases for Galloping with Results Obtained from Wind Tunnel Facilities. Validation of a Finite Element Model.” *IEEE Trans. on Power Delivery.* Vol. 15, No.1. pp. 367-374. January.

Kimura, K., M. Inoue, Y. Fujino, T. Yukino, H. Inoue and H. Morishima. Unsteady forces on an ice-accreted four-conductor bundle transmission line, *Proc. of the 10th Int. Conference on Wind Engineering, Copenhagen (Denmark), 21-24 June 1999, Wind Engineering into the 21st Century, Eds. A. Larsen, G.L. Larose and F.M. Livesey, A.A. Balkema*, pp.467-472.

Kimura, K., Y. Fujino, M. Inoue, T. Yukino, H. Inoue and H. Morishima. 2000. Unsteady aerodynamic force characteristics of ice-accreted four-conductor bundle transmission lines under large amplitude motion, *J. of Structural Engineering, JSCE*, Vol. 46A, No 2, pp. 1055-1062 (in Japanese).

Kortschinski, J. 1968. “Line Ice Detectors for the Indication and Study of Conductor Galloping.” IEEE Conference Paper C6867PWR. February.

Koutselos L.T. and M.J. Tunstall. 1986. “Collection and Reproduction of Natural Ice Shapes on Overhead Lines Conductors and Measurement of Their Aerodynamic Characteristics.” Third International Workshop on Atmospheric Icing of Structures (IWAIS’1986). Vancouver.

Koutselos, L.T. and M.J. Tunstall. 1988. “Further Studies of the Galloping Instability of Natural Ice Accretions on Overhead Line Conductors.” Paper A9.1. Fourth Int. Conf. on Atmospheric Icing of Structures. Paris.

Laneville, A. and G.V. Parkinson 1971. “Effects of turbulence on galloping bluff cylinders,” presented at the Third International Conference on Winds Effects on Buildings and Structures, Tokyo, Japan, Sept. 6-11.

Laneville, A. 1973. “Effects of turbulence on wind-induced vibrations of bluff cylinders,” Ph.D. Thesis, University of British Columbia.

Laneville, A., I.S. Gartshore and G.V.Parkinson. 1975. “An explanation of some effects of turbulence on bluff bodies” in Proc. Of 4th Int’l Conference on Buildings and Structures, London, England, Sept., Cambridge Univ. Press, pp. 333-342.

Laneville, A. 1977. “An Explanation of Some Effects of Turbulence on Bluff Bodies.” *Proceedings of the 4th International Conference of Wind Effects on Buildings and Structures.* Cambridge University Press. Pp. 333-341.

Laneville, A. 2005 “*Personal notes”*.

Leppers, P.H., R. Brand, and M. Couvreur. 1978. “Suppression of Galloping for Medium Size Bundle Conductors by Spacer Removal or Similar Means.” CIGRE Paper 22-09.

Leppers, P.H. and W.J. Wijker. 1979. “Short Review of Galloping in the Netherlands during Winter 1978-1979.” Presented at Corech galloping meeting in Leatherhead.

Liberman, A. J. 1974. *Subspan Oscillations and Conductor Galloping on HV Overhead Lines*. CIGRE Report 22-09.

Lilien, J.L. and J. P. Ponthot. 1988. “Overhead Lines Galloping—Modelisation.” Conference IMACS. Modelling and Simulation of Electrical Machines and Power Systems. Elsevier Science Publishers. North-Holland. Imacs. pp. 103-110.

Lilien, J.L. and H. Dubois. 1988. “Overhead Line Vertical Galloping on Bundle Configurations: Stability Criterions and Amplitude Prediction.” *IEE Overhead Line Design and Construction: Theory and Practice (up to 150 kV).* November. Proceedings. pp. 65-69.

Lilien, J.L., H. Dubois, and F. Dal Maso. 1989. *General Mathematical Formulation for Overhead Line Galloping.* AIM study day on galloping. March 10.

Lilien, J.L. 1991. *Galloping and Compact Line*. CIGRE Symposium on Compacting Overhead Transmission Lines. Leningrad. June. Report 200-01.

Lilien, J.L., P. Pirotte, T. Smart, and M. Wolfs. 1993. *A New Way to Solve Galloping on Bundled Lines.* Revue AIM Liège No. 2 and CIGRE WG11 Task Force on Galloping. Report 93-04. August.

Lilien, J.L., J. Wang, O. Chabart, and P. Pirotte. 1994. *Overhead Transmission Lines Design. Some Mechanical Aspects*. ICPST'94 (International Conference on Power System Technology). October 18-21. Beijing, China. 5 pages.

Lilien, J.L. and O. Chabart. 1995. “High Voltage Overhead Lines—Three Mechanisms to Avoid Bundle Galloping.” International Conference on Cable Dynamics. Liège. October 19-21. Report 47.

Lilien, J.L., M. Erpicum, and M. Wolfs. 1998. “Overhead Lines Galloping. Experience during One Event in Belgium on Last February 13th, 1997.” IWAIS ‘98. International Conference. Reykjavik, Iceland. June. Proceedings. pp. 293-299.

Lilien, J.L. and D.G. Havard. 2000. “Galloping Data Base on Single and Bundle Conductors. Prediction of Maximum Amplitudes.” *IEEE Trans on Power Delivery.* Vol. 15, No. 2. Pp. 670-674. April.

Lilien, J.L. and A. Vinogradov. 2002. “Full-scale Tests of TDD Antigalloping Device (Torsional Damper and Detuner).” *IEEE Trans on Power Delivery*. Vol.17. No. 2. pp. 638-643. April.

Loudon, D. 2003. Private correspondence from D. Loudon.

Lozowski, E.P., J.R. Stallabrass and P.F. Hearty. 1983. “The Icing of an Unheated, Non-rotating Cylinder, Part I: A Simulation Model,” *Journal of Climate and Applied Meteorology*, Vol. 22, pp. 2053-2062.

Matsubayashi, Y., I. Matsubara, and Y. Yoshida. 1977. “*Torsion Controlling type Galloping Damper.”* Sumitomo Electric Industries Limited. Japan, October.

Matsuura, Y., Y. Suzuki, K. Arakawa and K. Tanaka. 1990. “Technical aspects on long-term performance of suspension insulators and its laboratory evaluation methods,” Canadian Electrical Association Symposium on Insulators, Power System Planning and Operating Section, Engineering and Operating Division, Montreal, Canada, pp. 14-25, March 28.

Matsuzaki, Y., T. Ikeya, R. Kimata, A. Bognar, P. Szaplonczay and M. Teglas. 1991. “Interphase Spacers for Overhead Lines.” Symposium Leningrad, CIGRE S33-91. pp. 200-08.

Morishita, S., K. Tsujimoto, M. Yasui, N. Mori, K. Shimojima, and K. Naito. 1984. *Galloping Phenomena of Large Bundle Conductors: Experimental Results of the Field Test Lines.* CIGRÉ Paper 22-04.

Nakamura, Y. and Y. Tomonari, 1977. “Galloping of rectangular prisms in a smooth and in a turbulent flow,” Journal of Sound and Vibration, Bol. 52, Issue 2, May, pp. 233-241.

Nakamura, Y. and Y. Tomonari. 1980. *The Aerodynamic Characteristics of D-section Prisms in a Smooth and in a Turbulent Flow*. April.

Nakamura, Y. 1980. “Galloping of Bundled Power Line Conductors.” *Journ. Sound & Vibration.* Vol. 73, No. 3. pp. 363-377.

Nigol, O. and G.J. Clarke. 1974. “Conductor Galloping and Control Based on Torsional Mechanism.” IEEE C-74 116-2. Conference Paper.

Nigol, O., G.J. Clarke, and D.G. Havard. 1977. “Torsional Stability of Bundle Conductors.” *IEEE Trans, PAS*. Vol. 96. No. 5. September. pp. 1666-1674.

Nigol, O. and D.G. Havard. 1978. “Control of Torsionally Induced Galloping with Detuning Pendulums.” IEEE Paper A78 125-7. Presented at the IEEE PES Winter Meeting. New York.

Nigol, O. and P.G. Buchan. 1981. “Conductor Galloping, Part 1: Den Hartog Mechanism; Part II: Torsional Mechanism.” *IEEE Trans., PAS*. 100-699. February.

Noiseux, D.U. 1992. “Similarity Laws of the Internal Damping of Stranded Cables in Transverse Vibrations.” *IEEE Transactions on Power Delivery*. Vol. 7. No. 3. July. pp. 1574-1581.

Novak, M. 1969. “Aeorelastic galloping of prismatic bodies,” ASCE Journal of the Engineering Mechanics Division, 96, pp. 115-142.

Novak, M. 1971. “Galloping and vortex induced oscillations of structures,” in Proceeding of the third International Conference on wind effects on buildings and structures, Tokyo, Japan, Sept. 6-11, Paper IV-16, p. 11.

Novak, M. 1972. “Galloping Oscillations of Prismatic Structures.” *A.S.C.E. Journ. Engrg. Mech. Div*. Vol. 98. February.

Novak, M. and H. Tanaka. 1974. “Effect of Turbulence on Galloping Instability.” *ASCE Journal of Engineering and Mechanical Division.* Vol. 100. No. EM1. February. pp. 27-47.

Novak, M., A. Davenport and H. Tanaka. 1978. “Vibration of towers due to galloping of iced cables,” ASCE Journal of the Engineering Mechanics Division, 104, pp. 457-473.

Otsuki, A. and O. Kajita. 1975. “Galloping Phenomena of Overhead Transmission Lines.” *Fujikura Technical Review*. No.7. pp. 33-46.

Otsuki, A. and Y. Kojima. 1981. “Research on Galloping and Development of Anti-Galloping Device.” CEA International Symposium on Overhead Conductor Dynamics. Toronto.

Ottens, H.H. 1980. *Some Theoretical Considerations on the Effect of Cable Torsion on Gallop* NRL. Netherlands. NRL TR 81003 L. July 22.

Oura, H., T. Ito, Y. Suzuki, and O. Fujii. 1995. “Development of Phase-to-phase Spacer for 275 kV Transmission Lines in Hokkaïdo Electric Power Co., Inc.” Electricity ’95 Conference. Canadian Electric Association. Vancouver, Canada. March.

Ozaka, A., J. Kagami, K. Takeda, and T. Oka. 1996. “Observations of Galloping on Overhead Transmission Test Lines with Artificial Snow Accretion Models.” 7th International Workshop on Atmospheric Icing of Structures. Chicoutimi, Canada. pp. 300-305.

Parkinson, G.V. and J.D. Smith. 1964. “The Square Prism as an Aeroelastic Non-linear Oscillator.” *Quarterly Journal of Mechnical and Applied Mathematics.* Vol. XVII. Pt. 2.

Parkinson, G.V. 1971. “Wind-induced instability of structures.” Philosophical Transactions of the Royal Society of London, A269, 395-409.

Parkinson, G.V. 1974. “Mathematical models of flow-induced vibrations”. In Flow Induced Structural Vibrations, ed. E. Naudascher, pp. 81-127.

Parkinson, G.V. 1989. “Phenomena and modelling of flow-induced vibrations of bluff bodies.” Progress in Aerospace Sciences 26, pp. 169-224.

Personne, P. and J.F. Gayet. 1988. “Ice Accretion on Wires and Anti-Icing Induced by Joule Effect,” *Journal of Applied Meteorology*, Vol. 27, pp.101-115.

Pon, C.J., D.G. Havard, and A.T. Edwards. 1982. *Performance of Interphase Spacers for Galloping Control*. Ontario Hydro Research Division Report No.82-216-K. July 6.

Pon, C.J. and D.G. Havard. 1993. *Control of Distribution Line Galloping*. Final Report on CEA R&D Project 196 D 367. October.

Pon, C.J. and D.G. Havard. 1994. *Field Trials of Galloping Control Devices for Bundle Conductor Lines*. Report on R & D Project 133 T 386. Canadian Electrical Association. Montréal. March.

Poots, G. 1996. "*Ice and Snow Accretion on Structures*," Research Studies Press Ltd., Taunton.

Ratkowski, J.J. 1963. "Experiments with Galloping Spans." *IEEE Trans PAS*. Vol. 82. pp. 661-669. October.

Ratkowski, J.J. 1968. "Factors Relative to High Amplitude Galloping." *IEEE Trans. PAS* (Special Supplement). Vol. PAS-87. No. 6. June.

Rawlins, C.B. 1979. *Transmission Line Reference Book*: *Wind-Induced Conductor Motion.* - Chapter 4: Galloping conductors Electrical Power Research Institute. Palo Alto, California.

Rawlins, C.B. and J.C. Pohlman. 1988. "On the State of Galloping Conductor Technology." 4th International Workshop on Atmospheric Icing of Structures. Paris. September 5-7.

Rawlins, C.B. 1993. *Numerical Studies of the Galloping Stability of Single Conductors.* Technical Paper No. 30. Alcoa Conductor Products Company. Spartanburg, SC. June.

Rawlins, C.B. 2001. *Galloping Eigenmodes in a Multispan Overhead Line Section.* Proceedings of Fourth International Symposium on Cable Dynamics. Montreal (Canada). May 28-30. pp. 85-92.

Richardson, A.S., J.R. Martucelli, and W.S. Price. 1963a. "Research Study on Galloping of Electric Power Transmission Lines." Paper 7. First Symposium on Wind Effects on Buildings and Structures. Teddington, England. June. p. 612.

Richardson, A.S., J.R. Martuccelli, and W.S. Price. 1963b. "An Investigation of Galloping Transmission Line Conductors." *IEEE Transactions Paper*. Vol. PAS-82. pp. 4 1 1-3 1.

Richardson, A.S. 1979a. "Some Effects of Conductor Twisting on Galloping." IEEE Summer Power Meeting. Vancouver. (*Trans. IEEE Power Apparatus and Systems. PAS-99*. 1980. p. 811).

Richardson, A.S. 1979b. "Some Effects of Twisting on Galloping." IEEE Symposium on Mechanical Oscillations of Overhead Transmission Lines. Vancouver, B.C. July.

Richardson, A.S. 1989. *AR Twister* ™. Flyer from Research Consulting Associates. January.

Rogier, J., J. Goossens, M. Wolfs, A. Van Overmeere, J.L. Lilien, and L. Lugentz. 1998. *L'expérience des mesures occasionnelles et permanentes sur des lignes aériennes belges*. CIGRE 1998. Session Plénière. August. Vol. No. 145. CE 22.

Sakamoto, Y. 2000. "Snow accretion on overhead wires," *Phil. Trans, R. Soc. Lond.* A 358, pp. 2941-2970.

Sasaki S., M. Komoda, T. Akiyama, M. Oishi, Y. Kojima, T. Okumura, and Y. Maeda. 1986. *Development of Galloping Control Devices and their Operation Records in Japan*. CIGRÉ Report 22-07.

Schmidt, J. and C. Jürdens. 1989. "Design of Interphase Spacers with Composite Insulators and Service Experience." Presentation to CIGRÉ SC22-WG11 Task Force on Galloping. Rijeka, Yugoslavia.

Shimizu, M., T. Ishihara and P.V. Phuc. 2004. "A wind tunnel study on steady and unsteady aerodynamic characteristics of ice-accreted transmission lines," *Proc. of the 18th Symposium on Wind Engineering, Tokyo (Japan), 2-3 Dec.*, pp.245-250 (in Japanese).

Smith, J.D. 1962. “The square prism as an aeroelastic non-linear oscillator,” M.A.Sc. Thesis, University of British Columbia.

Stewart, D.C. 1937. “Experimental Study of Dancing Cables.” AIEE North Eastern District Meeting, Buffalo, NY. May.

Tattelman, P. and I.I. Gringorten. 1973. *Estimated Glaze Ice and Wind Loads at the Earth’s Surface for the Contiguous United States.* Report AFCRL-TR-73-0646. Air Force Cambridge Research Laboratories. L. G. Hanscom Field. Bedford, MA. October 16.

Tebo, G.B. 1941. “Measurement and control of conductor. vibration,” Trans. AIEE, vol. 60 , pp. 1188-1193.

Tombeur, F. 1984. *Mesure de la résistance à la torsion de câble en alliage d'aluminium.* EBES. Rapport Interne. November 15.

Tornquist, E.L. and C. Becker. 1947. “Galloping Conductors and a Method for Studying Them.” *AIEE Transactions Paper.* Vol. 66. pp. 1154-61.

Tsujimoto, K., H. Iisaka, K. Shimojima, H. Kubokawa, T. Okumura, and K. Fujii. 1983. “Report on Experimental Observation of Galloping Behaviour in 8-bundled Conductors.” *IEEE Transactions on Power Apparatus and Systems.* Vol. PAS-102. No. 5. May. pp. 1193-1201.

Tunstall, M. and L.T. Koutselos. 1988. “Further Studies of the Galloping Instability & Natural Ice Accretions on Overhead Line Conductors.” 4th Int. Conf. on Atmospheric Icing of Structures. Paris. September.

Van Dyke, P., C. Hardy, R. Dansereau, Y. Blanchette, and J.G. Gagne. 1995. “Hydro-Québec's Experience with Anti-galloping Pendulums.” Canadian Electrical Association. Transmission Section. Conductor and Hardware Session. Vancouver. March.

Van Dyke, P. and A. Laneville. 2004. “Galloping of a Single Conductor Covered with a D-section on a High Voltage Overhead Test Line.” 5th International Colloquium on Bluff Body Aerodynamics and Applications. Ottawa, Canada. pp. 377-380. July.

Van Dyke, P. 2005. Oral presentation. CIGRÉ WG11 meeting. Bilbao, Spain.

Van Dyke, P. and A. Laneville. 2005. “HAWS Clamp Performance on a High Voltage Overhead Test Line.” Sixth International Symposium on Cable Dynamics. Charleston, SC.

Van Dyke, P., A. Laneville, and D. Bouchard. 2006. “Galloping Experimental Analysis of Conductors Covered with a D-section on a High Voltage Overhead Test Line. 6th FSI, AE & FIV+N Symposium. Proceedings of ASME. Vancouver, Canada.

Wang, J. and J.L. Lilien. 1994. “Overhead Transmission Line Galloping. A Comparative Study between 2-DOF and 3-DOF Models.” 3ème Congrès National Belge de Mécanique Théorique et Appliquée. Liège. May. Acte du Congrès. pp. 257, 261.

Wang, J. 1996. *Large Vibrations of Overhead Electrical Lines: A Full 3-DOF Model for Galloping Studies.* Ph.D. Thesis. Collection des Publications de la Faculté des Sciences Appliquées de l’Université de Liège. No. 151. pp. 1-227.

Wang, J. and J.L. Lilien. 1998a. “A New Theory for Torsional Stiffness of Multi-span Bundle Overhead Transmission Lines.” February. *IEEE Trans. on Power Delivery.* Vol. 13. No. 4. pp. 1405-1411.

Wang, J. and J.L. Lilien. 1998b. “Overhead Electrical Transmission Line Galloping. A Full Multi-span 3-dof Model, Some Applications and Design Recommendations.” *IEEE Trans. on Power Delivery*. Vol. 13. No. 3. pp. 909-916. July.

Washizu, K. and A. Ohya. 1978. “Aeroelastic instability of rectangular cylinders in a heaving mode,” Journal of Sound and Vibration, 59, pp. 195-210.

Whapham, R. 1982. “Field Research for Control of Galloping with Air Flow Spoilers.” Missouri Valley Electrical Association Conference. Kansas City, MO.

Winkelman, P.F. 1974. *Investigations of Ice and Wind Loads, Galloping, Vibrations and Subconductor Oscillations (Transmission Line Conductor Problems*). U. S. Department of the Interior. Bonneville Power Administration. September.

Yamaguchi H., C.B. Gurung and T. Yukino. 2003. *"Characterization of wind-induced vibrations in transmission lines by single-channel field data analysis"*, Proc. of the 5th Int. Symposium on Cable Dynamics, Santa Margherita (Italy), 15-18 Sept.

Yanagisawa, T., T. Sukegawa, H. Akasaka, and Y. Matsuzaki. 1990. "Verification Test of an 8-Bundle Conductor on the Oku-Nikko UHV Test Line."Fifth International Workshop on Atmospheric Icing of Structures. Tokyo.

Yutaka, F., K. Toshio, and S. Toshihiro. 1998. "Countermeasures against Conductor Galloping." Overhead Transmission Lines New Technology in Japan. CIGRE SC22. Japanese Panel. pp. 122-132.

Appendix A Symbols

A	cross section
$A_{pk\text{-}pk}$	peak-to-peak galloping amplitude
a	spacing between a pair of subconductors
a_R	angle of reattachment
b	zero-to-peak amplitude
B_i	i^{th} weighing factor in Prony equation
C_D	aerodynamic drag coefficient
C_L	aerodynamic lift coefficient
$C_{L\alpha}$	$dC_L/d\alpha$
C_M	aerodynamic pitching moment coefficient
$C_{M\alpha}$	aerodynamic pitching moment coefficient
c	wave velocity
D	energy actually dissipated in a full cycle
D_f	energy per cycle lost to bending hysteresis
d	cable diameter (without ice)
d	droplet diameter (precipitation)
d	transverse dimension of the section
d_i	distance from the wire's neutral axis to the conductor's neutral axis
d_{ice}	distance between cable centre and ice gravity centre
E	cable young modulus
E_D	power dissipation during one cycle at a given amplitude
e	streamwise dimension of the section
F	amplitude of applied force
f	sag
f_D	aerodynamic drag force per unit length
f_L	aerodynamic lift force per unit length
f_{t1}	fundamental torsional frequency
f_{B^v}	frequency of the vertical mode

f_{v1} fundamental vertical frequency

f_W aerodynamic vertical force per unit length acting on the cable

f_Θ frequency of the torsional mode

G_{ice} center of gravity of ice accretion

g gravitational acceleration

I moment of inertia relative to a given axis

I moment of inertia per unit length

I_i moment of inertia relative to the neutral axis of the cable

i turbulence intensity of the flow

K tower longitudinal stiffness

K_{ev} equivalent longitudinal stiffness of the cable plus anchoring towers

k spring constant representing the rigidity of the support

k modal contribution

L section length of the cable between two anchoring towers

L loop length

L span length

L_s span length

L_p length of pendulum

LWC liquid water content of precipitation

Δl cable's length variation

M total mass of all pendulums in a span

M_w pitching moment per unit length

M_α aerodynamic moment per unit length of conductor

m mass per unit of length of cable

m_{ice} mass of ice per unit length

N_s total number of span

n order of Prony's expansion

n_c number of subconductors in the bundle

P longitudinal force applied to the cable

Q cross-load applied on the cable

R	arm length of pendulum
s	torsional stiffness of the conductor
s	span no
T	cable tension
T	temperature
T_o	initial cable tension
t	time
t_{acc}	accretion duration
U	maximum stored energy of strain
U_f	bending energy
U_k	kinetic energy
U_{os}	Stored energy of the oscillating system that supplies the force
V	wind velocity
v_r	relative wind velocity
$x(t)$	original galloping signal as a function of time
$\hat{x}(t)$	estimated response by Prony's method
$x(t)$	original signal
$y_{s,k0}$	modal contribution k to the initial sag in the span s
y	vertical displacement of cable
$\dot{y}$	vertical velocity of cable
$\ddot{y}$	vertical acceleration of cable
α	angle of attack of section due to vertical velocity
α_1	efficiency of collision
α_2	sticking efficiency
α_3	accretion efficiency
γ	curve fitting factor defined in equation (8.9)
δ	deflection
δ	logarithmic decrement
ε	eccentricity

ε	loss factor or loss tangent
η	loss coefficient of a solid
Θ	torsional displacement of cable due to dynamic forces
Θ	angle of rotation due to a static moment on the cable
Θ_o	initial torsional displacement of cable
λ_i	i^{th} eigenvalue in Prony equation
ξ_{eq}	equivalent percentage of critical damping due to drag effect
ξ_v	vertical damping ratio
ξ_Θ	torsional damping ratio
ρ_{air}	air density
φ	total angle of attack of section to relative wind
ω_v	circular frequency of the vertical mode
ω_θ	circular frequency of the torsional mode
ω_v	modal pulsation of the observed eigenmode (rad/s)
$\Delta\vartheta$	torsional excursion of cable